VOLUME: 17 NO: 1 YEAR: 2020

ISSN: 1304-530X

TURKISH JOURNAL OF PHARMACEUTICAL SCIENCES

An Official Journal of the Turkish Pharmacists' Association, Academy of Pharmacy

TURKISH JOURNAL OF PHARMACEUTICAL SCIENCES VOLUME: 17 NO: 1 YEAR: 2020

TURKISH
JOURNAL OF PHARMACEUTICAL SCIENCES

TÜRK ECZACILIK BİLİMLERİ DERGİSİ

TURKISH JOURNAL OF PHARMACEUTICAL SCIENCES

AIMS AND SCOPE

The Turkish Journal of Pharmaceutical Sciences is the only scientific periodical publication of the Turkish Pharmacists' Association and has been published since April 2004.

Turkish Journal of Pharmaceutical Sciences is an independent international open access periodical journal based on double-blind peer-review principles. The journal is regularly published 6 times a year and the publication language is English. The issuing body of the journal is Galenos Yayinevi/Publishing House.

The aim of Turkish Journal of Pharmaceutical Sciences is to publish original research papers of the highest scientific and clinical value at an international level.

The target audience includes specialists and physicians in all fields of pharmaceutical sciences.

The editorial policies are based on the "Recommendations for the Conduct, Reporting, Editing, and Publication of Scholarly Work in Medical Journals (ICMJE Recommendations)" by the International Committee of Medical Journal Editors (2016, archived at http://www.icmje.org/) rules.

Editorial Independence

Turkish Journal of Pharmaceutical Sciences is an independent journal with independent editors and principles and has no commerical relationship with the commercial product, drug or pharmaceutical company regarding decisions and review processes upon articles.

ABSTRACTED/INDEXED IN

Web of Science-Emerging Sources Citation Index (ESCI)
SCOPUS SJR
Directory of Open Access Journals (DOAJ)
ProQuest
Chemical Abstracts Service (CAS)
EBSCO
EMBASE
Analytical Abstracts
International Pharmaceutical Abstracts (IPA)
Medicinal & Aromatic Plants Abstracts (MAPA)
TÜBİTAK/ULAKBİM TR Dizin
Türkiye Atıf Dizini
UDL-EDGE

OPEN ACCESS POLICY

This journal provides immediate open access to its content on the principle that making research freely available to the public supports a greater global exchange of knowledge.

Open Access Policy is based on the rules of the Budapest Open Access Initiative (BOAI) http://www.budapestopenaccessinitiative.org/. By "open access" to peer-reviewed research literature, we mean its free availability on the public internet, permitting any users to read, download, copy, distribute, print, search, or link to the full texts of these articles, crawl them for indexing, pass them as data to software, or use them for any other lawful purpose, without financial, legal, or technical barriers other than those inseparable from gaining access to the internet itself. The only constraint on reproduction and distribution, and the only role for copyright in this domain, should be to give authors control over the integrity of their work and the right to be properly acknowledged and cited.

CORRESPONDENCE ADDRESS

Editor-in-Chief, Feyyaz ONUR, Prof.Dr.
Address: Lokman Hekim University, Faculty of Pharmacy, Department of Analytical Chemistry, 06100 Tandoğan-Ankara, TURKEY
E-mail: onur@pharmacy.ankara.edu.tr

PERMISSION

Requests for permission to reproduce published material should be sent to the editorial office. Editor-in-Chief, Prof. Dr. Feyyaz ONUR

ISSUING BODY CORRESPONDING ADDRESS

Issuing Body : Galenos Yayınevi
Address: Molla Gürani Mah. Kaçamak Sk. No: 21/1, 34093 İstanbul, TURKEY
Phone: +90 212 621 99 25 Fax: +90 212 621 99 27
E-mail: info@galenos.com.tr

INSTRUCTIONS FOR AUTHORS

Instructions for authors are published in the journal and on the website http://turkjps.org

MATERIAL DISCLAIMER

The author(s) is (are) responsible for the articles published in the JOURNAL.

The editor, editorial board and publisher do not accept any responsibility for the articles.

Publisher Contact
Address: Molla Gürani Mah. Kaçamak Sk. No: 21/1
34093 İstanbul, Turkey
Phone: +90 (212) 621 99 25 Fax: +90 (212) 621 99 27
E-mail: info@galenos.com.tr/yayin@galenos.com.tr
Web: www.galenos.com.tr | Publisher Certificate Number: 14521

Printing at: Üniform Basım San. ve Turizm Ltd. Şti.
Matbaacılar Sanayi Sitesi 1. Cad. No: 114 34204 Bağcılar, İstanbul, Turkey
Phone: +90 (212) 429 10 00 | Certificate Number: 42419
Printing Date: February 2020
ISSN: 1304-530X
International scientific journal published quarterly.

TURKISH
JOURNAL OF PHARMACEUTICAL SCIENCES

INSTRUCTIONS TO AUTHORS

Turkish Journal of Pharmaceutical Sciences is the official double peer-reviewed publication of The Turkish Pharmacists' Association. This journal is published every 3 months (4 issues per year; March, June, September, December) and publishes the following articles:

- Research articles
- Reviews (only upon the request or consent of the Editorial Board)
- Preliminary results/Short communications/Technical notes/Letters to the Editor in every field or pharmaceutical sciences.

The publication language of the journal is English.

The Turkish Journal of Pharmaceutical Sciences does not charge any article submission or processing charges.

A manuscript will be considered only with the understanding that it is an original contribution that has not been published elsewhere.

The Journal should be abbreviated as "Turk J Pharm Sci" when referenced.

The scientific and ethical liability of the manuscripts belongs to the authors and the copyright of the manuscripts belongs to the Journal. Authors are responsible for the contents of the manuscript and accuracy of the references. All manuscripts submitted for publication must be accompanied by the Copyright Transfer Form [copyright transfer]. Once this form, signed by all the authors, has been submitted, it is understood that neither the manuscript nor the data it contains have been submitted elsewhere or previously published and authors declare the statement of scientific contributions and responsibilities of all authors.

Experimental, clinical and drug studies requiring approval by an ethics committee must be submitted to the JOURNAL with an ethics committee approval report including approval number confirming that the study was conducted in accordance with international agreements and the Declaration of Helsinki (revised 2013) (http://www.wma.net/en/30publications/10policies/b3/). The approval of the ethics committee and the fact that informed consent was given by the patients should be indicated in the Materials and Methods section. In experimental animal studies, the authors should indicate that the procedures followed were in accordance with animal rights as per the Guide for the Care and Use of Laboratory Animals (http://oacu.od.nih.gov/regs/guide/guide.pdf) and they should obtain animal ethics committee approval.

Authors must provide disclosure/acknowledgment of financial or material support, if any was received, for the current study.

If the article includes any direct or indirect commercial links or if any institution provided material support to the study, authors must state in the cover letter that they have no relationship with the commercial product, drug, pharmaceutical company, etc. concerned; or specify the type of relationship (consultant, other agreements), if any.

Authors must provide a statement on the absence of conflicts of interest among the authors and provide authorship contributions.

All manuscripts submitted to the journal are screened for plagiarism using the 'iThenticate' software. Results indicating plagiarism may result in manuscripts being returned or rejected.

The Review Process

This is an independent international journal based on double-blind peer-review principles. The manuscript is assigned to the Editor-in-Chief, who reviews the manuscript and makes an initial decision based on manuscript quality and editorial priorities. Manuscripts that pass initial evaluation are sent for external peer review, and the Editor-in-Chief assigns an Associate Editor. The Associate Editor sends the manuscript to at least two reviewers (internal and/or external reviewers). The reviewers must review the manuscript within 21 days. The Associate Editor recommends a decision based on the reviewers' recommendations and returns the manuscript to the Editor-in-Chief. The Editor-in-Chief makes a final decision based on editorial priorities, manuscript quality, and reviewer recommendations. If there are any conflicting recommendations from reviewers, the Editor-in-Chief can assign a new reviewer.

The scientific board guiding the selection of the papers to be published in the Journal consists of elected experts of the Journal and if necessary, selected from national and international authorities. The Editor-in-Chief, Associate Editors may make minor corrections to accepted manuscripts that do not change the main text of the paper.

In case of any suspicion or claim regarding scientific shortcomings or ethical infringement, the Journal reserves the right to submit the manuscript to the supporting institutions or other authorities for investigation. The Journal accepts the responsibility of initiating action but does not undertake any responsibility for an actual investigation or any power of decision.

The Editorial Policies and General Guidelines for manuscript preparation specified below are based on "Recommendations for the Conduct, Reporting, Editing, and Publication of Scholarly Work in Medical Journals (ICMJE Recommendations)" by the International Committee of Medical Journal Editors (2016, archived at http://www.icmje.org/).

Preparation of research articles, systematic reviews and meta-analyses must comply with study design guidelines:

CONSORT statement for randomized controlled trials (Moher D, Schultz KF, Altman D, for the CONSORT Group. The CONSORT statement revised recommendations for improving the quality of reports of parallel group randomized trials. JAMA 2001; 285: 1987-91) (http://www.consort-statement.org/);

PRISMA statement of preferred reporting items for systematic reviews and meta-analyses (Moher D, Liberati A, Tetzlaff J, Altman DG, The PRISMA Group. Preferred Reporting Items for Systematic Reviews and Meta-Analyses: The PRISMA Statement. PLoS Med 2009; 6(7): e1000097.) (http://www.prisma-statement.org/);

STARD checklist for the reporting of studies of diagnostic accuracy (Bossuyt PM, Reitsma JB, Bruns DE, Gatsonis CA, Glasziou PP, Irwig LM, et al., for the STARD Group. Towards complete and accurate reporting of studies of diagnostic accuracy: the STARD initiative. Ann Intern Med 2003;138:40-4.) (http://www.stard-statement.org/);

STROBE statement, a checklist of items that should be included in reports of observational studies (http://www.strobe-statement.org/);

MOOSE guidelines for meta-analysis and systemic reviews of observational studies (Stroup DF, Berlin JA, Morton SC, et al. Meta-analysis of observational studies in epidemiology: a proposal for reporting Meta-analysis of observational Studies in Epidemiology (MOOSE) group. JAMA 2000; 283: 2008-12).

Authorship

Each author should have participated sufficiently in the work to assume public responsibility for the content. Any portion of a manuscript that

TURKISH
JOURNAL OF PHARMACEUTICAL SCIENCES

INSTRUCTIONS TO AUTHORS

is critical to its main conclusions must be the responsibility of at least 1 author.

GENERAL GUIDELINES

Manuscripts can only be submitted electronically through the Journal Agent website (http://journalagent.com/tjps/) after creating an account. This system allows online submission and review.

The manuscripts are archived according to ICMJE, Web of Science-Emerging Sources Citation Index (ESCI), SCOPUS, Chemical Abstracts, EBSCO, EMBASE, Analytical Abstracts, International Pharmaceutical Abstracts, MAPA(Medicinal & Aromatic Plants Abstracts), Tübitak/ Ulakbim Turkish Medical Database, Türkiye Citation Index Rules.

Format: Manuscripts should be prepared using Microsoft Word, size A4 with 2.5 cm margins on all sides, 12 pt Arial font and 1.5 line spacing.

Abbreviations: Abbreviations should be defined at first mention and used consistently thereafter. Internationally accepted abbreviations should be used; refer to scientific writing guides as necessary.

Cover letter: The cover letter should include statements about manuscript type, single-Journal submission affirmation, conflict of interest statement, sources of outside funding, equipment (if applicable), for original research articles.

The ORCID (Open Researcher and Contributor ID) number of the all authors should be provided while sending the manuscript. A free registration can be done at http://orcid.org.

REFERENCES

Authors are solely responsible for the accuracy of all references.

In-text citations: References should be indicated as a superscript immediately after the period/full stop of the relevant sentence. If the author(s) of a reference is/are indicated at the beginning of the sentence, this reference should be written as a superscript immediately after the author's name. If relevant research has been conducted in Turkey or by Turkish investigators, these studies should be given priority while citing the literature.

Presentations presented in congresses, unpublished manuscripts, theses, Internet addresses, and personal interviews or experiences should not be indicated as references. If such references are used, they should be indicated in parentheses at the end of the relevant sentence in the text, without reference number and written in full, in order to clarify their nature.

References section: References should be numbered consecutively in the order in which they are first mentioned in the text. All authors should be listed regardless of number. The titles of Journals should be abbreviated according to the style used in the Index Medicus.

Reference Format

Journal: Last name(s) of the author(s) and initials, article title, publication title and its original abbreviation, publication date, volume, the inclusive page numbers. Example: Collin JR, Rathbun JE. Involutional entropion: a review with evaluation of a procedure. Arch Ophthalmol. 1978;96:1058-1064.

Book: Last name(s) of the author(s) and initials, book title, edition, place of publication, date of publication and inclusive page numbers of the extract cited. Example: Herbert L. The Infectious Diseases (1st ed). Philadelphia; Mosby Harcourt; 1999:11;1-8.

Book Chapter: Last name(s) of the author(s) and initials, chapter title, book editors, book title, edition, place of publication, date of publication and inclusive page numbers of the cited piece.

Example: O'Brien TP, Green WR. Periocular Infections. In: Feigin RD, Cherry JD, eds. Textbook of Pediatric Infectious Diseases (4th ed). Philadelphia; W.B. Saunders Company;1998:1273-1278.

Books in which the editor and author are the same person: Last name(s) of the author(s) and initials, chapter title, book editors, book title, edition, place of publication, date of publication and inclusive page numbers of the cited piece. Example: Solcia E, Capella C, Kloppel G. Tumors of the exocrine pancreas. In: Solcia E, Capella C, Kloppel G, eds. Tumors of the Pancreas. 2nd ed. Washington: Armed Forces Institute of Pathology; 1997:145-210.

TABLES, GRAPHICS, FIGURES, AND IMAGES

All visual materials together with their legends should be located on separate pages that follow the main text.

Images: Images (pictures) should be numbered and include a brief title. Permission to reproduce pictures that were published elsewhere must be included. All pictures should be of the highest quality possible, in

JPEG format, and at a minimum resolution of 300 dpi.

Tables, Graphics, Figures: All tables, graphics or figures should be enumerated according to their sequence within the text and a brief descriptive caption should be written. Any abbreviations used should be defined in the accompanying legend. Tables in particular should be explanatory and facilitate readers' understanding of the manuscript, and should not repeat data presented in the main text.

MANUSCRIPT TYPES

Original Articles

Clinical research should comprise clinical observation, new techniques or laboratories studies. Original research articles should include title, structured abstract, key words relevant to the content of the article, introduction, materials and methods, results, discussion, study limitations, conclusion references, tables/figures/images and acknowledgement sections. Title, abstract and key words should be written in both Turkish and English. The manuscript should be formatted in accordance with the above-mentioned guidelines and should not exceed 16 A4 pages.

Title Page: This page should include the title of the manuscript, short title, name(s) of the authors and author information. The following descriptions should be stated in the given order:

1. Title of the manuscript (Turkish and English), as concise and explanatory as possible, including no abbreviations, up to 135 characters

2. Short title (Turkish and English), up to 60 characters

3. Name(s) and surname(s) of the author(s) (without abbreviations and academic titles) and affiliations

4. Name, address, e-mail, phone and fax number of the corresponding author

5. The place and date of scientific meeting in which the manuscript was presented and its abstract published in the abstract book, if applicable

TURKISH
JOURNAL OF PHARMACEUTICAL SCIENCES

INSTRUCTIONS TO AUTHORS

Abstract: A summary of the manuscript should be written in both Turkish and English. References should not be cited in the abstract. Use of abbreviations should be avoided as much as possible; if any abbreviations are used, they must be taken into consideration independently of the abbreviations used in the text. For original articles, the structured abstract should include the following sub-headings:

Objectives: The aim of the study should be clearly stated.

Materials and Methods: The study and standard criteria used should be defined; it should also be indicated whether the study is randomized or not, whether it is retrospective or prospective, and the statistical methods applied should be indicated, if applicable.

Results: The detailed results of the study should be given and the statistical significance level should be indicated.

Conclusion: Should summarize the results of the study, the clinical applicability of the results should be defined, and the favorable and unfavorable aspects should be declared.

Keywords: A list of minimum 3, but no more than 5 key words must follow the abstract. Key words in English should be consistent with "Medical Subject Headings (MESH)" (www.nlm.nih.gov/mesh/MBrowser.html). Turkish key words should be direct translations of the terms in MESH.

Original research articles should have the following sections:

Introduction: Should consist of a brief explanation of the topic and indicate the objective of the study, supported by information from the literature.

Materials and Methods: The study plan should be clearly described, indicating whether the study is randomized or not, whether it is retrospective or prospective, the number of trials, the characteristics, and the statistical methods used.

Results: The results of the study should be stated, with tables/figures given in numerical order; the results should be evaluated according to the statistical analysis methods applied. See General Guidelines for details about the preparation of visual material.

Discussion: The study results should be discussed in terms of their favorable and unfavorable aspects and they should be compared with the literature. The conclusion of the study should be highlighted.

Study Limitations: Limitations of the study should be discussed. In addition, an evaluation of the implications of the obtained findings/results for future research should be outlined.

Conclusion: The conclusion of the study should be highlighted.

Acknowledgements: Any technical or financial support or editorial contributions (statistical analysis, English/Turkish evaluation) towards the study should appear at the end of the article.

References: Authors are responsible for the accuracy of the references. See General Guidelines for details about the usage and formatting required.

Review Articles

Review articles can address any aspect of clinical or laboratory pharmaceuticals. Review articles must provide critical analyses of contemporary evidence and provide directions of or future research. Most review articles are commissioned, but other review submissions are also welcome. Before sending a review, discussion with the editor is recommended.

Reviews articles analyze topics in depth, independently and objectively. The first chapter should include the title in Turkish and English, an unstructured summary and key words. Source of all citations should be indicated. The entire text should not exceed 25 pages (A4, formatted as specified above).

CORRESPONDENCE

All correspondence should be directed to the Turkish Journal of Pharmaceutical Sciences editorial board;

Post: Turkish Pharmacists' Association

Address: Willy Brandt Sok. No: 9 06690 Ankara, TURKEY

Phone: +90 312 409 8136

Fax: +90 312 409 8132

Web Page: http://turkjps.org/home/

E-mail: onur@pharmacy.ankara.edu.tr

TURKISH
JOURNAL OF PHARMACEUTICAL SCIENCES

CONTENTS

TURKISH
JOURNAL OF PHARMACEUTICAL SCIENCES

CONTENTS

PUBLICATION NAME	Turkish Journal of Pharmaceutical Sciences
TYPE OF PUBLICATION	Vernacular Publication
PERIOD AND LANGUAGE	Quarterly- English
OWNER	Erdoğan ÇOLAK on behalf of the Turkish Pharmacists' Association
EDITOR-IN-CHIEF	Feyyaz ONUR
ADDRESS OF PUBLICATION	Cinnah Mah. Willy Brandt Sok. No: 9 Çankaya-Ankara/TURKEY

TURKISH
JOURNAL OF PHARMACEUTICAL
SCIENCES

Volume: 17, No: 1, Year: 2020

CONTENTS

Turk J Pharm Sci 2020;17(1):1-6
DOI: 10.4274/tjps.galenos.2018.97759

ORIGINAL ARTICLE

An *In Vitro* Study on the Interactions of Pycnogenol® with Cisplatin in Human Cervical Cancer Cells

İnsan Servikal Kanser Hücrelerinde Piknogenol®'ün Sisplatin ile Etkileşmesi Üzerine *İn Vitro* Çalışma

Merve BECİT[1], Sevtap AYDIN[2]*

[1]Atatürk University, Faculty of Pharmacy, Department of Pharmacology, Erzurum, Turkey
[2]Hacettepe University, Faculty of Pharmacy, Department of Pharmaceutical Toxicology, Ankara, Turkey

ABSTRACT

Objectives: In the treatment of cancer, it is intended to increase the anticancer effect and decrease cytotoxicity using various plant-derived phenolic compounds with chemotherapeutic drugs. Pycnogenol® (PYC), a phenolic compound, has been the subject of many studies. Since the mechanisms of the interactions of PYC with cisplatin need to be clarified, we aimed to determine the effects of PYC on cisplatin cytotoxicity in human cervix cancer cells (HeLa) and to evaluate the genotoxicity of PYC.

Materials and Methods: The cytotoxicity of cisplatin and PYC was measured by 3-(4,5-dimethylthiazol-2-yl)-2,5-diphenyltetrazolium bromide (MTT) assay in HeLa cells for 24 h and 48 h. The effect of PYC against oxidative DNA damage was evaluated using the comet assay.

Results: The IC_{50} values of cisplatin were 22.4 μM and 12.3 μM for 24 h and 48 h, respectively. The IC_{50} values of PYC were 261 μM and 213 μM for 24 h and 48 h, respectively. For 24 h exposure, PYC significantly reduced the IC_{50} value of cisplatin at the selected concentrations (15.6-500 μM). For 48 h exposure, PYC did not change the cytotoxicity of cisplatin at concentrations between 15.6 and 125 μM, but significantly reduced it at concentrations of 250 μM and 500 μM. PYC alone did not induce DNA damage at concentrations of 10 μM or 25 μM; however, it significantly induced DNA damage at higher concentrations (50-100 μM). It also significantly reduced H_2O_2-induced DNA damage at all concentrations studied (10-100 μM).

Conclusion: Our results suggest that PYC may increase the cisplatin cytotoxicity in HeLa cells at nongenotoxic doses. The results might contribute to the anticancer effect of cisplatin with PYC in cervical carcinoma, but in order to confirm this result further *in vitro* studies with cancer cell lines and *in vivo* studies are needed.

Key words: Pycnogenol, cisplatin, cytotoxicity, genotoxicity, human cervix cancer cells

ÖZ

Amaç: Kanser tedavisinde antikanser etkiyi artırmak ve sitotoksisiteyi azaltmak amacıyla kemoterapötik ilaçlar ile birlikte çeşitli bitkisel kökenli fenolik bileşiklerin kullanımı hedeflenmektedir. Bir fenolik bileşik olan Piknogenol® (PYC), birçok çalışmanın konusu olmaktadır. PYC'nin sisplatin ile etkileşme mekanizması tam olarak aydınlatılamadığı için insan serviks kanser hücrelerinde (HeLa) sisplatin sitotoksisitesi üzerine PYC'nin etkilerini belirlemeyi ve PYC'nin sitotoksik olmayan dozlarında PYC'nin genotoksisitesini değerlendirilmeyi hedefledik.

Gereç ve Yöntemler: HeLa hücrelerinde, 24 ve 48 saatlik maruziyetlerde, PYC varlığında ve yokluğunda sisplatinin sitotoksisitesi 3-(4,5-dimetiltiyazol-2-il)-2,5-difeniltetrazolyum bromür (MTT) yöntemi ile ölçüldü. Oksidatif DNA hasarına karşı PYC'nin etkisi Comet yöntemi ile değerlendirildi.

Bulgular: Sisplatinin IC_{50} değeri 24 saat ve 48 saat için sırasıyla 22,4 μM ve 12,3 μM idi. PYC'nin IC_{50} değerleri 24 saat ve 48 saat için sırasıyla 261 μM ve 213 μM idi. Yirmi dört saatlik maruziyet için, PYC'nin, seçilen konsantrasyonlarda (15,6-500 μM) sisplatinin IC_{50} değerini önemli ölçüde azalttı. Kırk sekiz saat maruziyet için, PYC sisplatinin sitotoksisitesini 15,6-125 μM arasındaki konsantrasyonlarda değiştirmedi, ancak 250 μM ve 500 μM konsantrasyonlarda önemli ölçüde azalttı. PYC tek başına 10 μM ve 25 μM konsantrasyonlarında DNA hasarına neden olmadı, ancak daha yüksek konsantrasyonlarında (50-100 μM) DNA hasarını önemli ölçüde indükledi. Ayrıca, çalışılan tüm konsantrasyonlarında (10-100 μM) 50 μM H_2O_2 tarafından indüklenen DNA hasarını önemli ölçüde azalttı.

*Correspondence: E-mail: sevtapaydin@hotmail.com, Phone: +90 538 543 76 57 ORCID-ID: orcid.org/0000-0002-6368-2745
Received: 27.07.2018, Accepted: 20.09.2018

Sonuç: Sonuçlarımız PYC'nin genotoksik olmayan dozlarında HeLa hücrelerindeki sisplatin sitotoksisitesini arttırabileceğini göstermektedir. Bu sonuçlar, sisplatinin PYC ile birlikte servikal karsinomadaki antikanser etkisine katkıda bulunabilir, ancak bunu doğrulamak üzere kanser hücre hatları üzerinde daha ileri *in vitro* çalışmalara ve *in vivo* çalışmalara ihtiyaç vardır.

Anahtar kelimeler: Piknogenol, sisplatin, sitotoksisite, genotoksisite, HeLa hücresi

INTRODUCTION

Oxidative stress is one of the hypotheses involved in the etiology of a number of diseases, including cancer. Considerable attention has been focused on antioxidant agents such as phenolic compounds in recent years, because it is stated that the development of oxidative stress-related diseases may be prevented or delayed by using them.[1-4] Pycnogenol® (PYC) is a phenolic compound and a natural dried extract obtained from the bark of the French maritime pine (Pinus pinaster). It is a proprietary mixture of procyanidins containing 65%-75% catechin and epicatechin subunits.[5,6] It is commonly consumed as a dietary food supplement owing to its strong antioxidant activity. As shown in many studies, PYC has potential therapeutic and protective effects against cancer.[6] However, there are not sufficient studies on the interactions between antineoplastic drugs and PYC. Antineoplastic drugs are clinically used in therapy of cancers, aiming to reduce tumor cell growth. Cisplatin (CIS) is a powerful antineoplastic drug to treat many types of cancer including esophageal, lung, breast, ovarian, bladder, cervical, and prostate cancers.[7] Nowadays, combinatorial therapies have been investigated with the aim of increasing anticancer activity and minimizing drug resistance. Recent studies yielded positive findings using various phenolic compounds combined with an antineoplastic drug.[8-12] Nevertheless, further investigations are needed to clarify the effects of phenolic compounds on cancer and the effects of combining them with antineoplastic drugs in different doses. The aim of the present study was to determine the effects of PYC on the cytotoxic profile of CIS in human cervical cervix carcinoma (HeLa) cells using the 3-(4,5-dimethylthiazol-2-yl)-2,5-diphenyltetrazolium bromide (MTT) assay. The genotoxic/antigenotoxic effects of PYC against oxidative DNA damage were evaluated using alkaline single cell gel electrophoresis (Comet assay).

MATERIALS AND METHODS

Chemicals

The chemicals used and their suppliers were as follows: CIS from Koçak Farma (Turkey); dimethyl sulfoxide (DMSO), Dulbecco's modified Eagle's medium, ethanol, ethidium bromide (EtBr), ethylenediamine tetra acetic acid disodium salt dihydrate (EDTA-2Na), fetal bovine serum (FBS), hydrogen peroxide (35%) (H_2O_2), low melting point agarose (LMA), MTT, n-lauroyl sarcosinate, normal melting point agarose (NMA), penicillin-streptomycin, sodium chloride (NaCl), sodium hydroxide (NaOH), Tris, Triton X-100, trypan blue, trypsin-EDTA, RPMI 1640 medium, Dulbecco's phosphate buffered saline (PBS) from Sigma (St. Louis, MO, USA); Millipore filters from Millipore (Billerica, MA, USA); all other plastic materials from Cornings (Corning Inc., NY, USA). PYC was purchased from Horphag Research Ltd. (Geneva, Switzerland). The quality of standardized PYC extract is specified in the United States Pharmacopeia (USP 28).[5]

Cell culture

HeLa cells were obtained from the American Type Culture Collection (Rockville, MD, USA). HeLa cells were grown in RPMI-1640 medium supplemented with 10% heat-inactivated FBS, 1% penicillin-streptomycin solution (10,000 units of penicillin and 10 mg of streptomycin in 0.9% NaCl), and 2 mM L-glutamine at 37°C in a humidified atmosphere of 5% CO_2. The cells were subcultured in 75 cm^2 cell culture flasks. The medium was changed every 2-3 days. The passage numbers used in our study for both cell lines were between passage 8 and passage 10.

Determination of cytotoxicity

After growing for 2 weeks, the cells were plated at 1×10^4 cells/well by adding 200 µL of a 5×10^4 cells/mL suspension to each well of a 96 well tissue culture plate and allowed to grow for 24 h before treatment. The number of cells was calculated by trypan blue dye exclusion. The stock solution of PYC was freshly prepared in PBS and filtered with Millipore filters (0.20 µm). The cells were treated with PYC at a wide range of concentrations (1.95-2000 µM) or CIS (0.49-500 µM) in the related culture medium for 24 h and 48 h. Control experiments were carried out with the culture medium containing only PBS (1%). After the values of IC_{50} were determined, the cytotoxic profiles of PYC on the IC_{50} of CIS were evaluated at wide doses of PYC in HeLa cells for 24 h and 48 h.

The cytotoxicity of PYC and CIS was measured in HeLa cells using the MTT assay, which is a colorimetric assay that measures the reduction of yellow MTT by mitochondrial succinate dehydrogenase.[13,14] At the end of the incubation (24 h and 48 h), 5 mg/mL MTT solution was added to each well, followed by incubation for another 4 h at 37°C. Then the medium was discarded. The formazan crystals were dissolved in 100 µL of DMSO and absorbance of each sample was measured at 570 nm using a microplate reader (SpectraMax M2, Molecular Devices Limited, Wokingham, UK).

The percentage of cell viability was calculated using the following formula:

Percentage of cell viability= (the absorbance of sample/control) ×100

The cytotoxic concentration that killed cells by 50% (IC_{50}) was determined from the absorbance versus concentration curve.

Determination of genotoxicity

HeLa cells were incubated with PYC at noncytotoxic doses (0, 10, 25, 50, and 100 µM) for 2 h (preincubation) with/without

genotoxic doses of H_2O_2 (50 µM) for 5 min. Thus, the possible protective effect of PYC against oxidative DNA damage induced by H_2O_2 was also evaluated. Moreover, 50 µM H_2O_2 was applied as a positive control. Medium containing 10% PBS was applied as a negative control. The comet assay was performed to assess DNA damage. The basic alkaline technique described by Singh et al.[15] was used for the detection of DNA damage in the cells. The concentrations of the cells were adjusted to 2×10^5 cells/mL, suspended in 5% LMA, and were then embedded on slides precoated with a layer of 1% NMA. The slides were allowed to solidify on ice for 5 min. The cover slips were then removed. All slides were immersed in cold lysing solution (pH 10) for a minimum of 1 h at 4°C. The slides containing the cells were removed from the lysing solution, drained, and then placed in a horizontal gel electrophoresis tank filled with freshly prepared alkaline electrophoresis solution (300 mmol/L NaOH, 1 mmol/EDTA-2Na, pH 13.0) for 20 min at 4°C to allow unwinding of the DNA and expression of DNA damage. Electrophoresis was then conducted at 4°C for 20 min at 24 V/300 mA. The slides were neutralized at room temperature by washing 3 times in neutralization buffer (0.4 mol/L Tris-HCl, pH 7.5) for 5 min. After neutralization, the slides were then incubated in 50%, 75%, and 98% of alcohol for 5 min successively. The dried microscope slides were stained with EtBr (20 µg/mL in distilled water, 60 µL/slide), covered with a cover glass prior to analysis with a fluorescence microscope (Leica DM1000, Wetzlar, Germany) equipped with an excitation filter of 515-560 nm. The microscope was connected to a charge-coupled device camera and a personal computer-based analysis system (Comet Analysis Software, Version 3.0, Kinetic Imaging Ltd., Liverpool, UK) to determine the extent of DNA damage after electrophoretic migration of the DNA fragments in the agarose gel. In order to visualize the DNA damage, the slides were examined at 400×. For each condition, 100 randomly selected comets from each of two replicate slides were scored (without knowledge of the group codes). DNA damage parameters were expressed as DNA tail intensity %.

Statistical analysis

All experiments were carried out in quadruplicate. The results were given as the mean ± standard deviation. The statistical analysis was performed with SPSS 10.5 (SPSS, Chicago, IL, USA). The distribution of the data was checked for normality using the Kolmogorov-Smirnov test. The means of data were compared by One-way variance analysis test and *post hoc* analysis of group differences was performed by least significant difference test. A p value of less than 0.05 was considered statistically significant.

RESULTS

Pycnogenol cytotoxicity

The results of PYC cytotoxicity are given in Table 1 and Figure 1. PYC did not cause significant cytotoxic effects at the concentration range of 1.95-125 µM when compared to the negative control for 24 h and 48 h incubation; however, the cell viabilities were significantly decreased above 250 µM concentrations of PYC ($p<0.05$) (Table 1). The IC_{50} values of PYC were 261 µM and 213 µM for 24 h and 48 h, respectively (Figure 1).

Cisplatin cytotoxicity

The results of CIS cytotoxicity are given in Table 2 and Figure 2. CIS did not cause significant cytotoxic effects at the concentration range of 0.49-7.81 µM or at the concentration range of 0.49-3.91 µM when compared to the negative control for 24 h and 48 h, respectively; however, the cell viabilities were significantly decreased above 15.2 µM and 7.81 µM of CIS for 24 h and 48 h incubation, respectively ($p<0.05$) (Table 2). The IC_{50} values of CIS were 22.4 µM and 12.3 µM for 24 h and 48 h, respectively (Figure 2).

Effects of Pycnogenol on cisplatin cytotoxicity

The effects of PYC at the concentration range of 15.6-500 µM on CIS cytotoxicity in HeLa cells are shown in Figure 3 for 24 h and 48 h incubation. As shown in Figure 3a, at all studied concentrations (15.6-500 µM) PYC significantly decreased the

Table 1. Effects of pycnogenol on the cell viability of HeLa cells for 24 h and 48 h*

Group	24 h (%)	48 h (%)
(-) Control	100.0±0	100.0±0
1.95 µM PYC	91.9±12.9	94.4±6.2
3.91 µM PYC	84.1±9.6	87.0±3.3
7.81 µM PYC	84.0±6.9	86.6±11.9
15.63 µM PYC	92.2±7.6	89.9±8.2
31.25 µM PYC	91.8±4.7	92.3±7.9
62.5 µM PYC	89.6±9.7	86.2±12.9
125 µM PYC	86.2±10	84.3±10.4
250 µM PYC	52.2±10.8[a]	36.1±5.5[a]
500 µM PYC	7.0±1.6[a]	3.8±0.3[a]
1000 µM PYC	6.6±0.7[a]	3.7±0.4[a]
2000 µM PYC	5.7±0.8[a]	2.8±0.7[a]

*Values are given as the mean ± standard deviation (n=4), [a]$p<0.05$, compared to negative control (Pharmaceutical Benefits Scheme), PYC: Pygnogenol

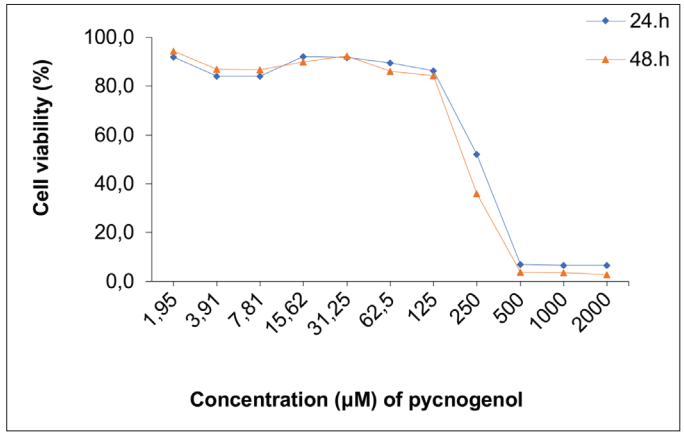

Figure 1. Effects of pycnogenol on the cell viability of HeLa cells for 24 h and 48 h*

* Values are given as the mean ± standard deviation (n=4), [a]$p<0.05$, compared to negative control (Pharmaceutical Benefits Scheme)

Table 2. Effects of cisplatin on the cell viability of HeLa cells for 24 h and 48 h*

Treatment group	24 h (%)	48 h (%)
(-) Control	100.0±0	100.0±0
0.49 µM CIS	100.1±4.2	94.2±6
0.98 µM CIS	100.4±9.1	93.0±7.4
1.95 µM CIS	99.5±7.5	93.2±13.5
3.91 µM CIS	100.1±4.6	94.3±14.2
7.81 µM CIS	86.5±14	77.6±7[a]
15.63 µM CIS	64.7±6.6[a]	29.4±2[a]
31.25 µM CIS	31.6±5.6[a]	6.7±0.9[a]
62.5 µM CIS	21.0±4.5[a]	5.9±0.7[a]
125 µM CIS	12.3±6.1[a]	6.3±0.7[a]
250 µM CIS	7.8±0.8[a]	6.9±0.9[a]
500 µM CIS	5.8±0.6[a]	7.3±1.7[a]

*Values are given as the mean ± standard deviation (n=4), [a]p<0.05, compared to negative control (Pharmaceutical Benefits Scheme), CIS: Cisplatin

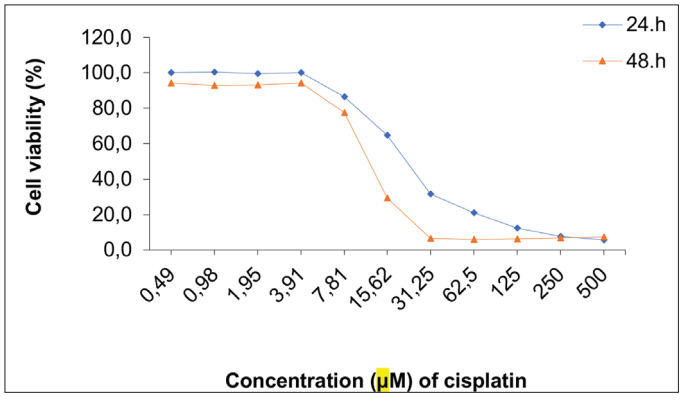

Figure 2. Effects of cisplatin on the cell viability of HeLa cells for 24 h and 48 h*

*Values are given as the mean ± standard deviation (n=4), ap<0.05, compared to negative control (Pharmaceutical Benefits Scheme)

IC_{50} value of CIS (20 µM, approximately) in a dose-dependent manner (1.53 fold, 1.84 fold, 1.87 fold, 1.94 fold, 2.28 fold, and 2.86 fold for 15.6 µM, 31.3 µM, 62.5 µM, 125 µM, 250 µM, and 500 µM, respectively, vs. the positive control) when compared to the negative control for 24 h incubation (p<0.05). As shown in Figure 3b, when compared to the negative control, PYC did not change the IC_{50} value of CIS (10 µM, approximately) at the concentration range of 15.6-125 µM for 48 h incubation; however, the IC_{50} value of CIS was significantly reduced at concentrations of 250 µM and 500 µM of PYC (1.11 fold and 1.57 fold for 250 µM and 500 µM, respectively, vs. the positive control) (p<0.05).

Effect of pycnogenol on DNA damage

The results of genotoxicity and antigenotoxicity of PYC at noncytotoxic doses (10 µM, 25 µM, 50 µM, and 100 µM) in HeLa cells using the comet assay were evaluated. DNA damage, expressed as DNA tail intensity in the HeLa cells, is shown in

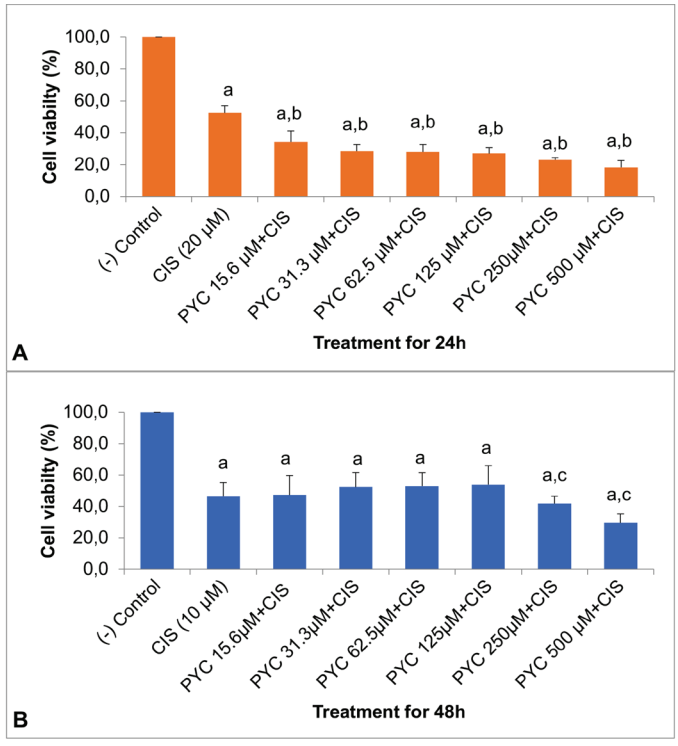

Figure 3. Effects of pycnogenol on the cisplatin cytotoxicity in HeLa cells for 24 h (A) and 48 h (B)

Values are given as mean ± standard deviation (n=4), a p<0.05, compared to negative control (Pharmaceutical Benefits Scheme), [b]p<0.05, compared to cisplatin (20 µM), [c]p<0.05, compared to cisplatin (10 µM), PYC: Pygnogenol, CIS: Cisplatin

Figure 4. We observed that PYC did not significantly increase DNA damage at all studied concentrations when compared to the negative control (p>0.05). In addition, PYC significantly decreased the DNA damage induced by H_2O_2 (50 µM) in a dose-dependent manner at all studied concentrations (10 µM=36.6%; 25 µM=36.7%; 50 µM= 40.1%; 75 µM=50.8%; 100 µM=58.6%) when compared to the positive control (p<0.05).

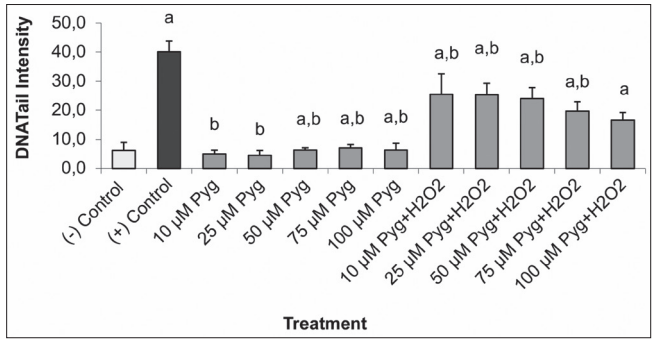

Figure 4. Effect of pycnogenol against oxidative DNA damage in HeLa cells. DNA damage was expressed as DNA tail intensity. Values are given as the mean ± standard deviation (n=4), [a]p<0.05, significantly different from negative control (1% Pharmaceutical Benefits Scheme), [b]p<0.05, significantly different from positive (50 µM H_2O_2) control, Pyg: Pygnogenol.

DISCUSSION

As is well known, CIS is clinically used in the therapy of many types of cancers (including esophageal, lung, breast, ovarian,

bladder, cervical, prostate, etc.), aiming to reduce tumor cell viability. However, it has important side effects, mainly nephrotoxicity.[7] Side effects and drug resistance are two of the major problems in antineoplastic therapy; hence recent studies have focused on new approaches, like combinational therapies with phenolic compounds, in order to prevent drug resistance, minimize side effects, and increase anticancer activity.[8-12] PYC, a phenolic compound, is commonly consumed as a dietary food supplement because of its strong antioxidant activity. It has potential therapeutic and protective effects against cancer, as shown in many studies.[5,6] However, there are not sufficient studies on the interactions between antineoplastic drugs and some natural phenolic compounds, including PYC. In the present study, after the determination of the cytotoxicities of PYC and CIS alone, the effects of PYC in combination with CIS were evaluated. The cytotoxicity of PYC and CIS increased approximately 1.22 fold and 1.82 fold, respectively, after 48 h incubation, when compared to 24 h incubation. The cytotoxicity profiles of PYC and CIS alone were different. It seems that the cytotoxicities of PYC and CIS are dose and time dependent. In our study, PYC (15.6-500 µM) significantly decreased the cytotoxicity of CIS in a dose-dependent manner with 24 h incubation. However, for 48 h incubation, PYC did not increase the cytotoxicity in the cells treated with CIS (10 µM, approximately) at the concentration range of 15.6-125 µM when compared to the negative control; however, the cell viability was reduced significantly at concentrations of 250 µM and 500 µM of PYC in the CIS-treated cells ($p<0.05$). According to our results, PYC seems to have the desired effect on the cytotoxic profile of CIS in HeLa cells for anticancer activity in a time- and dose-dependent manner. The possible mechanism underlying the cytotoxic effect of PYC has been associated with apoptosis.[16,17] In the study investigating the apoptotic effects of PYC, PYC induced apoptosis in human fibrosarcoma cells (HT1080), using flow cytometric analysis and RNA microarray.[16] In another study, it was reported that PYC significantly decreased cell viability and also induced caspase-independent apoptosis. Furthermore, PYC induced the translocation of apoptosis-inducing factor into the nucleus and regulated apoptosis.[17] In a study investigating the antitumor effect of PYC, the IC_{50} values of PYC in human leukemia cells (HL-60, U937, and K562) were reported to be 150 µg/mL (~516.8 µM), 40 µg/mL (~137.8 µM), and 100 µg/mL (~344.5 µM), respectively, for 24 h incubation, by propidium iodide exclusion.[18] In another study, in which the apoptotic effect of PYC in human oral squamous carcinoma (HSC-3) cells was investigated by the MTS assay, the IC_{50} value of PYC was reported as 20 µg/mL (~68.9 µM) for 24 h incubation.[19] However, the IC_{50} value of PYC was determined to be 285 µg/mL (~982 µM) for 24 h incubation in Chinese hamster ovary cells by Neutral Red Uptake test.[12] The genotoxicity and antigenotoxicity potential of PYC was evaluated with the commonly used alkaline comet assays at noncytotoxic doses in the HeLa cells. In the present study, we observed that PYC alone did not induce DNA damage at concentrations below 50 µM. However, it significantly reduced H_2O_2-induced DNA damage at all studied concentrations (10-100 µM). Our study using the comet assay showed that PYC might have a protective effect against H_2O_2-induced DNA damage in cells. The results were in good correlation with those of studies conducted previously. The antigenotoxic studies using the comet assay show that PYC may have a protective effect against oxidative DNA damage. For instance, Taner et al.[12] reported that PYC caused no genotoxic effects alone at low concentrations (5-50 µg/mL) as compared with the controls, and it might reduce H_2O_2-induced chromosome breakage and loss and DNA damage in cultured human lymphocytes in the comet assay. It seems that PYC may have potential for the treatment of diseases related to oxidative DNA damage. The IC_{50} value of CIS in the selected human cancer cells was reported to be 54.07 µM and 96.38 µM in cervical cancer cells (HeLa and Caco-2, respectively), 97.20 µM and 85.66 µM in pancreatic cancer cells (MIA PaCa-2 and BxPC-3, respectively), and 14.87 µM and 77.89 µM in hepatocellular carcinoma cells (Hep-G2 and SK-HEP-1, respectively), for 24 h incubation, using the MTT method.[20] Although there are some *in vivo* studies on the protective effect of PYC on CIS cytotoxicity, there are limited *in vitro* studies on the chemotherapeutic activity of PYC.[21-23] It has been reported that in CIS cytotoxicity CIS-induced prooxidant enzymes (myeloperoxidase, xanthine oxidase), malondialdehyde, and nitric oxide levels were corrected by PYC and chromosomal defects were reduced. These findings suggest that PYC may be a protective agent against CIS-induced oxidative, inflammatory, and genotoxic damage.[24] It has also been suggested that increased oxidative damage through radiotherapy can be prevented by strong antioxidant activity of PYC.[25] It was shown that grape seed extract (GSE), a polyphenolic compound like PYC, exerted synergistic anticancer effects with doxorubicin in human breast carcinoma (MCF-7 and MDA-MB468) cells.[26] In that study, GSE and doxorubicin alone and in combination strongly inhibited cell growth but there was no increase in apoptotic cell death caused by doxorubicin. These results suggest a strong possibility of synergistic anticancer effects of GSE and doxorubicin in combination for breast cancer treatment and also promising effects of combination of PYC and CIS for cancer. In recent studies, it has been aimed to decrease cytotoxicity and to increase anticancer activity using various phenolic compounds with antineoplastic drugs.[8-10,19] Many researchers have reported that CIS has positive effects in combination with antioxidants to increase its efficacy in cancer chemotherapy, reduce resistance development, and reduce toxicity. Nevertheless, more investigations are necessary to clarify the effects of phenolic compounds on cancer and the effects of combining with antineoplastic drugs in different doses.[11,24]

CONCLUSION

At the end of the study, it was considered that the use of PYC in the treatment of CIS revealed positive effects on HeLa cells. These findings suggest that PYC might contribute to the anticancer effect of CIS in cervical carcinoma. Therefore, combinatorial therapy may be therapeutically used in order to increase anticancer activity and minimize drug resistance

and side effects. It will be a new point of view in anticancer treatment, and further *in vitro* studies with other cancer cell lines as well as *in vivo* studies are suggested.

ACKNOWLEDGEMENTS

This study was supported by the Hacettepe University Research Fund (Grant Number: THD-2016-11838).

Conflicts of interest: No conflict of interest was declared by the authors. The authors alone are responsible for the content and writing of the paper.

REFERENCES

1. Russo GL. Ins and outs of dietary phytochemicals in cancer chemoprevention. Biochem Pharmacol. 2007;74:533-544.
2. Ramos AA, Lima CF, Wilson CP. DNA damage protection and induction of repair by dietary phytochemicals and cancer prevention: What do we know? Select Topics in DNA Repair. 2011;237-270.
3. Manach C, Williamson G, Morand C, Scalbert A, Remesy C. Bioavailability and bioefficacy of polyphenols in humans. I. Review of 97 bioavailability studies. Am J Clin Nutr. 2005;81(1 Suppl): 230-242.
4. Kyselova Z. Toxicological aspects of the use of phenolic compounds in disease prevention. Interdiscip Toxicol. 2011;4:173-183.
5. Packer L, Rimbach G, Virgili F. Antioxidant activity and biologic properties of a procyanidin-rich extract from pine (Pinus maritima) bark, pycnogenol. Free Radic Biol Med. 1999;27:704-724.
6. D'Andrea G. Pycnogenol: A blend of procyanidins with multifaceted therapeutic applications? Fitoterapia. 2010;81:724-736.
7. Rosenberg B. Fundamental studies with cisplatin. Cancer. 1985;55:2303-2316.
8. Adahoun MA, Al-Akhras MH, Jaafar MS, Bououdina M. Enhanced anti-cancer and antimicrobial activities of curcumin nanoparticles. Artif Cells Nanomed Biotechnol. 2017;45:98-107.
9. Perrone D, Ardito F, Giannatempo G, Dioguardi M, Troiano G, Russo L, DE Lillo A, Laino L, Lo Muzio L. Biological and therapeutic activities and anticancer properties of curcumin. Exp Ther Med. 2015;10:1615-1623.
10. Taner G, Aydın S, Bacanlı M, Sarigöl Z, Sahin T, Başaran AA, Başaran N. Modulating effects of pycnogenol(R) on oxidative stress and DNA damage induced by sepsis in rats. Phytother Res. 2014;28:1692-1700.
11. Florea AM, Busselberg D. Cisplatin as an anti-tumor drug: cellular mechanisms of activity, drug resistance and induced side effects. Cancers (Basel). 2011;3:1351-1371.
12. Taner G, Aydın S, Aytaç Z, Başaran AA, Başaran N. Assessment of the cytotoxic, genotoxic, and antigenotoxic potential of Pycnogenol® in *in vitro* mammalian cells. Food Chem Toxicol. 2013; 61:203-208.
13. Mosmann T. Rapid colorimetric assay for cellular growth and survival: Application to proliferation and cytotoxicity assays. J Immunol Methods. 1983;65:55-63.
14. Hansen MB, Nielsen SE, Berg K. Re-examination and further development of a precise and rapid dye method for measuring cell growth/cell kill. J Immunol Methods. 1989;119:203-210.
15. Singh NP, McCoy MT, Tice RR, Schneider EL. A simple technique for quantitation of low levels of DNA damage in individual cells. Exp Cell Res. 1988;175:184-191.
16. Harati K, Slodnik K, Chromik AM, Behr B, Goertz O, Hirsch T, Kapalschinski N, Klein-Hitpass L, Kolbenschlag J, Uhl W, Lehnhardt M, Daigeler A. Pro-apoptotic effects of pycnogenol on HT1080 human fibrosarcoma cells. Int J Oncol. 2015;46:1629-1636.
17. Yang IH, Shin JA, Cho SD. Pycnogenol Induces Nuclear Translocation of Apoptosis in MC-3 Human Mucoepidermoid Carcinoma Cell Line. J Cancer Prev. 2014;19:265-272.
18. Huang WW, Yang JS, Lin CF, Ho WJ, Lee MR. Pycnogenol induces differentiation and apoptosis in human promyeloid leukemia HL-60 cells. Leuk Res. 2005;29:685-692.
19. Yang IH, Shin JA, Kim LH, Kwon KH, Cho SD. The caspase 3-dependent apoptotic effect of pycnogenol in human oral squamous cell carcinoma HSC-3 cells. J Clin Biochem Nutr. 2016;58:40-47.
20. Nurcahyanti AD, Wink M. L-Canavanine potentiates the cytotoxicity of doxorubicin and cisplatin in arginine deprived human cancer cells. Peer J. 2016;4:e1542.
21. Lee IC, Ko JW, Park SH, Shin NR, Shin IS, Kim YB, Kim JC. Ameliorative effects of pine bark extract on cisplatin-induced acute kidney injury in rats. Ren Fail. 2017;39:363-371.
22. Eryilmaz A, Eliyatkin N, Demirci B, Basal Y, Kurt Omurlu I, Gunel C, Aktas S, Toka A, Basak S. Protective effect of Pycnogenol on cisplatin-induced ototoxicity in rats. Pharm Biol. 2016;54:2777-2781.
23. Ko JW, Lee IC, Park SH, Moon C, Kang SS, Kim SH, Kim JC. Protective effects of pine bark extract against cisplatin-induced hepatotoxicity and oxidative stress in rats. Lab Anim Res. 2014;30:174-180.
24. Aydin B, Unsal M, Sekeroglu ZA, Gülbahar Y. The antioxidant and antigenotoxic effects of pycnogenol(®) on rats treated with cisplatin. Biol Trace Elem Res. 2011;142:638-650.
25. de Moraes Ramos FM, Schönlau F, Novaes PD, Manzi FR, Bóscolo FN, de Almeida SM. Pycnogenol protects against Ionizing radiation as shown in the intestinal mucosa of rats exposed to X-rays. Phytother Res. 2006;20:676-679.
26. Sharma G, Tyagi AK, Singh RP, Chan DC, Agarwal R. Synergistic anti-cancer effects of grape seed extract and conventional cytotoxic agent doxorubicin against human breast carcinoma cells. Breast Cancer Res Treat. 2004;85:1-12.

Turk J Pharm Sci 2020;17(1):7-19
DOI: 10.4274/tjps.galenos.2018.04880

ORIGINAL ARTICLE

Formulation and Characterization of Solid Dispersions of Etoricoxib Using Natural Polymers

Doğal Polimerleri Kullanarak Etoricoxib Katı Dispersiyonunun Formülasyonu ve Karakterizasyonu

Sandip Babarao SAPKAL*, Vaibhav Suresh ADHAO, Raju Rambhau THENGE, Rahul Ashok DARAKHE, Sushilkumar Ananda SHINDE, Vinayak Natthuji SHRIKHANDE

Dr. Rajendra Gode College of Pharmacy, Department of Pharmaceutics, Malkapur, Dist. Buldana, Maharashtra, India

Objectives: The main objective of the present investigation to develop and evaluate solid dispersions of BCS Class II drugs etoricoxib employing various natural polymers, compatible with conventional manufacturing method to enhance solubility of poorly soluble drugs.

Materials and Methods: In this study, etoricoxib solid dispersion were prepared using xanthan gum, gaur gum and acacia and their combinations by solvent evaporation method. Solid dispersions and pure etoricoxib in the form of powder were characterized in comparison with pure drug and corresponding physical mixtures in the same ratios by Fourier transform infrared spectroscopy, differential scanning calorimetry (DSC), powder X-ray diffractogram, and *in vitro* drug release.

Results: Solid dispersion (ET11) prepared with 1: 2: 2: 2 drug carrier ratios were showed highest solubility in different solvents. Hence the solid dispersion (ET11) of 1: 2: 2: 2 ratios were selected for characterization. The DSC study indicated that the crystalline nature of etoricoxib was reduced to amorphous. The diffraction pattern of the solid dispersions in each figure indicates that diffraction peaks at 2ɵ values has less intensity than that of pure drugs. This indicated that the crystalline nature of drug sample was converted to amorphous with ET11. Scanning electron microscope photographs of solid dispersion seem to be more porous in nature. From the *in vitro* drug release profile, it can be seen that formulation ETM11 shows higher dissolution rate i.e. 98.2±1.3% compared with other formulations. It is predicted that, increasing concentration of carrier, increases the drug dissolution rate.

Conclusion: This study has shown that the solid dispersion of etoricoxib using natural carrier can be promising formulation for solubility and dissolution enhancement. Natural polymers used have shown promising results in the modification of drug release from the formulations.

Key words: Etoricoxib, solid dispersions, Xanthan gum, guar gum, gum acacia

ÖZ

Amaç: Bu araştırmanın temel amacı, zayıf çözünen ilaçların çözünürlüğünü arttırmak için geleneksel üretim yöntemiyle uyumlu, çeşitli doğal polimerler kullanarak BCS Sınıf II ilaçların katı dispersiyonlarını geliştirmek ve değerlendirmektir.

Gereç ve Yöntemler: Bu çalışmada, ksantan zamkı, gaur zamkı ve akasya ve bunların kombinasyonları kullanılarak çözücü buharlaştırma yöntemi ile etoricoxib katı dispersiyonu hazırlanmıştır. Katı dispersiyonlar ve toz halindeki saf etoricoxib, Fourier transform kızılötesi spektroskopisi, diferansiyel tarama kalorimetrisi (DSC), toz x-ışını difraktogramı ve *in vitro* etken madde salımı saf ilaç ve aynı oranlara karşılık gelen fiziksel karışımlarla karşılaştırmalı olarak karakterize edilmiştir.

Bulgular: 1: 2: 2: 2 ilaç taşıyıcı oranları ile hazırlanan katı dispersiyon (ET11), farklı çözücüler içinde en yüksek çözünürlüğü göstermiştir. Bu nedenle, karakterizasyon için 1: 2: 2: 2 oranlarındaki ET11 seçilmiştir. DSC çalışması, etoricoxib'in kristal yapısının amorf hale geçtiğini göstermiştir. Her bir şekildeki katı dispersiyonların kırınım modeli, 2ɵ değerlerindeki kırınım piklerinin saf etken maddeninkinden daha az gerilime sahip olduğunu göstermiştir. Bu, etken madde örneğinin kristal yapısının, ET11 ile amorf hale dönüştürüldüğünü göstermiştir. Katı dispersiyonun taramalı elektron mikroskobu fotoğrafları daha gözenekli yapıda görünmektedir. *İn vitro* etken madde salım profilinden, ETM11 formülasyonunun diğer formülasyonlara kıyasla %98,2±1,3 gibi daha yüksek çözünme oranı gösterdiği görülebilir. Artan taşıyıcı konsantrasyonunun etken maddenin çözünme hızını arttırdığı tahmin edilmektedir.

Sonuç: Bu çalışma, doğal taşıyıcı kullanılarak hazırlanan etoricoxibin katı dispersiyonunun çözünürlük ve çözünme artışı için umut verici bir formülasyon olabileceğini göstermiştir. Kullanılan doğal polimerler, formülasyonlardan etken madde salımının değiştirilmesinde ümit verici sonuçlar göstermiştir.

Anahtar kelimeler: Etorikoxib, katı dispersiyonlar, Xanthan zamkı, guar zamkı, acacia zamkı

*Correspondence: **E-mail:** sandipsapkal1985@gmail.com, **Phone:** 91+9975908070 **ORCID-ID:** orcid.org/0000-0001-5626-8469
Received: 31.07.2018, **Accepted:** 27.09.2018

INTRODUCTION

Poorly water-soluble drugs are expected to have dissolution-limited absorption. Increasing drug solubility may contribute substantially to improved drug absorption and consequently drug bioavailability. There are several pharmaceutical strategies available to improve the aqueous solubility of poorly soluble drugs: solid dispersion, solubilization using surfactants, the use of cosolvents, reduction of particle size, hydrotrophy, and the use of aqueous soluble derivative or salts.[1,2] Solid dispersion techniques have been used to enhance the dissolution and oral bioavailability of many poorly soluble drugs.[3] One aspect of solid dispersion technology on which most researchers in the field would agree is that the number of marketed products arising from this approach has been disappointing. Indeed,the sheer simplicity of the manufacturing method, the fact that in general only the drug andcarrier are required, and the frequently reported improvements in both the dissolution rate andbioavailability would lead one to expect that the transfer to the marketplace would be rapid andwidespread. Research for alternative carriers has been increasing to suit the industrial applications as well as to reduce the production cost and toxic effects. Recently, many natural polymers have been evaluated for their use in new applications. The dissolution rate of drugs from formulations containing viscous carriers is generally low due to the formation of a gel layer on the hydrated surfaces, which prevents drug release during dissolution. This can be overcome during tablet formulation by adding disintegrants. Pulverization of the product is also another important drawback with the high viscosity carriers;it can be overcome by using a decreasing order of polymer/drug ratio during formulation.[4,5] The poor aqueous solubility and wettability of etoricoxib, 5-chloro-6-methyl-3 [4-(methyl sulfonyl)phenyl]-2, 3-bypyridine, a highly selective second generation cyclooxygenage-2 inhibitor administered orally as an analgesic and nonsteroidal anti-inflammatory drug, cause difficulties in the formulation oforal dosage forms and lead to variable bioavailability.[6] It is used in the treatment of rheumatoid arthritis, osteoarthritis, postoperative dental pain, chronic back pain, and acute gout. Moreover, recent studies have evidenced its efficacy in patients with ankylosing spondylitis. However, its very low aqueous solubility and poor dissolution can cause formulation problems and limit its therapeutic application by delaying the rate of absorption and the onset of action.[7-10] Hence, enhancement of the solubility and/or dissolution rate of etoricoxib can be achieved by preparation of solid dispersions. Many authors have formulated solid dispersions of etoricoxib using a number of various polymers and methods. However, few attempts have been made to prepare solid dispersions of etoricoxib using natural polymers like xanthan gum, guar gum, and gum acacia as carriers to improve its aqueous solubility and dissolution. In the present study, a solvent evaporation technique was used to prepare solid dispersions with natural carriers, mainly xanthan gum, guar gum, and gum acacia and combinations of them. Solid dispersions and pure etoricoxib in the form of powder were characterized in comparison with pure drug and corresponding physical mixtures in the same ratios by Fourier transform infrared spectroscopy (FTIR), differential scanning calorimetry (DSC), X-ray powder diffractogram (XRPD), and *in vitro* drug release.

MATERIALS AND METHODS

Pure etoricoxib was a gift sample from Abbott Health Care Pvt Ltd, Mumbai, India. Xanthan gum, guar gum, and gum acacia were obtained from standard deviation (SD) Fine Chemicals, Mumbai. All other chemicals used were of analytical grade.

Ultraviolet-visible absorption spectroscopy[11]

A ultraviole (UV) spectrophotometer from Shimadzu, UV-1800, was used for all UV-visible spectroscopic studies. For the quantitative determination of the drug in various samples, the Beer-Lambertlaw was used. The first step was to create a standard calibration curve. To prepare a calibration curve the drug was dissolved in a suitable solvent. An aliquot was withdrawn from this and diluted. Various concentrations were made by serial dilution of this basic stock solution. The various solutions were measured, in triplicate, using UV-visible absorption spectroscopy to obtain absorption data. The data, which were the mean of the three readings obtained, were used to prepare a calibration curve. This curve was further used for the determination of the concentration of the drug in any formulation or during the dissolution studies.

Development of a calibration curve for etoricoxib

The stock solution of etoricoxib was accordingly diluted to obtain a concentration range of 0-10 µg/mL. The absorbance was observed against methanol as a blank and the calibration curve was plotted between concentration (x axis) and absorbance (y axis).

Partition coefficient determination of drug

Partition coefficient (oil/water) is a measure of a drug's lipophilicity and an indication of its ability to cross cell membranes. It is defined as the ratio of un-ionized drug distributed between the organic and aqueous phases at equilibrium.

$Po/w = (C_{oil}/C_{water})$ equilibrium

The partition coefficient is commonly determined using an oil phase of octanol or chloroform and water. Drugs having values of P much greater than 1 are classified as lipophilic, whereas partition coefficients much less than 1 are indicative of a hydrophilic drug. Before the partition coefficient was determined, the phases of the solvent system were mutually saturated by shaking at the temperature of the experiment by the shake flask method for Po/w, in which an accurately weighed sample of etoricoxib (10 mg each) was taken in a conical flask containing a presaturated mixture of known quantities of high purity analytical grade n-octanol and double distilled water in 1:1 v/v ratio (25 mL:25 mL), which were then shaken for 100 rotations in 5 min and allowed to stand long enough again to allow the phases to separate. Afterwards the aqueous phase was sampled by a procedure that minimizes the risk of including traces of n-octanol by syringe. The quantity

of substance present in the n-octanol phase was calculated by subtracting the quantity of substance in the aqueous phase from the quantity of the substance originally introduced. Finally, the partition coefficient was calculated using the equation. The same procedure was performed three times and the average Po/w was calculated.

Solubility determination and phase solubility study

The solubility of etoricoxib was determined by the equilibrium solubility method in which a saturated solution of the material was obtained by stirring an excess of drug in a constant quantity of solvent until saturation or equilibrium was achieved in a vortex mixer. Then it was filtered through Whatman filter paper (no.1) and concentration was analyzed by UV spectrophotometer at 284 nm. The solubility of etoricoxib was determined in distilled water and pH across the gastrointestinal tract, i.e. in pH 1.2, 4.5, and 6.8. Phase solubility studies of etoricoxib were carried out to evaluate the possible solubilizing effect of the carrier by adding an excess of drug to 10 mL of aqueous solutions containing increasing concentrations of gum acacia, guar gum, and xanthan gum (0%-2% w/v) and shaking at 25°C in a temperature controlled bath for 72 h. Drug concentrations were assessed spectrophotometrically.[12]

Preparation of solid dispersions and physical mixtures

Solid dispersions of etoricoxib were prepared using xanthan gum, guar gum, and gum acacia by the solvent evaporation method. A 1 g quantity of etoricoxib and natural carrier were dissolved separately in 100 mL of absolute ethanol. The solution was stirred for 1 h and the solvent was allowed to evaporate at room temperature. The solid dispersions obtained (ET1) were pulverized and sieved through 22 mesh and then stored in screw cap vials at room temperature pending further use. The same procedure was carried out for all the formulations presented in Table 1.

Physical mixtures of the etoricoxib and carriers having the same composition as the solid dispersions were prepared (ETM1) by simply triturating the drugs and the polymers in a porcelain mortar.[13] The mixtures were sieved and stored in screw cap vials at room temperature pending further use. The same procedure was carried out for all the formulations presented in Table 2.

Table 1. Composition of etoricoxib solid dispersions

Formulation	Formulation code	Etoricoxib:xanthan gum:guar gum:gum acacia ratios
Solid dispersion	ET1	1:1:0:0
	ET2	1:2:0:0
	ET3	1:0:1:0
	ET4	1:0:2:0
	ET5	1:0:0:1
	ET6	1:0:0:2
	ET7	1:1:1:1
	ET8	1:2:1:1
	ET9	1:1:2:1
	ET10	1:1:1:2
	ET11	1:2:2:2

Determination of solubility of various solid dispersions

Etoricoxib loaded solid dispersions, physical mixtures, and pure etoricoxib equivalent to 30 mg were weighed and transferred to four flasks containing 50 mL of distilled water, pH 1.2 acetate buffer, phosphate buffer pH 6.8, and phosphate buffer pH 7.4. The sample was agitated at 80 rpm in a thermostated shaking water bath at 37±0.5°C for 8 h. The supernatant solution was then filtered through Whatman filter paper. The filtrate was diluted and the absorbance was measured using a UV-Vis spectrophotometer.[12]

Determination of percent yield

The percent yield of etoricoxib solid dispersions was determined according to the method described using the following expression:

$$\% \text{ yield} = \frac{\text{weight of prepared SD}}{\text{Wt. of drug + carrier}} \times 100 \quad \text{Eq. 1}$$

Estimation of drug content of solid dispersions and physical mixtures

Solid dispersions equivalent to 60 mg of etoricoxib were weighed accurately and dissolved in a suitable quantity of methanol. The solutions were filtered through a membrane filter (0.45 mm). The drug content was determined at 284 nm by UV spectrophotometer after suitable dilution.[14]

Dissolution studies

The dissolution studies were performed using a US Pharmacopeia 24 type II dissolution test apparatus. Samples equivalent to 60 mg of etoricoxib were placed in a dissolution vessel containing 900 mL of phosphate buffer (pH 6.8) maintained at 37°C and stirred at 100 rpm. Samples were collected periodically and replaced with a fresh dissolution medium. After filtration

Table 2. Composition of etoricoxib physical mixture

Formulation	Formulation code	Etoricoxib:xanthan gum:guar gum:gum acacia ratios
Physical mixture	ETM1	1:1:0:0
	ETM2	1:2:0:0
	ETM3	1:0:1:0
	ETM4	1:0:2:0
	ETM5	1:0:0:1
	ETM6	1:0:0:2
	ETM7	1:1:1:1
	ETM8	1:2:1:1
	ETM9	1:1:2:1
	ETM10	1:1:1:2
	ETM11	1:2:2:2

through Whatman filter paper no. 41, the concentration of etoricoxib was determined spectrophotometrically at 284 nm. Dissolution studies were performed in triplicate (n=3) and the calculated mean values of cumulative drug release were used while plotting the release curves.

Fourier transform infrared studies

Compatibility studies of the drug (etoricoxib) with xanthan gum, guar gum, and gum acacia were carried out using FTIR spectroscopy. Sample from the drug alone, carrier alone, and physical mixture of drug and polymer was examinedby ATR sampling technique and the spectrum was scanned over the frequency range between 4000 and 600 cm^{-1} and at 4 cm resolution. The appearance, disappearance, or broadening of absorption band(s) on the spectra of the solid dispersions and the polymeric carriers in comparison with the spectrum of the drug were used to determine possible interactions between pure drug and polymers.

Differential scanning calorimetry

A Mettler Toledo DSC STAR^e systemwas used for all the DSC studies performed on the drug, polymer, physical mixtures, and solid dispersions. The DSC uses STAR^e software V8.10 for its operation. Samples ranging from 8 to 15 mg were used and the results were normalized using the software so that the results could be compared. The samples were placed in a 100 µL pan. The pans were covered with a lid and the lid was crimped into place. A pinhole was made in the lid to vent out any gas that might result while heating. The pan was then placed inside the furnace using an empty pan as a blank. The DSC was calibrated using indium (5-10 mg) with a melting onset temperature at 156±0.2°C and zinc with a melting onset temperature of 419.6±0.7°C as the standards. The two processes show a heat flow of 28.45±0.6 J/g and 107.5±3.2 J/g for indium and zinc, respectively.

Powder X-ray diffraction

Powder X-ray diffraction studies were performed to check for any crystallinity in the formulation after it was made and after the stability studies were performed. Avoiding recrystallization of the drug in the formulation was one of the goals of the present study. PAN analytical X-Pert Pro V1.6 with X Pert Data Collector V2.1 software was used equipped with a CuKa2 anode tube and diffractometer of radius 240 mm. The X-ray powder diffraction scan was performed using a BB004 flat stage. The powdered sample was placed in an aluminum sample holder that had a 2.5 cm square with a depth of 0.5 mm. The data were collected by scanning the sample at 45 kV and 40 mA. Samples were scanned from 5 to 50°C 2θ at a step size of 0.0170 and scan rate of 1.0°C/min.

Scanning electron microscopy

The surface morphology of the raw materials and the formulated product were studied using a scanning electron microscope equipped with a JEOL JSM 7500. Snappy 4 software was used to obtain the digital picture. Samples were placed on brass stubs using double-sided adhesive tape. The samples were coated with a layer of gold using a gold sputter technique to improve the conductivity of the surface of the sample to obtain good images. A Denton Vacuum Desk II was used for the gold sputter technique. Pictures were taken at magnifications whereby they could be compared with each other, showing best the surface features of the various materials.

RESULTS AND DISCUSSION

Preformulation studies of etoricoxib

The standard drug absorbance in methanol at 0 to 10 µg/mL concentration at 284 nm is reported in Table 3. The standard curve obeyed the Beer-Lambert law in the range of 0 to 10 µg/mL. Data in this range were subjected to linear regression analysis. The graphical presentation of the linear curve of etoricoxib in methanol is shown in Figure 1 and was linear.

Correlation coefficient (R^2)=0.999

Equation of regressed line: Y=0.0071x+0.023, where

X=value of concentration,

Y=Regressed value of absorbance.

In the preformulation study of the drug, the λ-maxof etoricoxib was found at 284 nm. Similarly the partition coefficient of etoricoxib was found to be 3.9 by the shake flask method, which indicates that it is lipophilic. Thus it can pass the cell membrane easily once solubilized.

Saturation solubility and phase solubility

The solubility data of etoricoxib in distilled water, acetate buffer pH 1.2, phosphate buffer pH 6.8, and phosphate buffer pH 7.4 at 25°C are given in Table 4. The comparison of etoricoxib in different solvents is presented graphically in Figure 2. The

Table 3. Standard absorbance of etoricoxib in methanol

Conc. of drug (µg/mL)	Absorbance at 284 nm
0	0
2	0.18
4	0.321
6	0.494
8	0.655
10	0.793

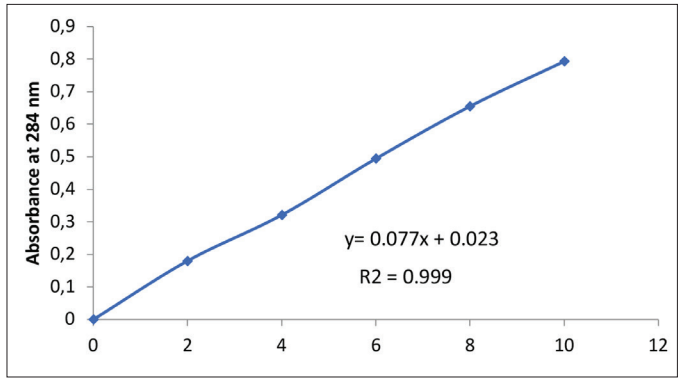

Figure 1. Standard calibration curve of etoricoxib

phase solubility curve of etoricoxib in the presence of natural carriers, i.e.xanthan gum, guar gum, and gum acacia, is shown in Figure 3. A systematic increase in the solubility of drug was observed with an increasing concentration of natural polymers in water. The increased solubility may be due to improved dissolution of drug in water by natural polymers. This might be due to the solubilization effect of carrier, which increased the wetting property of the drug. The data obtained from the phase solubility study are given in Table 5.

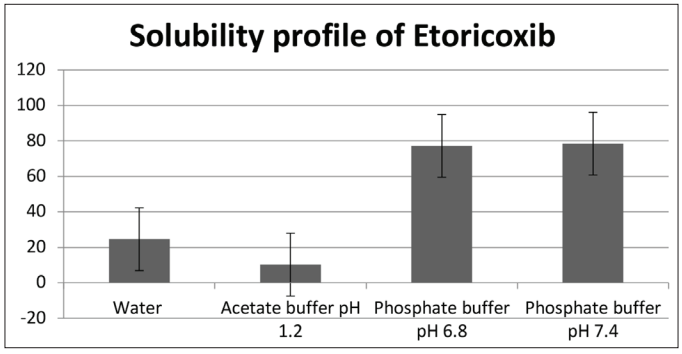

Figure 2. Solubility profile of etoricoxib

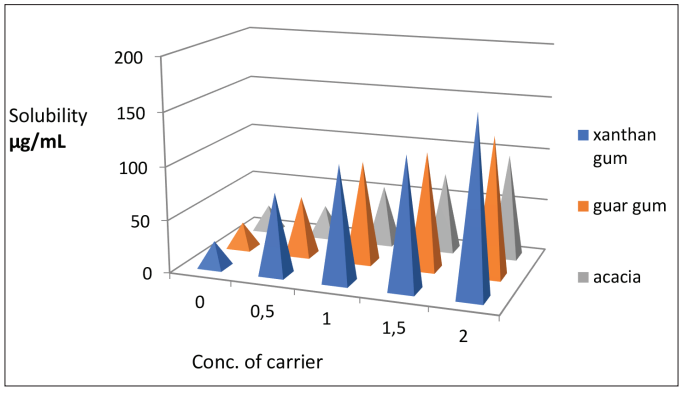

Figure 3. Phase solubility of etoricoxib with carrier

Table 4. Solubility data of etoricoxib in different solvents

Solubility solvents	Concentration (µg/mL)
Water	24.49
Acetate buffer pH 1.2	10.25
Phosphate buffer pH 6.8	77.16
Phosphate buffer pH 7.4	78.48

Table 5. Phase solubility data for etoricoxib in carriers

Conc.	Xanthan gum	Guar gum	Gum acacia
	µg/mL		
0.25%	77.16	56.25	30.16
0.50%	109.13	96.23	56.12
1%	123.23	110.51	74.58
2%	165.08	130.81	98.16
Pure drug	24.49 µg/mL		

Solubility study of solid dispersions and physical mixtures

The solubility data of pure etoricoxibare shown in Table 4 and they indicated that 24.49 µg/mL pure etoricoxib was soluble in distilled water; hence it is considered a poorly water soluble drug. The solubility data of the physical mixtures containing etoricoxib and xanthan gum, guar gum, and gum acaciaare shown in Table 6. The solubility profile of the physical mixtures of etoricoxib is shown in Figure 4. The solubility of etoricoxib in the solid dispersions prepared by solvent evaporation in different solvents was also studied and the data for the same are given in Table 7. As compared to pure drug and the physical mixtures, the solid dispersions prepared by solvent evaporation showed higher solubility in distilled water, pH 1.2 acetate buffers, phosphate buffer pH 6.8, and phosphate buffer pH 7.4 (Figure 5). The present investigation suggested thatthis might be possible due to the preparation of solid dispersions using varying concentrations of natural carriers, which formed a eutectic mixture and increased the wettability of etoricoxib and hence its solubility.

Percentage yield of solid dispersions

Etoricoxib solid dispersion with xanthan gum had a yield of 90.5% and 91.8% for the etoricoxib:xanthan gum combination

Table 6. Solubility of physical mixture of etoricoxib and xanthan gum, guar gum, and gum acacia

Formulation code	Distilled water (µg/mL)	pH 1.2 (µg/mL)	pH 6.8 (µg/mL)	pH 7.4 (µg/mL)
ETM1	25±0.66	56±0.97	84±0.66	88±0.83
ETM2	28±0.16	64±0.24	104±0.28	125±0.45
ETM3	37±0.41	42±0.66	90±0.68	165±0.74
ETM4	33±0.66	59±0.88	130±0.10	146±0.23
ETM5	42±0.61	70±0.56	82±0.96	196±0.84
ETM6	55±0.32	96±0.45	148±0.78	220±0.26
ETM7	98±0.84	162±0.51	182±0.24	250±0.92
ETM8	96±0.14	145±0.42	164±0.28	210±0.12
ETM9	70±0.16	110±0.66	183±0.44	232±0.26
ETM10	90±0.44	150±0.60	185±0.28	190±0.20
ETM11	112±0.62	186±0.36	206±0.55	284±0.86

Mean ± standard deviation (n=3)

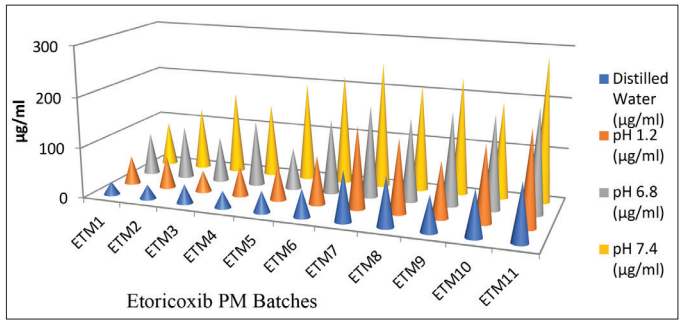

Figure 4. Solubility profile of etoricoxib physical mixture

ratios of 1:1 and 1:2 (ET1 and ET2), respectively. The yield recorded for etoricoxib:guar gum solid dispersions at ratios of 1:1 and 1:2 was 94.2% and 96.4% (ET3 and ET4), respectively. Solid dispersion of etoricoxib with gumacacia at a ratio of 1:1 and 1:2 had yields of 93.0% and 98.12% (ET5 and ET6), respectively. Solid dispersion of etoricoxib with xanthan gum, guar gum, and gum acacia at a ratio of 1:1:1:1 had a yield of 97.10% (ET7). Solid dispersion of etoricoxib with xanthan gum, guar gum, and gumacacia at a ratio of 1:2:1:1 had a yield of 98.2% (ET8). Solid dispersion of etoricoxib with xanthan gum, guar gum, and gum acacia at a ratio of 1:1:2:1 had a yield of 96.0% (ET9). Solid dispersion of etoricoxib with xanthan gum, guar gum, and gum acacia at a ratio of 1:1:1:2 had a yield of 94.0% (ET10). Solid dispersion of etoricoxib with xanthan gum, guar gum, and gum acacia at a ratio of 1:2:2:2 had a yield of 93.0% (ET11) (Table 8) (Figure 6).

Drug content of solid dispersions and physical mixtures

A fundamental quality attribute for all pharmaceutical preparations is the requirement for a constant dose of drug between dispersions. In each of the mentioned formulae, no single preparation found outside thelimit. All the formulations and physical mixture contained active ingredients within the general limit of 90%-110%. Etoricoxib content (%) with xanthan gum, guar gum, and gum acacia in physical mixture and solid dispersion with different drug:carrier ratios is shown in Table 9 and Table 10, respectively. The entire percent drug shown in the tables was found within the general specification. It is proved that the formulation prepared can be continue for further evaluation.

Table 7. Solubility of solid dispersion of etoricoxib and xanthan gum, guar gum, and gum acacia

Formulation code	Distilled water (µg/mL)	pH 1.2 (µg/mL)	pH 6.8 (µg/mL)	pH 7.4 (µg/mL)
ET1	50±0.86	86±0.17	104±0.66	88±0.83
ET2	89±0.66	114±0.34	120±0.28	125±0.45
ET3	70±0.48	92±0.76	132±0.68	95±0.74
ET4	120±0.16	129±0.87	160±0.10	136±0.23
ET5	60±0.68	110±0.36	112±0.96	96±0.84
ET6	96±0.22	156±0.55	188±0.78	120±0.26
ET7	160±0.44	212±0.61	252±0.24	250±0.92
ET8	96±0.14	155±0.42	264±0.28	210±0.12
ET9	170±0.17	210±0.76	233±0.44	242±0.26
ET10	99±0.74	240±0.80	285±0.28	260±0.20
ET11	192±0.92	286±0.26	306±0.55	364±0.86

Mean ± Standard deviation (n=3)

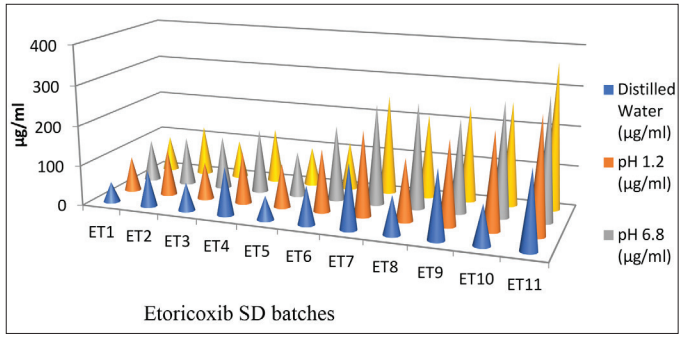

Figure 5. Solubility profile of etoricoxib solid dispersion

In vitro dissolution study of solid dispersions and physical mixtures of etoricoxib using natural carrier

Dissolution studies were performed to compare the drug release from the physical mixtures and solid dispersions to that of the pure drug etoricoxib. The dissolution test was carried out for a period of 90 min in pH 6.8 phosphate buffer. The drug release data obtained for formulations ETM1-ETM11 are tabulated in Table 11. They show the cumulative percent drug released as a function of time for all formulations. The cumulative percent drug released after 90 min is shown in the table. *In vitro* studies reveal that there is a marked increase in the dissolution rate of

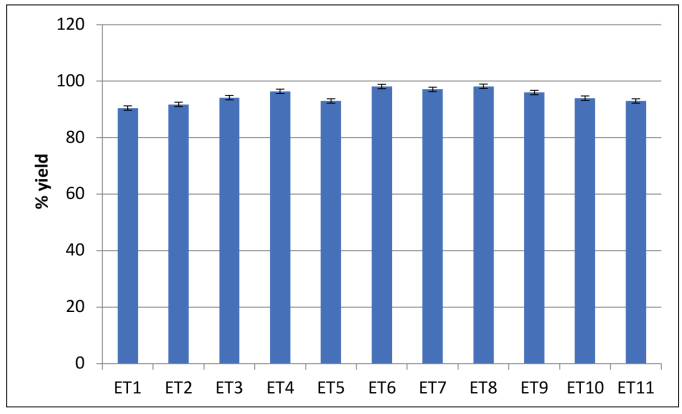

Figure 6. Effect of composition of polymers on yield of etoricoxib solid dispersion

Table 8. Percent yield of etoricoxib solid dispersion

Formulation code	Ratios of etoricoxib:xanthan gum:guar gum:gum acacia	% yield
ET1	1:1:0:0	90.5
ET2	1:2:0:0	91.8
ET3	1:0:1:0	94.2
ET4	1:0:2:0	96.4
ET5	1:0:0:1	93
ET6	1:0:0:2	98.12
ET7	1:1:1:1	97.1
ET8	1:2:1:1	98.2
ET9	1:1:2:1	96
ET10	1:1:1:2	94
ET11	1:2:2:2	93

Mean ± Standard deviation (n=3)

etoricoxib from all the physical mixtures when compared to pure etoricoxib itself. From the *in vitro* drug release profile, it can be seen that formulation ETM11 containing etoricoxib, xanthan gum, guar gum, and gum acacia (1:2:2:2) shows a higher dissolution rate, i.e. 98.2±1.3%, compared with the other formulations. It is predicted thatan increasing concentration of carrier will increase the drug dissolution rate. The dissolution profile of the physical mixture of etoricoxib, xanthan gum, guar gum, and gum acacia over the period of 1.5 h is shown in Figure 7.

The percentage of drug released from the solid dispersions of etoricoxib using natural carrier is shown in Table 12. As compared to the physical mixtures of etoricoxib with natural carrier, the solid dispersions showed a higher dissolution rate for etoricoxib. Over the period of 90 min, a maximum of 98% drug was released.The percent drug released increased with increasing concentration of carrier. The increase in dissolution of etoricoxib from the solid dispersions might be attributed to factors such as a reduction in the particle size of the drug in

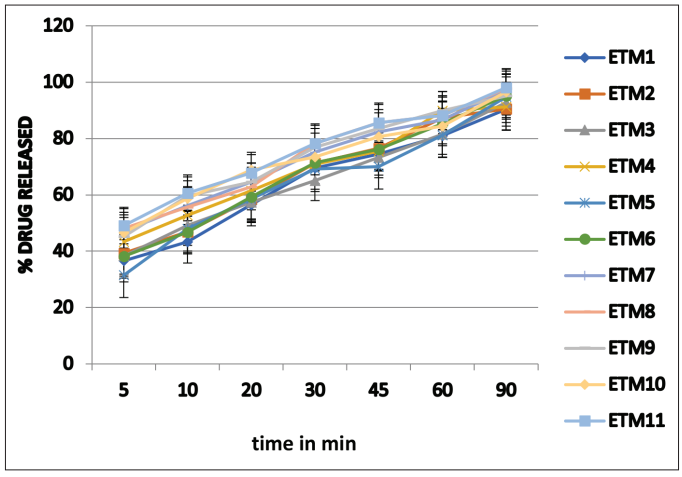

Figure 7. Drug release pattern of physical mixtures of etoricoxib using natural carrier

Table 9. Drug content of etoricoxib solid dispersion

Formulation code	Ratios of etoricoxib:xanthan gum:guargum:gum acacia	Drug amount (%)
ET1	1:1:0:0	97.99
ET2	1:2:0:0	98.18
ET3	1:0:1:0	98.14
ET4	1:0:2:0	98.56
ET5	1:0:0:1	98.45
ET6	1:0:0:2	98.90
ET7	1:1:1:1	99.12
ET8	1:2:1:1	99.68
ET9	1:1:2:1	99.78
ET10	1:1:1:2	99.45
ET11	1:2:2:2	99.89

Mean ± Standard deviation (n=3)

the matrix, increase in the surface area, reduced crystallinity, and an increase in the solubility of the drug in the presence of the lipid carriers. The drug release is shown in Figure 8. The literature reveals that the solvent evaporation method of solid dispersion solubilizes the drug and carrier at molecular level,hence forming a eutectic mixture and increasing the solubility of poorly water soluble drugs.

FTIR spectral studies

The infrared spectrum of etoricoxib is shown in Figure 9. The characteristic peaks of functional groups present in the drugs were checked and are given in Table 13. The functional groups present in the structure of etoricoxib were identified correctly and hence the drug was confirmed and considered for further uses.

The IR spectra of pure etoricoxib showed characteristic peaks at 1596.9 cm^{-1} (C=N stretching vibration); 1431 cm^{-1}, 1300 cm^{-1}, 1141.8 cm^{-1}, and 1085.8 cm^{-1} (S=O stretching vibrations); and

Table 10. Drug content of etoricoxib physical mixture

Formulation code	Ratios of etoricoxib:xanthan gum:guar gum:gum acacia	Drug amount (%)
ETM1	1:1:0:0	98.01
ETM2	1:2:0:0	98.74
ETM3	1:0:1:0	98.57
ETM4	1:0:2:0	98.88
ETM5	1:0:0:1	98.71
ETM6	1:0:0:2	99.10
ETM7	1:1:1:1	99.12
ETM8	1:2:1:1	99.23
ETM9	1:1:2:1	99.14
ETM10	1:1:1:2	99.38
ETM11	1:2:2:2	99.78

Mean ± Standard deviation (n=3)

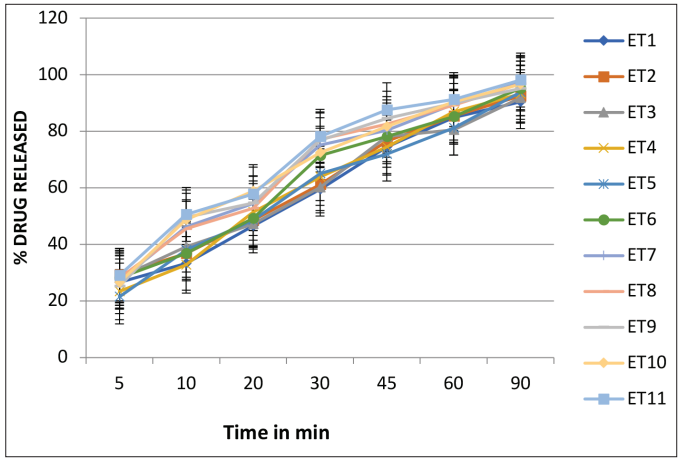

Figure 8. Drug release pattern of solid dispersions of etoricoxib using natural carrier

840.9 cm^{-1}, 775.3 cm^{-1}, and 638 cm^{-1} (C-Cl stretching vibrations), respectively (Figure 9). Figures 10, 11, and 12 show theinfrared spectrum of xanthan gum, guar gum, and gum acacia, respectively. From the spectrum it was observed that chemical groups C=N stretching vibration, S=O stretching vibrations, and C-Cl stretching vibrationshad the same wave number as etoricoxib did (Figure 13).

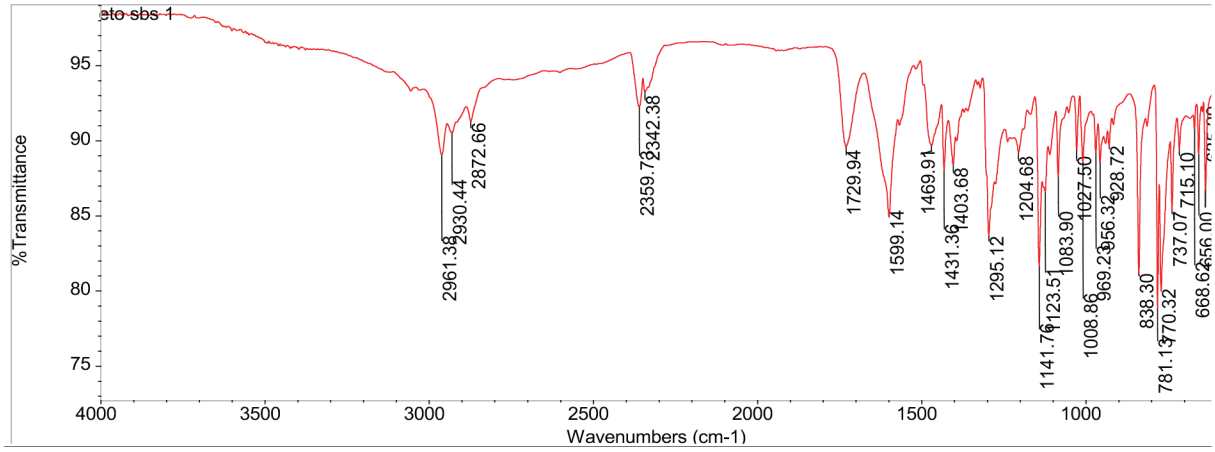

Figure 9. Infrared spectrum of etoricoxib

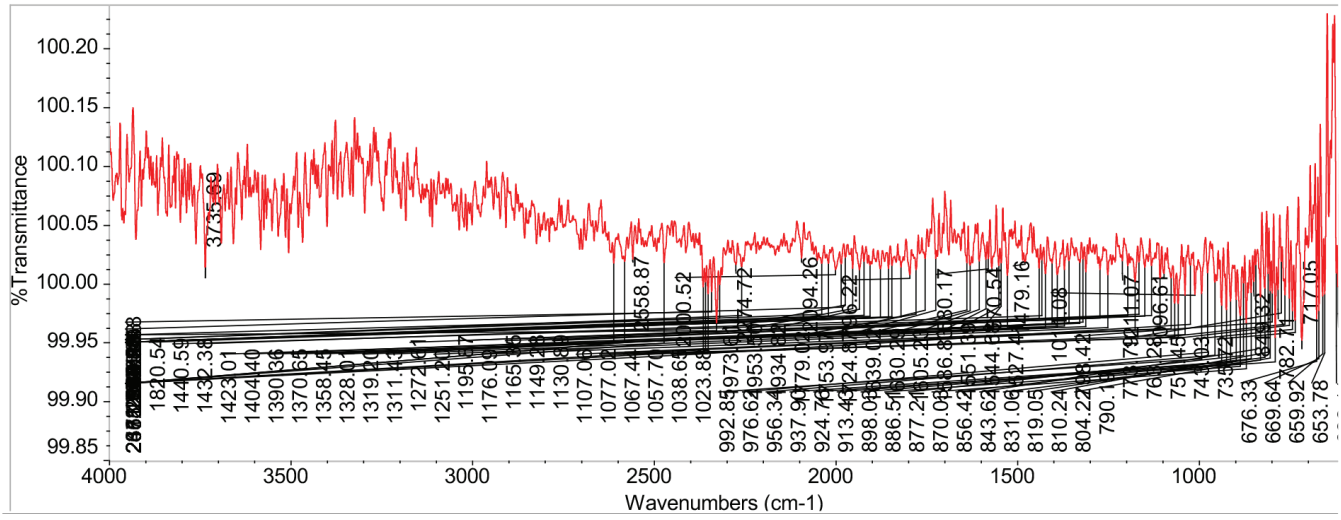

Figure 10. Infrared spectrum of xanthan gum

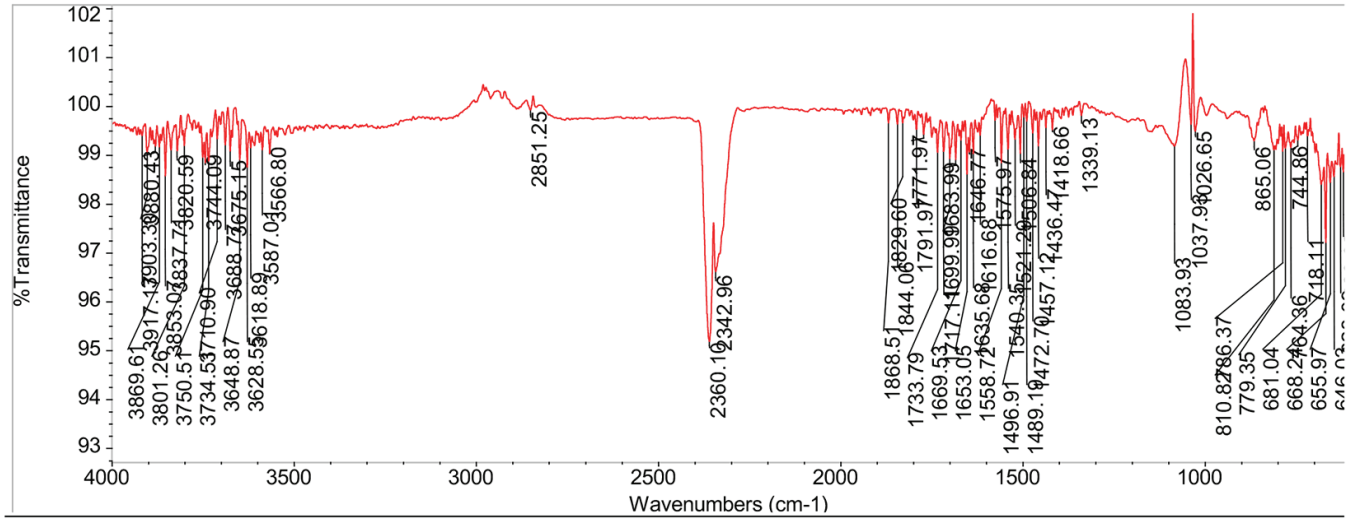

Figure 11. Infrared spectrum of guar gum

DSC studies

The DSC thermogram of etoricoxib, xanthan gum, guar gum, and gum acacia and its solid dispersion ET11 (1:2:2:2) is shown in Figure 14. The DSC thermogram of pure etoricoxib shows a single sharp endothermic peak at 140.05°C, indicating that the drug is highly crystalline. The DSC thermogram of the solid dispersion of etoricoxib showed a shallow endothermic peak at 74.88°C, indicating glass transition temperature, a recrystallization peak at 112°C, and a melting peak at 132°C. This confirmed the transformation of crystalline etoricoxib into

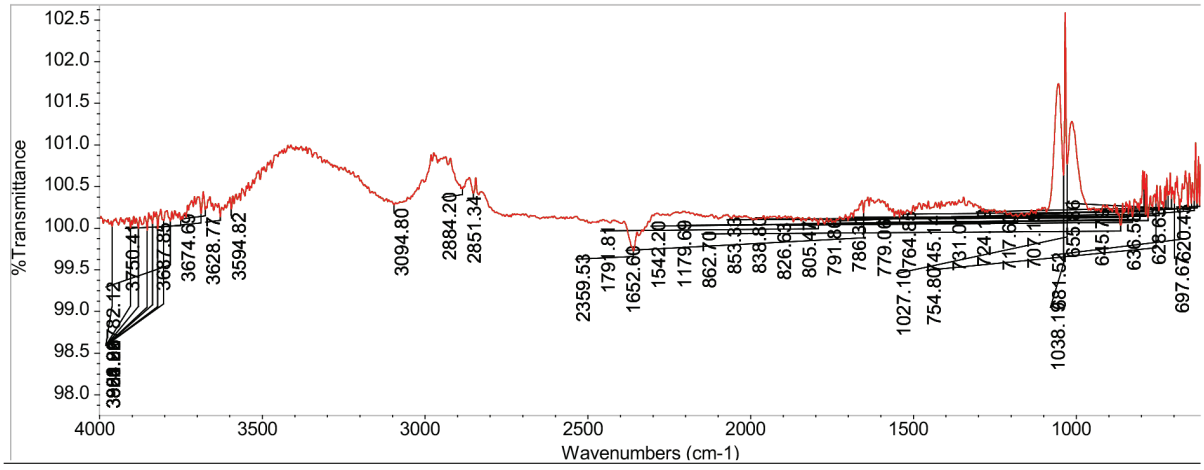

Figure 12. Infrared spectrum of gum acacia

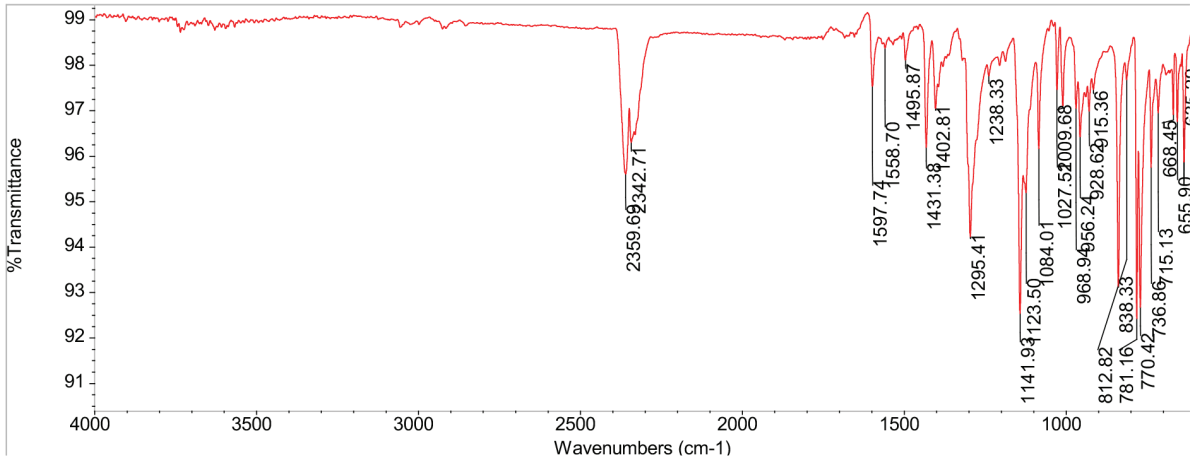

Figure 13. Infrared spectrum of etoricoxib and carrier mixture

Table 11. Drug release profile of physical mixtures of etoricoxib using natural carrier

Time in min	% drug release										
	ETM1	ETM2	ETM3	ETM4	ETM5	ETM6	ETM7	ETM8	ETM9	ETM10	ETM11
0	0	0	0	0	0	0	0	0	0	0	0
5	36.6±2	39.3±2	38.3±3	43.4±2	31.5±1	38.2±2	47.1±2	48.1±1	45.2±3	46.6±2	49.1±1
10	43.3±2	46.9±1	49.2±1	52.8±2	48.0±2	46.8±3	56.2±2	55.6±2	59.6±1	58.7±3	60.6±2
20	56.5±3	58.5±2	57.3±2	61.5±1	58.5±3	59.2±2	64.5±2	62.8±2	64.6±2	68.8±2	67.8±2
30	69.5±3	71.2±2	65.1±2	70.8±1	69.1±2	71.4±2	75.2±2	78.2±2	76.8±1	73.4±1	78.2±2
45	74.5±1	76.5±2	73.2±1	75.5±1	70.0±2	76.2±2	82.4±3	85.6±3	83.5±2	80.7±3	85.6±3
60	80.9±3	87.3±2	81.5±3	89.9±1	81.2±4	85.2±2	86.6±1	88.2±2	89.9±2	84.4±2	88.2±2
90	90.4±1	90.5±2	92.8±3	91.2±1	94.8±3	95.2±2	97.2±2	97.8±2	95.1±3	96.6±1	98.1±3

Mean ± Standard deviation (n=3)

amorphous etoricoxib and hence improved dissolution. The physical mixture of etoricoxib and xanthan gum, guar gum, and gum acacia did not show such change in Figure 15.

XRPD studies

The XRPD pattern of etoricoxib, xanthan gum, guar gum, and gum acacia and solid dispersion ET11 is shown in Figure 16. The XRPD patterns of pure etoricoxib showed numerous distinctive peaks in the region of 10 to 50° (2ɵ), i.e. 17°, 18.2°, 24.2°, and 29.2°, indicating the crystalline nature of etoricoxib. The XRPD study of etoricoxib solid dispersion (ET11) indicated a halo pattern. It showed broad and diffuse maxima attributable to the relatively random arrangement of the constituent molecules, which produced poorly coherent scatters. These patterns were quite distinct from those produced by the crystalline etoricoxib.

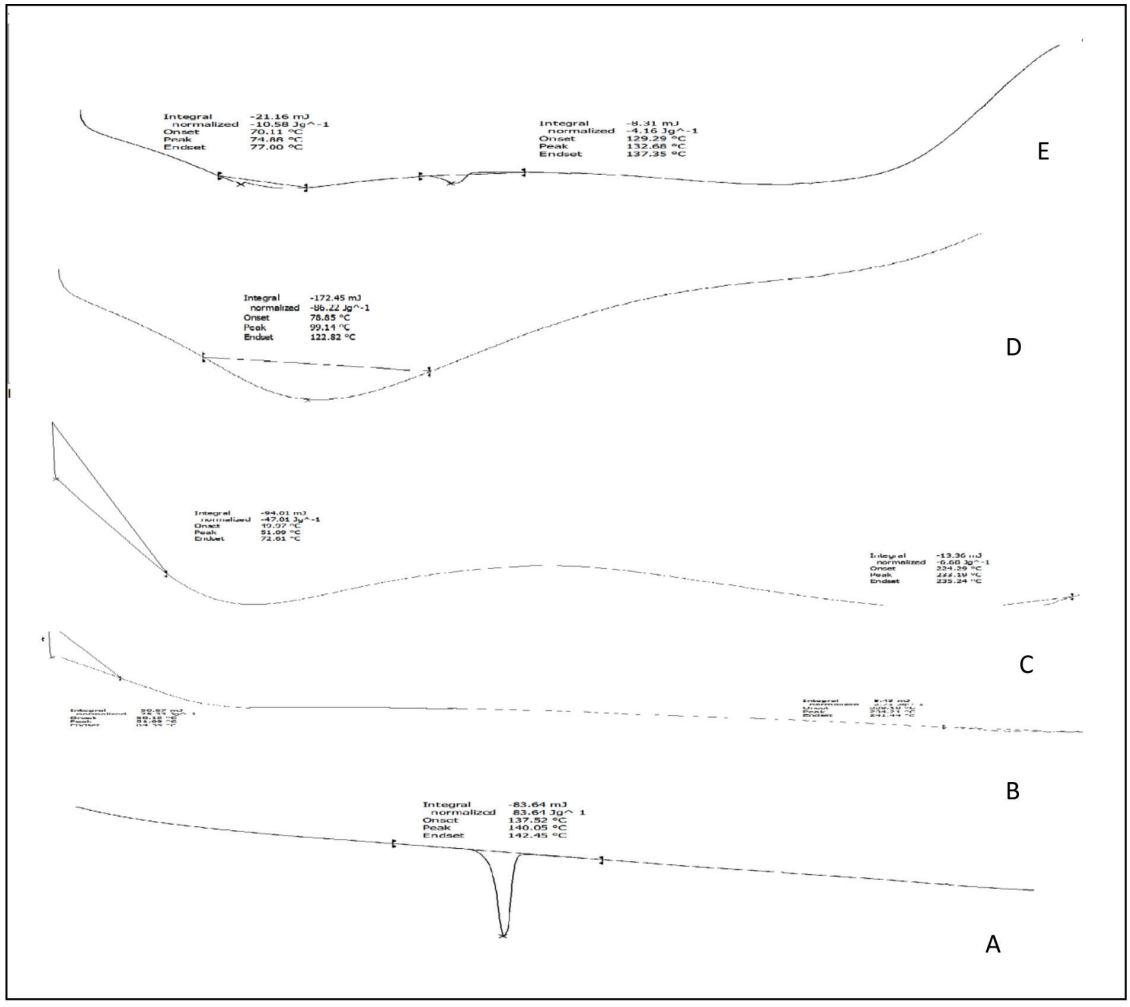

Figure 14. Differential scanning calorimetry thermogram of A) etoricoxib, B) gum acacia, C) guar gum, D) xanthan gum, and E) etoricoxib and xanthan gum, guar gum, and gum acacia solid dispersion

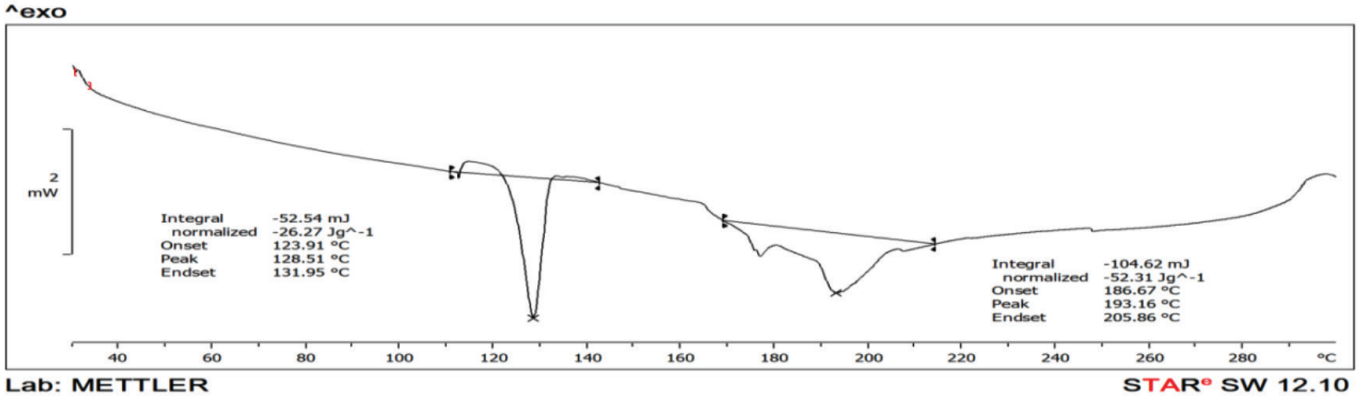

Figure 15. Differential scanning calorimetry thermogram ofetoricoxib and xanthan gum, guar gum, and gum acacia physical mixture

This confirmed the transformation of crystalline etoricoxib into amorphous etoricoxib and was also supported by DSC results. The enhancement in the dissolution rate of the drug from the solid dispersion is ascribed to the marked reduction in the crystallinity of the drug.

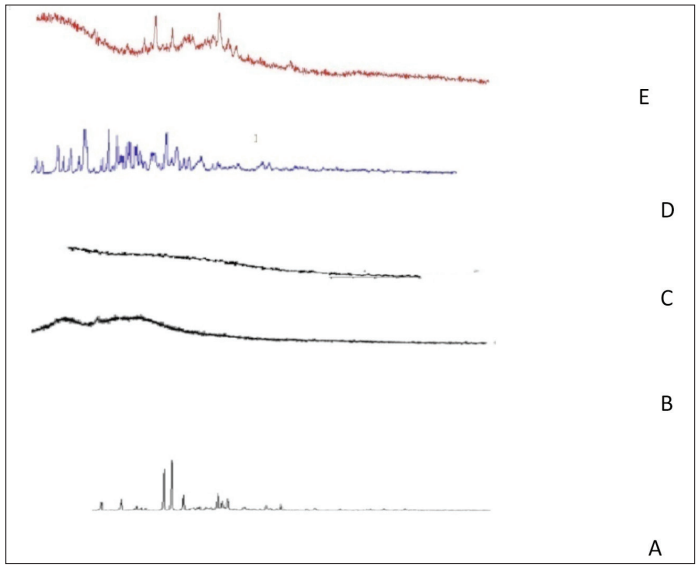

Figure 16. X-ray powder diffractionof A) etoricoxib, B) gum acacia, C) guar gum, D) xanthan gum, and E) etoricoxib and xanthan gum, guar gum, and gum acacia solid dispersion

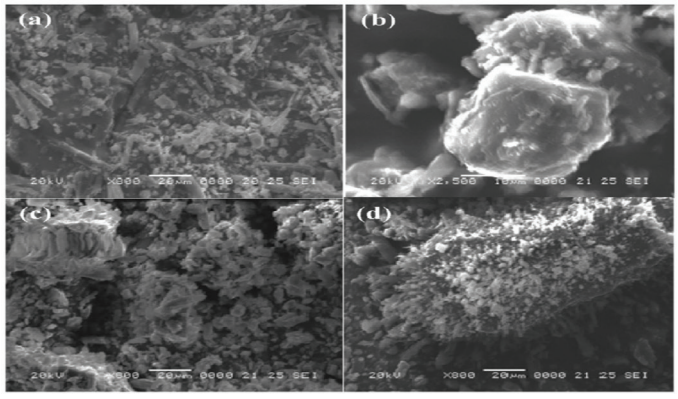

Figure 17. Scanning electron microscopy of A) etoricoxib, B) gum acacia, C) gaur gum and, D) xanthan gum

Scanning electron microscopy studies

Scanning electron microscopy (SEM) photographs for pure drug and optimized formulation ET11 are shown in Figures 17 and 18, respectively. It was found that the presence of polymer in the solid dispersion influenced the particle size of the resultant agglomerates. The size of the particles increased with an increase in deposition of polymer on the surface of the drug. The surface morphology studies revealed that the solid dispersion was closely compacted into small spherical form.

CONCLUSION

In the present study it was clearly demonstrated that etoricoxib solid dispersion formulation can be effectively produced by processing via solvent evaporation with enhanced solubility and dissolution rates. Natural polymer combinations were optimized and stable solid dispersion systems were developed successfully. Utilization of xanthan gum, guar gum, and gum acacia offers excellent possibilities to develop stable amorphous solid dispersions. Furthermore, this etoricoxib incorporated solid dispersion gave higher dissolution and solubility values compared to the pure etoricoxib drug. *In vitro* drug release studies of optimized formulation ET11 exhibited a cumulative release of 98.1±3% after 90 min. The FTIR spectrum revealed that no chemical interaction occurred between the

Table 13. Characteristic peaks of etoricoxib

Peak (cm^{-1})	Intensity (%T)	Chemical groups
1596.9	89.614	C=N stretching vibration
1431	83.682	S=O stretching vibrations
1300	83.682	
1141.8	81.631	
840.9	81.097	C-Cl stretching vibrations
775.3	78.861	
638	86.694	

Table 12. Drug release profile of solid dispersions of etoricoxib using natural carrier

Time in min	% drug release										
	ET1	ET2	ET3	ET4	ET5	ET6	ET7	ET8	ET9	ET10	ET11
0	0	0	0	0	0	0	0	0	0	0	0
5	26.6±2	29.3±2	28.3±3	23.4±2	21.5±1	28.2±2	27.1±2	28.1±1	25.2±3	26.6±2	29.1±1
10	33.3±2	36.9±1	39.2±1	32.8±2	38.0±2	36.8±3	46.2±2	45.6±2	49.6±1	48.7±3	50.6±2
20	46.5±3	48.5±2	47.3±2	51.5±1	48.5±3	49.2±2	54.5±2	52.8±2	54.6±2	58.8±2	57.8±2
30	59.5±3	61.2±2	60.1±2	63.8±1	65.1±2	71.4±2	75.2±2	77.2±2	76.8±1	72.4±1	78.2±2
45	74.5±1	76.5±2	78.2±1	74.5±1	72.0±2	78.2±2	80.4±3	82.6±3	84.5±2	81.7±3	87.6±3
60	84.9±3	85.3±2	80.5±3	86.9±1	81.2±4	85.2±2	89.6±1	89.2±2	89.9±2	90.4±2	91.2±2
90	90.4±1	92.5±2	91.8±3	93.2±1	93.8±3	95.2±2	97.2±2	96.8±2	95.1±3	96.6±1	98.1±3

Mean ± Standard deviation (n=3)

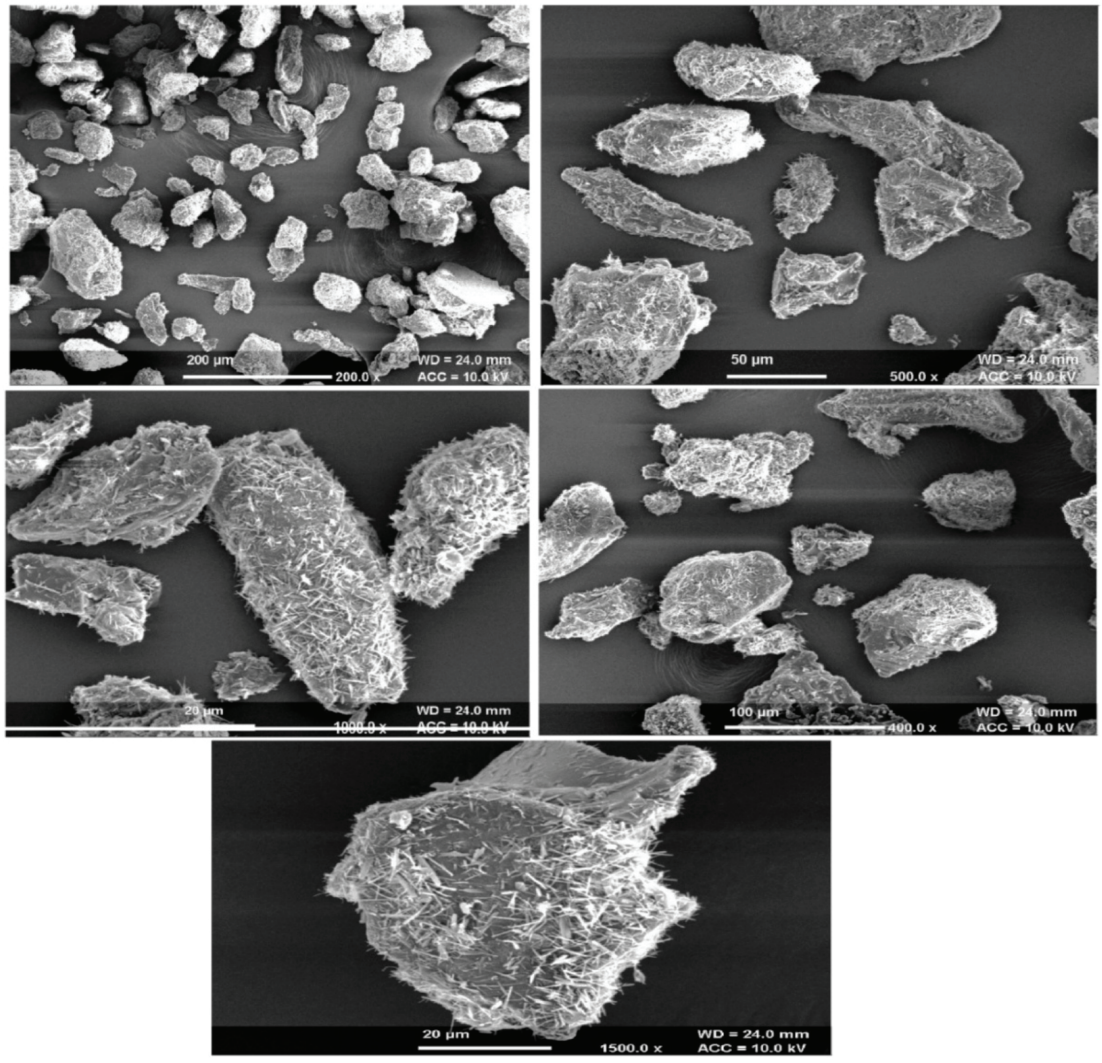

Figure 18. Scanning electron microscopy study of etoricoxib solid dispersion using natural carrier

drug and excipients used in the formulation. Analysis by DSC and powder X-ray diffraction showed that etoricoxib existed in amorphous form within the solid dispersion formulation fabricated using the solvent evaporation process. Additionally, scanning electron microscopy studies suggested the conversion of crystalline etoricoxib to an amorphous form. The dissolution rate and solubility of etoricoxib solid dispersions were improved significantly using the natural carriers xanthan gum, guar gum, and gum acacia.

ACKNOWLEDGEMENTS

The authors are grateful to Abbott Health Care Private Limited (India) for providing etoricoxib as a gift sample.

Conflicts of interest: No conflict of interest was declared by the authors.

REFERENCES

1. Amidon GL, Lennernäs H, Shah VP, Crison JR. A theoretical basis for a biopharmaceutical drug classification: Correlation of *in vitro* drug product dissolution and *in vivo* bioavailability. Pharm Res. 1995;12:413-420.
2. Ain S, Ain Q, Parveen S. An overview on various approaches used for solubilization of poorly soluble drugs. Pharm Res. 2009;2:84-104.
3. Habib MJ. Pharmaceutical solid dispersion technology. CRC, New York; 2000.
4. Murali Mohan Babu GV, Prasad ChD, Ramana Murthy KV. Evaluation of modified gum karaya as carrier for the dissolution enhancement of poorly water soluble drug nimodipine. Int J Pharm. 2002;234:1-17.
5. Sapkal S, Narkhede M, Babhulkar M, Mehetre G, Rathi A. Natural polymers: Best carriers for improving bioavailability of poorly water soluble drugs in solid dispersion. Marmara Pharm J. 2013;17:65-72.
6. Leclercq P, Malaise MG. Etoricoxib (Arcoxia). Revue Medicale de Liege. 2004; 59: 345-349.
7. Capone ML, Tacconelli S, Patrignani P. Clinical pharmacology of etoricoxib. Expert Opin Drug MetabToxicol. 2005;1:269-282.
8. Cochrane DJ, Jarvis B, Keating GM. Etoricoxib. Drugs. 2002;62:2637-2651.
9. Patel DM, Patel MM. Optimization of fast dissolving etoricoxib tablets prepared by sublimation technique. Indian J Pharm Sci. 2008;70:71-76.

10. Patel HM, Suhagia BN, Shah SA, Rathod IS, Parmar VK. Preparation and characterization of etoricoxib-β-cyclodextrin complexes prepared by the kneading method. Acta Pharm. 2007;57:351-359.
11. Shavi GV, Nayak UY, Raghavendra R, Shrawan B, Sreenivasa Reddy M. Enhanced Dissolution and Bioavailability of Etoricoxib in Solid Dispersion Systems: An Investigation into the Role of Carrier Matrix on Stability, *In vitro* and *In vivo* Performance. RRJPPS. 2016;5:55-63.
12. Higuchi T, Connors KA, Phase solubility techniques. Adv Anal Chem Instrum. 1965;4:117.
13. Rao M, Mandage Y, Thanki K, Bhise S. Dissolution improvement of simvastatin by surface solid dispersion technology. Dissolution Technologies. 2010:27-34.
14. Ketkar AR, Patil VB, Paradkar AR. Computer Aided Exploratory Data Analysis Model Fitting for Dissolution Kinetics. 4th International Symposium on Advances in Technology and Business Potential of New Drug Delivery System. Mumbai, India. 2002.

Turk J Pharm Sci 2020;17(1):20-6
DOI: 10.4274/tjps.galenos.2018.15870

ORIGINAL ARTICLE

Deposition Pattern of Polydisperse Dry Powders in Andersen Cascade Impactor - Aerodynamic Assessment for Inhalation Experimentally and *In Silico*

Andersen Cascade Impactor'da Polidispers Kuru Tozların Birikim Şekli - İnhalasyon için Deneysel ve *İn Silico* Aerodinamik Değerlendirme

Janwit DECHRAKSA[1], Tan SUWANDECHA[2], Teerapol SRICHANA[1]*

[1]Prince of Songkla University, Faculty of Pharmaceutical Sciences, Department of Pharmaceutical Technology, Drug Delivery System Excellence Center, Hat Yai, Songkhla, Thailand
[2]Prince of Songkla University, Faculty of Sciences, Department of Pharmacology, Hat Yai, Songkhla, Thailand

ABSTRACT

Objectives: An impactor is a standard instrument that applied for particle deposition assessment in the pharmaceutical aerosols. It provides data comparison between inhaler formulations. However, the deposition pattern in the impactor is not clearly understood. In practice monodisperse aerosols were employed to calibrate the impactor.

Materials and Methods: This study used polydisperse aerosols together with the computer simulation to track the particles in the impactor to understand the deposition pattern. Particles deposited on each stage of the Andersen cascade impactor were compared with its stage cut-off diameter using polydisperse aerosols by three particle sizing techniques. The relationship of cut-off diameter with particle size distribution was established for each stage. Also, the computational verification was used to complement the real experiments.

Results: Projected diameters from microscope images showed that the size of particles varied on the stage's collection plate, and the median size of each stage decreased along the lower stages from 8.53 to 0.92 μm. The median sizes measured by laser diffraction were close to the impactor's cut-off diameters. *In silico* data showed that the outlet mass fractions gradually changed in size towards the lower stages.

Conclusion: Polydisperse aerosols and *in silico* computer fluid dynamics may compliment to standard calibration method.

Key words: Particle size distribution, computer fluid dynamic, andersen cascade impactor, polydisperse aerosols

ÖZ

Amaç: Impactor farmasötik aerosollerde partikül birikiminin değerlendirmesi için uygulanan standart bir araçtır. İnhalasyon formülasyonları arasında veri karşılaştırması sağlar. Bununla birlikte, impactordeki birikim şekli tam olarak anlaşılamamıştır. Uygulamada, impactorü kalibre etmek için monodispers aerosoller kullanılmıştır.

Gereç ve Yöntemler: Bu çalışmada, birikim şeklini anlamak için impactordeki partikülleri izlemek için bilgisayar simülasyonu ile birlikte polidispers aerosoller kullanılmıştır. Andersen cascade impactorün her kademesinde biriken partiküller, üç partikül boyutlandırma tekniği ile polidispers aerosoller kullanılarak ilgili limit çapı ile karşılaştırılmıştır. Limit çapı, her kademe için partikül büyüklüğü dağılımı ile ilişkilendirilmiştir. Ayrıca gerçek deneyleri tamamlamak için hesaba dayalı doğrulaması kullanılmıştır.

Bulgular: Mikroskop görüntülerinden projeksiyon çapı, partikül boyutunun kademe plakası üzerinde değiştiğini ve her bir kademenin medyan boyutunun alt kademelerde 8,53'den 0,92 μm'ye düştüğünü göstermiştir. Lazer kırınımı ile ölçülen ortalama boyutlar, impactorün limit çaplarına yakındı. *In silico* verileri, çıkış kütle fraksiyonlarının boyut olarak alt kademelere doğru yavaş yavaş değiştiğini göstermiştir.

Sonuç: Polidispers aerosoller ve *in silico* bilgisayar sıvı dinamiği standart kalibrasyon yöntemine uygun olabilir.

Anahtar kelimeler: Partikül büyüklüğü dağılımı, bilgisayar sıvı dinamiği, andersen cascade impactor, polidispers aerosoller

*Correspondence: **E-mail:** teerapol.s@psu.ac.th, **Phone:** +6674286960 **ORCID-ID:** orcid.org/0000-0002-4772-2276
Received: 29.08.2018, **Accepted:** 04.10.2018

INTRODUCTION

The particle deposition pattern and air flow in the pulmonary system are of great importance for pulmonary drug delivery. An impactor is a standard instrument applied for particle deposition assessment of pharmaceutical aerosols. Even if the impactor does not perfectly represent a realistic respiratory tract, it provides data for comparing formulations and products.[1] The Andersen cascade impactor (ACI) is a conventional cascade impactor that has been used in various aerosol studies.[2-4] The ACI has been developed to characterize aerodynamic particle size distribution (PSD) and particle deposition, by using an inertial impactor so that the aerodynamic size affects the inertial forces, and different sizes are collected on individual collection plates.[5] The standard ACI has eight stages. Each stage has been designed to collect particles in a range of inertial forces that are affected by nozzle size and flow patterns. The impactor stage specifically traps aerosol particles according to a cut-off diameter, and the collected mass represents the aerosol amount in the size range of that stage.

Other particle assessment techniques include laser diffraction, time of flight, and microscopy, giving PSD. De Boer et al.[6] successfully developed a laser diffraction technique to measure micronized powder aerosols. Laser diffraction has been used to determine the size of deposited particles either prior to or subsequent to entering through the impactor.[7,8] Haynes et al.[9] showed a good correlation between the volume median diameter and the mass median aerodynamic diameter (MMAD) obtained by Spraytec® and the ACI, respectively, with R^2=0.8037. The particle deposition is reproducible and there is a strict correlation with the impactor in the case of liquid formulations.[8] Microscopy can allow direct particle size measurement and observation of particle morphology. This technique provides both qualitative and quantitative data for characterizing aerosols from dry powder inhalers. The projected area diameter is used to describe the particle size in its most stable plane.[10]

Monodisperse aerosols are defined as those with narrow PSD, and they are widely used in many applications, including aerosol sizing apparatus calibration, medical delivery systems, and experimental testing of models.[7,11-14] Monodisperse aerosols are applied in the calibration of aerosol sizing apparatuses, and for example fluorescent dye monodisperse aerosols are generated in specific calibration particle sizes by a vibrating orifice aerosol generator and are immediately fed to the impactor.[7,12] Polydisperse aerosols are more common in pharmaceutical formulations as defined by a broader PSD, specifically having a geometric standard deviation (GSD) higher than 1.25.[15,16] Polydisperse aerosols are rarely used as calibrants, although there are some studies using polydisperse aerosols to compare two impactors.[16,17] However, the well-known calibration procedures use monodisperse aerosols. Srichana et al.[13] published a calibration method using spherical silica for the ACI; the monodisperse particle sizes were separately introduced to determine the collection efficiency curve of the preseparator and stages 0 to stage 4. In addition, dry powder polydisperse aerosols from blends of monodisperse silica powders have been employed for calibration.[13] Computational fluid dynamics (CFD) has been employed in the simulation of fluid flow and in particle tracking in the impactor. In our previous study, a preseparator-equipped ACI showed airflow smoothing to the next stage.[18] Moreover, the single jet model and the quarter ACI model have been validated in the sense that the particle collection efficiency showed excellent correlation with experiments.[14,19] However, prior information on polydisperse particle deposition in the ACI is lacking. The aim of the current research was to study the particle paths and deposition using polydisperse aerosols in an ACI and assess the behavior of polydisperse aerosols regarding deposition in the impactor. The particles on the collection plates were collected and analyzed by particle sizing techniques, namely by laser diffraction and microscopy. The research was conducted by observation of the PSD using actual experiments and by particle tracking simulations of each stage using CFD.

MATERIALS AND METHODS

Particle production

Polydisperse mannitol particles were obtained by spray drying mannitol solution using a mini spray dryer (Buchi B-290, Switzerland) with a high-performance cyclone and nano spray dryer (Buchi B-90, Switzerland) under different conditions until 5 size ranges of particles were obtained (1-10 µm). Three size ranges of silica microspheres were prepared by dispersing in 3 mL of methanol and adjusting the volume with HFA-134a to make a 10 mL pressurized silica suspension (0.2-1.2 µm). These mannitol and silica particles were first characterized by scanning electron microscopy (SEM) before being subjected to the ACI for particle deposition.

ACI operation

The eight stages of the ACI include the preseparator and stage -1 to stage 6, and the filter and base stage were operated to monitor particle deposition. First, 20 mg of spray-dried mannitol was placed in the in-house dry powder inhaler device[20] or the pressurized silica suspension, and the sources were coupled with the ACI by a metal inlet. Then the ACI was first tested at 60 L/min for 10 s to ensure all aerosol particles were delivered completely into the ACI. The trapped particles on each stage were analyzed for their deposition pattern by laser diffraction and microscopy. For spray-dried mannitol, the collection plates were separately rinsed with de-ionized water and the dissolved mannitol contents for each stage were analyzed using HPLC.[21] Samples (100 µL) were injected into a resolved C-18 column (5 µm, 150 mm×3.9 mm, Waters, Milford, MA, USA) using de-ionized water as a mobile phase, at a flow rate of 1 mL/min. The retention time was about 4 min. A refractive index detector (Model RID-10A; Shimadzu, Kyoto, Japan) was used. A calibration curve was constructed using standard solutions of mannitol from 10 to 400 µg/mL. The MMAD and GSD were calculated simultaneously.

Laser diffraction

Pre-ACI: A Spraytec® (Malvern, Worcestershire, UK) equipped with a USP inlet was used in place of the inhalation cell. The

equipment was connected directly to a particle-collecting filter and vacuum pump. The PSDs of spray-dried mannitol particles were characterized by suspending in air using the laser diffraction technique via the Spraytec®. The flow rate was set at 60 L/min in the measurement zone and 2% obscuration was set as a trigger for all measurements. Post-ACI: The collected mannitol particles were gently removed from the collection plates. The Spraytec® was then used to characterize the particle size deposition on each stage. Second, the silica particles on the last three stages (S4-S6) were rinsed individually using methanol and particle samples were allowed to equilibrate at 25°C for 2 min. Then size distribution was determined by the Zetasizer Nano ZS (Malvern, UK). Dynamic light scattering measurements were carried out at 173° scattering angle (backscatter detection) using the Malvern Zetasizer Nano ZS. Three measurements were made for 10 runs for each sample. The viscosity and refractive index of the dispersant were set at 0.5476 cP and 1.326, respectively. For the silica particles, the refractive index (1.458) and absorption (0.001) were used to calculate the size distributions by volume and by particle count. The Z-average, polydisperse index, and median values were used for comparison of the different techniques.

Microscopic analysis

Double adhesive discs (3M, Bangkok, Thailand) were prepared and placed on each collection plate to trap the particles that lost their momentum. Five hundred particles were examined by light microscopy using particle sizing analysis software (cell^P, Olympus Soft Imaging Solutions GmbH, Münster, Germany). After the number count based size distribution had been determined by microscopy this PSD was compared with those from other techniques. The Hatch–Choate transformation equation was used to convert the by number distribution to the by weight distribution. The logarithm of the particle size (x-axis) was plotted against the cumulative percent frequency on a probability scale (y-axis).

Experimentally, spray-dried mannitol was continuously introduced into the ACI, where the Spraytec® was operated at 60 L/min with the assistance of a dry powder device to deagglomerate the dry powder into single particles.[22,23] Then the projected diameters of trapped particles were analyzed by microscopy.

Computational simulation

Figure 1 shows the ACI model developed from previous work including face sizing for continuation of the face to completely transfer to the mathematical model.[18] One-third of the model was used instead of the whole cascade impactor to simplify the complex calculation. The Navier–stokes equations were solved by the finite volume method. The turbulence model used was realizable k-ε and standard wall functions were selected to solve the fluid flow equations as a good fit was given with the empirical data.

Particle motion equation: model description

The particle tracking employed the discrete phase simulation in Fluent by Lagrangian discrete phase model based on one-way coupling. The discrete phase simulation was based on the assumption that the discrete phase occupies a low volume fraction ($V_p \ll V_{air}$) with a high loading mass ($m_p \leq m_{air}$). The original particle condition is gravitation and the initial velocity was specified as a constant with a fully turbulent profile, and no-slip conditions were applied at the walls.[24] The spherical particle model was employed for particles larger than 1 µm, whereas those in the size range 0.1-0.9 µm were treated with the Stokes–cunningham model, which provides a slip correction factor. The stochastic tracking approach was used to predict the turbulent dispersion of the particles to mimic the real situation as the particles were traveling in the air (Equation 1).

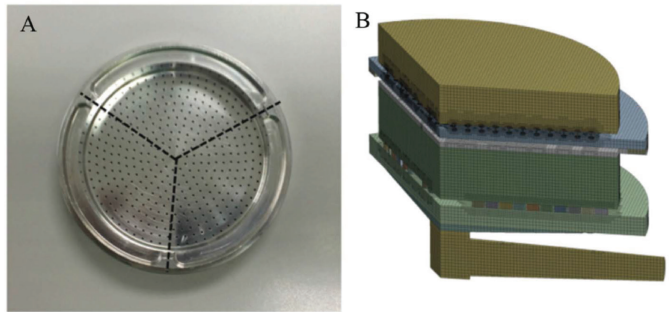

Figure 1. Divided Andersen cascade impactor stage dimensions A) and the computation model of impactor B)

$$\upsilon_p = \bar{\upsilon}_0 + \dot{u}, \quad \textbf{Equation 1}$$

where
- $\bar{\upsilon}_0$ is the mean air velocity
- υ_p is the particle velocity
- $\dot{u}$ is the turbulent velocity fluctuation

Impaction parameter and particle kinetic energy

Kinetic energy (K_e) is employed in trapping particles on the collection plate. The regular trap boundary condition leads to underestimation of the collection plate cut-off diameter.[25] Therefore, a user defined function (UDF) was developed following the kinetic Equations 2-4. The density of silica particles was 1.8 g/mL and mannitol had density 1.5 g/mL.

$$K_e = \frac{1}{2} Mass_p \times v_p^2 \quad \textbf{Equation 2}$$

$$Mass = Volume \times Density \quad \textbf{Equation 3}$$

$$\text{Volume of sphhere} = \frac{4}{3}\pi r^3, \quad \textbf{Equation 4}$$

where
- K_e is the particle's kinetic energy
- $Mass_p$ is the mass of the particle in kilograms
- v_p is the particle's velocity in meters per second

Particle deposition simulation

The deposition factor was the total deposition within the stage of interest and could be explained by the Lagrangian model simulations as the number of discrete particles that were deposited on the collection plate. The deposition efficiency (DE) was defined by Equation 5.

$$DE = \frac{\text{number of particles depositing in region}}{\text{number of particles entering region}} \quad \textbf{Equation 5}$$

Particle size distribution model for tracking a group of particles

The chosen PSD was Rosin–Rammler. The Rosin–Rammler distribution function gives an exponential relationship between the particle diameter (d) and the mean particle diameter[26] as shown in Equation 6.

$$Yp = e^{-(d/\bar{d})^n}, \quad \textbf{Equation 6}$$

where Y_p is the retained weight fraction of particles with a diameter greater than d

$\bar{d}$ is the mean particle diameter

d is the particle diameter

n is the spread of PSD

In this case, the spread parameter was 2.071 and the maximum diameter was 8.71 µm, while the minimum diameter was 0.21 µm and the number-average mean diameter of the Rosin–rammler distribution was 3.36 µm with 28 segments of particle size. The trajectory of the sample histograms was used to describe the PSDs on each collection plate and at the outlet of each stage. The diameter of the particles was set as a variable. In the present study, the particle deposition efficiency of each stage was calculated by the number of particles trapped on the collection plate divided by the number of particles entering each stage. The simulated PSD from the outlet of the upper stage was used as an inlet PSD of particles of the following stage. The PSD was introduced into a computer simulation and the particle distributions on each stage of the ACI were computationally modeled.

The submitted protocol entitled "Deposition pattern of polydisperse dry powders in Andersen cascade impactor" including all related documents has been reviewed by the Health Science Human Research Ethics Committee, Prince of Songkla University (ref:161/2760).

RESULTS AND DISCUSSION

Particle morphology and surface characteristics

Figures 2 and 3 show the morphology and surface of spray-dried mannitol and silica microspheres, viewed under SEM. The mannitol prepared using a spray dryer and nano spray dryer presented perfectly spherical shapes with smooth surfaces. All silica microspheres were perfectly spherical with smooth surfaces.

Particle size distribution of spray-dried mannitol and silica microspheres

The median size ($Dv_{0.5}$ ± SD) was 3.53±0.09 µm with size at 90% cumulative ($Dv_{0.9}$) of 8.62±0.66 µm and size at 10% cumulative ($Dv_{0.1}$) of 0.92±0.47 µm. The spray-dried mannitol had polydisperse PSD with a span of 2.18. The span is the measurement of the width of the size distribution. The smaller the value the narrower the distribution. The width is calculated by $(Dv_{0.9}-Dv_{0.1})/Dv_{0.5}$. The PSDs revealed a spread of particle sizes in spray-dried mannitol. The specific sizes of silica were 0.261, 0.690, and 1.18 µm with narrow distribution.

Depositions of mannitol and silica particles on each ACI stage

The mean diameters of mannitol and silica particles from microscopy are shown in Table 1. Microscopy also confirmed the spherical shape of particles captured on the adhesive film (Figure 4). Large particles were mostly isolated and had been collected on an early stage of the impactor, while agglomeration of some primary particles may have occurred during ACI processing. The spray-dried mannitol particles exhibited some agglomeration of small particles. The agglomerates behaved like larger particles and were trapped by the early stages of the ACI. However, individual particles did not change their sizes when viewed under the microscope. From the microscopy results, the particle size of deposited particles decreased along the stages, for example the particle mean diameter of deposited particles on stage 6 was 0.92 µm, which was close to the limits of optical microscopy. Particle deposition depends on the stage cut-off diameter and on the inertial forces of the particles, which relate directly to particle morphology and size. Most of the particle population stayed under the stage nozzle of similar sizes, where the smaller particles escaped to the next stage via the air

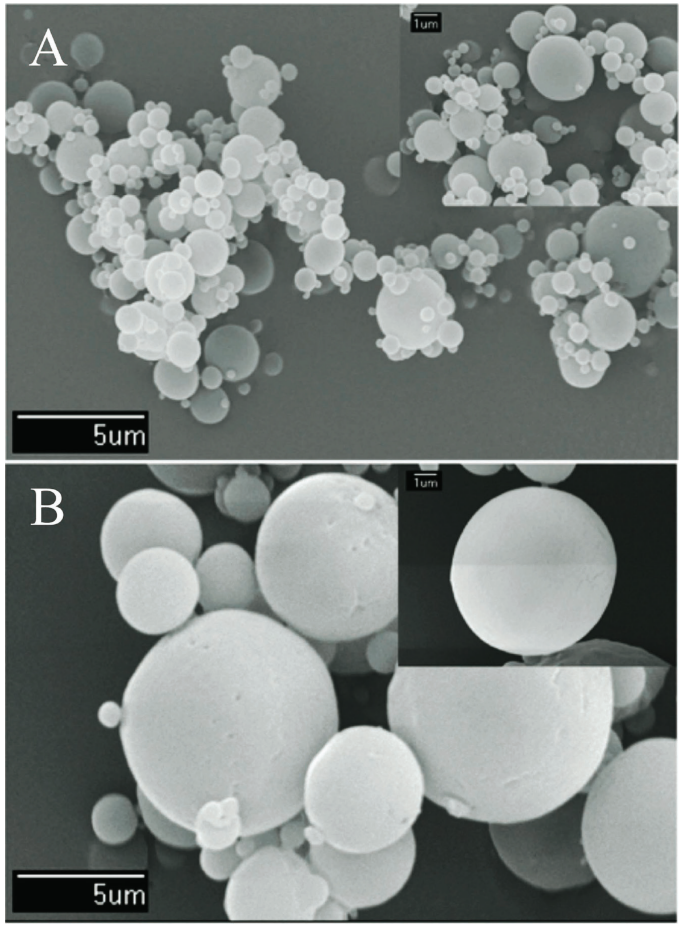

Figure 2. Morphology and surface characteristics of spray-dried mannitol by scanning electron microscopy imaging: mannitol spray-dried using a mini spray dryer A) and mannitol spraydried using a nano spray dryer B)

stream because of their lower inertial forces.[18] Each collection plate trapped the particles with sufficient inertial force.

The spray-dried mannitol had median diameters of 3.02, 3.91, 7.02, and 9.59 µm. Therefore, the particle size range covered the cut-off diameters of stage -1 to stage 3 at a flow rate of 60 L/min. The spray-dried mannitol was introduced into the ACI. The comparison between the manufacture's nominal cut-off and the actual deposition of particles (spray-dried mannitol) is shown in Figure 5. The median particle size deposition on each stage's collection plate matched reasonably well with the nominal cut-off diameters. The cut-off diameters usually were obtained by the amount of specific trapped particle size on the stage of interest compared with the whole impactor using individual monodisperse particle size. The results for spray-dried mannitol showed a good match of the median size of deposited spray-dried mannitol and the manufacturer's nominal data on impactor stages. However, it was not possible to evaluate with this spray-dried mannitol the particle deposition in the lower stages (stage 4 or lower) because the cut-off diameters are too small relative to the prepared particle sizes.

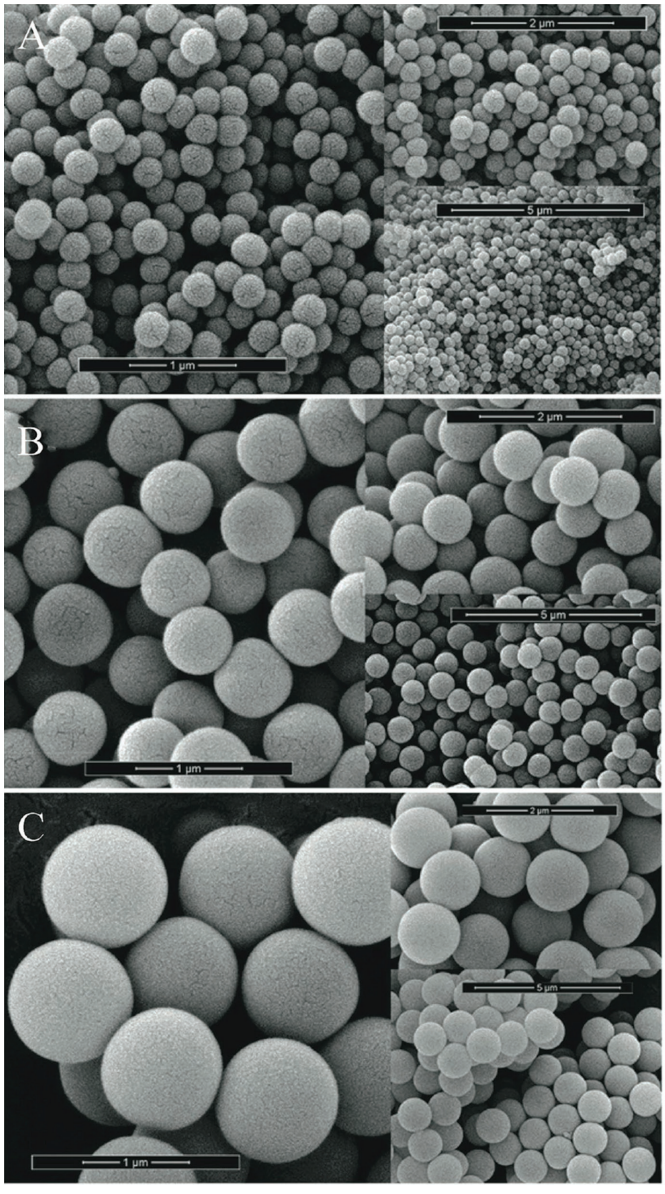

Figure 3. Morphology and surface characteristics of monodisperse silica microspheres:monodisperse silica microspheres of sizes 0.261, 0.690, and 1.18 µm, respectively

Silica microsphere deposition on each ACI stage

The mean particle size trapped by each collection plate is shown in Figure 5. For stages 4 to 6, the spherical silica particles were in the appropriate size range. Three size ranges of silica particles (0.261, 0.690, and 1.180 µm) were introduced into the ACI (n=5). Three cases of silica microspheres clearly escaped through the nozzle of stage 4, with mean size of trapped silica particles close to the manufacturer's cut-off data with relative accuracies from 71.4% to 127.6%. The higher error of the correlation could be explained by particle aggregation. The mean particle size of trapped particles on stage 5's collection plate showed good agreement with the stage cut-off using

Table 1. The geometric mean diameter (µm) on weight basis, obtained using the Hatch-Choate equation with microscopy data

Stage	d_g	σ_g	Log d_{ln}	d'_g
S_{-1}	7.79	0.84	0.90	8.53
S_0	5.57	0.82	0.75	6.27
S_1	3.96	0.89	0.60	4.12
S_2	2.77	0.81	0.45	3.16
S_3	1.89	0.83	0.28	2.10
S_4	1.40	0.78	0.16	1.68
S_5	1.06	0.78	0.04	1.28
S_6	0.78	0.79	-0.10	0.92

d_g is a geometric mean diameter, σ_g is a geometric standard deviation, d_{ln} is a length-number mean diameter, d'_g is a geometric mean diameter on a weight basis

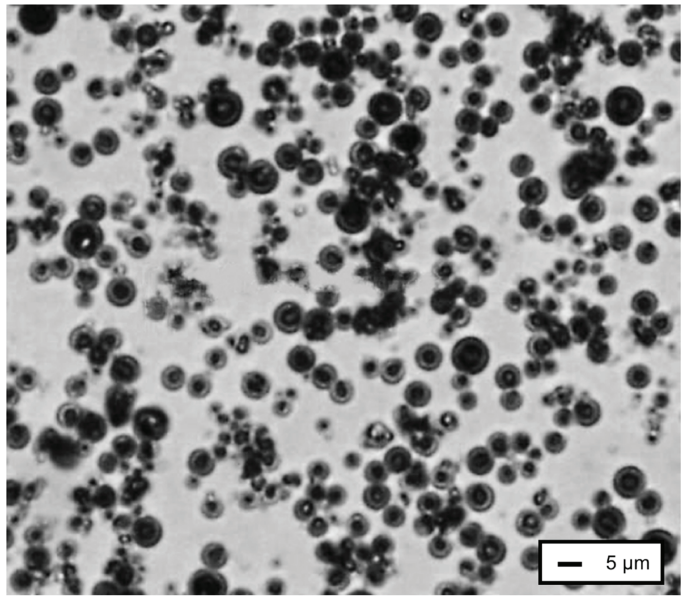

Figure 4. Deposition pattern of spray-dried mannitol on stage 0 collection plate observed with optical microscope: 50× magnification

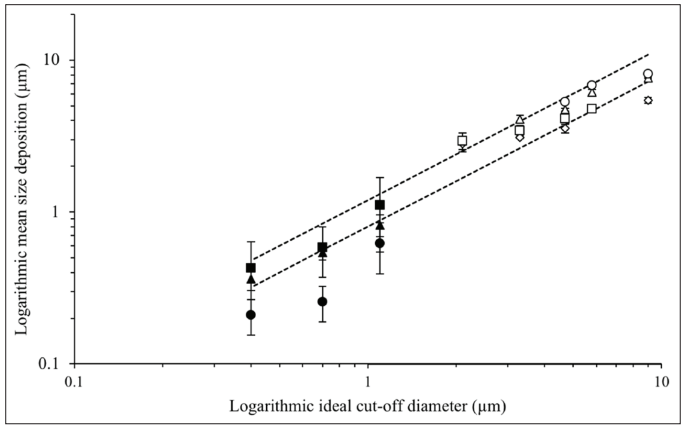

Figure 5. The correlation between logarithmic ideal size cut-off and logarithmic mean size deposition of spray dried mannitol: 3.02 μm (◇), 3.91 μm (□), 7.02 μm (△), 9.59 μm (○), and microsphere silica: 0.26 μm (■), 0.69 μm (▲), and 1.18 μm (●) on each stage

silica microspheres within 94.4% and 106.3% relative accuracy. For the trapped particles on stage 6's collection plate, the data showed good correlation between the microsphere deposition and the stage's cut-off diameter with 90.85%-106.90% correlation. In brief, the particle depositions on the collection plate show the aggregated particles could form a larger diameter clump and be prematurely trapped on the earlier stage of the impactor. Moreover, the laser diffraction results showed good correlation of deposition on each collection plate with the respective nominal cut-off diameters.[13,27,28] The mean size of trapped particles on each stage could be representative of the stage cut-off diameter, while the PSD allowed estimation of collection efficiency curves.

Computational particle tracking and deposition

The particles were tracked along the computational ACI model (60 L/min) to study particle paths in the impactor. The validation of the computational model had been confirmed using the collection efficiency curves of the computational simulation obtained by injecting individual particles from 0.3 μm to 11 μm in size. The simulated capture rate curves at 50% collection efficiency gave cut-off diameter estimates matching the manufacturer's nominal values well. The experimental particle deposition results were comparable to the simulation results for the ACI. The particle deposition in the ACI was expressed as percent by mass across the distribution of particle sizes in the aerosol. The amounts of spray-dried mannitol on each collection plate were analyzed by LC with an RI detector as shown in Figure 6. The MMAD of spray-dried mannitol was 4.08 μm with a GSD of 1.75 for 60 L/min. Figure 7 shows the simulated PSDs at outlets of each stage, by mass fractions of spray-dried mannitol following injection with Rosin–Rammler PSD. These simulations at the outlet of stage -1 showed that 50% of particles were around 4 μm. The MMAD of the simulated particles at the outlet exhibited decreasing size when they passed through the impactor stage with the smaller cut-off diameter. The simulated PSD had an MMAD at 4.08 μm, whereas the experimental particle size was 4.15 μm. PSD was not significantly distorted until stage 3, which has a cut-off

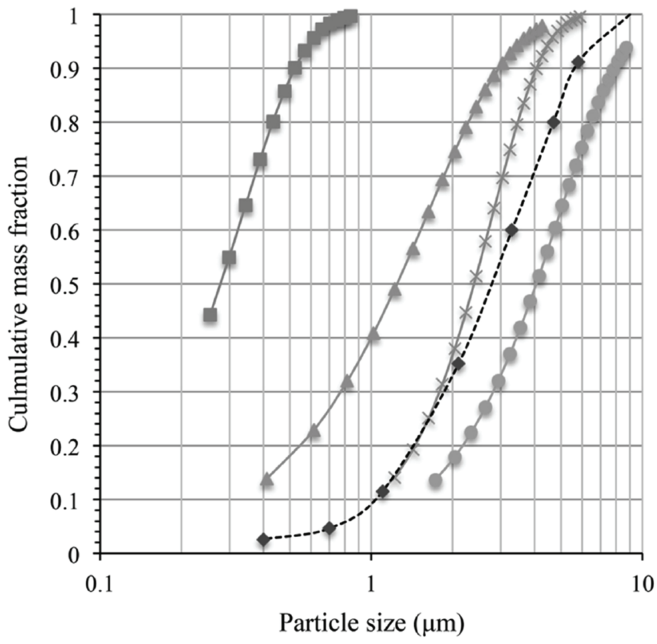

Figure 6. PSD by mass across particle sizes at the outlet of each individual stage as simulated outlet: Stage 1 (□), Stage 1 (□), Stage 3 (□), Stage 4 (□) and experimental data (□), spraydried mannitol

PSD: Particle size distribution

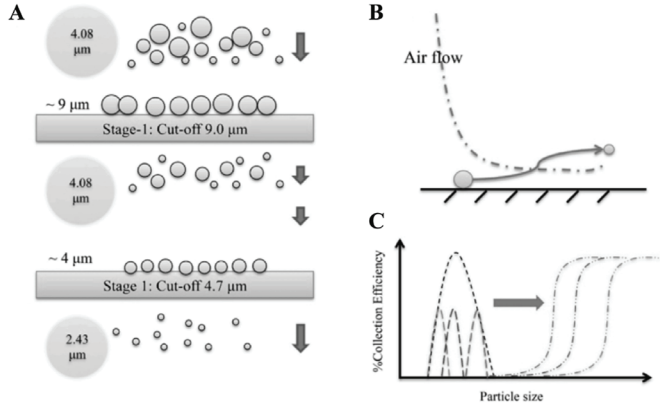

Figure 7. Illustrations of polydisperse particles passing by impactors A) and B), and particle distribution on each stage of a polydisperse mixture in impactor C)

diameter below the MMAD. For example, the diameter was close to 1.20 μm at the outlet of stage 3, while the cut-off diameter of stage 4 is 1.10 μm. The simulations provided an explanation of how spray-dried mannitol was deposited and traveled across the ACI. Even if the aerosol particles were polydisperse, they were trapped by specific collection plates. In the present study, the particle deposition simulation gave for each particle size a capture probability and it confirmed that monodisperse aerosols are ideal for calibrating the ACI.[13,28,29] However, the simulation of polydisperse spray-dried mannitol explained the particle flow behavior by mass fraction captured of each particle size. In the case of polydisperse aerosols, the impactor should separate the polydisperse samples as they were fed into the impactor.

CONCLUSION

Polydisperse aerosols were characterized and used to test an ACI successfully. This study assessed particle deposition in a cascade impactor using both experiments and computational simulations of dry particulate powder. Polydisperse dry powders behaved in accordance with the computational simulation based on inertial and aerodynamic drag forces one particle at a time. The tested particle sizing techniques, based on laser diffraction and optical microscopy, showed results comparable with the impactor manufacturer's nominal cut-off data with polydisperse dry powders. The use of polydisperse dry powders in determining separation characteristics of the ACI was demonstrated using particle travelling path.

ACKNOWLEDGEMENTS

We would like to thank the Drug Delivery System Excellence Center for the use of their facilities. This work was supported by the Higher Education Research Promotion and National Research University Project of Thailand, Office of the Higher Education Commission. We would also like to thank the reviewers of this article and Dr. Seppo Karrila for assistance with manuscript preparation

Conflicts of interest: No conflict of interest was declared by the authors. The authors alone are responsible for the content and writing of this article.

REFERENCES

1. Mitchell J, Newman S, Chan HK. *In vitro* and *in vivo* aspects of cascade impactor tests and inhaler performance: A review. AAPS PharmSciTech. 2007;21:110.
2. Duan Q, An JL, Wang HL, Miao Q. Pollution characteristics of organic and elemental carbon in atmospheric particles in Nanjing northern suburb in summer. Huan J ing Ke Xue. 2014;35:2460-2467.
3. Li Y, Zhang H, Qiu X, Zhang Y, Wang H. Dispersion and risk assessment of bacterial aerosols emitted from rotating-brush aerator during summer in a wastewater treatment plant of xi'an, china. Aerosol Air Qual Res. 2013;13:1807-1814.
4. Srichana T, Juthong S, Thawithong E, Supaiboonpipat S, Soorapan S. Clinical equivalence of budesonide dry powder inhaler and pressurized metered dose inhaler. Clin Respir J. 2016;10:74-82.
5. Marple VA, Liu BYH. Characteristics of laminar jet impactors. Environ Sci Technol. 1974;8:648-654.
6. De Boer AH, Gjaltema D, Hagedoorn P, Frijlink HW. Characterization of inhalation aerosols: A critical evaluation of cascade impactor analysis and laser diffraction technique. Int J Pharm. 2002;249:219-231.
7. Kwon SB, Lim KS, Jung JS, Bae GN, Lee KW. Design and calibration of a 5-stage cascade impactor (K-JIST cascade impactor). J Aerosol Sci. 2003;34:289-300.
8. Wachtel H, Ziegler J. Laser diffraction method for particle size distribution measurements in pharmaceutical aerosols. US. 2005.
9. Haynes A, Shaik MS, Krarup H, Singh M. Evaluation of the Malvern Spraytec® with inhalation cell for the measurement of particle size distribution from metered dose inhalers. J Pharm Sci. 2004;93:349-363.
10. Concessio NM, Hickey AJ. Descriptors of irregular particle morphology and powder properties. Adv Drug Deliv Rev. 1997;26:29-40.
11. Biddiscombe MF, Usmani OS, Barnes PJ. A system for the production and delivery of monodisperse salbutamol aerosols to the lungs. Int J Pharm. 2003;254:243-253.
12. Rader DJ, Mondy LA, Brockmann JE, Lucero DA, Rubow KL. Stage response calibration of the Mark III and Marple personal cascade impactors. Aerosol Sci Technol. 1991;14:365-379.
13. Srichana T, Martin GP, Marriott C. Calibration method for the Andersen cascade impactor. J Aerosol Sci. 1998;29:761-762.
14. Vinchurkar S, Longest PW, Peart J. CFD simulations of the Andersen cascade impactor: Model development and effects of aerosol charge. J Aerosol Sci. 2009;40:807-822.
15. Arefin AME, Masud MH, Joardder MUH, Akhter S. A monodisperse-aerosol generation system: Design, fabrication and performance. Particuology. 2017;34:118-125.
16. Rosati JA, Brown JS, Peters TM, Leith D, Kim CS. A polydisperse aerosol inhalation system designed for human studies. J Aerosol Sci. 2002;33:1433-1446.
17. Yoshida H, Kuwana A, Shibata H, Izutsu KI, Goda Y. Comparison of aerodynamic particle size distribution between a next generation impactor and a cascade impactor at a range of flow rates. AAPS PharmSciTech. 2017;18:646-653.
18. Dechraksa J, Suwandecha T, Maliwan K, Srichana T. The comparison of fluid dynamics parameters in an Andersen cascade impactor equipped with and without a preseparator. AAPS PharmSciTech. 2014;15:792-801.
19. Gulak Y, Jayjock E, Muzzio F, Bauer A, McGlynn P. Numerical calibration of the Andersen cascade impactor using a single jet model. Int J Pharm. 2009;377:45-51.
20. Sukasame N, Nimnoo N, Suwandecha T, Srichana T. Pharmacodynamics of dry powder formulations of salbutamol for delivery by inhalation. Asian Biomedicine. 2011;5:475-483.
21. Adi H, Young PM, Chan HK, Agus H, Traini D. Co-spray-dried mannitol-ciprofloxacin dry powder inhaler formulation for cystic fibrosis and chronic obstructive pulmonary disease. Eur J Pharm Sci. 2010;40:239-247.
22. Ding Y, Riediker M. A system to assess the stability of airborne nanoparticle agglomerates under aerodynamic shear. J Aerosol Sci. 2015;88:98-108.
23. Miansari M, Qi A, Yeo LY, Friend JR. Vibration-induced deagglomeration and shear-induced alignment of carbon nanotubes in air. Adv Funct Mater. 2015;25:1014-1023.
24. Worth Longest P, Vinchurkar S. Validating CFD predictions of respiratory aerosol deposition: Effects of upstream transition and turbulence. J Biomech. 2007;40:305-316.
25. Matida EA, Finlay WH, Lange CF, Grgic B. Improved numerical simulation of aerosol deposition in an idealized mouth-throat. J Aerosol Sci. 2004;35:1-19.
26. Bailey AG, Balachandran W, Williams TJ. The rosin--rammler size distribution for liquid droplet ensembles. J Aerosol Sci. 1983;14:39-46.
27. Garmise RJ, Hickey AJ. Calibration of the Andersen cascade impactor for the characterization of nasal products. J Pharm Sci. 2008;97:3462-3466.
28. Nichols SC, Brown DR, Smurthwaite M. New concept for the variable flow rate Andersen cascade impactor and calibration data. J Aerosol Med. 1998;11:133-138.
29. Dodge LG. Calibration of the Malvern particle sizer. Appl Opt. 1984;23:2415-2419.

Turk J Pharm Sci 2020;17(1):27-35
DOI: 10.4274/tjps.galenos.2018.34392

ORIGINAL ARTICLE

Levocetirizine Dihydrochloride-Loaded Chitosan Nanoparticles: Formulation and *In Vitro* Evaluation

Levosetirizin Dihidroklorür Yüklü Kitosan Nanopartikülleri: Formülasyonu ve *İn Vitro* Değerlendirilmesi

Gülsel YURTDAŞ KIRIMLIOĞLU*, A. Alper ÖZTÜRK

Anadolu University, Faculty of Pharmacy, Department of Pharmaceutical Technology, Eskişehir, Turkey

ABSTRACT

Objectives: The aim of the present study was to formulate levocetirizine hydrochloride (LCD)-loaded chitosan nanoparticles at submicron level with high entrapment efficiency and prolonged effect for optimizing the plasma drug concentration enhancing bioavailability.

Materials and Methods: LCD was successfully incorporated into chitosan nanoparticles by spray drying for the purpose of oral application. *In vitro* characteristics were evaluated in detail.

Results: LCD was successfully loaded into the polymeric matrices by spray drying. Characterization of the nanoparticles including encapsulation efficiency, particle size, zeta potential, morphology, polydispersity index, solid-state characterizations, and LCD quantification by high performance liquid chromatography was performed. The release pattern of LCD from the nanoparticles was determined using a dialysis tube in simulated intestinal fluid (pH 6.8). *In vitro* release profiles indicated prolonged release of LCD from the nanoparticles that followed the Korsmeyer-Peppas kinetic model.

Conclusion: Chitosan-based LCD-loaded polymeric nanoparticles appear to be a promising drug delivery system for the active agent.

Key words: Levocetirizine dihydrochloride, chitosan, polymeric nanoparticle, spray drying

ÖZ

Amaç: Bu çalışmanın amacı, biyoyararlanımı iyileştirerek plazma ilaç konsantrasyonunu optimize etmek için uzatılmış etkiye ve yüksek yükleme kapasitesine sahip, mikron altı düzeyde levosetirizin dihidroklorür (LCD) yüklü kitosan nanopartijkülleri formüle etmektir.

Gereç ve Yöntemler: Bu çalışmada LCD, oral uygulama amacı ile kitosan nanopartiküllerine püskürterek kurutma yöntemi kullanılarak yüklenmiştir. Nanopartiküllerin *in vitro* karakteristik özellikleri detaylıca incelenmiştir.

Bulgular: LCD püskürterek kurutma yöntemi ile polimerik matrise başarıyla yüklenmiştir. Nanopartiküllerin karakterizasyonu yüklenme etkinliği, parçacık büyüklüğü, zeta potansiyel, morfoloji, polidisperslik indisi ve yüksek basınçlı sıvı kromatografisi ile LCD tayini dahil olmak üzere yapılmıştır. Nanopartiküllerden LCD salımı simüle edilmiş bağırsak vasatında (pH 6,8) diyaliz tübü kullanılarak gerçekleştirilmiştir. Nanopartiküllerden LCD salımına ait *in vitro* salım profilleri Korsmeyer-Peppas modeline uygunluk gösterek uzatılmış salım göstermiştir.

Sonuç: Kitosan bazlı LCD yüklü polimerik nanopartiküllerin etkin madde için umut verici bir ilaç taşıyıcı sistem olduğu sonucuna varılabilir.

Anahtar kelimeler: Levosetirizin dihidroklorür, kitosan, polimerik nanopartikül, püskürterek kurutma

*Correspondence: **E-mail:** gyurtdas@anadolu.edu.tr, **Phone:** +90 532 167 98 92 **ORCID-ID:** orcid.org/0000-0001-8897-0885
Received: 20.06.2018, **Accepted:** 04.10.2018

INTRODUCTION

Levocetirizine dihydrochloride (LCD) is an orally active, third generation nonsedative antihistaminic agent widely used in the treatment of chronic idiopathic urticaria, seasonal allergic rhinitis, and hay fever.[1,2] It has more affinity for H_1 receptors when compared to cetirizine hydrochloride (CD).[1] LCD is rapidly and extensively absorbed after oral administration, with the peak plasma concentration attained in 0.9-1 h.[3] LCD undergoes a low degree of first pass metabolism in the liver; it is metabolized to a limited extent by oxidative dealkylation to metabolite negligible antihistaminic activity. It is approximately 93% bound to plasma proteins and has a plasma elimination half-life of 8-9 h that does not change with multiple dosing.[4] The fast disintegration behavior of conventional LCD formulations may result in initial burst-released kinetics, permitting the drug to be absorbed very quickly and resulting in high serum concentrations. Under these conditions, local irritation to gastrointestinal (GI) mucous membranes and other side effects such as drowsiness, tiredness, dry mouth, fever, cough, oculogyric crisis, and somnolence are inevitable.[2,5] Therefore, it is desirable to design and develop a rational delivery system for LCD. Many efforts towards designing CD and LCD (active enantiomer of CD) sustained delivery systems by encapsulating, forming flexible vesicles, microparticles, and nanoparticles were made during the last decade.[2,4-6] Nanoparticles have attracted considerable attention due to their advantageous properties such as decreased particle size, increased surface area, enhanced reactivity, promoted drug release, reformed targeting, reduced toxicity, and improved sustained-release efficacy.[7] Surface charges of nanoparticles have a significant effect on internalization with cells and also on their uptake. Positively charged nanoparticles seem to allow a higher extent of internalization apparently as a consequence of ionic interactions established between cationic nanoparticles and negatively charged membranes.[8] Chitosan is a polycationic polymer that is a naturally occurring polysaccharide found abundantly in marine crustaceans, insects, and fungi.[9,10] Chitosan is composed of 2-amino-2-deoxy-β-D-glucan combined with glycosidic linkages.[11] Positively charged amino groups of polymer interact with negatively charged biological membranes, ensuring a mucoadhesive character of the chitosan matrices.[12] Chitosan is one of the most extensively studied materials in the pharmaceutical field. Properties such as biodegradability, low toxicity, good biocompatibility, and no risk of accumulation/retention in the body make it suitable for use in biomedical and pharmaceutical formulations.[13] Spray drying is a single-step, cheap, continuous, and scalable process that enables the production of particles with controlled size and morphological aspects.[14] Spray drying also eliminates the addition of crosslinking agent and minimizes the swelling of chitosan-based nanoparticles.[15] Therefore, spray drying technology was utilized in the present study for the formulation of cationic nanoparticles using the advantages of the method. Our study may provide valuable information for the design and development of new LCD-loaded controlled-release dosage forms. The aim of the present study was to formulate positively charged LCD-loaded nanoparticles at submicron level with high encapsulation efficiency (EE), reduced local irritation to GI mucous membranes and other side effects, and prolonged plasma level drug concentration enhancing the bioavailability and protection of sensitive drugs against light thus improving their stability.

MATERIALS AND METHODS

Materials

The LCD was a kind gift from Neutec (İstanbul, Turkey). Chitosan (low molecular weight with 20-200 mPas.s viscosity) was purchased from Sigma (Steinheim, Germany). All other reagents used were of analytical grade.

Preparation of nanoparticles

Chitosan nanoparticles were prepared using a mini spray dryer (B-190, Buchi, Switzerland). The spray dryer was connected to an Inert Loop B-295 (Buchi, Switzerland) due to the organic solvent. Carbon dioxide gas was used at a flow rate of 120 $L.min^{-1}$. The residual oxygen level in the system was kept below 4%. When preparing particulate systems by spray drying, it has to be kept in the mind that production parameters such as size of nozzle, feeding pump rate, inlet temperature, and compressed air flow rate affect particle size.[15,16] It was reported that smaller particles are formed with a lower feeding pump rate and smaller nozzle size. In addition, smaller particles are formed with greater volume of air input where particle size is not dependent on inlet temperature in the range of 120-180°C.[15] Therefore, the inlet temperature was maintained at 120°C using the slowest pump rate that can spray the solution.

Accurately weighed chitosan (1 g) was dissolved in acetic acid solution (2% v/v, 120 mL). Ethanol (96% v/v, 120 mL) was added to the acidic solution in order to decrease the viscosity of the chitosan solution. LCD was added to the mixture under constant stirrer speed (300 rpm) on a magnetic stirrer. The final clear solution was then spray dried with an inlet temperature of 120±1°C and outlet temperature of 60±5°C and delivered to a drying zone via a 4 µm nozzle. White dry powders were obtained and kept in tightly closed vials at room temperature until being analyzed. Placebo nanoparticles were prepared as described above without the addition of active agent.

The spray-drying conditions are shown in Table 1.

Characterization of nanoparticles

Morphology

The particle shape and surface characteristics of the freshly prepared nanoparticle formulations and LCD were investigated by scanning electron microscope (SEM) (Hitachi TM3030Plus Tabletop Microscope, Japan) at 25±2°C. Samples were coated with a thin layer of gold under argon to avoid charging under the electron beam.

Table 1. Spray-drying conditions

Inlet temperature	Outlet temperature	Flow rate mL/min	Pump control level	Aspirator control level
120°C	60°C	450	3	3

Particle size and zeta potential

Particle size, polydispersity index (PI), and zeta potential measurements were carried out on freshly prepared samples using a Malvern Nano ZS (Zetasizer Nano Series, Malvern, Worcestershire, UK). Samples of all nanoparticles were dispersed in double distilled water (adjusted to a constant conductivity of 50 μS.cm^{-1} using 0.9% NaCl) just prior to analyses. All analyses were repeated in triplicate at 25±2°C. The data obtained were evaluated by span values calculated using volume distribution as diameter (d) values of 10%, 50%, and 90%. The diameter values indicate the percentage of particles possessing a diameter equal to or lower than the given value. The span value is a statistical parameter useful for evaluating the particle size distribution and calculated by the following equation:[17]

Span value=[d(90)-d(10)]/d(50) (1)

Differential scanning calorimetry

Structural and crystallinity changes in LCD and the polymer due to the thermal impacts during the formulation steps were evaluated using differential scanning calorimetry (DSC) (DSC-60, Shimadzu Scientific Instruments, Columbia, MI, USA). Analyses were performed under nitrogen at a flow rate of 50 mL.min^{-1} at 30-250°C with a rate of increase of 10°C.min^{-1}.

Fourier transform infrared spectrophotometry

Fourier transform infrared (FT-IR) analysis spectra were recorded using a Shimadzu IR Prestige-21 (Shimadzu Corporation, Kyoto, Japan) at the wavelength range of 4000-500 cm^{-1}.

Nuclear magnetic resonance spectroscopy

Nuclear magnetic resonance (NMR) spectroscopy (^{1}H-NMR) analyses were performed using an UltraShield™ CPMAS NMR (Bruker, Rheinstetten, Germany). Samples were prepared by dissolving nanoparticles in deuterated dimethyl sulfoxide. Pure chitosan and LCD were analyzed by DSC, FT-IR, and ^{1}H-NMR and were used as reference evaluating the interaction between polymer and LCD.

Determination of LCD

High performance liquid chromatography (HPLC) was used for the determination of LCD. A Shimadzu 20-A (Tokyo, Japan) equipped with a reversed phase Nucleosil 120-5 column (column diameter: 4.6 mm, column length: 250 mm, C_{18} gravity, 5 μm) was used. Acetonitrile: water: 1 M sulfuric acid (93:66:4, v/v/v) was used as mobile phase with a flow rate of 1 mL.min^{-1}; 20 μL constant amount of samples injected via an automatic injector (Shimadzu, Tokyo, Japan) was used and a photodiode detector was used at 230 nm.[18] Column temperature was set to 30°C. Validation studies were carried out for data reliability.

Encapsulation efficiency

In order to determine the amount of LCD in drug-loaded nanoparticles, drug EE was determined by validated HPLC method. Accurately weighed nanoparticles (5 mg) were dispersed in acetonitrile (1 mL), vortexed for 1 min, and centrifuged at 2500 rpm for 5 min for the determination of LCD remaining on the chitosan sphere surface (LCD_s).[12] The quantity of LCD encapsulated in nanoparticles was calculated as the difference between the amount initially added (LCD_t) and the LCD_s.[5] Each experiment was repeated three times.

EE %=[(LCD_t-LCD_s)/LCD_t]×100 (2)

In vitro drug release

A dialysis membrane method was used to identify the release behavior of nanoparticles. *In vitro* release profiles of LCD were investigated in freshly prepared simulated intestinal fluid (SIF, pH 6.8) over 72 h. Briefly, drug-loaded nanoparticles containing 1.5 mg of LCD were put in dialysis bags (with a molecular cut-off 12-14 kD, Sigma) and capped with closures. The bags were immersed into dissolution medium containing 80 mL of SIF at 37±1°C on a water bath using a continuous magnetic stirring rate of 100 rpm.[7] Next 1-mL samples were withdrawn at predetermined time intervals and LCD contents in the receptor chamber were determined by HPLC and the release profile of pure LCD was used as a reference for better evaluation of the profiles. Sink conditions were maintained in the receptor compartment during the *in vitro* release studies. Each experiment was repeated three times.

In vitro release kinetics

Release kinetics were investigated using the software DDSolver in order to evaluate the mechanism of drug release from nanoparticles.[19]

RESULTS AND DISCUSSION

Different methods were used to prepare chitosan nanoparticles. The method chosen depended on factors such as particle size, thermal and chemical stability of the active agent, reproducibility of the release profiles, stability of the final product, and residual toxicity associated with the final product.[11]

Spray drying is a well-known technique to produce powders, granules, or agglomerates from mixtures of drug and excipient solutions as well as suspensions.[15] In the present study, spray drying was chosen for preparing chitosan nanoparticles since it does not involve toilsome procedures and avoids the use of harsh cross-linking agents and organic solvents that might trigger chemical reactions with the active agent.[11] The compositions of the chitosan nanoparticles prepared are given in Table 2.

Characterization of nanoparticles

Morphology

SEM images of pure LCD and polymeric nanoparticles are given in Figure 1. The images showed that all formulations prepared

Table 2. Compositions of nanoparticles prepared

Code	Chitosan (g)	LCD (g)	Acetic acid solution (2%, v/v, mL)	Methanol (mL)
Placebo	1	-	120	120
F-1	1	0.05	120	120
F-2	1	0.1	120	120

LCD: Levocetirizine dihydrochloride

were spherical.[5] The placebo nanoparticles' images resembled deflated balloons with wrinkled surfaces (Figure 1b), while the LCD-loaded spray-dried formulations demonstrated spherical shapes with the general morphology of spray-dried amorphous materials.[12,20] The crystalline structure of LCD was not observed in the formulations, indicating successful incorporation of LCD into polymeric matrices.

Particle size and zeta potential

Mean particle size, PI, and zeta potential values of the chitosan nanoparticles are presented in Table 3. The particle size and size distribution of nanoparticles play a key role in their adhesion and interaction with cells.[7] Particle sizes of the nanoparticles were 521.70±8.50 nm and 538.46±5.74 nm for F-1 and F-2, respectively. It was found that the decrease in the amount of LCD in nanoparticles was in parallel with the relative decrease in average particle size.[21] PI values were used to define the particle size distribution. All prepared nanoparticles were nanometer sized and the size distributions were relatively monodisperse with PI values of 0.512±0.090 and 0.498±0.074 for F-1 and F-2, respectively. PI values higher than 0.7 are indicative of a very large particle size distribution.[22,23] All nanoparticles prepared in the present study had PI values lower than 0.7; therefore, particle size distribution was uniform.

The span index measures the width of the particle size distribution, as described in the literature.[24] Formulations show a relatively narrow particle size distribution (span index <1). The narrower size distribution reported previously was confirmed by the span values, i.e. the lower span the narrower the particle size distribution.[17] Zeta potential is a scientific notion for electrokinetic potential in colloidal systems and is one of the most important properties, playing a major role in the efficiency of nanomedicine. Zeta potential can affect the physical and pharmacokinetic properties of nanosystems in the body or may affect the phagocytosis of nanoparticles in the blood stream.[25] The results showed that zeta potentials were 25.7±1.8 mV and 25.9±2.5 mV for F-1 and F-2, respectively, which may be attributed to the positive charges on polymeric matrices, indicating adequate physical stability. Considering negatively charged cell membranes, cationic nanoparticles have great potential in the enhancement of internalization with the cells and also on their uptake.[15,26]

Differential scanning calorimetry

Thermodynamic variations related to morphological changes during and after the formulation steps can be detected by thermal analysis.[27] Figure 2 displays the thermal behavior of the LCD and nanoparticles prepared. Pure LCD demonstrated an endothermic peak at 228°C, showing a crystalline structure.[28] According to DSC analyses, no endothermic peaks were revealed in the thermograms of the nanoparticles prepared, showing the amorphous state of the polymeric lattice. The disappearance of LCD peaks in all thermograms of nanoparticles prepared indicated that LCD was molecularly dispersed in the polymeric structure.[7,21,23]

Fourier transform infrared spectrophotometry

FT-IR spectroscopy reveals information about the molecular interactions of chemical components and is beneficial for assessing microstructural changes in the polymeric structure.[29]

The FT-IR spectrum of LCD showed bands assigned to the aromatic -CH (3110-3000 cm^{-1}) and aliphatic -CH_2 (2985.6-2914.2 cm^{-1}). While the OH dimer of the amino-carboxylic acid appeared at 2628.98 cm^{-1}, the tertiary amine salt was observed at 2349.30 cm^{-1} (Figure 3). The absorption bands at 1745.58 cm^{-1} and 1600.32 cm^{-1} were a result of the carbonyl group and phenyl nucleus skeletal stretching, respectively. The presence of two adjacent benzene rings was shown at 844.8-808.1 cm^{-1}. While

Table 3. Mean particle size, PI, zeta potential of formulations prepared (n=3)

Code	Particle size (nm) ± SE	PI ± SE	Span values ± SD	Zeta potential (mV) ± SE
Placebo	487.42±7.25	0.426±0.085	0.782±0.058	24.3±2.1
F-1	521.70±8.50	0.512±0.090	0.992±0.073	25.7±1.8
F-2	538.46±5.74	0.498±0.074	0.855±0.081	25.9±2.5

PI: Polydispersity index, SE: Standard error

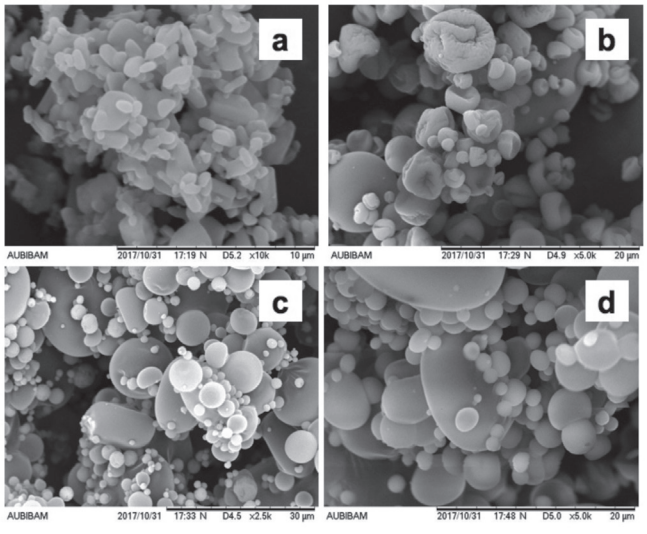

Figure 1. Scanning electron microscope images of pure LCD and formulations; a) LCD, b) placebo, c) F-1, d) F-2

LCD: Levocetirizine dihydrochloride

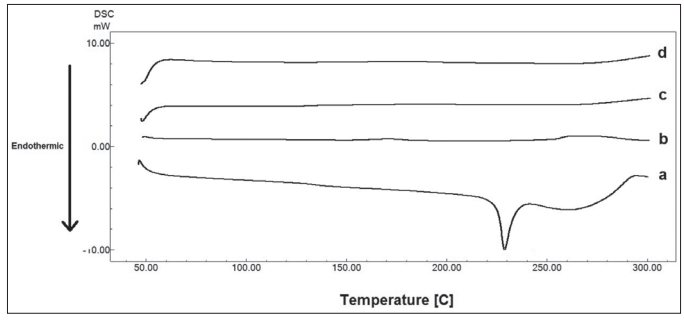

Figure 2. Differential scanning calorimetry thermograms of pure LCD and formulations; a) LCD, b) placebo, c) F-1, d) F-2

LCD: Levocetirizine dihydrochloride, SD: Standard deviation

the carboxylic C-O bond frequency was observed at 1463-1263 cm^{-1}, the aliphatic chain C-O bond in $CH_2CH_2OCH_2COOH$ appeared at 1180.4 cm^{-1} and at 758 cm^{-1}.[30] The placebo formulation showed similar absorption bands with pure chitosan. The FT-IR spectrum of the placebo formulation showed characteristic absorption bands at 3352, 2918, and 2850 cm^{-1}, which represent -OH, -CH_2, and CH_3 aliphatic groups, and bands at 1558 and 1417 cm^{-1} represent the -NH group bending vibration and vibrations of the -OH group of the primary alcohol, respectively. The amino group has a characteristic band at 3400-3500 cm^{-1} that is concealed by the broad absorption band of the -OH group.[31] Distinctive peaks of LCD were not seen in the spectra of F-1 or F-2 formulations, indicating the molecular dispersion of LCD in the polymeric matrices, which was supported by the DSC results.[7] The absence of LCD distinctive peaks confirmed encapsulation of the drug within the polymeric structure.[6]

Nuclear magnetic resonance spectroscopy

The physicochemical properties of nanoparticles can be identified by NMR analysis in a variety of dosage forms to elucidate the status of active agent incorporated into matrices, its molecular mobility, and molecular interactions between the active agent and the excipients.[12] Peaks appeared in the broad multiplet between 7 and 8 ppm belonging to peaks of 16 aromatic CH protons and 2 NH protons (Figure 4).[32] A singlet was observed at 3.33 ppm for the methyl diphenyl CH proton. A triplet at 3.83 ppm was obvious due to four protons on the acyclic CH_2 groups. Another singlet at 3.51 ppm with two protons was shown for the CH_2 in CH_2CH_2O entity. The CH_2 in the CH_2COOH group appeared as a singlet at 3.73 ppm. A very weak singlet was present at 10.6 ppm for the one proton of the carboxylic acid group.[33] Some characteristic peaks of LCD were found also in the spectra of nanoparticle formulations, indicating successful incorporation of drug into the nanoparticles with no chemical changes.[34] The data were also supported by the DSC and FT-IR results.

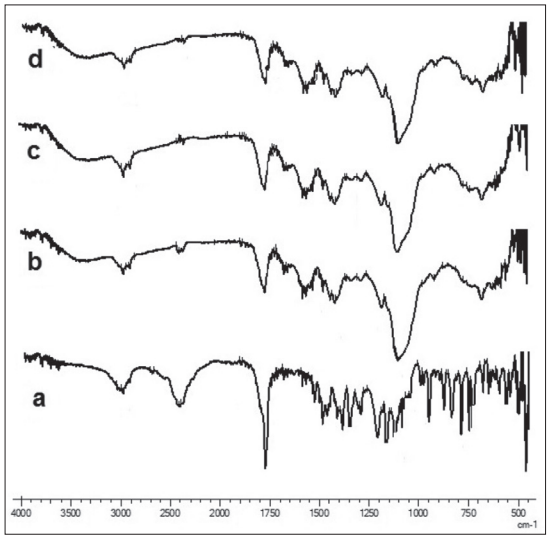

Figure 3. Fourier transform infrared spectra of pure LCD and formulations; a) LCD, b) placebo, c) F-1, d) F-2

LCD: Levocetirizine dihydrochloride

Determination of LCD

The analytical process validation method of the International Harmonization Committee was used in the present study. The method was validated for linearity, accuracy, precision, sensitivity, and specificity with reference to the guidelines.[35] The separation and resolution of the LCD from formulations could be achieved using a mixture of acetonitrile:water:1 M sulfuric acid (93:66:4, v/v/v) as the mobile phase with UV detection at 230 nm.[18] The calibration curve was constructed by plotting the peak area ratio (y) of the LCD concentration. The linearity of the method was examined in the range of 2.5-250 $\mu g.mL^{-1}$ and the calibration curve was chosen in this range (Figure 5). Good fit of the equation was found, y=2398.3252x+6416.2523, with a correlation coefficient of 0.9996. The limit of detection (LOD) and limit of quantification (LOQ) values were 0.7968 $\mu g.mL^{-1}$ and 2.4146 $\mu g.mL^{-1}$, respectively. Accuracy is the similarity of the

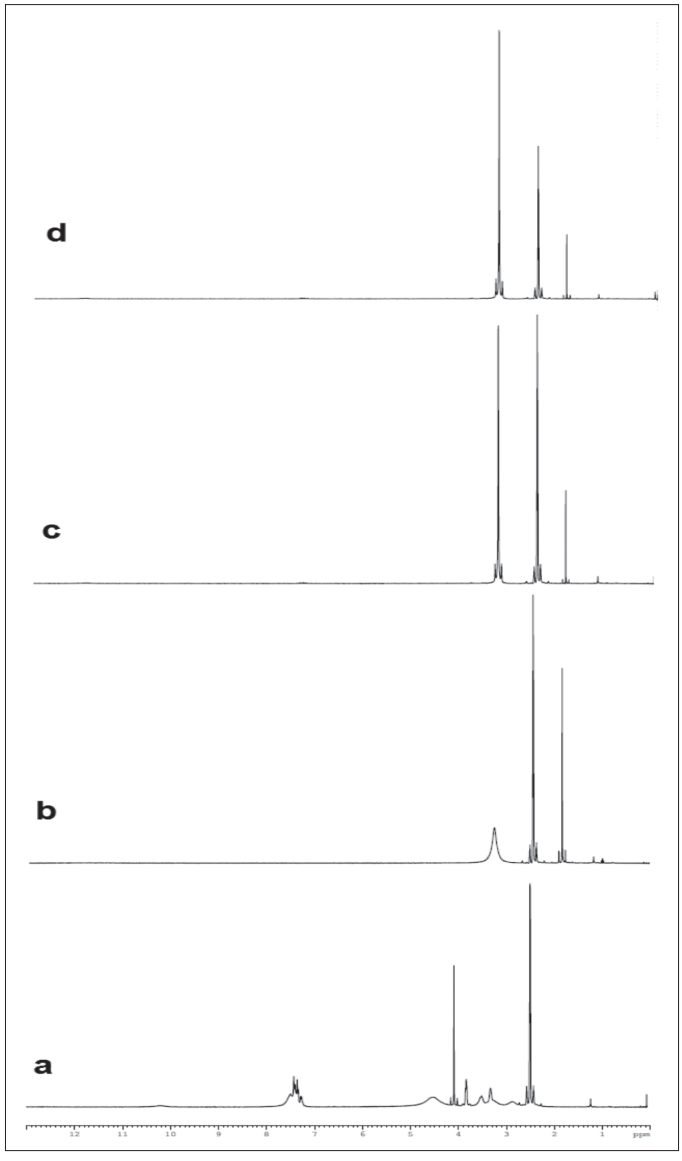

Figure 4. Nuclear magnetic resonance spectra of pure LCD and formulations; a) LCD, b) placebo, c) F-1, d) F-2

LCD: Levocetirizine dihydrochloride

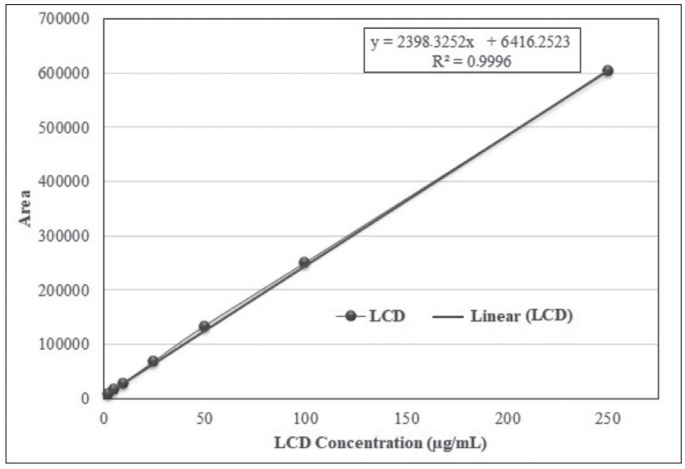

Figure 5. Calibration curve of levocetirizine dihydrochloride
LCD: Levocetirizine dihydrochloride

test results obtained by the analytical method to the true values. It was reported that recovery values must be in the range of 98%-102% to decide on the accuracy of the method used. The HPLC method used in this study yielded high recovery values (98%-100%) (Table 4), which indicated the accuracy of the method used. Measurements obtained with three different concentrations (low, medium, and high) evaluating repeatability and reproducibility of the analytical method used seem to verify the precision of the method since the percentage of relative standard deviation (RSD) was below 2%, which is within the targeted interval (Table 5).[36] Meanwhile this method was specific for the determination and quantification of LCD. The method validation conducted proved the accuracy, reliability, and specificity of the method. It was found that all the results of the present coefficient of variation are below 2%, showing the method was valid.[37,38]

Encapsulation efficiency

The EE is the percentage of the amount of the drug loaded into polymeric matrices. In the present study, EE % was 71.37±1.32 and 67.328±2.09 (EE % ± SE) for F-1 and F-2, respectively. Drug-polymer composition is most likely one of the reasons for the *in vitro* release rate; however, it seems that a complex phenomenon between active agent and polymer molecules may occur, including entrapment of drug within the polymeric network and the adsorption of drug molecules on the surface of polymeric matrices as a result of electrostatic adhesion.[39,40]

In vitro drug release

Dissolution testing has been recognized as an important tool for both drug development and quality control.[41] It can be used not only as a primary tool to monitor the consistency and stability of drug products but also as a relatively rapid and inexpensive technique to predict *in vivo* absorption of a drug formulation.[19] The release profiles obtained from chitosan nanoparticles are given in Figure 6. The release profile of pure LCD was used as reference. LCD release from nanoparticles was much slower than that of its pure form, showing a time-dependent release manner in release media. Moreover, there was no significant

Table 4. Accuracy and recovery results

LCD (µg.mL^{-1})	Recovery (µg.mL^{-1})	Recovery (%)	SE	RSD
5	4.9039	98.0775	0.7582	1.3391
50	50.0427	100.0855	1.4125	2.4445
250	248.8017	99.5207	0.1239	0.2157

SE: Standard error; RSD: Relative standard deviation, LCD: Levocetirizine dihydrochloride

Table 5. Interday and intraday precision results

LCD (µg. mL^{-1})	Intraday (n=3)				Interday (n=9)
		Day 1	Day 2	Day 3	
5	Mean area	18466	18137	18203	18269
	SD	0.0981	0.0885	0.0666	0.0725
	RSD	1.9535	1.8111	1.3560	1.4680
50	Mean area	132707	132835	12858	131353
	SD	0.2954	0.8360	0.6790	1.0241
	RSD	0.5610	1.5860	1.3336	1.9660
250	Mean area	609100	610793	603723	607842
	SD	0.4775	0.7398	0.7237	1.5391
	RSD	0.1900	0.2936	0.2906	0.6137

SE: Standard error; RSD: Relative standard deviation, LCD: Levocetirizine dihydrochloride, SD: Standard deviation

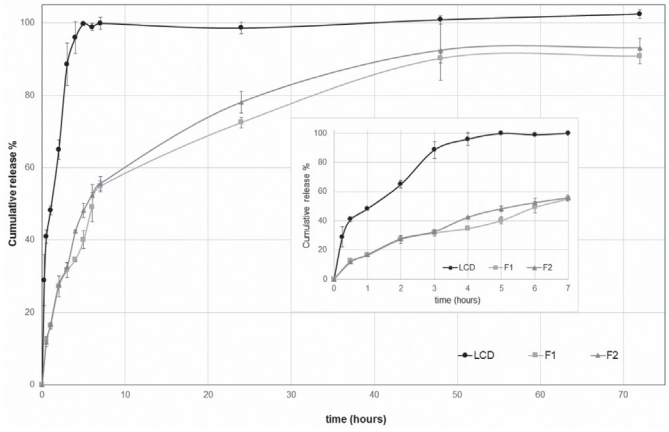

Figure 6. *In vitro* release profiles of levocetirizine dihydrochloride from nanoparticles prepared (n=3) (mean ± standard error)

difference between F-1 and F-2 formulations as stated by the release profiles ($p>0.05$).[21] The release rate was not affected significantly by increasing the amount of LCD used in the nanoparticles. Moreover, drug release was extended more than 2-fold with nanoparticles, which enhances their possible use for better treatment.

In vitro release kinetics

Quantitative evaluation of drug dissolution characteristics is of great interest to pharmaceutical scientists. Drug release data were evaluated using many mathematical and statistical parameters.[19]

Fitting *in vitro* release profiles to mathematical models describing drug release as a function of time gives valuable data about the *in vivo* release behavior of optimal delivery systems.[42] Therefore, *in vitro* release kinetics were also evaluated for nanoparticles in comparison with pure LCD using DDSolver.[19]

In vitro dissolution data were transferred to DDSolver to determine five important and the most popular criteria. These criteria were based on the coefficient of determination (Rsqr, R^2, or COD), the adjusted coefficient of determination ($R^2_{adjusted}$), the Akaike information criterion (AIC), the model selection criterion (MSC), and n for only Korsmeyer–Peppas models. The highest R^2, $R^2_{adjusted}$, and MSC values and the lowest AIC values were used for the evaluation of the best fitted models.[19,43] Zero-order kinetics, first-order kinetics, Higuchi, Hixson–Crowell, Korsmeyer–Peppas, and Hopfenberg models were selected for evaluation in DDSolver. The majority of these models usually have nonlinear equations. DDSolver has been developed to utilize the hardships encountered in comparing free profiles with several different dissolution parameters for eliminating many experimental mistakes and the other mistakes due to the user.[19] The R^2, $R^2_{adjusted}$, MSC, and AIC values obtained as a result of applying *in vitro* release study data to different kinetic models using DDSolver are shown in Table 6. Release of pure LCD fit best the first-order model, where drug release is concentration dependent. *In vitro* release from chitosan nanoparticles fit best the Korsmeyer–Peppas model according to all the criteria. This model indicates diffusion controlled release from a polymeric matrix nano-system developed.[9,23] 'n' is the diffusional release exponent that could be used to characterize the different release mechanisms [n≤0.45 (Fickian diffusion), 0.45<n<1 (anomalous transport), and n=1 (case II transports; i.e. zero-order release)]. The Korsmeyer–Peppas equation proposed that release of LCD from the polymeric matrices was through Fickian diffusion (n=0.290 and n=0.420 for F-1 and F-2, respectively). This information suggests that LCD release from the nanoparticles was through diffusion.[44]

CONCLUSION

In this study, LCD was used as a model drug to be entrapped in a natural biodegradable material (chitosan) using spray drying. The results of analyses demonstrated that nanometer-sized spherical nanoparticles were achieved with this technique. Moreover, the nanoparticles showed a narrow size distribution, cationic characteristic, and relatively high EE. Solid state characterization studies such as DSC, FT-IR, and ^{1}H-NMR confirmed the successful incorporation into the polymeric matrices. It was shown that all nanoparticles displayed a prolonged release pattern without a burst effect in comparison

Table 6. Release kinetic modeling of levocetirizine dihydrochloride-loaded nanoparticles

Code	Model and equation	Evaluation criteria					
		k	R^2	$R^2_{adjusted}$	AIC	MSC	n
LCD	Zero-order model* $F=k_0*t$	2.100	-8.446	-8.446	120.841	-2.427	-
F-1		1.682	-0.180	-0.180	101.939	-0.347	-
F-2		1.745	-0.335	-0.335	103.943	-0.471	-
LCD	First-order model* $F=100*[1-Exp(-k_1*t)]$	0.805	0.932	0.932	66.594	2.504	-
F-1		0.060	0.745	0.745	85.068	1.186	-
F-2		0.068	0.741	0.741	85.904	1.169	-
LCD	Higuchi model* $F=k_H*t^{0.5}$	19.106	-3.304	-3.304	112.194	-1.641	-
F-1		13.298	0.794	0.794	82.722	1.400	-
F-2		13.931	0.738	0.738	86.047	1.156	-
LCD	Hixson–Crowell model* $F=100*[1-(1-k_{HC}*t)^3]$	0.027	-4.977	-4.977	115.807	-1.970	-
F-1		0.014	0.565	0.565	90.958	0.651	-
F-2		0.016	0.521	0.521	92.659	0.555	-
LCD	Korsmeyer–Peppas* $F=k_{KP}*t^n$	97.701	-0.321	-0.468	101.200	-0.642	0.000
F-1		25.722	0.929	0.921	73.074	2.277	0.290
F-2		20.211	0.843	0.826	82.370	1.490	0.420
LCD	Hopfenberg model* $F=100*[1-(1-k_{HB}*t)^n]$	0.081	0.132	0.035	96.584	-0.222	3.000
F-1		0.014	0.565	0.517	92.958	0.469	3.000
F-2		0.016	0.522	0.469	94.652	0.374	3.000

*In all models, *F* is the fraction (%) of drug released in time t, k_0: zero-order release constant, k_1: first-order release constant, k_H: Higuchi release constant, k_{HC}: Hixson-Crowell release constant k_{KP}: release constant incorporating structural and geometric characteristics of the drug-dosage form, *n*: is the diffusional exponent indicating the drug-release mechanism, F_0 is the initial fraction of the drug in the solution resulting from a burst release, k_{HB}: Hopfenberg release constant, LCD: Levocetirizine dihydrochloride

with the pure drug. According to the criteria, formulations were fitted to the Korsmeyer–Peppas model demonstrating the diffusion mechanism of polymeric matrices. *In vitro* studies showed that cationic chitosan nanoparticles containing LCD are effective carrier candidates for reducing local irritation to GI membranes and other side effects and optimizing plasma drug concentration improving bioavailability and protection of sensitive drugs against light, thus also improving their stability. However, *in vivo* analyses are required for a final decision to be made.

ACKNOWLEDGEMENTS

The authors would like to thank BIBAM (Anadolu University) management for the spray dryer equipment and Exp. Serkan Levent (DOPNA-LAB, Anadolu University) for FT-IR and NMR studies.

Conflicts of interest: No conflict of interest was declared by the authors.

REFERENCES

1. Prabhu P, Malli R, Koland M, Vijaynaryana K, D'Souza U, Harish NM, Shastry CS, Charyulu RN. Formulation and evaluation of fast dissolving films of levocetirizine dihydrochloride. Int J Pharm Investig. 2011;1:99-104.
2. Goindi S, Kumar G, Kaur A. Novel flexible vesicles based topical formulation of levocetirizine: *in vivo* evaluation using oxazolone-induced atopic dermatitis in murine model. J Liposome Res. 2014;24:249-257.
3. Takahashi H, Ishida-Yamamato A, Iizuka H. Effects of bepotastine, cetirizine, fexofenadine, and olopatadine on histamine-induced wheal- and flare-response, sedation, and psychomotor performance. Clin Exp Dermatol. 2004;29:526-532.
4. El-Say KM, El-Hewl ARM, Ahmed OAA, Hosny KM, Ahmed TA, Kharshoum RM, Fahmy UA, Alsawahli M. Statistical optimization of controlled release microspheres containing cetrizine hydrochloride as a model for water soluble drugs. Pharm Dev Technol. 2015;20:738-746.
5. Li F, Ji R, Chen X, You B, Pan Y, Su J. Cetrizine dihydrochloride loaded microparticles design using ionotropic cross-linked chitosan nanoparticles by spray-drying method. Arch Pharm Res. 2010;33:1967-1973.
6. Vino S, Preethi LR, Gopika M, Ghosh AR. Controlled release formulation of levocetirizine dihydrochloride by casein microparticles. Afr J Pharm Pharmaco. 2013;7:1046-1053.
7. Yurtdaş-Kırımlıoğlu G, Yazan Y. Formulation and *in vitro* characterization of polymeric nanoparticles designed for oral delivery of levofloxacin hemihydrate. Euro Int J Sci Technol. 2016;5:148-157.
8. Foged C, Brodin B, Frokjaer S, Sundblad, A. Particle size and surface charge affect particle uptake by human dendritic cells in an *in vitro* model. Int J Pharm. 2005;298:315-322.
9. Dash M, Chiellini F, Ottenbrite RM, Chiellini E. Chitosan - a versatile semi-synthetic polymer in biomedical applications. Prog Polym Sci. 2011;36:981-1014.
10. Vino S, Paryani P, Sajitha LS, Ghosh AR. Formulation and evaluation of chitosan beads of levocetirizine dihydrochloride. J Appl Pharm Sci. 2012;2:221-225.
11. Agnihotri SA, Mallikarjuna NN, Aminabhavi TA. Recent advances on chitosan-based micro-and nanoparticles in drug delivery. J Control Release. 2004;100:5-28.
12. Başaran E, Yenilmez E, Berkman MS, Büyükköroğlu G, Yazan Y. Chitosan nanoparticles for ocular delivery of cyclosporine A. J Microencapsul. 2014;31:49-57.
13. Sinha VR, Singla AK, Wadhawan S, Kaushik R, Kumria R, Bansal K, Dhawan S. Chitosan microspheres as a potential carrier for drugs. Int J Pharm. 2004;274:1-33.
14. Re M. Formulating drug delivery systems by spray drying. Dry Technol. 2006;24:433-446.
15. He P, Davis SS, Illum L. Chitosan microspheres prepared by spray drying. Int J Pharm. 1999;187:53-65.
16. Corrigan DO, Healy AM, Corrigan OI. Preparation and release of salbutamol from chitosan and chitosan co-spray dried compacts and multiparticulates. Eur J Pharm Biopharm. 2006;62:295-305.
17. Teeranachaideekul V, Souto EB, Junyaprasert VB, Müller RH. Cetyl palmitate-based NLC for topical delivery of Coenzyme Q_{10} - development, physicochemical characterization and in vitro release studies. Eur J Pharm Biopharm. 2007;67:141-148.
18. USP (The United States Pharmacopeia), Levocetirizine Dihydrochloride, 2017. Available from: http://www.uspnf.com/sites/default/files/usp_pdf/EN/USPNF/iras/levocetirizine-dihydrochloride-m3460-ira.pdf
19. Zhang Y, Huo M, Zhou J, Zou A, Li W, Yao C, Xie S. DDSolver: an add-in program for modelling and comparison of drug dissolution profiles. AAPS Journal. 2010;12:263-271.
20. Sormoli ME, Islam MIU, Langrish TAG. The effect of chitosan hydrogen bonding on lactose crystallinity during spray drying. J Food Eng. 2012;108:541-548.
21. Yenilmez E, Yurtdaş-Kırımlıoğlu G, Şenel B, Başaran E. Preparation, characterization and *in vitro* evaluation of dirithromycin loaded Eudragit RS 100 nanoparticles for topical application. Lat Am J Pharm. 2017;36:2203-2212.
22. Lopedota A, Trapani A, Cutrignelli A, Chiarantini L, Pantucci E, Curci R, Manuali E, Trapani G. The use of Eudragit RS 100/cyclodextrin nanoparticles for the transmucosal administration of glutathione. Eur J Pharm Biopharm. 2009;72:509-520.
23. Öztürk AA, Yenilmez E, Arslan R, Şenel B, Yazan Y. Dexketoprofen trometamol-loaded Kollidon® SR and Eudragit® RS 100 polymeric nanoparticles: formulation and *in vitro-in vivo* evaluation. Lat Am J Pharm. 2017;36:2153-2165.
24. Tan CP, Nakajima M. β-Carotene nanodispersions: preparation, characterization and stability evaluation. Food Chem. 2005;92:661-667.
25. Honary S, Zahir F. Effect of zeta potential on the properties of nano-drug delivery systems - a review (part 1). Trop J Pharm Res. 2013;12:255-264.
26. Radomska-Soukharev A. Stability of lipid excipients in solid lipid nanoparticles. Adv Drug Deliver Rev. 2007;59:411-418.
27. Castelli F, Puglia C, Sarpietro MG, Rizza L, Bonina F. Characterization of indomethacin-loaded lipid nanoparticles by differential scanning calorimetry. Int J Pharm. 2005;304:231-238.
28. Choudhury P, Deb P, Dash S. Formulation and statistical optimization of bilayer sublingual tablets of levocetirizine hydrochloride and ambroxol hydrochloride. Asian J Pharm Clin Res. 2016;9:228-234.

29. Saito Y, Iwata T. Characterisation of hydroxyl groups of highly crystalline-chitin under static tension detected by FT-IR. Carbohydr Polym. 2012;87:2154-2159.

30. Kenawi IM, Barsoum BM, Youssef MA. Drug-drug interaction between diclofenac, cetirizine and ranitidine. J Pharm Biomed Anal. 2005;37:655-661.

31. Sionkowska A, Wisniewski M, Skopinska J, Kennedy CJ, Wess TJ. Molecular interactions in collagen and chitosan blends. Biomaterials. 2004;25:795-801.

32. Ali SM, Upadhyay SK, Maheshwari A. NMR spectroscopic study of inclusion complexes of cetirizine dihydrochloride and β-cyclodextrin in solution. Spectroscopy. 2007;21:177-182.

33. Shamshad H, Arayne MS, Sultana N. Spectroscopic characterization of *in vitro* interactions of cetirizine and NSAIDS. J Anal Sci Technol. 2014;5:1-8.

34. Yurtdaş-Kırımlıoğlu G, Yazan Y. Development, characterization and *in vitro* release characteristics of rabeprazole sodium in halloysite nanotubes. Euro Int J Sci Technol. 2016;5:99-109.

35. ICH, Q2R1 2005. Harmonised Tripartite Guideline, Validation of Analytical Procedure: Text and Methodology, Complementary Guideline on Methodology, in: Proceedings of the International Conference on Harmonization, Canada. Available from: https://www.ema.europa.eu/en/documents/scientific-guideline/ich-q-2-r1-validation-analytical-procedures-text-methodology-step-5_en.pdf

36. Shabir GA. Validation of high-performance liquid chromatography methods for pharmaceutical analysis. Understanding the differences and similarities between validation requirements of the US Food and Drug Administration, the US Pharmacopeia and the International Conference on Harmonization. J Chromatogr A. 2003;987:57-66.

37. Yurtdaş-Kırımlıoğlu G, Yazan Y. Determination of gamma-aminobutyric acid by HPLC: its application to polymeric nanoparticles and stability studies. Int J Develop Res. 2016;6:8277-8282.

38. Öztürk AA, Yenilmez E, Yazan Y. Development and validation of high performance liquid chromatography (HPLC) modified method for dexketoprofen trometamol. Euro Int J Sci Technol. 2017;6:33-41.

39. Adibkia K, Javadzadeh Y, Dastmalchi S, Mohammadi G, Niri FK, Alaei-Beirami M. Naproxen-Eudragit® RS100 nanoparticles: preparation and physicochemical characterization. Colloids Surf B Biointerfaces. 2011;83:155-159.

40. Thagele R, Mishra A, Pathak AK. Formulation and characterization of clarithromycin based nanoparticulate drug delivery system. Int J Pharm Life Sci. 2011;2:510-515.

41. Zuo J, Gao Y, Bou-Chacra N, Löbenberg R. Evaluation of the DDSolver software applications. Biomed Res Int. 2014;ArticleID204925:1-9.

42. Costa P, Sousa Lobo JM. Modeling and comparison of dissolution profiles. Eur J Pharm Sci. 2001;13:123-133.

43. Victor OB, Francis OA. Evaluation of the kinetics and mechanism of piroxicam release from lipophilic and hydrophilic suppository bases. Int J ChemTech Res. 2017;10:189-198.

44. Sharma UK, Verma A, Prajapati SK, Pandey H, Pandey AC. *In vitro, in vivo* and pharmacokinetic assessment of amikacin sulphate laden polymeric nanoparticles meant for controlled ocular drug delivery. Appl Nanosci. 2015;5:143-155.

Turk J Pharm Sci 2020;17(1):36-42
DOI: 10.4274/tjps.galenos.2018.26056

ORIGINAL ARTICLE

GC/MS Analysis of Alkaloids in *Galanthus fosteri* Baker and Determination of Its Anticholinesterase Activity

Galanthus fosteri Baker'da Alkaloitlerin GC/MS Analizi ve Antikolinesteraz Aktivitesinin Belirlenmesi

Ahmet EMİR*, Ceren EMİR, Buket BOZKURT, Nehir ÜNVER SOMER

Ege University, Faculty of Pharmacy, Department of Pharmacognosy, Bornova, İzmir, Turkey

ABSTRACT

Objectives: Amaryllidaceae alkaloids are well known for their wide range of pharmacological activities. Galanthamine, an Amaryllidaceae alkaloid, is an effective, selective, reversible, and competitive cholinesterase inhibitor marketed under different commercial names in several countries for the treatment of Alzheimer's disease. The aim of this work was to study the alkaloid profiles of the aerial parts and bulbs of both flowering and fruiting periods of *Galanthus fosteri* Baker (Amaryllidaceae), as well as analyzing their inhibitory activities on both acetylcholinesterase (AChE) and butyrylcholinesterase (BuChE) for the first time.

Materials and Methods: The alkaloid profiles of the four samples were determined by means of gas chromatography-mass spectrometry, and AChE and BuChE inhibition assays were performed by the modified Ellman method.

Results: Totally, 22 compounds with mass spectral characteristics of Amaryllidaceae alkaloids were detected in the extracts. Significant AChE and BuChE inhibitory activities were observed in the tested samples (IC_{50} between 0.189 and 91.23 µg/mL).

Conclusion: This study shows that *G. fosteri*, collected from Akdağ, Amasya (Turkey), is a potential source of diverse chemical structures of Amaryllidaceae alkaloids with cholinesterase inhibitory properties.

Key words: *Galanthus fosteri*, Amaryllidaceae alkaloids, anticholinesterase activity

ÖZ

Amaç: Amaryllidaceae alkaloitleri geniş yelpazedeki farmakolojik aktiviteleriyle iyi bilinmektedir. Bir Amaryllidaceae alkaloidi olan Galantamin, Alzheimer hastalığının tedavisi için çeşitli ülkelerde farklı ticari isimler altında pazarlanan etkili, seçici, geri dönüşümlü ve kompetitif kolinesteraz inhibitörüdür. Bu çalışma, ilk kez *Galanthus fosteri* Baker'in (Amaryllidaceae), hem çiçekli hem de meyveli dönemlerinin toprak üstü ve soğanlarının alkaloit profilini incelemenin yanı sıra hem asetilkolinesteraz (AChE) hem de butirilkolinesteraz (BuChE) üzerindeki inhibitör aktivitelerini analiz etmeyi amaçlamıştır.

Gereç ve Yöntemler: Dört örneğin alkaloit profilleri gaz kromatografisi-kütle spektrometrisi ile belirlendi ve AChE ve BuChE inhibisyon analizleri modifiye Ellman yöntemi ile yapılmıştır.

Bulgular: Ekstrelerde Amaryllidaceae alkaloitlerinin kütle spektral özellikleri olan toplam yirmi iki bileşik tespit edilmiştir. Test edilen örneklerde belirgin şekilde AChE ve BuChE inhibitör aktiviteler gözlenmiştir (IC*50* 0,189 ile 91,23 µg/mL arasında).

Sonuç: Bu çalışma, Amasya Akdağ'dan (Türkiye) toplanan *G. fosteri*'nin kolinesteraz inhibitör özelliğine sahip çeşitli kimyasal yapıdaki Amaryllidaceae alkaloitlerinin kaynağı olma potansiyeline sahip olduğunu göstermiştir.

Anahtar kelimeler: *Galanthus fosteri*, Amaryllidaceae alkaloitleri, antikolinesteraz aktivite

***Correspondence: E-mail:** ahmet.emir@ege.edu.tr, **Phone:** +90 505 393 21 09 **ORCID-ID:** orcid.org/0000-0002-0971-7716
Received: 09.07.2018, **Accepted:** 11.10.2018

INTRODUCTION

Galanthus fosteri (*G. fosteri*) Baker (snowdrop) is a bulbous monocotyledon plant belonging to the family Amaryllidaceae occurring mainly in south- and north-central Turkey.[1] Plants of this family are known to possess alkaloids with diverse chemical structures and a wide spectrum of biological activities such as cholinesterase inhibitory, antimalarial, hepatoprotective, antitumoral, anti-inflammatory, and antiviral.[2-7] Alzheimer's disease (AD), the most common cause of dementia and affecting approximately 46.8 million people worldwide, is a neurodegenerative disease characterized by widespread loss of central cholinergic function.[8] The human central nervous system contains two cholinesterases: acetylcholinesterase (AChE), encoded by a gene on chromosome 7, and butyrylcholinesterase (BuChE), encoded by a gene on chromosome 3. Although the role of AChE in the cholinergic system is well known, the role of BuChE is poorly understood. However, each enzyme alone is not sufficient for acetylcholine metabolism and cholinergic transmission.[9,10] Therefore, in the treatment of AD, it is important to inhibit AChE as well as BuChE. Galanthamine, the most important alkaloid found in Amaryllidaceae plants, marketed under the commercial name of Reminyl® in Europe and elsewhere and Razadine® in the USA, is used to treat AD owing to its cholinesterase inhibitory properties.[11]

It has been found that Amaryllidaceae alkaloids can be analyzed by gas chromatography-mass spectrometry (GC/MS) without any previous derivatization, and they show a mass spectral fragmentation pattern very similar to those recorded.[12] In the present study, the alkaloid profile of *G. fosteri* was determined by GC/MS, using both bulbs and aerial parts of the flowering and fruiting periods. In addition, cholinesterase inhibitory activity potentials of the extracts were examined spectrophotometrically using a microplate assay modified from Ellman's *in vitro* method with a 96-well micro-plate reader.[13,14]

MATERIALS AND METHODS

Plant material

G. fosteri was collected from Akdağ, Amasya, on March 28, 2012 and April 1, 2013 during the flowering and fruiting periods, respectively. The plants were identified by Prof. M. Ali Onur from the Department of Pharmacognosy, Faculty of Pharmacy, Ege University, İzmir, Turkey. Voucher samples of *G. fosteri* (No: 1516, 1525) are deposited in the Herbarium of the Department of Pharmacognosy, Faculty of Pharmacy, Ege University.

Alkaloid extraction

The alkaloidal extracts were prepared from air-dried and powdered aerial parts and bulbs of *G. fosteri* Baker to be used in GC/MS analysis and in the anticholinesterase activity assay. Plant material (500 mg) was separately extracted 3 times with methanol (5 mL) at room temperature. The solvent was evaporated under reduced pressure, the residues were dissolved in 10 mL of 2% sulfuric acid, and the neutral compounds were removed with diethyl ether (3×10 mL). The acidic aqueous phases were basified with 25% ammonia to pH 9-10 and the alkaloids were extracted with chloroform (3×10 mL). The combined chloroform extracts were then dried over anhydrous sodium sulfate, filtered, and the organic solvent was distilled *in vacuo* to afford the alkaloidal extract.[15] The obtained extracts were used for GC/MS analysis and also screened for anticholinesterase activity.

GC/MS analysis

The GC/MS analysis was performed using Thermo GC-Trace Ultra Ver: 2.0., Thermo MS DSQ II (Thermo Fisher Scientific, San Jose, CA, USA) operating in electron impact mode (EI, 70 eV). The oven temperature was programmed as 80°C for 1 min, 80-250°C (10°C min^{-1}), 250°C for 2 min, 250-300°C (10°C min^{-1}), and a 10 min hold at 300°C. The injector temperature was 250°C. Helium was used as carrier gas at a flow rate of 0.8 mL min^{-1}. A TR-5 MS column (30 m×0.25 mm×0.25 µm) was used. The extracts were dissolved in methanol (1 mg of extract in 500 µL of methanol). All injections were run in splitless mode. The spectra of co-eluting chromatographic peaks were investigated and deconvoluted by the use of Xcalibur (version 2.07; Thermo Fisher Scientific San Jose, CA, USA). The compounds were identified by comparing their mass spectral fragmentation with standard reference spectra from the NIST 05 database (NIST Mass Spectral Database, PC-Version 5.0 (2005), National Institute of Standardization and Technology, Gaithersburg, MD, USA), or applying co-chromatography with previously isolated authentic standards and in comparison with data obtained from the literature. The percentage of total ion current for each compound is given in Table 1. The area of the GC/MS peaks depends both on the concentration of the corresponding compound and on the intensity of their mass spectral fragmentation. Moreover, they can be used for a relative comparison of alkaloids.

Anticholinesterase activity

The alkaloidal extracts of the aerial parts and bulbs were tested for their AChE and BuChE inhibitory activities by 96-well microplate assay modified from Ellman's method at the concentration range of 0.006-600 µg/mL (final concentrations in the assay 0.0015-150 µg/mL).[13,14] Galanthamine was used as a positive control. The enzyme inhibitory activity was calculated as the percentage compared to the blank. IC_{50} values were analyzed by the software package Prism V5.0 (GraphPad Inc., San Diego, CA, USA).

RESULTS

A great number of alkaloids present in Amaryllidaceous plant extracts have been separated effectively and identified very quickly by GC/MS, indicating that this method for chemical analysis is useful and reliable for studies on the alkaloid metabolism in this family.[12,16] To the best of our knowledge, this is the first report of a GC/MS study on the alkaloids of *G. fosteri* growing in Turkey. The alkaloid patterns of the samples were normalized and presented as a % of individual compounds in the total alkaloidal mixture based on the deconvoluted peak area (Table 1). The structures of the alkaloids are given in Figure 1. Totally, 22 compounds with mass spectral characteristics

Table 1. GC/MS data and relative composition of the alkaloids in the extracts of *G. fosteri*

Compound	R.T. (min)	[M+]	m/z (relative intensity, %)	Content (percentage of TIC)				References
				Flowering period		Fruiting period		
				Aerial parts	Bulbs	Aerial parts	Bulbs	
Hordenine[a] (1)	11.2	165 (1)	121 (2), 107 (4), 91 (3), 77 (7), 58 (100)	1.86	7.40	6.08	5.85	[17]
M+ 255[a] (2)	16.91	255 (22)	240 (42), 181 (100) 153 (37), 152 (47), 97 (27), 73 (51)	-	-	-	0.11	[18]
Ismine[b] (3)	20.13	257 (29)	238 (100), 211 (6), 196 (11), 168 (8)	0.16	0.22	t	1.35	[19]
Trisphaeridine[b] (4)	21.05	223 (100)	222 (38), 167 (11), 138 (27), 111 (19), 69 (21)	-	0.35	t	1.18	[19]
5,6-Dihydrobicolorine[b] (5)	21.05	239 (36)	238 (100), 180 (15), 129 (65), 113 (18), 112 (25), 111 (27), 71 (37)	t	-	0.16	1.51	[15]
Crinine[c] (6)	21.40	271 (100)	270 (35), 254 (5), 228 (37), 214 (10), 199 (26),185 (31), 150 (51), 122 (54)	0.13	0.27	0.16	-	[20]
Galanthamine[d] (7)	21.60	287 (80)	286 (100), 270 (14), 244 (39), 230 (19), 216 (38)	0.21	0.94	3.18	0.33	S, NIST 05
Galanthindole[e] (8)	22.74	281 (100)	262 (23), 207 (26), 191 (30), 149 (20), 97 (21), 73 (26)	-	-	-	0.33	[21]
9-*O*-Demethylmaritidine[f] (9)	22.84	273 (81)	202 (29), 201 (100), 189 (71), 175 (28), 115 (27)	-	9.07	-	2.62	[22]
Anhydrolycorine[g] (10)	22.98	251 (41)	250 (100), 224 (17), 192 (16), 191 (14), 96 (11)	-	-	-	1.24	[23]
O,N-dimethylnorbelladine[h] (11)	23.22	303 (9)	180 (29), 137 (100), 122 (6), 94 (5), 77 (7)	1.48	2.37	1.04	1.36	[24]
Assoanine[g] (12)	23.56	267 (52)	266 (100), 250 (31), 222 (14), 207 (14), 193 (12), 180 (15)	t	-	-	0.72	[15]
11,12-Didehydroanhydrolycorine[g] (13)	24.03	249 (57)	248 (100), 207 (10), 191 (16) 190 (30), 95 (23),	-	0.67	-	0.96	[25, 26]
Galanthine[g] (14)	24.54	317 (15)	316 (11), 284 (10), 268 (16), 266 (10), 244 (16), 243 (92), 242 (100)	0.36	3.08	0.33	1.08	[19]
11-Hydroxyvittatine[f] (15)	24.89	287 (9)	258 (100), 242 (12), 211 (15), 186 (20), 181 (20), 153 (10), 115 (17)	-	8.37	2.38	13.51	S, [19]
Incartine[g] (16)	25.10	333 (30)	332(77), 259(72), 258(100), 244(18)	24.88	40.03	22.21	32.70	S, [17]
Lycorine[g] (17)	25.28	287 (19)	268 (17), 250 (14), 228 (11), 227 (67), 226 (100), 147 (12)	-	5.39	-	0.97	[23]
9-*O*-methylpseudolycorine[g] (18)	25.36	303 (18)	302 (16), 284 (16), 243 (72), 242 (100), 240 (11), 227 (21), 226 (30), 207 (34)	-	1.34	-	0.99	S, [24]
11-*O*-acetyl-9-*O*-demethylmaritidine[f] (19)	25.8	331 (100)	272 (54), 271 (86), 254 (51), 242 (58), 226 (74), 181 (66), 115 (47)	64.51	12.57	62.79	9.12	S, [24]
3,11-*O*-diacetyl-9-*O*-demethylmaritidine[f] (20)	26.28	373 (42)	254 (38), 242 (48), 229 (69), 227 (66), 226 (98), 211 (90), 181 (100)	5.25	-	3.22	-	S, [24]
Galwesine[i] (21)	26.78	361 (12)	207 (43), 155 (88), 140 (100), 112 (20), 96 (16), 73 (20)	0.21	-	-	-	[20]
Oxoincartine[g] (22)	29.52	347 (40)	273 (100), 258 (68), 207 (42), 73 (16)	0.32	1.54	0.43	2.70	S, [24]

[a]: Other, [b]: Phenanthridine, [c]: Crinine, [d]: Galanthamine, [e]: Indole, [f]: Haemanthamine, [g]: Lycorine, [h]: Norbelladine, [i]: Homolycorine, t: Trace <0.1, S: Standard, TIC: Total ionic concentration, *G. fosteri*: *Galanthus fosteri*

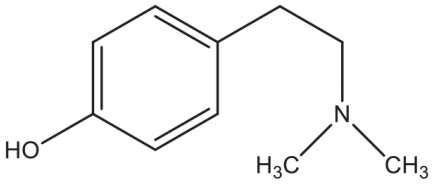
HO
N
H3C
CH3

1

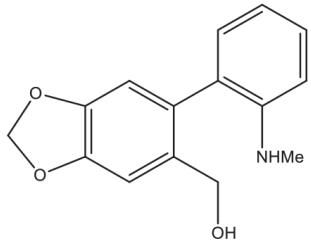
O
O
NHMe
OH

3

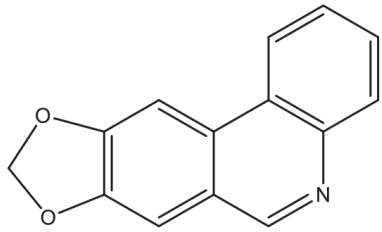
O
O
N

4

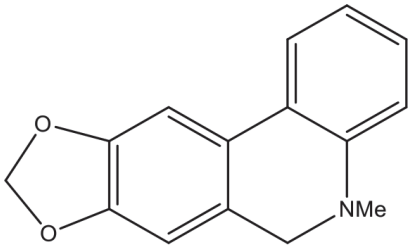
O
O
NMe

5

6

7

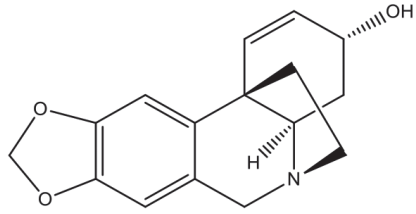
OH
O
O
H
N

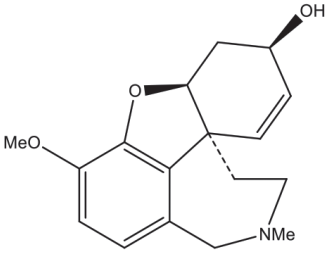
OH
O
MeO
NMe

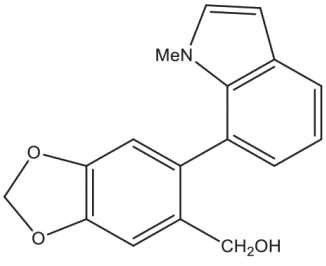
MeN
O
O
CH2OH

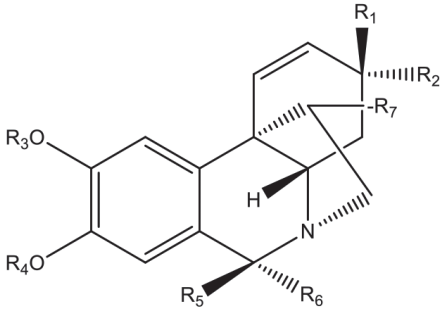
R1
R2
R7
R3O
H
N
R4O
R5
R6

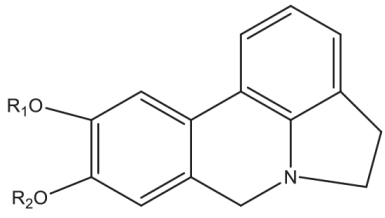
R1O
R2O
N

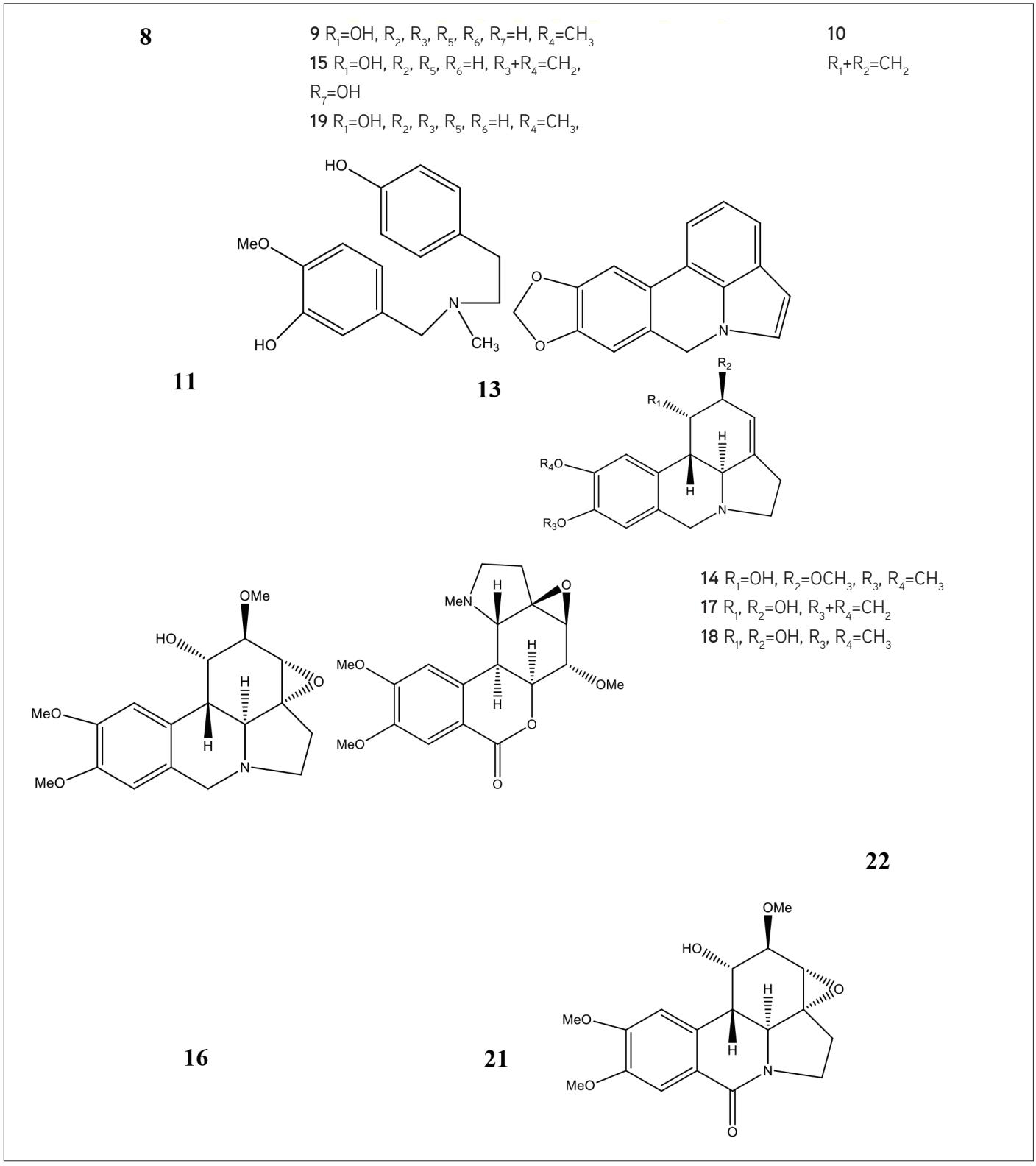

Figure 1. Structures of alkaloids identified in *Galanthus fosteri*: hordenine (1), ismine (3), trisphaeridine (4), 5,6-dihydrobicolorine (5), crinine (6), galanthamine (7), galanthindole (8), 9-*O*-demethylmaritidine (9), anhydrolycorine (10), *O*,N-dimethylnorbelladine (11), assoanine (12), 11,12-didehydroanhydrolycorine (13), galanthine (14), 11-hydroxyvittatine (15), incartine (16), lycorine (17), 9-*O*-methylpseudolycorine (18), 11-O-acetyl-9-*O*demethylmaritidine (19), 3,11-*O*-diacetyl-9-*O*-demethylmaritidine (20), galwesine (21), oxoincartine (22)

of Amaryllidaceae alkaloids were detected in the extracts of the aerial parts and bulbs of both the flowering and fruiting periods (Table 1). The identified compounds possessed various Amaryllidaceae alkaloid skeleton types including lycorine,

haemanthamine, narciclasine, homolycorine, norbelladine, galanthamine, and crinine types and additionally indole alkaloid and another base hordenine. Hordenine is not typical for plants of the family Amaryllidaceae. It has been found mainly in other plant families like Poaceae (*Hordeum vulgare*), Cactaceae (in a very wide range of species), and in a few algae and fungi.[20] In addition, one compound showing mass spectral fragmentation characteristic of Amaryllidaceae alkaloids was left unidentified due to lack of reference MS spectra. Of the 22 alkaloids identified, only seven, hordenine, galanthamine, *O,N*-dimethylnorbelladine, galanthine, incartine, 11-*O*-acetyl-9-*O*-demethylmaritidine, and oxoincartine, were common in all the samples. The results obtained from the microplate assay for cholinesterase inhibitory activity of the samples ranged between 0.189 µg/mL and 91.23 µg/mL; IC_{50} values (µg/mL) are shown in Table 2.

Table 2. Cholinesterase inhibitory activity of extracts

Sample		AChE [IC_{50} (µg/mL)]	BuChE [IC_{50} (µg/mL)]
Flowering period	Aerial parts	13.15	91.23
	Bulbs	8.63	37.125
Fruiting period	Aerial parts	0.189	21.98
	Bulbs	7.12	20.65
Galanthamine		0.043	0.711

AChE: Acetylcholinesterase, BuChE: Butyrylcholinesterase

CONCLUSION

The findings of the present study demonstrate the potential of *G. fosteri* collected in north-central Turkey as a source of cholinesterase inhibitor compounds with diverse chemical structures of Amaryllidaceae alkaloids. The alkaloidal patterns of the aerial parts and bulbs were dominated by 11-*O*-acetyl-9-*O*-demethylmaritidine, which has remarkable AChE and BuChE inhibitory activities with IC_{50} values of 6.04 µM and 29.72 µM, respectively. Furthermore, incartine is the main alkaloid in bulbs and it has shown low anticholinesterase activity.[24] The number of alkaloids in the bulbs was considerably higher in comparison with the aerial parts. Generally, lycorine and haemanthamine type alkaloids were the major components in the tested samples. Thus, the products of *ortho–para'* and *para–para'* oxidative phenolic coupling dominate in samples. Both groups of alkaloids have quite pronounced biological activities. Lycorine type alkaloids have antitumor, antiviral, antibacterial, antifungal, anticholinesterase, and analgesic activities, while haemanthamine type alkaloids have antitumor, antimalarial, antibacterial, analgesic, and anti-inflammatory activities.[27-30] The highest anticholinesterase activity was shown in the aerial parts of the fruiting period, which have the highest relative amount of galantamine. Moreover, the highest BuChE inhibitory activity was detected in the bulbs of the same period, which have the highest number of lycorine type alkaloids. Compared to the other *Galanthus* species[31,32] in which both activities were examined, the aerial parts of the fruiting period stand out with their high AChE inhibitor activity, while BuChE inhibitor activity has similar values. In conclusion, the present study clearly suggests that GC/MS is an appropriate method for the rapid analysis of the qualitative and relative amounts of alkaloid composition in *G. fosteri* specimens, which have diverse alkaloid structures and anticholinesterase activity.

ACKNOWLEDGEMENTS

We thank the Pharmaceutical Science Research Centre (FABAL) and Ege University Research Fund (2014/ECZ/20) for their financial support.

Conflicts of interest: No conflict of interest was declared by the authors.

REFERENCES

1. Davis AP. The genus *Galanthus*-snowdrops in the wild. In: Snowdrops, A Monograph of Cultivated Galanthus. Cheltenham; Griffin Press Publishing Ltd. 2006:9-63.
2. McNulty J, Nair JJ, Little JR, Brennan D, Bastida J. Structure-activity studies on acetylcholinesterase inhibition in the lycorine series of Amaryllidaceae alkaloids. Bioorg Med Chem Lett. 2010;20:5290-5294.
3. Cedrón JC, Gitiérrez D, Flores N, Ravelo ÁG, Estévez-Braun A. Synthesis and antimalarial activity of new haemanthamine-type derivatives. Bioorg Med Chem. 2012;20:5464-5472.
4. Ilavenil S, Kaleeswaran B, Ravikumar S. Protective effects of lycorine against carbon tetrachloride induced hepatotoxicity in Swiss albino mice. Fundam Clin Pharmacol. 2012;26:393-401.
5. Dalecká M, Havelek R, Královec K, Brucková L, Cahlíková L. Amaryllidaceae family alkaloids as potential drugs for cancer treatment. Chem Listy. 2013;107:701-708.
6. Çitoğlu G, Tanker M, Gümüşel B. Antiinflammatory effects of lycorine and haemanthidine. Phytother Res. 1988;12:205-206.
7. He J, Qi WB, Wang L, Tian J, Jiao PR, Liu GQ, Ye WC, Liao M. Amaryllidaceae alkaloids inhibit nuclear-to-cytoplasmic export of ribonucleoprotein (RNP) complex of highly pathogenic avian influenza virus H5N1. Influenza Other Respir Viruses. 2012;7:922-931.
8. Cummings J, Aisen PS, DuBois B, Frölich L, Jack CR Jr, Jones RW, Morris JC, Raskin J, Dowsett SA, Scheltens P. Drug development in Alzheimer's disease: the path to 2025. Alzheimers Res Ther. 2016:8;39.
9. Xie W, Stribley JA, Chatonnet A, Wilder PJ, Rizzino A, Mccomb RD, Taylor P, Hinrichs SH, Lockridgeet O. Postnatal developmental delay and supersensitivity to organophosphate in gene-targeted mice lacking acetylcholinesterase. J Pharmacol Exp Ther. 2000;293:896-902.
10. Mesulam M, Guıllozet A, Shaw P, Levey A, Duysen EG, Lockridge O. Acetylcholinesterase knockouts establish central cholinergıc pathways and can use butyrylcholinesterase to hydrolyze acetylcholine. Neuroscience. 2002;110:627-639.
11. Torras-Claveria L, Berkov S, Codina C, Viladomat F, Bastida J. Daffodils as potential crops of galanthamine. Assessment of more than 100 ornamental varieties for their alkaloid content and acetylcholinesterase inhibitory activity. Ind Crops Prod. 2013;43:237-244.

12. Kreh M, Matusch R, Witte L. Capillary gas chromatography-mass spectrometry of Amaryllidaceae alkaloids. Phytochemistry. 1995;38:773-776.

13. Ellman L, Courtney KD, Andres V Jr, Feather-Stone RM. New and rapid colorimetric determination of acetylcholinesterase activity. Biochem Pharmacol. 1961;7:88-95.

14. López S, Bastida J, Viladomat F, Codina C. Acetylcholinesterase inhibitory activity of some Amaryllidaceae alkaloids and *Narcissus* extracts. Life Sci. 2002;71:2521-2529.

15. Bozkurt B, Emir A, Kaya GI, Önür MA, Berkov S, Bastida J, Somer NÜ. Alkaloid profiling of *Galanthus woronowii* Losinsk. by GC-MS and evaluation of its biological activity. Marmara Pharmaceutical Journal. 2017;21:915-920.

16. Berkov S, Pavlov A, Ilieva M, Burrus M, Popov S. Stanilova M. CGC-MS of alkaloids in *Leucojum aestivum* plants and their in vitro cultures. Phytochem Anal. 2005;16:98-103.

17. Berkov S, Bastida J, Sidjimova B, Francesc V, Codina C. Phytochemical differentiation of Galanthus nivalis and Galanthus elwesii (Amaryllidaceae): A case study. Biochem Syst Ecol. 2008;36:638-645.

18. Cortes N, Alvarez R, Osorio EH, Alzate F, Berkov S, Osorio E. Alkaloid metabolite profiles by GC/MS and acetylcholinesterase inhibitory activities with binding-mode predictions of five Amaryllidaceae plants. J Pharm Biomed Anal. 2015;102:222-228.

19. Torras-Claveria L, Berkov S, Jáuregui O, Caujapé J, Viladomat F, Codina C, Bastida J. Metabolic Profiling of bioactive *Pancratium canariense* extracts by GC-MS. Phytochem Anal. 2010;21:80-88.

20. Berkov S, Romani S, Herrera M, Viladomat F, Codina C, Momekov G, Ionkova I, Bastida J. Antiproliferative alkaloids from *Crinum zeylanicum*. Phytother Res. 2011;25:1686-1692.

21. de Andrade JP, Pigni NB, Torras-Claveria L, Berkov S, Codina C, Viladomat F, Bastida J. Bioactive alkaloid extracts from *Narcissus broussonetii*: Mass spectral studies. J Pharm Biomed. 2012;70:13-25.

22. Bastida J, Llabrés JM, Viladomat F, Codina C, Rubiralta M, Feliz M. 9-O-Demethylmaritidine: A New Alkaloid from *Narcissus radinganorum*. Planta Med. 1988;54:524-526.

23. Berkov S, Evstatieva L, Popov S. Alkaloids in Bulgarian *Pancratium maritimum* L. Z Naturforsch C J Biosci. 2004;59:65-69.

24. Emir A, Emir C, Bozkurt B, Onur MA, Bastida J, Somer NU. Alkaloids from *Galanthus fosteri*. Phytochem Lett. 2016;17:167-172.

25. Berkov S, Bastida J, Tsvetkova R, Viladomat F, Codina C. Alkaloids from Sternbergia colchiciflora. Z Naturforsch C J Biosci 2009;64:311-316.

26. Berkov S, Bastida J, Sidjimova B, Viladomat F, Codina C. Alkaloid diversity in Galanthus elwesii and Galanthus nivalis. Chem Biodivers. 2011;8;115-130.

27. Bastida J, Berkov S, Torras L, Pigni NB, de Andrade JP, Martínez V, Codina C, Viladomat F. Chemical and biological aspects of Amaryllidaceae alkaloids. Transworld Research Network. 2011:65-100.

28. Cedrón JC, Arco-Aguilar MD, Estévez-Braun A, Ravelo AG. Chemistry and Biology of *Pancratium* Alkaloids. 2010;68:1-37.

29. Ding Y, Qu D, Zhang KM, Cang XX, Kou ZN, Xiao W, Zhu JB. Phytochemical and biological investigations of Amaryllidaceae alkaloids: a review. J Asian Nat Prod Res. 2016;19;53-100.

30. He M, Qu C, Gao O, Hu X, Hong X. Biological and pharmacological activities of amaryllidaceae alkaloids. RSC Adv. 2015;5:16562-16574.

31. Kaya GI, Uzun K, Bozkurt B, Onur MA, Somer NU, Glatzel DK, Fürst R. Chemical characterization and biological activity of an endemic Amaryllidaceae species: *Galanthus cilicicus*. S Afr J Bot. 2017;108:256-260.

32. Bozkurt B, Coban G, Kaya GI, Onur MA, Unver-Somer N. Alkaloid profiling, anticholinesterase activity and molecular modeling study of *Galanthus elwesii*. S Afr J Bot. 2017;113;119-127.

Turk J Pharm Sci 2020;17(1):43-8
DOI: 10.4274/tjps.galenos.2018.87699

ORIGINAL ARTICLE

In Vitro Skin Permeation and Antifungal Activity of Naftifine Microemulsions

Naftifin Mikroemülsiyonlarının *İn Vitro* Deriden Permeasyonu ve Antifungal Aktivitesi

Meryem Sedef ERDAL[1]*, Aslı GÜRBÜZ[1], Seher BİRTEKSÖZ TAN[2], Sevgi GÜNGÖR[1], Yıldız ÖZSOY[1]

[1]İstanbul University, Faculty of Pharmacy, Department of Pharmaceutical Technology, İstanbul, Turkey
[2]İstanbul University, Faculty of Pharmacy, Department of Pharmaceutical Microbiology, İstanbul, Turkey

ABSTRACT

Objectives: Microemulsions are fluid, isotropic, colloidal systems that have been widely studied as drug delivery systems. The percutaneous transport of active agents can be enhanced by their microemulsion formulation when compared to conventional formulations. The purpose of this study was to evaluate naftifine-loaded microemulsions with the objective of improving the skin permeation of the drug.

Materials and Methods: Microemulsions comprising oleic acid (oil phase), Kolliphor EL or Kolliphor RH40 (surfactant), Transcutol (co-surfactant), and water were prepared and physicochemical characterization was performed. *In vitro* skin permeation of naftifine from microemulsions was investigated and compared with that of its conventional commercial formulation. Attenuated total reflectance-Fourier transform infrared (ATR-FTIR) spectroscopy was used to evaluate the interaction between the microemulsions and the stratum corneum lipids. *Candida albicans* American Type Culture Collection (ATCC) 10231 and *Candida parapsilosis* were used to evaluate the antifungal susceptibility of the naftifine-loaded microemulsions.

Results: The microemulsion formulation containing Kolliphor RH40 as co-surfactant increased naftifine permeation through pig skin significantly when compared with the commercial topical formulation ($p<0.05$). ATR-FTIR spectroscopy showed that microemulsions increased the fluidity of the stratum corneum lipid bilayers. Drug-loaded microemulsions possessed superior antifungal activity against *Candida albicans* ATCC 10231 and *Candida parapsilosis*.

Conclusion: This study demonstrated that microemulsions could be suggested as an alternative topical carrier with potential for enhanced skin delivery of naftifine.

Key words: Naftifine, microemulsion, colloidal drug carrier system, topical antifungal

ÖZ

Amaç: Mikroemülsiyonlar, ilaç taşıyıcı sistemler olarak çok çalışılan; sıvı, izotropik, kolloidal sistemlerdir. Aktif maddelerin mikroemülsiyonlardan perkütan absorpsiyonu konvansiyonel formülasyona göre iyileşebilmektedir. Bu çalışmanın amacı, naftifin yüklü mikroemülsiyonların, ilacın deriden permeasyonunun iyileştirilmesine yönelik olarak değerlendirilmesidir.

Gereç ve Yöntemler: Oleik asit (yağ fazı), Kolliphor EL veya Kolliphor RH40 (surfaktan), Transcutol (ko-surfaktan) ve sudan oluşan mikroemülsiyonlar hazırlanarak fizikokimyasal karakterizasyonları gerçekleştirilmiştir. Naftifinin *in vitro* deriden permeasyonu çalışılmış ve konvansiyonel ticari preparatı ile karşılaştırılmıştır. Zayıflatılmış toplam yansıma-Fourier dönüşümü (ATR-FTIR) spektroskopisi, mikroemülsiyonlar ile stratum corneum lipitleri arasındaki etkileşimin araştırılması için kullanılmıştır. Naftifin yüklü mikroemülsiyonların antifungal aktiviteleri *Candida albicans* Amerikan Tip Kültür Koleksiyonu (ATCC) 10231 ve *Candida parapsilosis* kullanılarak değerlendirilmiştir.

Bulgular: Ko-surfaktan olarak Kolliphor RH40 içeren mikroemülsiyon formülasyonu, naftifinin topikal ticari formülasyonu ile karşılaştırıldığında, domuz derisinden naftifin permeasyonunu istatistiksel olarak anlamlı derecede arttırmıştır ($p<0,05$). ATR-FTIR spektroskopisi, mikroemülsiyonların stratum corneum lipit çifte tabakalarının akışkanlığını arttırdığını göstermiştir. İlaç yüklü mikromülsiyonlar, *Candida albicans* ATCC 10231 ve *Candida parapsilosis* türlerine karşı yüksek antifungal aktivite göstermişlerdir.

Sonuç: Sonuç olarak, bu çalışmada mikroemülsiyonların, naftifinin deriden permeasyonunun iyileştirilmesinde alternatif topikal taşıyıcılar olarak kabul edilebilecekleri gösterilmiştir.

Anahtar kelimeler: Naftifin, mikroemülsiyon, kolloidal ilaç taşıyıcı sistem, topikal antifungal

*Correspondence: **E-mail:** serdal@istanbul.edu.tr, **Phone:** +90 532 302 16 16 **ORCID-ID:** orcid.org/0000-0001-6220-2036
Received: 13.07.2018, **Accepted:** 18.10.2018

INTRODUCTION

Naftifine hydrochloride (naftifine) is a synthetic, topical allylamine antifungal compound that is effective in the management of superficial dermatomycoses. Naftifine shows primarily fungicidal activity against *Candida* species including *Candida albicans* (*C. albicans*) and *Candida parapsilosis* (*C. parapsilosis*) and it has been proven to be especially effective in moderate to severe cutaneous candidiasis caused by these two species.[1,2]

The strongly lipophilic nature of naftifine (log p: 5.4) leads to its accumulation in high concentrations within the stratum corneum, which is the outermost barrier layer of the skin. However, the therapeutic efficacy of antifungal drugs applied topically depends on the ability of the formulation to overcome the stratum corneum barrier and improve the uptake in deeper skin layers.[3] Therefore, a drug delivery system aiming to increase the topical penetration of naftifine is important to enhance its local antifungal efficacy. Microemulsions are colloidal nano-sized carriers with a dynamic microstructure that form spontaneously by combining appropriate amounts of oil, water, surfactant, and a co-surfactant.[4,5] They are thermodynamically stable and isotropic systems and they have been extensively explored for a variety of pharmaceutical applications, including dermal and transdermal drug delivery.[6-9] The high solubilization capacity of microemulsions and their ability to modify the diffusional barrier of the stratum corneum can facilitate drug penetration into deeper skin layers compared to conventional formulations.[10,11] The aim of the present study was to formulate and evaluate the *in vitro* skin permeation and antifungal activity of naftifine-loaded microemulsion formulations comprising oleic acid (oil phase), Kolliphor EL or Kolliphor RH40 (surfactant), Transcutol (co-surfactant), and water. Attenuated total reflectance-Fourier transform infrared (ATR-FTIR) spectroscopy was used to evaluate the interaction between the microemulsions and the stratum corneum lipids. The antifungal susceptibility of naftifine-loaded microemulsions was assessed against two *Candida* species, namely *C. albicans* American Type Culture Collection (ATCC) 10231 and *C. parapsilosis*.

MATERIALS AND METHODS

Materials

Naftifine was kindly provided by Eczacıbaşı Drug Company (İstanbul, Turkey), and the polyoxyl castor oils (Kolliphor® EL and Kolliphor® RH40) were kind gifts from BASF (Limburgerhof, Germany). Oleic acid was purchased from Sigma (St. Louis, MO, USA). Diethylene glycol monoethyl ether (Transcutol P®) was kindly provided by Gattefossé (Lyon, France). RPMI-1640 medium and 4-morpholinepropanesulfonic acid (MOPS) were purchased from Sigma (St. Louis, MO, USA). All other chemicals used in the study were of analytical grade.

Preparation and characterization of microemulsions

We previously reported the preparation and physicochemical characterization of microemulsions loaded with naftifine.[12] Briefly, the concentration range of components necessary for the formation of microemulsions was determined by construction of pseudoternary phase diagrams based on water titration at ambient temperature (25±0.5°C). The oil phase to surfactant/cosurfactant mixture ratio varied from 1:9 to 9:1 (w/w) and the ratio of surfactant/co-surfactant (km) was fixed as 1:2. The microemulsions were formed spontaneously at room temperature as a clear monophasic liquid (Table 1). Naftifine was solubilized in the oil phase at 1% concentration before preparation of the microemulsions. In order to verify the isotropic nature of the optimized microemulsions ME1 and ME2, cross-polarized light microscopy (Olympus BX51 U-AN 360, Tokyo, Japan) imaging was performed. The droplet size and the polydispersity index of the microemulsions were determined using dynamic light scattering (Malvern Zetasizer Nano ZS, Malvern Instruments, Malvern, Worcestershire, UK) after pre-filtering (0.45 mm, Millex) of the microemulsions. The electric conductivity and pH of the microemulsions were measured using a combined device (EuTech PC 700; Eutech Instruments, Landsmeer, the Netherlands) at room temperature. The refractive index of the microemulsions was determined by a digital Abbe Refractometer (Atogo Co. Ltd., Tokyo, Japan). In order to measure the viscosity and rheological behavior of the microemulsions a Brookfield Rheometer (Brookfield DV3THACJ0, Middleboro, MA, USA) with a cone-plate measuring device was used. All measurements were conducted in triplicate in a temperature-controlled environment at 25°C.

In vitro permeation study

Preparation of skin

Pig skin (obtained from a local slaughterhouse) was carefully cleaned of fat and muscle and then dermatomed to a thickness of 750 µm (Zimmer Electric Dermatome, Warsaw, IN, USA). The integrity of the skin was confirmed by transepidermal water loss measurement with an open chamber device (Tewameter TM 300; Courage + Khazaka Electronic, Cologne, Germany) as stated in the literature.[4]

Permeation experiments

In vitro permeation experiments were performed using Franz type diffusion cells (diffusion area of 1.76 cm^2, Permegear V6A Stirrer, Hellertown, PA, USA). Pig skin was placed on the receiver chambers with the stratum corneum facing upwards

Table 1. The composition of naftifine loaded microemulsion formulations

Formulation components	ME1 (% w/w)	ME2 (% w/w)
Oleic acid	8.0	8.7
Kolliphor® RH40	19.0	-
Kolliphor® EL	-	17.2
Transcutol P®	38.0	34.8
Naftifine HCl	1.0	1.0
Water	34.0	38.1

HCl: Hydrochloride

and then the donor chambers were clamped in place. The receptor chamber was filled with 12 mL of phosphate buffer pH 5.0 containing 30% ethanol to ensure sink conditions. The receptor phase maintained at 37°C under constant stirring (300 rpm) with a magnetic bar. Microemulsion formulation (500 µL) was placed in the donor compartments of diffusion cells. The compartments were sealed by Parafilm M® (Bemis, Oshkosh, WI, USA) immediately after the addition of the formulation in order to prevent evaporation. The permeation of naftifine from microemulsions was followed for 8 h. The commercial topical cream formulation naftifine (Exoderil) was used as the control formulation. Samples of 500 µL were removed at appropriate time intervals for analysis and replaced immediately with fresh receptor medium. The samples were analyzed for their drug content by HPLC. Permeation profiles of naftifine were constructed by plotting time (h) against the cumulative amount of the drug (µg/cm^2) as measured in the receptor medium. Steady state flux (J_{ss}, mg/cm^2.h) was calculated from the steady state part of the curve. The effect of microemulsions as carrier on dermal administration [enhancement ratio, (ER)] is determined by the following equation:

ER=Flux from microemulsion formulation/Flux from commercial formulation

Data were determined from the average of at least six experiments.

HPLC analysis

For the HPLC (Shimadzu Model LC 20AT, Kyoto, Japan) analysis of naftifine we used a reversed phase C18 column (4.6 mm×150 mm, 5 µm, Merck, Darmstadt, Germany) preceded by a guard column (4×4 mm, 5 µm, Merck, Darmstadt, Germany). The mobile phase consisted of acetonitrile:tetrahydrofuran:tetram ethyl-ammonium hydroxide buffer (pH 7.8) (62:10:28) and the flow rate was fixed at 1.2 mL/min. The wavelength of detection was set at 280 nm. The limit of quantification was found to be 0.025 µg/mL. The method was validated for selectivity, linearity, accuracy, and precision. It was found to be linear between the concentration range of 0.025-100 µg/mL with a high correlation coefficient (r^2=0.999) and was precise (intra- and interday variation 2%) and accurate (mean recovery 99%).

ATR-FTIR spectroscopy

The effect of microemulsions ME1 and ME2 and marketed formulation (Exoderil) on pig skin was investigated by ATR-FTIR spectroscopy. For this purpose, the surface of 4 cm^2 pieces of dermatomed pig skin was treated with 300 µL of ME1, ME2, or commercial cream for 8 h. At the end of the treatment period ATR-FTIR spectra were recorded as the average of 40 scans with a spectral resolution of 4 cm^{-1} in the 4000-650 cm^{-1} range using a Perkin Elmer Spectrum 100 FTIR spectrometer (UK) equipped with a ZnSe ATR crystal. Attention was focused on characterizing the occurrence of peaks near 2850 and 2920 cm^{-1}, which were due to the symmetric and asymmetric CH_2 stretching vibrations, respectively. In order to minimize intersample variation, the same piece of skin before treatment was used for normalization.[13]

In vitro antifungal activity

Yeasts

C. albicans ATCC 10231 and C. parapsilosis were used to evaluate the antifungal susceptibility of naftifine-loaded microemulsions. The yeasts were cultured and maintained on Sabouraud dextrose agar for 24 h at 30°C prior to testing.

Assay

The minimum inhibitory concentration (MIC) of microemulsion formulations was determined by the microdilution technique using 96-well microplates. Serial two-fold dilutions ranging from 5000 to 5 mg/mL were done following the Clinical Laboratory Standards Institute (CLSI) recommendations, rule CLSI M27-A3 for yeasts.[14,15] RPMI-1640 medium (Sigma, St. Louis, MO, USA) buffered to pH 7.0 with MOPS (Sigma, St. Louis, MO, USA) was used for the dilutions. The inoculum was prepared with RPMI-1640 medium, using 24 h cultures adjusted to a turbidity equivalent to a 0.5 McFarland standard, to give a final concentration of 0.5×10^3 to 2.5×10^3 cfu/mL in the test tray. The trays were covered and placed in plastic bags to prevent evaporation and incubated at 35°C for 46-50 h. The MICs were defined as the lowest concentration of compound giving complete inhibition of visible growth.[16] Naftifine was used as reference antifungal for yeast. The MIC values of the naftifine were within the accuracy range in CLSI throughout the study.[14] All tests were performed in triplicate.

Statistical analysis

All results are the mean ± standard deviation of at least three experiments. The statistical analysis was performed using Tukey's multiple comparison test, with $p<0.05$ as level of significance (GraphPad Prism 5 Software, La Jolla, CA, USA).

RESULTS AND DISCUSSION

Physicochemical characterization of microemulsions

The small droplet size (7.34±0.03-11.17±0.25 nm) together with its narrow distribution (0.15±0.01-0.19±0.01) indicated the homogeneous nature of the microemulsions and explained the clarity and isotropicity of the systems. The conductivity values revealed that the microemulsions were in oil in water (o/w) form and naftifine in salt form led to increased conductivity. The pH values of the microemulsions were reasonable for their cutaneous application (4.26±0.01-5.71±0.03). The refractive indices of the microemulsions confirmed the transparency of the formulations. The apparent viscosity values of the microemulsions were 70.76±0.12-83.58±0.46 Cp and they showed Newtonian flow behavior.[12]

In vitro permeation study

The permeability of naftifine from microemulsions was measured *in vitro* using excised pig skin. The cumulative percutaneous penetrating amounts of naftifine from the microemulsions and from the commercial cream are illustrated in Figure 1 and the permeation parameters are summarized in Table 2. Flux of naftifine from the microemulsion ME1 (109.99±1.58 µg.cm^{-2}.h^{-1}) was significantly higher than that of ME2 (45.59±2.10 µg.cm^{-}

^{2}.h^{-1}) and commercial cream (21.32±1.56 µg.cm^{-2}.h^{-1}) ($p<0.05$). It has been reported that percutaneous permeation is an essential requirement for satisfactory topically applied antifungals in order to achieve therapeutic concentration for deep fungal infections.[17] The ability of a microemulsion to improve the transport of drugs to and across the skin is largely influenced by the composition and concentration of the microemulsion components, as well as the internal structure and type of the microemulsion used (o/w, w/o, or bicontinuous systems).[10,18] Various oils have been used as components of the oil phase in microemulsions. Oleic acid is one of the most frequently selected ones and it has been demonstrated that oleic acid containing microemulsions increased the penetration of lipophilic drugs through the skin.[19,20] Transcutol P is a well-known penetration enhancer in skin delivery and by its amphiphilic nature it has been known to reduce interfacial tension, resulting in balanced microemulsion systems.[21] Although both of the microemulsions contained oleic acid and Transcutol P, the highest permeation was obtained by ME1, demonstrating a possible synergistic effect of the added surfactant Kolliphor® RH40. The content of the surfactant mixture in ME1 influenced the permeation rate of naftifine. In addition, the lower viscosity of ME1 (75.62±0.24 cP) than ME2 (83.58±0.46 cP) might provide better mobility for the drug molecules and consequently a faster release with a diffusion-controlled mechanism.[12,22] The permeability coefficient (Kp) of naftifine in ME1 was fivefold higher than the value obtained for the commercial formulation. The microemulsion formulation ME1 had the highest ER_{Flux} (5.16) with a ~5-fold enhancement rate compared to the commercial formulation. It was also found that the lag times were shortened when microemulsions were used (Table 2). This result was consistent with previous studies reporting that microemulsions remarkably shortened the lag time of formulations.[23]

ATR-FTIR spectroscopy

In Figure 2, the spectra of untreated pig skin (control) and pig skin treated with either microemulsion formulations (ME1 and ME2) or commercial cream (Exoderil) are shown. The most characteristic bands are the asymmetric and symmetric CH_2 stretching absorbances at 2920 cm^{-1} and 2850 cm^{-1} arising from endogenous skin lipids. We observed that both the CH_2 stretching vibration bands shifted towards higher wave numbers after microemulsion application, which could be attributed to a decrease in the conformational order of the stratum corneum lipids. Thus, disorder of the barrier might further have enhanced permeation of naftifine across the stratum corneum.[17,24]

In vitro antifungal activity of naftifine microemulsions

Naftifine is a topical antifungal agent having shown a specific inhibitory effect in sterol biosynthesis of *C. albicans* and *C. parapsilosis*.[25] The *in vitro* antifungal activity of naftifine-loaded microemulsions ME1 and ME2 against *C. albicans* ATTC 10231 and *C. parapsilosis* (port blood) was higher than that of the commercial topical cream (Exoderil) as can be seen in Figure 3. These results proved that microemulsions had superior fungicidal efficacies due to considerable penetration of the drug into fungal cell membranes.[26] Jadhav et al.[27] observed greater activity of fluconazole-loaded microemulsions than of conventional gel formulations and this was attributed to the better diffusion of the drug provided by the presence of surfactants and oil phase. Similarly, El-Hadidy et al.[28]

Table 2. Effect of microemulsions (ME1 and ME2) on percutaneous permeation of naftifine

Formulation	Flux (J_{ss}) (µg.cm^{-2}.h^{-1})	Permeability coefficient (K_p) (cm.h^{-1})×10^{-3}	Lag time (h)	ER_{Flux}
ME1	109.99±1.58	10.10±0.23	1.22±0.87	5.16
ME2	45.59±2.10	4.56±0.41	1.55±0.56	2.14
Exoderil	21.32±1.56	2.13±0.85	3.50±0.49	1.00

Each data point is the mean ± standard deviation of six determinations

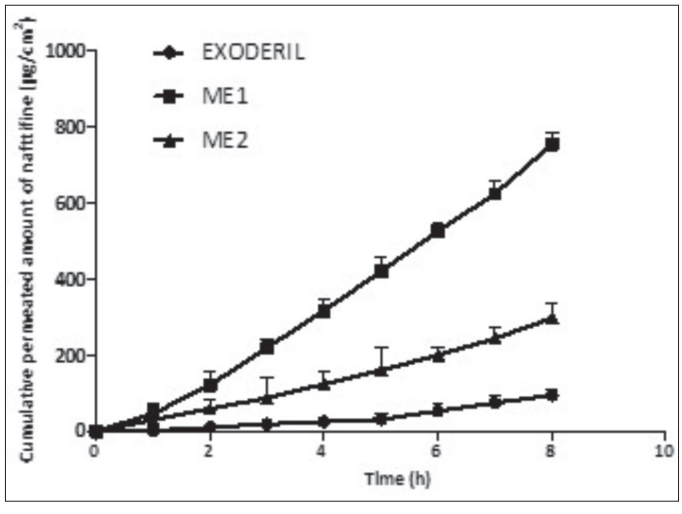

Figure 1. Comparison of skin permeation rates of naftifine from microemulsions and from the topical commercial formulation. At least 6 experiments (n≥6) were performed for each formulation

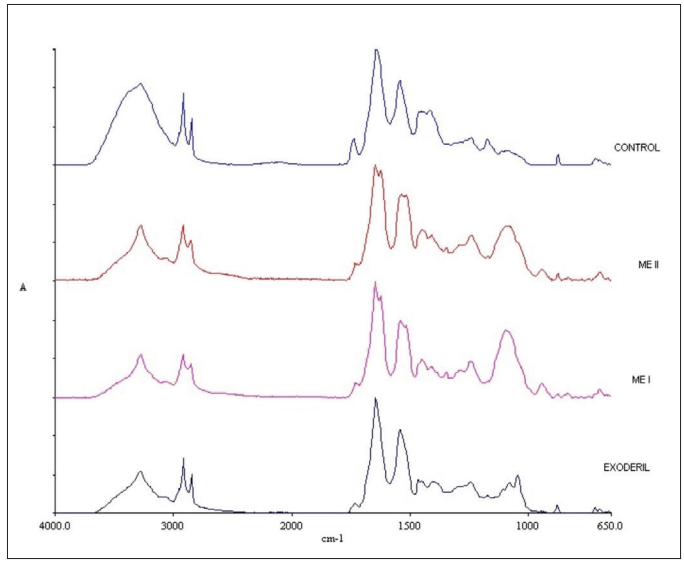

Figure 2. Comparison of Attenuated total reflectance-Fourier transform infrared spectra of untreated and formulation (ME1, ME2, and commercial cream) treated pig skin samples

(2012) observed considerably higher antifungal activity with voriconazole microemulsions against *C. albicans* when compared to the supersaturated solution of the same drug. Microemulsion formulation M1, which contains Kolliphor EL as surfactant, showed higher antifungal activity compared to that of the microemulsion M2 and Exoderil. Kolliphor EL is a nonionic surfactant and it is a well-known formulation vehicle for various hydrophobic drugs, including anesthetics, photosensitizers, sedatives, immunosuppressive agents, and anticancer drugs.[29] Kolliphor EL-containing microemulsions have been considered effective topical carriers to deliver the antifungal agents oxiconazole and terconazole.[30,31] The composition of microemulsion M1 in our study might alter the permeation of fungal cells more than the formulation M2 and commercial cream, which consequently resulted in higher penetration of microemulsion globules containing naftifine through fungal cell walls.

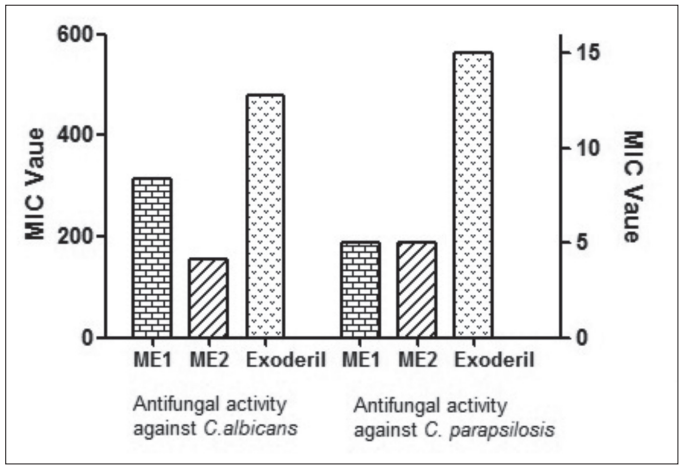

Figure 3. Values of minimum inhibitory concentration determined either for naftifine-containing microemulsions (ME1 and ME2) or for the commercial topical formulation (Exoderil)

CONCLUSION

Our results showed significant naftifine permeation enhancement by a microemulsion formulation comprising oleic acid, Kolliphor RH40, Transcutol, and water when compared with its conventional topical formulation. ATR-FTIR spectra revealed that microemulsions increased the fluidity of the stratum corneum lipid bilayers. Drug-loaded microemulsions showed superior antifungal activity against two *Candida* species. In conclusion, this study demonstrated that a microemulsion formulation of naftifine could be a potential alternative to the conventional formulation of the drug.

ACKNOWLEDGEMENTS

This work was supported by the Scientific Research Projects Coordination Unit of İstanbul University (Project number NP-512 and BYP-2017-26514).

Conflict of Interest: No conflict of interest was declared by the authors.

REFERENCES

1. Gupta AK, Ryder JE, Cooper EA. Naftifine: A Review. J Cutan Med Surg. 2008;12:51-58.
2. Bondaryk M, Kurzątkowski W, Staniszewska M. Antifungal agents commonly used in the superficial and mucosal candidiasis treatment: mode of action and resistance development. Postep Derm Alergol. 2013;30:293-301.
3. Güngör S, Erdal MS, Aksu B. New Formulation Strategies in Topical Antifungal Therapy. Journal of Cosmetics Dermatological Sciences and Applications. 2013;3:56-65.
4. Sintov AC, Shapiro l. New microemulsion vehicle facilitates percutaneous penetration in vitro and cutaneous drug bioavailability in vivo. J Control Release. 2004;95:173-183.
5. Teichmann A, Heuschkel S, Jacobi U, Presse G, Neubert RH, Sterry W, Ladermann J. Comparison of stratum corneum penetration and localization of a lipophilic model drug applied in an o/w microemulsion and an amphiphilic cream. Eur J Pharm Biopharm. 2007;67:699-706.
6. Baroli B, López-Quintela MA, Delgado-Charro MB, Fadda AM, Blanco-Méndez J. Microemulsions for topical delivery of 8-methoxsalen. J Control Release. 2000;69:209-218.
7. Zhao JH, Ji L, Wang H, Chen ZQ, Zhang YT, Liu Y, Feng NP. Microemulsion-based novel transdermal delivery system of tetramethylpyrazine: preparation and evaluation in vitro and in vivo. Int J Nanomedicine. 2011;6:1611-1619.
8. Coneac G, Vlaia V, Olariu I, Mu AM, Anghel DF, Ilie C, Popoiu C, Lupuleasa D, Vlaia L. Development and evaluation of new microemulsion-based hydrogel formulations for topical delivery of fluconazole. AAPS PharmSciTech. 2015;16:889-904.
9. Sintov AC. Transdermal delivery of curcumin via microemulsion. Int J Pharm. 2015;481:97-103.
10. Lopes LB. Overcoming the cutaneous barrier with microemulsions. Pharmaceutics. 2014;6:52-77.
11. Talegaonkar S, Azeem A, Ahmad FJ, Khar RK, Pathan SA, Khan ZI. Microemulsions: a novel approach to enhanced drug delivery. Recent Pat Drug Deliv Formul. 2008;2:238-257.
12. Erdal MS, Özhan G, Mat MC, Özsoy Y, Güngör S. Colloidal nanocarriers for the enhanced cutaneous delivery of naftifine: characterization studies and in vitro and in vivo evaluations. Int J Nanomedicine. 2016;11:1027-1037.
13. Bommannan D, Potts RO, Guy RH. Examination of stratum corneum barrier function in vivo by infrared spectroscopy. J Invest Dermatol. 1990;95:403-408.
14. CLSI. Performance Standards for Antimicrobial Susceptibility Testing. 27th ed. CLSI supplement M100. Wayne, PA: Clinical and Laboratory Standards Institute; 2017.
15. CLSI. Reference Method for Broth Dilution Antifungal Susceptibility Testing of Yeasts 4th ed. CLSI standard M27. Clinical and Laboratory Standards Institute; 2017.
16. Chryssanthou E, Cuenca-Estrella M. Comparison of the Antifungal Susceptibility Testing Subcommittee of the European Committee on Antibiotic Susceptibility Testing proposed standard and the E-test with the NCCLS broth microdilution method for voriconazole and caspofungin susceptibility testing of yeast species. J Clin Microbiol. 2002;40:3841-3844.

17. Ge S, Lin Y, Lu H, Li Q, He J, Chen B, Wu C, Xu Y. Percutaneous delivery of econazole using microemulsion as vehicle: Formulation, evaluation and vesicle-skin interaction. Int J Pharm. 2014;465:120-131.

18. Hosmer J, Reed R, Bentley MV, Nornoo A, Lopes LB. Microemulsions containing medium-chain glycerides as transdermal delivery systems for hydrophilic and hydrophobic drugs. AAPS PharmSciTech. 2009;10:589-596.

19. Rhee YS, Choi JG, Park ES, Chi SC. Transdermal delivery of ketoprofen using microemulsions. Int J Pharm. 2001;228:161-170.

20. Panapisal V, Charoensri S, Tantituvanont A. Formulation of microemulsion systems for dermal delivery of silymarin. AAPS PharmSciTech. 2012;13:389-399.

21. Kajbafvala A, Salabat A, Salimi A. Formulation, characterization, and *in vitro/ex vivo* evaluation of quercetin-loaded microemulsion for topical application. Pharm Dev Technol. 2018;23:741-750.

22. Butani D, Yewale C, Misra A. Amphotericin B topical microemulsion: formulation, characterization and evaluation. Colloids Surf B Biointerfaces. 2014;116:351-358.

23. Lin YH, Tsai MJ, Fang YP, Fu YS, Hung YB, Wu PC. Microemulsion formulation design and evaluation for hydrophobic compound: Catechin topical application. Colloids Surf B Biointerfaces. 2018;161:121-128.

24. Schwarz JC, Pagitsch E, Valenta C. Comparison of ATR-FTIR spectra of porcine vaginal and buccal mucosa with ear skin and penetration analysis of drug and vehicle components into pig ear. Eur J Pharm Sci. 2013;50:595-600.

25. Uzqueda M, Martín C, Zornoza A, Sánchez M, Martínez-Oharriz MC, Vélaz I. Characterization of complexes between naftifine and cyclodextrins in solution and in the solid state. Pharm Res. 2006;23:980-988.

26. Raju YP, N H, Chowdary VH, Nair RS, Basha DJ, N T. *In vitro* assessment of non-irritant microemulsified voriconazole hydrogel system. Artif Cells Nanomed Biotechnol. 2017;45:1539-1547.

27. Jadhav KR, Shetye SL, Kadam VJ. Design and Evaluation of Microemulsion Based Drug Delivery System. Int J Adv Pharm. 2010;1:156-166.

28. El-Hadidy GN, Ibrahim HK, Mohamed MI, El-Milligi MF. Microemulsions as vehicles for topical administration of voriconazole: formulation and *in vitro* evaluation. Drug Dev Ind Pharm. 2012;38:64-72.

29. Gelderblom H, Verweij J, Nooter K, Sparreboom A. Cremophor EL: the drawbacks and advantages of vehicle selection for drug formulation. Eur J Cancer. 2001;37:1590-1598.

30. Khattab A, Ismail S. Formulation and evaluation of oxiconazole mucoadhesive nanoemulsion based gel for treatment of fungal vaginal infection. Int J Pharmacy and Pharm Sci. 2016;8:33-40.

31. Abd-Elsalam WH, El-Zahaby SA, Al-Mahallawi AM. Formulation and *in vivo* assessment of terconazole-loaded polymeric mixed micelles enriched with Cremophor EL as dual functioning mediator for augmenting physical stability and skin delivery. Drug Deliv. 2018;25:484-492.

Turk J Pharm Sci 2020;17(1):49-55
DOI: 10.4274/tjps.galenos.2018.49389

ORIGINAL ARTICLE

Effects of Glycyrrhetic Acid on Human Chronic Myelogenous Leukemia Cells

Glisiretik Asidin İnsan Kronik Miyelojenöz Lösemi Hücreleri Üzerindeki Etkileri

Halilibrahim ÇİFTÇİ*

Kumamoto University, School of Pharmacy, Department of Bioorganic Medicinal Chemistry, Kumamoto, Japan

ABSTRACT

Objectives: Chronic myelogenous leukemia (CML) is a type of blood cancer that is initially treated with imatinib (first Abl kinase inhibitor). However, some patients with CML develop imatinib resistance. Several new generation drugs have been developed, but do not overcome this problem. Glycyrrhetic acid (GA) is a plant-derived pentacyclic triterpenoid that exhibits multiple pharmacological properties for the treatment of cancers. The current study aimed to investigate the effects of GA on the K562 cell line (Bcr-Abl positive leukemia).

Materials and Methods: The MTT cell proliferation assay was employed to evaluate the cytotoxic effect of GA compared with imatinib (positive control) against leukemia and normal blood cells. For detection of cell death, an apoptotic/necrotic/healthy assay was performed against the K562 cell line. To investigate the kinase inhibitory activity of GA, the Abl1 kinase profiling assay and a molecular docking study were performed.

Results: GA showed Abl kinase inhibitory activity with an IC_{50} value of 29.2 μM and induced apoptosis in the K562 cell line after 6 h of treatment.

Conclusion: The current findings indicate that this class of plant extract could be a potential candidate for treatment of CML.

Key words: Pentacyclic triterpenoid, glycyrrhetic acid, Abl kinase, apoptosis, K562 cells

ÖZ

Amaç: Kronik miyelojenöz lösemi (KML), başlangıçta imatinib (ilk Abl kinaz inhibitörü) ile tedavi edilen bir tür kan kanseridir. Fakat, KML'li bazı hastalar imatinibe karşı direnç geliştirebilmektedir. Değişik yeni nesil ilaçlar geliştirilmiştir, ancak bu problemin üstesinden gelinememiştir. Glisiretik asit (GA), kanser tedavisinde birçok farmakolojik özellik gösteren bitki kaynaklı bir pentasiklik triterpenoiddir. Bu çalışma, GA'nın K562 hücreleri (Bcr-Abl pozitif lösemi) üzerindeki etkilerini araştırmayı amaçlamaktadır.

Gereç ve Yöntemler: MTT hücre proliferasyon analizi, GA'nın imatinibe (pozitif kontrol) kıyasla lösemi ve normal kan hücrelerine karşı sitotoksik etkisini değerlendirmek için kullanıldı. Hücre ölümünün tespiti için, apoptotik/nekrotik/sağlıklı hücre analizi K562 hücrelerine karşı yapıldı. GA'nın kinaz inhibe edici aktivitesini araştırmak için, Abl1 kinaz profil tahlili ve moleküler doking çalışmaları yapıldı.

Bulgular: GA, 29,2 μM IC_{50} değeri ile Abl kinaz inhibitör aktivitesi gösterdi ve 6 saatlik tedaviden sonra K562 hücre hattında apoptoza sebep oldu.

Sonuç: Mevcut bulgular, bu bitki özütü sınıfının KML tedavisi için potansiyel bir aday olabileceğini göstermektedir.

Anahtar kelimeler: Pentasiklik triterpenoid, glisiretik asit, Abl kinaz, apoptoz, K562 hücreleri

*Correspondence: E-mail: hiciftci@kumamoto-u.ac.jp, Phone: 0819031996161 ORCID-ID: orcid.org/0000-0002-9796-7669
Received: 10.08.2018, Accepted: 18.10.2018

INTRODUCTION

One of the major health problems all over the world is cancer. In 2015, over 8.7 million patients died from cancer globally, with approximately 17.5 million new cases.[1,2] Despite extensive efforts over the last several decades, cancer is still one of the most common causes of death in many developing nations. The death rate from cancer is predicted to be 17 million with 26 million new cases each year by 2030.[3,4] Due to this global increase in the cancer burden, a massive research effort has been made for the discovery of effective and less toxic chemotherapeutic agents.[5-8] Over the past few years tyrosine kinases have attracted growing interest as drug targets in anticancer drug discovery that play an important role in signal transduction, mitogenesis, and other cellular activation processes.[9-11] More than 25 kinase inhibitors are available for cancer therapy and there are currently many more promising candidates in clinical development[12,13] after the approval of imatinib as the first Bcr-Abl tyrosine kinase inhibitor in 2002.[14] Although imatinib continues to be the initial choice in chronic myelogenous leukemia (CML) treatment, some patients with CML develop drug resistance to imatinib.[14,15] This major limitation is becoming a significant concern for patients with imatinib-resistant chronic-phase CML.[16] Several new generation drugs have been developed, but there are still no alternative drugs available to overcome this problem.[17,18] Pentacyclic triterpenoids have emerged as a unique class of natural compounds and have been studied extensively for more than a century due to their effective therapeutic applications for the treatment of a wide spectrum of diseases and their high safety profile.[19,20] Recent studies have indicated that two different types of pentacyclic triterpenoids, celastrol and gypsogenin, exert anti-Abelson kinase 1 (Abl1) and anti-CML leukemia effects.[21,22]

Glycyrrhetic acid (GA) is an olenane-type natural pentacyclic triterpenoid extracted from liquorice that exhibits promising anticancer activity on many cancer cells including human ovarian cancer, breast cancer, hepatocellular carcinoma, pituitary adenoma, human bladder cancer, lung cancer, and leukemia.[19,23-27] However, there is no reported research yet in the literature that displays Bcr-Abl inhibitory activity of GA. In the present study, we explored the biological activities of GA against leukemia cell lines (Jurkat, MT-2, and K562) and normal cells of human blood peripheral blood mononuclear cells (PBMCs) and then evaluated its antityrosine kinase activity. Furthermore, apoptotic/necrotic analysis against the K562 cell line and molecular docking with the Abl kinase domain were carried out using GA.

MATERIALS AND METHODS

Cell culture conditions and drug treatment

The K562, Jurkat, and MT-2 cell lines were cultured in RPMI 1640 (Wako Pure Chemical Industries, Osaka, Japan) medium with 10% fetal bovine serum (Equitech-Bio, Kerrville, TX, USA) and 89 μM/mL streptomycin (Meiji Seika Pharma, Tokyo, Japan) in a humid atmosphere at 37°C and 5% CO_2. PBMCs (Precision Bioservices, Frederic, MD, USA) were incubated in RPMI 1640 medium with 10% human serum AB (Gemini, Woodland, CA, USA) and 89 μM/mL streptomycin at 37°C (humid atmosphere, 5% CO_2). In the experiments, the leukemia and PBMCs were incubated in 24-well culture plates at 10^5 and 10^6 cells/mL concentration respectively for 48 h. The stock solutions of GA (Tokyo Chemical Industry Co. Ltd., Tokyo, Japan) and imatinib (Wako Pure Chemical Industries, Osaka, Japan) in concentrations of 2.5 mM, 5 mM, 10 mM, 20 mM, and 30 mM were prepared in DMSO (Wako Pure Chemical Industries, Osaka, Japan). The concentration of DMSO in the final culture medium was 1%.

MTT assay for cytotoxicity

The MTT test was performed routinely as described in the literature.[28,29] GA and imatinib were cultured with cells in different concentrations (3-300 μM). After 48 h of treatment, cells were incubated with MTT (Dojindo Molecular Technologies, Kumamoto, Japan) solution in medium for 4 h. At the end of incubation, the solution was taken out and 100 μL of DMSO was added to each well. The absorbance of the solution was measured in a microplate reader, Infinitive M1000 (Tecan, Groding, Austria), at a wavelength of 550 nm with background subtraction at 630 nm. All experiments were run in triplicate and cell viability was calculated as the percentage of viable control cells. IC_{50} values were estimated from the results of the MTT test described as the drug concentrations that reduced absorbance to 50% of control values.

Detection of cell death

After treatment of K562 cells with GA or imatinib at IC_{50} concentrations for 6 h, a apoptotic/necrotic/healthy detection kit (PromoKine, Heidelberg, Germany) was used according to PromoKine's instructions with modifications.[30] After the cells were harvested and washed with PBS, the cells were suspended with binding buffer (1X). After that, 50 μL of binding buffer, 4 μL of FITC-annexin V solution, 4 μL of ethidium homodimer III solution, and 4 μL of Hoechst 33342 solution were added to the cells for 30 min at room temperature in the dark. Then the cells were analyzed by a fluorescence microscope, Biorevo Fluorescence BZ-9000 (Keyence, Osaka, Japan). The number of apoptotic cells (annexin V), late apoptotic or necrotic cells (annexin V and ethidium homodimer III), and necrotic cells (ethidium homodimer III) were counted as previously described.[31]

Abl1 tyrosine kinase profiling system

The Abl1 kinase profiling assay (Promega Corporation, Madison, WI, USA) was performed as previously described with modifications.[21] In this system, Abl1 kinase strip and its substrate were diluted with 95 μL of 2.5X kinase reaction buffer and 15 μL of 100 μM ATP. Then 2 μL of kinase working stock and 2 μL of ATP/substrate working stock were dispensed in the 384-well plate wells along with 1 μL of compound solution at varying concentrations (10-300 μM) in a buffer. The kinase reaction was incubated for 1 h at room temperature and then the activity of Abl1 kinase was detected using the ADP-Glo kinase assay (Promega Corporation). Abl1 inhibition profiling of

GA in dose-response mode was measured by a luminescence microplate reader, Infinitive M1000 (Tecan). IC_{50} values of GA and imatinib required to reduce kinase activity by 50% were calculated using the software Image J.

Molecular modeling

To investigate the binding modes of GA with Abl1 kinase, a molecular docking study was performed using Molecular Operating Environment 2015.10 (Chemical Computing Group, Montreal, Canada). The co-crystal structure of Abl tyrosine kinase with imatinib was obtained as the docking template from the Protein Data Bank (PDB code: 1IEP).[32] Then the Abl kinase and GA were prepared for molecular docking analysis including the addition of hydrogen atoms, the assignment of bond order, assessment of the correct protonation state, and other default parameters. All molecular docking calculations were performed as previously described.[33,34]

RESULTS

In the present study, we first performed the MTT assay to investigate the antiproliferative effects of GA and imatinib against multiple human leukemia cells (K562 CML, Jurkat, and MT-2) at various concentrations (10-300 μM). Imatinib was selected as a model drug, considering its wide use in the treatment of CML. GA (Figure 1) and imatinib were dissolved in DMSO, diluted with culture medium, and then treated with cultured cells for 48 h. The IC_{50} values of these compounds on three cancer cell lines are shown in Table 1. GA exhibited a concentration-dependent inhibitory effect with IC_{50} values that were less than 75 μM against all three cancer cell lines. It possessed the most potent cytotoxic activity against imatinib-sensitive K562 cells with an IC_{50} value of 51.6 μM (Figure 2A), while the IC_{50} values of GA on Jurkat and MT-2 cells were 55.1 μM and 70.2 μM, respectively, weaker than those of the positive control. Next the activity of the target compound was examined on normal PBMCs and compared with imatinib (Figure 2B). GA did not show considerable cytotoxicity against PBMCs, with an IC_{50} value of 117.5 μM, and exhibited ~3.5 times lower cytotoxicity than imatinib (Figure 2B). These results indicate that GA can act as an anti-CML agent and exhibits good selectivity for K562 cell lines over normal cells.

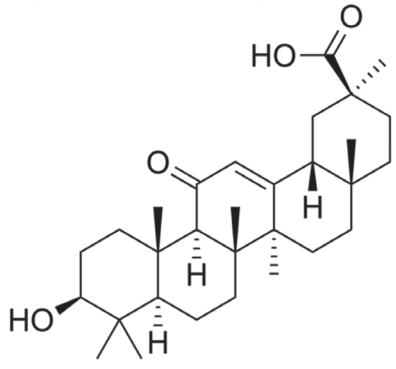

Figure 1. Structure of glycyrrhetic acid

Table 1. IC_{50} values of GA and imatinib for K562, Jurkat, MT-2 and peripheral blood mononuclear cells after 48 h treatment

Cells	IC_{50} (μM)*	
	GA	Imatinib
K562	51.6±6	7.0±3
Jurkat	55.1±6	4.9±4
MT-2	70.2±7	17.0±7
PBMC	117.5±9	33.1±6

*The IC_{50} values represent the mean ± standard deviation of triplicate experiments, PBMC: Peripheral blood mononuclear cell, GA: Glycyrrhetic acid

In order to investigate the process of apoptosis and necrosis, K562 cells treated with GA or imatinib at IC_{50} concentrations were subjected to the annexin V/ethidium homodimer III and Hoechst 33342 staining method and then observed by a fluorescence microscope (Figure 3). In the control experiment (1% DMSO), all cells were healthy (blue staining) at 6 h (Figure 3A). On the other hand, the cells treated with GA and imatinib were stained mostly with healthy cells (blue) and then apoptotic cells (green), and only a few necrotic cells (red) and late apoptotic or necrotic cells (both green and red) were detected at 6 h (Figure 3A), suggesting that the main cell death pathway

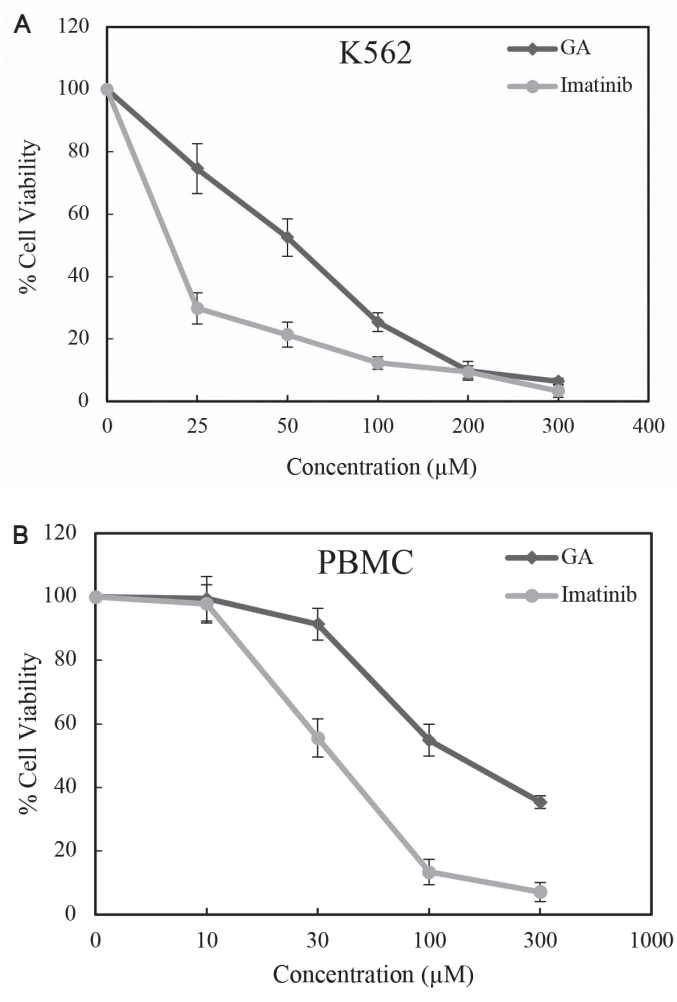

Figure 2. Cell proliferation inhibition of GA and imatinib on (A) K562 and (B) PBMC cells after 48 h incubation

PBMC: Peripherol blood mononuclear cell, GA: Glycyrrhetic acid

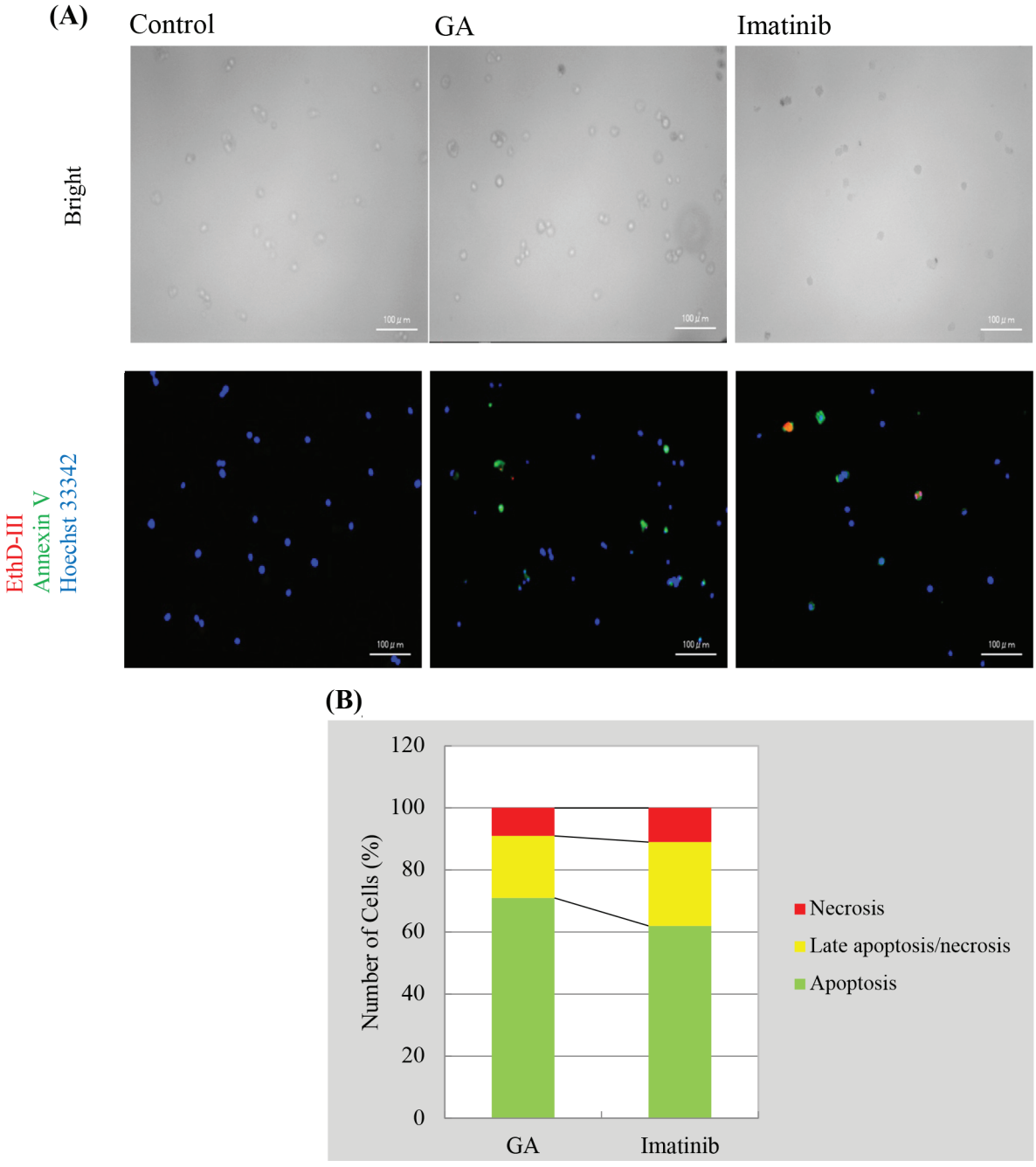

Figure 3. Alteration in K562 cells at IC_{50} concentrations of control, GA, and imatinib (A) for 6 h. (B) A total of approximate 100 stained cells were selected randomly in each experiment of (A) and were classified into 3 types: "apoptosis" (green), "necrosis or late apoptosis" (both green and red), and "necrosis" (red)

GA: Glycyrrhetic acid

of GA and imatinib was apoptosis at an earlier time. The results showed that GA has 71% apoptotic, 9% necrotic, and 20% late apoptotic/necrotic activities (Figure 3B). In contrast, the response of K562 cells upon 6 h imatinib treatment was 62% apoptosis, 11% necrosis, and 27% late apoptosis/necrosis (Figure 3B). Surprisingly, the results demonstrated that GA is able to induce more cell apoptosis than imatinib in Bcr-Abl positive cells.

To explore the inhibition profile of GA on Bcr-Abl, we used the Abl1 tyrosine activity-based kinase assay. In this system, GA was screened at multiple concentrations (10-300 μM) to determine its inhibitory profile on the target kinase (Abl1 tyrosine kinase). GA displayed potential Bcr-Abl inhibitory activity with an IC_{50} value of 29.2 μM as shown in Figure 4. Imatinib was included for comparison and showed a stronger inhibitory effect than GA on Abl1. In order to understand the

Bcr-Abl kinase inhibitory activity of GA, we next examined molecular modeling based on the co-crystal structure of Abl with imatinib as the docking model (PDB ID code: 1IEP). GA fitted into the pocket, forming five noncovalent interactions with four amino acid residues, namely His361, Arg362, Asp381, and Ala380 (Figure 5). It is clear that GA carboxylate plays a pivotal

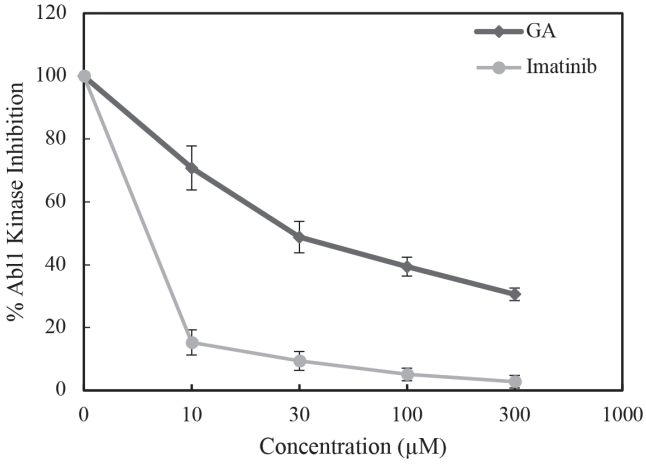

Figure 4. Effect of GA and imatinib on Abl1 tyrosine kinase at varying concentrations (10-300 μM), GA: Glycyrrhetic acid

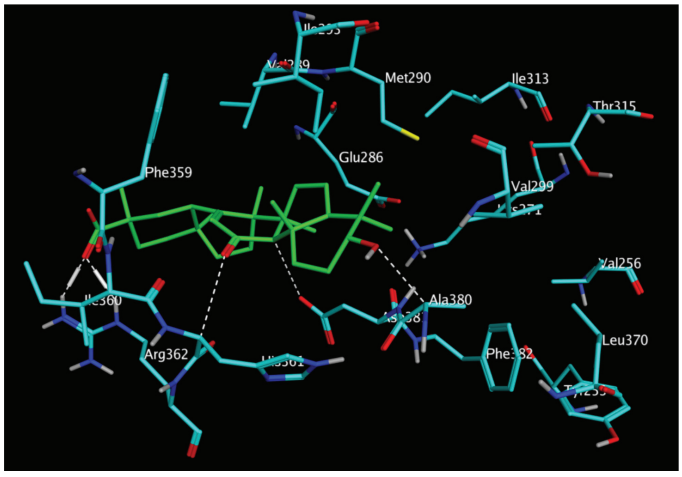

Figure 5. The binding poses of GA in Bcr-Abl tyrosine kinase (PDB ID: 1IEP). GA is shown as green sticks, key amino acid residues are visualized in cyan sticks, and settled interactions are indicated as dotted white lines

GA: Glycyrrhetic acid

role in activity by forming two H bonds with the basic amino acid Arg362. Binding energy values of GA and imatinib into the pocket are -7.2 and -11.1 kcal/mol, respectively, in agreement with the experimental results.

DISCUSSION

CML is a cancer of white blood cells mainly caused by Bcr-Abl. Bcr-Abl tyrosine kinase inhibitors including imatinib have demonstrated significant therapeutic effects in many CML patients. However, resistance and toxicity of these inhibitors have been frequently reported in recent years. Therefore, novel Bcr-Abl inhibitors with high efficacy and low toxicity for treatment of CML are still sought. The accumulated evidence shows that GA has antitumor activities in breast cancer, ovarian cancer, and acute promyelocytic leukemia, but its activity against CML is yet to be investigated.

In the present study, we explored the cytotoxic activity of GA against different leukemic cell lines (K562, Jurkat, and MT-2) and found that GA possesses a remarkable antiproliferative effect on the K562 Bcr-Abl positive cell line. Moreover, GA induced programmed cell death in CML cells more efficiently than imatinib at 6 h of treatment and showed significant tumor selectivity on blood cells (PBMC and K562). To get more insights into GA's molecular mechanism, we assessed its effect on Abl1 kinase, which is amplified in K562 cells. As anticipated, GA inhibited Abl1 kinase with an IC_{50} of 29.2 μM. Molecular modeling simulation provided mechanistic information on the possible binding mode of GA into the ATP binding site of Abl1 kinase.

CONCLUSION

Recently, we have also revealed the activity of gypsogenin, which is another pentacyclic triterpenoid, and its derivatives against the K562 cell line.[21] Considering previous and current data together, our findings suggest that PTs have promising anticancer roles and deserve particular attention in the treatment of CML. We think that derivatization of GA will enhance its binding affinity into Bcr-Abl kinase, which in turn will enhance its anticancer activity. Further derivatizations and biological investigations for improvement of GA activity are ongoing.

ACKNOWLEDGEMENTS

The author thanks Prof. Masami Otsuka, Dr. Mikako Fujita, Dr. Mohamad O. Radwan, and Dr. Nizar Turker for their helpful discussions on molecular modeling and English editing. The work was supported by Project P16111 from Japan Society for the Promotion of Science (JSPS).

Conflict of Interest: No conflict of interest was declared by the authors.

REFERENCES

1. Global Burden of Disease Cancer Collaboration, Fitzmaurice C, Allen C, Barber RM, Barregard L, Bhutta ZA, Brenner H, Dicker DJ, Chimed-Orchir O, Dandona R, Dandona L, Fleming T, Forouzanfar MH, Hancock J, Hay RJ, Hunter-Merrill R, Huynh C, Hosgood HD, Johnson CO, Jonas JB, Khubchandani J, Kumar GA, Kutz M, Lan Q, Larson HJ, Liang X, Lim SS, Lopez AD, MacIntyre MF, Marczak L, Marquez N, Mokdad AH, Pinho C, Pourmalek F, Salomon JA, Sanabria JR, Sandar L, Sartorius B, Schwartz SM, Shackelford KA, Shibuya K, Stanaway J, Steiner C, Sun J, Takahashi K, Vollset SE, Vos T, Wagner JA, Wang H, Westerman R, Zeeb H, Zoeckler L, Abd-Allah F, Ahmed MB, Alabed S, Alam NK, Aldhahri SF, Alem G, Alemayohu MA, Ali R, Al-Raddadi R, Amare A, Amoako Y, Artaman A, Asayesh H, Atnafu N, Awasthi A, Saleem HB, Barac A, Bedi N, Bensenor I, Berhane A, Bernabé E, Betsu B, Binagwaho A, Boneya

D, Campos-Nonato I, Castañeda-Orjuela C, Catalá-López F, Chiang P, Chibueze C, Chitheer A, Choi JY, Cowie B, Damtew S, das Neves J, Dey S, Dharmaratne S, Dhillon P, Ding E, Driscoll T, Ekwueme D, Endries AY, Farvid M, Farzadfar F, Fernandes J[69], Fischer F, G/Hiwot TT, Gebru A, Gopalani S, Hailu A, Horino M, Horita N, Husseini A, Huybrechts I, Inoue M, Islami F, Jakovljevic M, James S, Javanbakht M, Jee SH, Kasaeian A, Kedir MS, Khader YS, Khang YH, Kim D, Leigh J, Linn S, Lunevicius R, El Razek HMA, Malekzadeh R, Malta DC, Marcenes W, Markos D, Melaku YA, Meles KG, Mendoza W, Mengiste DT, Meretoja TJ, Miller TR, Mohammad KA, Mohammadi A, Mohammed S, Moradi-Lakeh M, Nagel G, Nand D, Le Nguyen Q, Nolte S, Ogbo FA, Oladimeji KE, Oren E, Pa M, Park EK, Pereira DM, Plass D, Qorbani M, Radfar A, Rafay A, Rahman M, Rana SM, Søreide K, Satpathy M, Sawhney M, Sepanlou SG, Shaikh MA, She J, Shiue I, Shore HR, Shrime MG, So S, Soneji S, Stathopoulou V, Stroumpoulis K, Sufiyan MB, Sykes BL, Tabarés-Seisdedos R, Tadese F, Tedla BA, Tessema GA, Thakur JS, Tran BX, Ukwaja KN, Uzochukwu BSC, Vlassov VV, Weiderpass E, Wubshet Terefe M, Yebyo HG, Yimam HH, Yonemoto N, Younis MZ, Yu C, Zaidi Z, Zaki MES, Zenebe ZM, Murray CJL, Naghavi M. Global, Regional, and national cancer incidence, mortality, years of life lost, years lived with disability, and disability-adjusted life-years for 32 cancer groups, 1990 to 2015: A Systematic Analysis for the Global Burden of Disease Study. JAMA Oncol. 2017;3:524-548.

2. Ferlay J, Soerjomataram I, Dikshit R, Eser S, Mathers C, Rebelo M, Parkin DM, Formann D, Bray F. Cancer incidence and mortality worldwide: sources, methods and major patterns in GLOBOCAN 2012. Int J Cancer. 2015;136:359-386.
3. Thun MJ, DeLancey JO, Center MM, Jemal A, Ward EM. The global burden of cancer: Priorities for prevention. Carcinogenesis. 2010;31:100-110.
4. Torre LA, Bray F, Siegel RL, Ferlay J, Lortet-tieulent J, Jemal A. Global cancer statistics, 2012. CA Cancer J Clin. 2015;65:87-108.
5. Hoelder S, Clarke PA, Workman P. Discovery of small molecule cancer drugs: Successes, challenges and opportunities. Mol Oncol. 2012;6:155-176.
6. Cragg GM, Pezzuto JM. Natural products as a vital source for the discovery of cancer chemotherapeutic and chemopreventive agents. Med Princ Pract. 2016;25(Suppl 2):41-59.
7. Ma X, Yu H. Global burden of cancer. Yale J Biol Med. 2006;79:85-94.
8. Altıntop MD, Ciftci HI, Radwan MO, Sever B, Kaplancıklı ZA, Ali TFS, Koga R, Fujita M, Otsuka M, Özdemir A. Design, synthesis, and biological evaluation of novel 1,3,4-thiadiazole derivatives as potential antitumor agents against chronic myelogenous leukemia: Striking effect of nitrothiazole moiety. Molecules. 2017:23.
9. Schenk PW, Snaar-Jagalska BE. Signal perception and transduction: The role of protein kinases. Biochim Biophys Acta. 1999;1449:1-24.
10. Fabbro D, Fendrich G, Guez V, Meyer T, Furet P, Mestan J, Griffin JD, Manley PW, Cowan-Jacob SW. Targeted therapy with imatinib: An exception or a rule? Handbook of Experimental Pharmacology. 2005;167:361-389.
11. Wang Z, Cole PA. Catalytic mechanisms and regulation of protein kinases. Methods Enzymol. 2014;548:1-21.
12. Borriello A, Caldarelli I, Bencivenga D, Stampone E, Perrotta S, Oliva A, Della Ragione F. Tyrosine kinase inhibitors and mesenchymal stromal cells: Effects on self-renewal, commitment and functions. Oncotarget. 2017;8:5540-5565.
13. Gross S, Rahal R, Stransky N, Lengauer C, Hoeflich KP. Targeting cancer with kinase inhibitors. J Clin Invest. 2015;125:1780-1789.
14. Mughal A, Aslam HM, Khan AM, Saleem S, Umah R, Saleem M. Bcr-Abl tyrosine kinase inhibitors- current status. Infec Agents Cancer. 2013;8:23.
15. Soverini S, Hochhaus A, Nicolini FE, Gruber F, Lange T, Saglio G, Pane F, Müller MC, Ernst T, Rosti G, Porkka K, Baccarani M, Cross NC, Martinelli G. BCR-ABL kinase domain mutation analysis in chronic myeloid leukemia patients treated with tyrosine kinase inhibitors: Recommendations from an expert panel on behalf of European LeukemiaNet. Blood. 2011;118:1208-1215.
16. Barouch-Bentov R, Sauer K. Mechanisms of drug-resistance in kinases. Expert Opin Investig Drugs. 2011;20:153-208.
17. Weisberg E, Manley PW, Cowan-Jacob SW, Hochhaus A, Griffin JD. Second generation inhibitors of BCR-ABL for the treatment of imatinib-resistant chronic myeloid leukaemia. Nat Rev Cancer. 2017;7:345-356.
18. Giles FJ, O'Dwyer M, Swords R. Class effects of tyrosine kinase inhibitors in the treatment of chronic myeloid leukemia. Leukemia. 2009;23:1698-1707.
19. Salvador JAR, Leal AS, Valdeira AS, Gonçalves BMF, Alho DPS, Figueiredo SAC, Silvestre SM, Mendes VIS. Oleanane-, ursane-, and quinone methide friedelane-type triterpenoid derivatives: Recent advances in cancer treatment. Eur J Med Chem. 2017;142:130.
20. Radwan MO, Ismail MAH, El-Mekkawy S, Ismail NSM, Hanna AG. Synthesis and biological activity of new 18β-glycyrrhetinic acid derivatives. Arab J Chem. 2016;9:390-399.
21. Ciftci HI, Ozturk SE, Ali TFS, Radwan MO, Tateishi H, Koga R, Ocak Z, Can M, Otsuka M, Fujita M. The first pentacyclic triterpenoid gypsogenin derivative exhibiting anti-Abl1 kinase and anti-chronic myelogenous leukemia activities. Biol Pharm Bull. 2018;141:570-574.
22. Lu Z, Jin Y, Qiu L, Lai Y, Pan J. Celastrol, a novel HSP90 inhibitor, depletes Bcr-Abl and induces apoptosis in imatinib-resistant chronic myelogenous leukemia cells harboring T315I mutation. Cancer Lett. 2010;290:182-191.
23. Sharma G, Kar S, Palit S, Das PK. 18β-glycyrrhetinic acid induces apoptosis through modulation of Akt/FOXO3a/Bim pathway in human breast cancer MCF-7 cells. J Cell Physiol. 2012;227:1923-1931.
24. Zhu J, Chen M, Chen N, Ma A, Zhu C, Zhao R, Jiang M, Zhou J, Ye L, Fu H, Zhang X. Glycyrrhetinic acid induces G1-phase cell cycle arrest in human non-small cell lung cancer cells through endoplasmic reticulum stress pathway. Int J Oncol. 2015;46:981-988.
25. Liu D, Song D, Guo G, Wang R, Lv J, Jing Y, Zhao L. The synthesis of 18β-glycyrrhetinic acid derivatives which have increased antiproliferative and apoptotic effects in leukemia cells. Bioorgan Med Chem. 2007;15:5432-5439.
26. Pirzadeh S, Fakhari S, Jalili A, Mirzai S, Ghaderi B, Haghshenas V. Glycyrrhetinic Acid induces apoptosis in leukemic HL60 cells through upregulating of CD95 / CD178. Int J Mol Cell Med. 2014;3:272-278.
27. Gao Z, Kang X, Hu J, Ju Y, Xu C. Induction of apoptosis with mitochondrial membrane depolarization by a glycyrrhetinic acid derivative in human leukemia K562 cells. Cytotechnology. 2012;64:421-428.
28. Ali TF, Iwamaru K, Ciftci HI, Koga R, Matsumoto M, Oba Y, Kurosaki H, Fujita M, Okamoto Y, Umezawa K, Nakao M, Hide T, Makino K, Kuratsu J, Abdel-Aziz M, Abuo-Rahma Gel-D, Beshr EA, Otsuka M. Novel metal chelating molecules with anticancer activity. Striking effect of the imidazole substitution of the histidine-pyridine-histidine system. Bioorg Med Chem. 2015;23:5476-5482.

29. Bayrak N, Yıldırım H, Tuyun AF, Kara EM, Celik BO, Gupta GK, Ciftci HI, Fujita M, Otsuka M, Nasiri HR. Synthesis, computational study, and evaluation of in vitro antimicrobial, antibiofilm, and anticancer activities of new sulfanyl aminonaphthoquinone derivatives. Lett Drug Des Discov. 2017;14:647-661.

30. Karabacak M, Altıntop MD, İbrahim Çiftçi H, Koga R, Otsuka M, Fujita M, Özdemir A. Synthesis and evaluation of new pyrazoline derivatives as potential anticancer agents. Molecules. 2015;20:19066-19084.

31. Tateishi H, Monde K, Anraku K, Koga R, Hayashi Y, Ciftci HI, DeMirci H, Higashi T, Motoyama K, Arima H, Otsuka M, Fujita M. A clue to unprecedented strategy to HIV eradication: "Lock-in and apoptosis." Sci Rep. 2017;7:8957.

32. Nagar B, Bornmann WG, Pellicena P, Schindler T, Veach DR, Miller WT, Clarkson B, Kuriyan J. Crystal structures of the kinase domain of c-Abl in complex with the small molecule inhibitors PD173955 and imatinib (STI-571). Cancer Res. 2002;62:4236-4243.

33. Radwan MO, Sonoda S, Ejima T, Tanaka A, Koga R, Okamoto Y, Fujita M, Otsuka M. Zinc-mediated binding of a low-molecular-weight stabilizer of the host anti-viral factor apolipoprotein B mRNA-editing enzyme, catalytic polypeptide-like 3G. Bioorgan Med Chem. 2016;24:4398-4405.

34. Koga R, Radwan MO, Ejima T, Kanemaru Y, Tateishi H, Ali TFS, Ciftci HI, Shibata Y, Taguchi Y, Inoue J, Otsuka M, Fujita M. A Dithiol Compound Binds to the Zinc finger protein TRAF6 and suppresses its ubiquitination. ChemMedChem. 2017;12:1935-1941.

Turk J Pharm Sci 2020;17(1):56-62
DOI: 10.4274/tjps.galenos.2018.91249

ORIGINAL ARTICLE

Investigation of the Presence of Sildenafil in Herbal Dietary Supplements by Validated HPLC Method

Bitkisel Diyet Takviyelerinde Sildenafil Varlığının Valide Bir HPLC Yöntemiyle Araştırılması

Emrah DURAL*

Sivas Cumhuriyet University, Faculty of Pharmacy, Department of Pharmaceutical Toxicology, Sivas, Turkey

ABSTRACT

Objectives: As the first FDA-approved phosphodiesterase type 5 inhibitor, sildenafil (SDF) is widely used in the treatment of erectile dysfunction due to its strong pharmacodynamic activity. Since many food supplements are now involved in illegal adulteration, the presence of SDF in food supplements is very important because of their toxicological risks. In this study a simple fast, reliable high-performance liquid chromatography method with ultraviolet (UV) detector has been developed and validated for SDF analysis in herbal dietary supplements (HDSs).

Materials and Methods: 10 mM phosphate buffer containing 0.1% triethylamine (pH 3.5) and acetonitrile (65:35, v/v), as mobile phase was applied isocratically to a reverse phase C18 analytical (4.6×250 mm, 5 µm) column. Chromatographic separation was achieved by a C_{18} reverse-phase analytical column 4.6×250 mm, 5 µm particle size, using acetonitrile, with 10 mM phosphate buffer containing 0.1% triethylamine (65:35, v/v, pH 3.5) as a mobile phase. The mobile phase flow rate was 1 mL min^{-1} and the column temperature was 35°C. The UV detector was set at 293 nm. The liquid-liquid extraction method used in the study provided a simple and practical method for the recovery of SDF in HDSs and their obtained values ranged from 87.6 to 111.7%.

Results: The method showed linearity with an excellent correlation coefficient (r^2>0.999). Moreover, it was specific and sensitive with the limit of quantification, 6.5 ng mL^{-1}. Intraday and interday method precision was ≤8.2 (relative standard deviation %). Intraday and interday method accuracy was between -4.0 and 7.1 (RE%). The method was strong according to the robustness test results obtained from UV detection, mobile phase buffer pH, column temperature, and flow rate changes. The described procedure was simple, fast, precise, and feasible for routine adulteration analysis of SDF, especially in food control or toxicology laboratories. This method was successfully applied to 50 individual solid and liquid form HDSs.

Conclusion: The results showed that 37 out of 50 samples of HDSs (represented 74.0%) examined contained SDF between 0.01 and 465.47 mg/g, 150.87±127.48 (mean ± standard deviation), which could lead to serious health problems and might even be fatal for consumers. The described procedure was found to be simple, rapid, precise and feasible for routine adulteration analysis of SDF, especially in food control or toxicology laboratories.

Key words: Sildenafil, adulteration, herbal dietary supplements, validation, high-performance liquid chromatographic-ultraviolet detection

ÖZ

Amaç: FDA tarafından onaylı ilk fosfodiesteraz-5 inhibitörü olan sildenafil (SDF), güçlü farmakodinamik etkinliği sebebiyle erektil fonksiyon bozukluğunun tedavisinde yaygın olarak kullanılmaktadır. Günümüzde birçok gıda takviyesi, yasadışı tağşiş işlemlerine dahil olduğundan, gıda takviyelerinin içerisindeki SDF varlığının belirlenmesi toksikolojik riskleri sebebiyle çok önemlidir. Bu çalışmada bitkisel gıda takviyelerinde (BGT) SDF analizi için basit, hızlı, güvenilir bir ultraviyole (UV) detektörlü yüksek performanslı sıvı kromatografi yöntemi geliştirilmiş ve valide edilmiştir.

Gereç ve Yöntemler: Mobil faz olarak içeriğinde %0,1 trietilamin bulunan 10 mM'lik fosfat tamponu (pH 3,5) ve asetonitril (65:35, v/v) bir ters faz C18 analitik kolonuna (4,6×250 mm, 5 µm) izokratik olarak uygulanmıştır. Mobil faz akış hızı 1 mL dk^{-1} ve kolon sıcaklığı 35°C idi. UV dedektör 293 nm'ye ayarlanmıştır. Çalışmada kullanılan sıvı-sıvı ekstraksiyon yöntemi, BGT'lerde SDF'nin geri kazanımı için basit ve pratik bir yöntem sağladı ve elde edilen değerleri %87,6 ila 111,7 arasındaydı.

Bulgular: Yöntem, mükemmel bir korelasyon katsayısı ile doğrusallık göstermiştir (r^2>0,999). Ayrıca, metot 6,5 ng mL^{-1}'lik tayin limitiyle seçici ve hassastı. Gün içi ve günler arası metot kesinlik ≤%8,2 (% bağıl standart sapma) idi. Gün içi ve günler arası metot doğruluk testi sonuçları (-4,0) ile

*Correspondence: E-mail: emrahdural@cumhuriyet.edu.tr, Phone: +90 346 219 10 10 (#39 20) ORCID-ID: orcid.org/0000-0002-9320-8008
Received: 24.07.2018, Accepted: 25.10.2018

7,1 (%RE) arasındaydı. Metodun UV tespiti, mobil faz tampon pH'sı, kolon sıcaklığı ve akış hızı değişimlerinden elde edilen sonuçlarla sağlam olduğu görüldü. Bu yöntem birbirinden ayrı katı ve sıvı formdaki 50 adet BGT'ye başarıyla uygulanmıştır.

Sonuç: Sonuçlar incelenen 50 adet BGT örneğinden 37'sinin (%74,0), 0,01 ile 465,47 mg/g, 150,87±127,48 (ortalama±standart sapma) ile kullananlarda ciddi sağlık sorunlarına yol açabilecek hatta ölümcül bile olabilecek kadar SDF içerdiğini gösterdi. Tanımlanan prosedürün, özellikle gıda kontrol veya toksikoloji laboratuvarlarında SDF'nin rutin tağşiş analizleri için basit, hızlı, kesin ve uygulanabilir olduğu görülmüştür.

Anahtar kelimeler: Sildenafil, tağşiş, bitkisel gıda takviyeleri, validasyon, yüksek-performanslı sıvı kromatografisi-ultraviyole dedeksiyon

INTRODUCTION

Sildenafil (SDF), 1-[(3-(6.7-dihydro-1-methyl-7-oxo-3-propyl-1H-pyrazolo(4.3-d)pyrimidin-5-yl)-4-ethoxyphenyl) sulfonyl)-4-methyl piperazine citrate] (Figure 1a) is a potent and selective inhibitor of the cyclic guanosine monophosphate (cGMP)-specific phosphodiesterase type 5 (PDE-5) mainly found in the penile corpus cavernosum that causes cGMP to accumulate in the corpus cavernosum.[1,2] cGMP, which is broken down by PDE-5, is directly responsible for producing smooth muscle relaxation in the corpus cavernosum and allowing the inflow of blood.[3]

SDF, the first synthetic PDE-5 inhibitor licensed for clinical use, has the ability to enhance relaxation of the corpus cavernosum and therefore can potentially improve penile erectile function.[4,5] Since SDF is considered an effective oral agent for the treatment of male erectile dysfunction, it has been extensively used to improve erectile dysfunction. In addition, SDF has been also used commonly in the treatment of pulmonary hypertension disease successfully.[6]

The structural formula is $C_{22}H_{30}N_6O_4S$. SDF is an ampholyte with pKa value 4 (pyridinium ion) and 8.8 (benzmidazole). SDF is soluble in both methanol and water.[7] SDF is rapidly absorbed with approximately 40% bioavailability by the gastrointestinal tract and rapidly and widely metabolized to active N-desmethyl sildenafil (N-SDF) as a major metabolite by the CYP3A4 and CYP2C9 hepatic microsomal enzymes after oral administration. The elimination half-life of both SDF and *N*-SDF is approximately 2.5 h.[8,9]

SDF is a relatively safe drug with an upper limit of 100 µg/day. However, it has some serious side effects that may create potential hazards. It has been reported to seriously potentiate the hypotensive effects of nitrates commonly employed in the treatment of certain heart impairments. This side effect, which occurs in combination with nitrates and can cause risk of death, is very important toxicologically. Clinical studies have also reported blindness in one eye as an adverse effect of administration of SDF. SDF also has a high affinity for phosphodiesterase type 6 (PDE-6), which is a retinal enzyme involved in phototransduction. The inhibition of PDE-6 can result in a situation known as blue tinge, which prevents the ability to distinguish between blue and green colors. Although only 3% of patients report visual disturbances, this blue-green impairment can cause problems when fulfilling certain tasks. For example, this degradation can lead to problems for pilots during night flights or adverse meteorological conditions.[10]

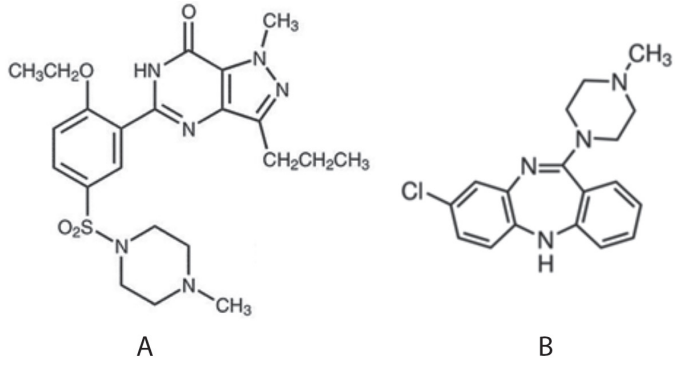

Figure 1. Chemical structure of SDF (A) and CZP (B) used as an internal standard

SDF: Sildenafil, CZP: Clozapine

Because people consider that natural substances are safer and healthier than synthetic derivatives, herbal dietary supplements (HDSs) have widely increased as alternatives to chemically synthetic products recently.[11] The adulteration with SDF in varying doses of herbal products sold for the treatment of erectile dysfunction is a serious potential health hazard. Although drugs containing SDF need to be prescribed under medical supervision, they are used without prescription in many countries, including Turkey. The sale of these medicines without medical advice causes patients to use them in high doses to gain more effect. It is known that the adulteration of HDSs with SDF is illegal and when a patient who is undergoing medical treatment with SDF also uses HDSs adulterated with SDF serious results may emerge. However, the presence of HDSs containing SDF marketed without controls in Turkey and around the world is frequently reported.

Therefore, consumption of HDSs that might be adulterated with SDF can produce serious toxic effects. For the purposes of quality control and product safety, analytical procedures need to be established that can selectively detect and quantify SDF in dosages in adulterated herbal products.

Several techniques are reported for the determination of SDF in many kinds of food supplements and pharmaceutical formulations, namely flow injection analysis,[2] thin layer chromatography (TLC),[12] spectrophotometry,[2,13] spectrofluorometry,[14] high-performance liquid chromatography (HPLC)-ultraviolet (UV),[7,15-17] HPLC-diode array detection,[12,18] HPLC-electrospray ionization-mass spectrometry (ESI-MS),[19] micellar electrokinetic chromatography,[4] electrospray tandem (ESI)-MS,[11] gas chromatography (GC)-MS,[20,21] liquid chromatography (LC)-MS,[12] and LC-MS.[22,23]

In addition, low analytical sensitivity, inadequate intraday and interday reproducibility values, and inappropriate recovery amounts cause problems with the use of these techniques.

Spectrophotometer analyses can lead to false positive results due to chemical interactions with molecules with similar chemical properties through the absence of pre-separation through a column. TLC assays do not show sufficient analytical sensitivity in routine assays with the long analysis times and difficulties of quantification. Analysis of SDF by GC-MS does not show sufficient analytical sensitivity due to its chemical properties, that is its low transition to the gas phase. Although the LC-MS is a device with high analytical sensitivity, it is less common in toxicological analysis laboratories due to its high cost. Moreover, its per analysis cost is higher than that of other techniques. HPLC-UV-based analytical techniques provide sufficient analytical sensitivity and reproducibility to determine the amount of SDF in food supplements, biological fluids, and other many matrices.

Our study of the analysis of SDF content in HDSs with HPLC-UV provides a significant advantage with high analytical accuracy and precision, low cost per analysis, and fast retrieval of results. This method was based on separation with an analytical column 4.6×250 mm, 5 µm particle size, using acetonitrile, and 10 mM phosphate buffer (pH 3.5) containing 0.1% triethylamine (65:35, v/v) as the mobile solvent. The UV detector was set at 293 nm and the total analysis time was 7.5 min. Clozapine (CZP) was used as an internal standard (ISTD). The developed method was also validated with linearity, accuracy, precision, sensitivity, recovery, and robustness according to the ICH-2005 guideline. The validity of the developed method has been proved by analyzing 50 HDSs that were liquid (liquid and paste) and solid (tablet, capsule, and powder) form. The results showed that products sold as HDSs for the treatment of erectile dysfunction seriously threatened public health, since SDF content was found to be in the range of 0.01 to 465.47 mg/g in 37 of the 50 samples (74%) analyzed in terms of SDF contents (150.87±127.48, $\bar{x}$ ± Standard deviation).

MATERIALS AND METHODS

Chemicals and reagents

Pure reference samples of SDF (Figure 1a) and CZP as the ISTD (Figure 1b) were purchased from Sigma-Aldrich (Steinheim, Germany). HPLC grade methanol and acetonitrile were obtained from Sigma-Aldrich (St. Louis, MO, USA). Analytical grade triethyl amine, orthophosphoric acid, potassium dihydrogen phosphate, sodium carbonate, and sodium sulfate were purchased from Merck (Darmstadt, Germany). Ultrapure water was made by Elga Purelab (High Wycombe, United Kingdom) system. A polytetrafluoroethylene disc filter (0.45 µm) was used to purify the HDSs. Membrane filters with a pore size of 0.45 µm from Millipore (Burlington, MA, USA) were used for filtration of the mobile phase.

Instrumentation

The separation and quantification were performed by HP Agilent 1100 series (Palo Alto, CA, USA) HPLC system, equipped with a UV detector. A HPLC system was employed in the present study; it consisted of a gradient pump (G1311A), a degasser (G1312), a column oven (G1316A), a UV detector (G1314A), and a Rheodyne 7725i manual injector with a 20-µL sample loop. ChemStation® version 08.03 software was employed for data collection and handling.

Chromatographic conditions

Separations were carried out on an ACE-5 (Aberdeen, Scotland) reverse phase C_{18} analytical column (4.6×250 mm, 5 µm particle size). The analysis was carried out under isocratic conditions using a flow rate of 1.0 mL min^{-1} at 35°C. Chromatographic quantitation was conducted at 293 nm. The mobile phase consisted 10 mM phosphate buffer (containing 0.1% triethyl amine) and acetonitrile (65:35, v/v) before delivery into the HPLC system. The mobile phase pH was adjusted to 3.5 with 1 M phosphoric acid. It was degassed before every use over 30 min using an ultrasonic bath.

Collection of samples and its preparation to analysis

Fifty-one different HDSs advertised to enhance sexual performance in men from individual brands were purchased online and from an herbal market in Sivas. All the solid drug and tablet samples were pulverized by a mortar. An exactly weighed 200 mg (liquid, solid, and powdered) sample was dissolved in a 10 mL mixture of methanol and 1.5% Na_2CO_3 (7:3, v/v). After that, the mixture was dried with 250 mg of Na_2SO_4. The extract was mixed over 10 min at 1200 rpm in a rotator shaker and dissolved in an ultrasonic bath over 30 min. The sample was centrifuged at 3000 rpm for 5 min and approximately 10 mL of the upper phase was transferred to a clean test tube and filtered by a 0.45-µm disc filter. Then 10 µL of sample filtrate and 10 µL of ISTD (100 µg mL^{-1}) were completed to 10 mL with the mobile phase and vortexed at 1200 rpm for 1 min. Finally, 20 µL of this mixture was applied to the liquid chromatograph under specified chromatographic conditions.

Preparation of standard solutions

A SDF stock solution (1 mg mL^{-1}) was prepared in methanol and stored at -20°C. It has been quantitatively determined that it is chemically stable for at least 3 months. Working solutions were prepared by main stock solution weekly in methanol at 10, 20, 30, 40, 60, 80, and 100 µg mL^{-1} concentrations. The ISTD main stock solution (10 mg mL^{-1}) was prepared with methanol to yield a 100 µg mL^{-1} working solution.

RESULTS AND DISCUSSION

Method validation

The method developed was validated in terms of specificity, linearity, accuracy, precision, sensitivity, recovery, and robustness. In order to obtain accurate and precise measurements in accordance with the International Harmonization Conference, the intraday and interday validity protocols were implemented taking into account the reproducibility of the method and instrument.[24]

Specificity

Specificity is the ability of the method to measure the analyte response in the presence of all the impurities that may arise from the analyte and other conditions. The UV detector was

set to a wavelength of 293 nm displaying optimum sensitivity. Figures 2a, 2b, and 2c show chromatograms of blank, spiked, and real samples illustrating the high resolution with no interference and too short separation time (7.5 min). The method demonstrated excellent chromatographic specificity with no endogenous interference at the retention times of SDF and CZP (6.2 and 6.7 min, respectively) as an ISTD.

Linearity and selectivity

After establishing the chromatographic conditions, the linearity of SDF was studied by preparing standard solutions at 7 different levels ranging from 10 to 1000 ng mL^{-1}. Calibration was performed by linear regression of peak-area ratios of SDF to the ISTD versus the respective standard concentration. For each concentration 3 individual replicates were injected and linearity was obtained for SDF with high correlation coefficients (r^2) over 0.999 (Table 1). System suitability parameters are tabulated in Table 2.

Precision and accuracy

The precision and accuracy of the method were examined on 5 consecutive days. Precision, defined as relative standard deviation (RSD), was determined by five individual replicates at three different concentrations, which were 20, 100, and 500 ng mL^{-1} (n=5). Table 3 shows the RSD values of low, medium, and high concentrations (20, 100, and 500 ng mL^{-1}, respectively) to present inter- and intraday precision. Accuracy, defined as relative error (RE%), was also determined for the same concentrations of analytes (Table 3).

Recovery

The recovery of the method was calculated by comparing the results obtained from the application of the standard sample prepared in methanol to the samples prepared in the same concentration in the herbal sample. The recovery results conducted at 20, 100, and 500 ng mL^{-1} are tabulated in Table 3.

Sensitivity

The limit of detection (LOD) and limit of quantification (LOQ) were determined based on the standard deviation of the response and the slope of the calibration curve, according to the International Council for Harmonisation of Technical Requirements for Pharmaceuticals for Human Use (ICH) guidelines.[24] (LOD=3.3σ/S, LOQ=10σ/S, where σ is the standard deviation of the response and S is the slope of the calibration curve). The LOD and LOQ values of the method were 1.94 ng mL^{-1} and 6.46 ng mL^{-1}, respectively.

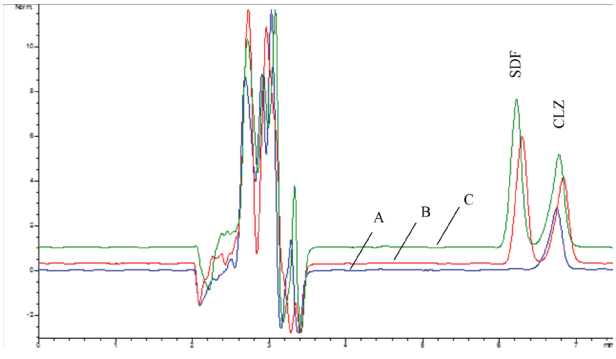

Figure 2. A. The chromatogram of the SDF blank sample that belongs to HDS extract used as a quality control sample in validation tests. B. The chromatogram of an HDS extract that was prepared by standard addition method containing 1000 ng mL-1 SDF. C. The chromatogram of a real HDS sample extract determined to be adulterated with SDF.

SDF: Sildenafil, HDS: Herbal dietary supplements, CLZ: Clozapine

Robustness

Significant changes were not observed in the analytical signals upon changing the UV wavelength value (±2 nm) ($p>0.05$), mobile phase buffer pH (±0.3) ($p>0.05$), column temperature (±4°C) ($p>0.05$), or mobile phase flow rate (±0.1 mL min^{-1}) ($p>0.05$). The statistics were evaluated by SPSS 15 - Kruskal-Wallis test. In addition, changes in analyst, analytical column, the source of chemical, and/or solvent did not lead to significant changes in chromatographic signals. Robustness experiments demonstrated that the method created data of acceptable precision and accuracy. After the data from the validation tests were found to be appropriate for safe analysis, the survey of the SDF in real HDSs was initiated.

Analysis of samples

A quantitative investigation of SDF contents in 50 HDSs used for the treatment of erectile dysfunction sold in an herbal market and on the Internet was conducted. Solid and liquid supplement samples were prepared according to the sample preparation

Table 1. The analytical parameters of the proposed HPLC method

Parameter	SDF[a]
Calibration curve (ng mL^{-1})	10.0-1000.0
Slope	0.0011
Standard error of slope	0.00013
Intercept	-0.0028
Standard error of intercept	0.0573
Coefficient of determination (r^2)	0.9992
LOD (ng mL^{-1})	1.9
LOQ (ng/mL)	6.5
Retention time for SDF (min)	6.2
Retention time of IS (min)	6.7

[a]Number of repeated measurement n=6, LOD: Limit of detection, LOQ: Limit of quantification SDF: Sildenafil, HPLC: Hight performance liquid chromatography

Table 2. System suitability parameters

Parameters	T_R	K	α	(Rs)	Symmetry factor
SDF	6.2	5.6	1.1	3.3	1.0
IS	6.7	6.3	-	-	1.0

T_R=Retention time, K= Capacity factor for SDF and IS, where k=the capacity factor for drug and IS,
α=Separation factor, calculated as K_2/K_1 Rs= Resolution 2 (t2-t1) / (w1+w2), where t2 and t1 are the retention times of the SDF and IS and w2 and w1 are the half-peak width of the drug and IS, respectively

procedure explained above. The measurement results are given in Table 4. Sample chromatograms are shown in Figure 3.

CONCLUSION

In our study, the presence of SDF was quantitatively investigated in 50 products described as ginseng, panax, epimedium, herbal mixtures, and herbal supplements on product packages by the developed and also validated method in accordance with ICH (2005) Guidelines.[24] The SDF positive samples known as HDSs were in the form of pills, capsules, powders, syrups, liquids, and pastes. These food supplements that were positive for SDF analysis were all different shades of green and brown. Some of the products analyzed gave the impression that they were malodorous herbal medicines. In addition, some analyzed herbal products were enriched with chocolate, lemon juice, and other sweeteners. In addition, there was a malodorous product that was difficult for a person to swallow in one go because of its size, 3 cm in diameter. Powdered products were usually brown and gray in color and had a sharp spice smell. Liquid products were light green. It is thought that these processes are intended to convince users that the products are natural.

It has been reported that SDF is a safe drug for therapeutic use. However, the use of SDF-containing medical tablets as well as a user who considers taking a natural product will cause an overdose. The tendency to use more of the recommended product for the expected increase in activity, as well as the product thought to be natural, is often common in individuals who use food supplements. It is also known that the use of SDF in combination with organic nitrates significantly increases systemic blood pressure lowering effects. An overdose can create a serious risk for the cardiovascular system. It is known that individuals who frequently use these products are men over 50 years old and cardiovascular system diseases increase in this group during this period.

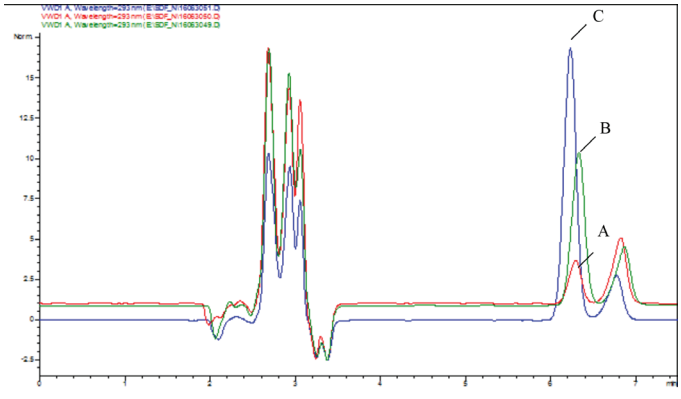

Figure 3. Real HDS sample chromatograms containing SDF (A=sample 50, B=sample 49, and C=sample 51)

HDS: Herbal dietary supplements, SDF: Sildenafil

However, SDF has been found in quantities of 0.01 to 465.47 mg/g (150.87±127.48, mean ± standard deviation) in 37 products with positive results, which could harm human health even after a single use (Table 4). It has been reported that these products have been sold at a higher rate than others with low SDF content. It has also appeared on product packages that the same products are more effective in the treatment of erectile dysfunction. It has been determined that some of the herbal products studied contain SDF in almost half of their weight.

This study was carried out due to the fact that there is no method in the literature that is analyzed with a simple, uncomplicated analytical device with low cost of analysis. In our study, a new HPLC-based analysis method was developed for the determination of illegal addition of SDF to herbal products and the method was validated and the applicability of the method was shown with 50 samples. The method developed has significant advantages, such as rapid analysis with a total analysis time of 7.5 min, a low sample requirement (0.2 g), and high analytical accuracy (LOD: 1.88 ng mL^{-1}). The method developed is noteworthy due to its intraday and interday reproducibility values, which were between 2.34 and 8.13 (RSD%) for precision and between -4.02 and 7.14 (RE%) for accuracy, and recovery values were between 87.57% and 111.65%. The method was also proven to be robust against changes in some analytical conditions such as mobile phase content, column temperature, and flow rate, as well as robustness tests. The method was also easily applied to 50 herbal products and the analyses were successfully completed in all products. In addition, during sample preparation and analysis only a small amount of solvent was used. Our study methodology was compared with the other HPLC study results in Table 5.

A total of 50 products marketed as herbal products for the treatment of erectile dysfunction were exposed to serious abuse. Measures to prevent international marketing of these products, which seriously threaten public health, are needed. Although the products examined are visually similar to a medicinal product, they are marketed as "herbal products" online and in markets selling herbal products. These synthetic

Table 3. Confidence parameters of the validated method; intraday and interday precision and accuracy and recovery parameters of validated method; at 20, 100, and 500 ng mL^{-1} concentration for determination of SDF

Expected conc. (ng mL^{-1})	Intraday (n=5)			Interday (n=5)			Observed concentration (n=5)	
	Estimated conc. $\bar{x}$±SD (ng mL^{-1})	Precision (RSD%)	Accuracy (RE%)	Estimated conc. $\bar{x}$±SD (ng mL^{-1})	Precision (RSD%)	Accuracy (RE%)	Values of the recovery (%)	Mean recovery %±SD
20	22.43±1.54	8.13	7.14	21.05±0.97	4.21	5.25	87.57-108.73	98.15±9.52
100	106.47±2.43	2.34	6.47	104.98±6.05	5.90	4.98	92.08-103.61	97.85±5.83
500	479.89±15.80	3.31	-4.02	486.07±22.46	4.58	-2.79	98.59-111.65	105.12±7.00

"Concentrations" are abbreviated as "conc.", SDF: Sildenafil, SD: Standard deviation, RSD: Relative standard deviation, RE: Relative error

Table 4. Results of SDF values determined in HDSs

Sample number	The presentation of the product	The detected SDF amount (mg/g)	Sample number	The presentation of the product	The detected SDF amount (mg/g)	Sample number	The presentation of the product	The detected SDF amount (mg/g)
1	Dust	0.01	18	Tablet	48.51	35	Dust	ND
2	Capsule	ND	19	Dual tablet	246.41	36	Dust	ND
3	Tablet	151.78	20	Dust	ND	37	Tablet	91.83
4	Capsule	34.15	21	Capsule	153.64	38	Dual tablet	30.77
5	Tablet	290.86	22	Tablet	188.53	39	Dust	ND
6	Capsule	1.95	23	Dual tablet	261.89	40	Dust	ND
7	Capsule	ND	24	Tablet	75.95	41	Tablet	55.35
8	Liquid	15.52	25	Tablet	148.68	42	Tablet	241.79
9	Capsule	287.56	26	Tablet	0.90	43	Capsule	392.85
10	Tablet	262.70	27	Tablet	116.18	44	Dual tablet	465.47
11	Dust	ND	28	Tablet	344.70	45	Dust	ND
12	Tablet	127.34	29	Dust	ND	46	Dust	ND
13	Tablet	201.85	30	Dust	ND	47	Tablet	91.72
14	Tablet	0.02	31	Tablet	288.74	48	Tablet	104.76
15	Dust	ND	32	Capsule	346.48	49	Capsule	25.60
16	Dust	0.40	33	Capsule	168.53	50	Tablet	247.32
17	Paste	13.36	34	Dual tablet	58.09			
Minimum detected concentration			0.01					
Maximum detected concentration			465.47					
Average			150.87					
Standard deviation			127.48					

SDF: Sildenafil, HDSs: Herbal dietary supplements, ND= Not detected

Table 5. The validation parameters and chromatographic properties of SDF determination methods in the literature

Study	LOQ	Retention times (min)	Linearity	Linear range	Mobile phase	Flow (mL min $^{-1}$)	Detector and detection value	Total analysis time (min)
Reddy and Reddy 2008[7]	8.2 ng mL^{-1}	4.1	0.9990	0.1-30 µg mL^{-1}	Phosphate buffer (pH 7.0) and acetonitrile/ (3:7, v/v)	0.8	UV 228	15
Daraghmeh et al.[15] 2001	12.2 µg mL^{-1}	9.5	0.9999	2-12 µg mL^{-1} 64-257 µg mL^{-1}	0.2 M ammonium acetate (pH 7.0) and acetonitrile (1:1, v/v)	1	UV 240	10
Dinesh et al.[16] 2002	0.05 µg mL^{-1}	10.0	0.9995	0.05-7.5 µg mL^{-1}	Water and acetonitrile (48:52, v/v)	1	UV 245	10
Nagaraju et al.[17] 2003	-	5.2	0.9950	90.5-99.9 µg mL^{-1}	0.05 M potassium dihydrogen orthophosphate and acetonitrile (3:7 v/v)	1	DAD 230	15
Yang et al.[18] 2010	2 ng mL^{-1}	2.0	1.0000	0.2- 200 µg mL^{-1}	30 mM ammonium formate (pH 3.0) and acetonitrile (7:3, v/v)	1.3	UV 230	7

SDF: Sildenafil, LOQ: Limit of quantification, UV: Ultraviolet, DAD: Diode array detection

products have been found to contain SDF in amounts that could threaten human health even after a single use.

In the present study, the established HPLC-UV method is fast, cheap, and accurate for reference laboratories concerned with food control or toxicology. The applicability of the developed method to herbal products was proved by analysis of 50 HDSs. At the same time, it was shown that herbal products marketed for the treatment of erectile dysfunction in the market contain high amounts of SDF, which can pose a risk to human health.

ACKNOWLEDGEMENTS

This research was supported by Scientific Research Projects Support Program of Sivas Cumhuriyet University (CÜBAP) under project number ECZ016.

Conflict of Interest: No conflict of interest was declared by the authors.

References

1. Ahn CY, Bae SK, Bae SH, Kang HE Kim SH, Lee MG, Shin WG. Pharmacokinetics of sildenafil and its metabolite, N-desmethylsildenafil, in rats with liver cirrhosis and diabetes mellitus, alone and in combination. Xenobiotica. 2011;41:164-174.
2. Alitokka G, Atkosar Z, Sener E, Tunçel M. FIA of sildenafil citrate using UV-detection. J Pharm Biomed Anal. 2001;25:339-342.
3. Langtry HD, Markham A. Sildenafil: a review of its use in erectile dysfunction. Drugs. 1999;57:967-989.
4. Berzas Nevado JJ, Flores JR, Peñalvo GC, Rodríguez FN. Determination of sildenafil citrate and its main metabolite by sample stacking with polarity switching using micellar electrokinetic chromatography. J Chromatogr A. 2002;953:279-286.
5. Cooper JD, Muirhead DC, Taylor JE, Baker PR. Development of an assay for the simultaneous determination of sildenafil (viagra) and its metabolite (UK-103,320) using automated sequential trace enrichment of dialysates and high-performance liquid chromatography. J Chromatogr B Biomed Sci Appl. 1997;701:87-95.
6. Barnett CF, Machado RF. Sildenafil in the treatment of pulmonary hypertension. Vasc Health Risk Manag. 2006;2:411-422.
7. Reddy BP, Reddy KA, Reddy MS. Validation and stability indicating RP-HPLC method for the determination of tadalafil API in pharmaceutical formulations. Res Pharm Biotechnol. 2010;2:1-6.
8. Al-Ghazawi M, Tutunji M, AbuRuz S. Simultaneous determination of sildenafil and N-desmethyl sildenafil in human plasma by high-performance liquid chromatography method using electrochemical detection with application to a pharmacokinetic study. J Pharm Biomed Anal. 2007;43:613-618.
9. Karatza AA, Bush A, Magee AG. Safety and efficacy of Sildenafil therapy in children with pulmonary hypertension. Int J Cardiol. 2005;100:267-273.
10. Lewis RJ, Johnson RD, Blank CL. Quantitative determination of sildenafil (Viagra) and its metabolite (UK-103,320) in fluid and tissue specimens obtained from six aviation fatalities. J Anal Toxicol. 2006;30:14-20.
11. Abdel-Hamid Me. Determination of sildenafil, tadalafil, and vardenafil in tablets and adulterated herbal products by ESI-MS-MS. J Liq Chromatogr Relat Technol. 2006;29:591-603.
12. Mikami E, Ohno T, Matsumoto H. Simultaneous identification/determination system for phentolamine and sildenafil as adulterants in soft drinks advertising roborant nutrition. Forensic Sci Int 2002;130:140-146.
13. Harikrishna K, Nagaralli BS, Seetharamappa J. Extractive Spectrophotometric Determination of Sildenafil Citrate (Viagra) in Pure and Pharmaceutical Formulations. 2008;16:11-17.
14. Chien C, Wang C, Fernandez LP. Spectrofluorimetric Determination of Sildenafil : A New Analytical Alternative for Its Analysis. J Chinese Med Res Dev. 2012;1:54-60.
15. Daraghmeh N, Al-Omari M, Badwan AA, Jaber AM. Determinaton of sildenafil citrate and related substances in the commercial products and tablet dosage form using HPLC. J Pharm Biomed Anal. 2001;25:483-492.
16. Dinesh ND, Vishukumar BK, Nagaraja P, Made Gowda NM, Rangappa KS. Stability indicating RP-LC determination of sildenafil citrate (Viagra) in pure form and in pharmaceutical samples. J Pharm Biomed Anal. 2002;29:743-748.
17. Nagaraju V, Sreenath D, Rao JT, Rao RN. Separation and determination of synthetic impurities of sildenafil (Viagra) by reversed-phase high-performance liquid chromatography. Anal Sci. 2003;19:1007-1011.
18. Yang YJ, Song DM, Jiang WM, Xiang BR. Rapid resolution RP-HPLC-DAD method for simultaneous determination of sildenafil, vardenafil, and tadalafil in pharmaceutical preparations and counterfeit drugs. Anal Lett. 2010;43:373-380.
19. Zhu X, Xiao S, Chen B, Zhang F, Yao S, Wan Z, Yang D, Han H. Simultaneous determination of sildenafil, vardenafil and tadalafil as forbidden components in natural dietary supplements for male sexual potency by high-performance liquid chromatography-electrospray ionization mass spectrometry. J Chromatogr A. 2005;1066:89-95.
20. Man CN, Nor NM, Lajis R, Harn GL. Identification of sildenafil, tadalafil and vardenafil by gas chromatography-mass spectrometry on short capillary column. J Chromatogr A. 2009;1216:8426-8430.
21. Popescu AM, Radu GL, Onisei T, Raducanu AE, Niculae CG. Detection by gas chromatography-mass spectrometry of adulterated food supplements. Rom Biotechnol Lett. 2014;19:9485-9492.
22. Tseng MC, Lin JH. Determination of sildenafil citrate adulterated in a dietary supplement capsule by LC/MS/MS. J Food Drug Anal. 2002;10:112-119.
23. Liang Q, Qu J, Luo G, Wang Y. Rapid and reliable determination of illegal adulterant in herbal medicines and dietary supplements by LC/MS/MS. J Pharm Biomed Anal. 2006;40:305-311.
24. ICH. International Conference on Harmonization (ICH) of Technical Requirements for the Registration of Pharmaceuticals for Human Use, Validation of Analytical Procedures: Methodology (ICB-Q2B) (1996). http://www.ich.org/fileadmin/Public_Web_Site/ICH_Products/Guidelines/Quality/Q2_R1/Step4/Q2_R1__Guideline.pdf

Turk J Pharm Sci 2020;17(1):63-7
DOI: 10.4274/tjps.galenos.2018.26566

ORIGINAL ARTICLE

In Vitro Activities of the Cationic Steroid Antibiotics CSA-13, CSA-131, CSA-138, CSA-142, and CSA-192 Against Carbapenem-resistant *Pseudomonas aeruginosa*

Katyonik Steroid Antibiyotiklerden CSA-13, CSA-131, CSA-138, CSA-142 ve CSA-192'nin Karbapenem Dirençli *Pseudomonas aeruginosa* Suşlarına Karşı *İn Vitro* Aktivitesi

Çağla BOZKURT GÜZEL[1]*, Nevin Meltem AVCI[1], Paul SAVAGE[2]

[1]İstanbul University, Faculty of Pharmacy, Department of Pharmaceutical Microbiology, İstanbul, Turkey
[2]Brigham Young University, Department of Chemistry and Biochemistry, Provo, Utah, USA

ABSTRACT

Objectives: *Pseudomonas aeruginosa* is an important opportunistic pathogen that is difficult to treat because of the antibiotic resistance that has developed in recent years. Increasing carbapenem resistance has led to a rise in hospital infections caused by this bacterium. As a result, researchers have begun to search for new molecules. Ceragenins are the general name for membrane-acting cationic steroid antimicrobial molecules that have activity similar to that of antimicrobial peptides. In this study, we investigated the *in vitro* activities of the cationic steroid antibiotics (CSAs) CSA-13, CSA-131, CSA-138, CSA-142, CSA-192, and colistin on carbapenem-resistant *Pseudomonas aeruginosa* (CRPA).

Materials and Methods: Minimum inhibitory concentrations (MICs) and minimum bactericidal concentrations (MBCs) were determined by broth dilution method.

Results: The MIC_{50} (µg/mL) values of CSA-13, CSA-131, CSA-138, CSA-142, CSA-192, colistin, and meropenem were 8, 4, 8, 16, 32, 1, and 16, respectively. The MBC values were equal to or twice the MIC values.

Conclusion: CSA-131 and CSA-138 appear to be good candidates for CRPA treatment. However, the lack of stability, efficacy, and pharmacokinetic properties of CSA requires further research in the future *in vivo* and *in vitro*.

Key words: Cationic steroid antibiotic, carbapenem-resistant *Pseudomonas aeruginosa*, colistin, minimum inhibitory concentrations, minimum bactericidal concentrations

ÖZ

Amaç: Son yıllarda geliştirdiği antibiyotik direnci nedeniyle tedavisi zorlaşan önemli bakterilerden biri de *Pseudomonas aeruginosa* (*P. aeruginosa*)'dır. Önemli bir hastane enfeksiyonu etkeni olan bu bakterinin karbapenem grubu antibiyotiklere karşı geliştirdiği direnç nedeniyle bu suşlarla meydana gelen enfeksiyonlarda önemli bir artış görülmüştür. Bu da araştırmacıları yeni moleküller üzerinde çalışmaya yönlendirmiştir. Cerageninler, antimikrobiyal peptidlere benzer şekilde aktivite gösteren, membrana etki edebilen katyonik steroid antimikrobiyal moleküllerin genel ismidir. Bu çalışmada katyonik steroid antibiyotiklerden katyonik steroid antibiyotikler (CSA) olan CSA-13, CSA-131, CSA-138, CSA-142 ve CSA-192'nin ve kolistinin karbapenem dirençli *P. aeruginosa* üzerine olan *in vitro* etkilerini araştırılmıştır.

Presented in: 26-29 April 2017 IVEK International Convention of Pharmaceuticals and Pharmacies - Poster and 27 May 2018 Eskişehir Competition of pharmacy graduation projects symposium

***Correspondence: E-mail:** caglabozkurt@hotmail.com, **Phone:** +90 532 624 89 86 **ORCID-ID:** orcid.org/0000-0003-1202-1266
Received: 02.04.2018, **Accepted:** 25.10.2018

Gereç ve Yöntemler: Minimum inhibitör konsantrasyonları (MİK) ve minimum bakterisidal konsantrasyonlar (MBK) değerleri mikrodilüsyon yöntemi ile belirlenmiştir.

Bulgular: $MİK_{50}$ (µg/mL) değerleri, CSA-13, CSA-131, CSA-138, CSA-142, CSA-192, kolistin ve meropenem için sırasıyla 16, 4, 8, 32, 32, 2 ve 32'dir. MBK değerleri, MİK değerlerine eşit ya da iki katı olarak saptanmıştır.

Sonuç: Sonuç olarak CSA-131 ve CSA-138'in karbepenem dirençli *P. aeruginosa* tedavisinde iyi birer aday olacağı düşüncesindeyiz. Ancak CSA'ların stabilite özellikleri, etkinlikleri ve farmakokinetik özelliklerindeki eksiklikler, gelecekte bu konuda daha fazla araştırma yapılmasını gerektirmektedir.

Anahtar kelimeler: Katyonik steroid antibiyotik, karbapenem dirençli *Pseudomonas aeruginosa*, kolistin, minimum inhibitör konsantrasyonları, minimum bakterisidal konsantrasyonlar

INTRODUCTION

Carbapenems are important frequently used antipseudomonal drugs, although high carbapenem resistance rates in *Pseudomonas aeruginosa* (*P. aeruginosa*) isolates have been increasingly reported worldwide.[1-3] In 2017, the World Health Organization published a list of antibiotic-resistant priority pathogens for which new antibiotics are urgently needed. One of the most critical groups of all is carbapenem-resistant *P. aeruginosa* (CRPA).[4] In such cases, colistin is the only option for treatment.[5] Moreover, the lack of effective antibiotics against CRPA isolates has led to the re-use of colistin. Colistin has shown good *in vitro* activity against gram-negative bacilli, including *P. aeruginosa*. However, resistance to colistin is emerging all across the globe.[6]

There is an urgent need to develop alternative compounds and approaches to combat CRPA. Antimicrobial peptides (AMPs) have recently been extensively researched as potential antimicrobial agents. AMPs have the advantages of selectivity, activity rate, and the ability of bacteria not to develop resistance to these peptides.[1,7] In addition to these properties of AMPs, there are problems in usage such as linear peptide structure, proteolysis, high cost of production in excess amount, short half-life in circulation, and less toxic effect against microorganisms in micromolar use.[8] Because of these reasons, researchers have sought new antimicrobial agents using peptide and peptide analogues. One of them, ceragenin, is a general name for membrane-acting cationic steroid antibiotics (CSAs) and they have been developed as nonpeptide forms of endogenous cationic AMPs. CSAs are cationic, amphiphilic molecules that mimic AMP but do not have the undesirable properties of AMPs. Due to their lipophilic nature they target pathogen membranes, causing morphological changes in membrane structure, leading to cell death. Many CSAs display broad-spectrum antimicrobial activities against both gram-positive and gram-negative bacteria, including multiresistant strains, parasites, some viruses, and fungi.[9-18]

CSA-13, the first generation prototype of CSA molecule, is highly effective against gram-positive and gram-negative bacteria.[12,19] The low toxicity of CSA-13 in animal studies supports the possible application of this compound in human therapy.[20] CSA-131, CSA-138, CSA-142, and CSA-192 molecules are in a later generation group. There are few published studies about these second generation molecules against resistant *P. aeruginosa* strains.[6,19] Therefore, in the present study, we assessed the *in vitro* activities of CSA-13, CSA-131, CSA-138, CSA-142, and CSA-192 against CRPA strains and compared their activity to colistin.

MATERIALS AND METHODS

Bacterial isolates

Twenty clinical strains of unrelated CRPA were isolated from various samples from Çanakkale Onsekiz Mart University, Health Practice and Research Center Microbiology Laboratory, Turkey, in 2016-2017. The isolates were defined as carbapenem-resistant strains using disc diffusion and microdilution. All strains were identified by the Vitek2 Compact System. *P. aeruginosa* ATCC 27853 (Rockville, MD, USA) was used as a quality control strain.

Antimicrobial agents

CSA-13, CSA-131, CSA-138, CSA-142, and CSA-192 were synthesized from a cholic acid scaffold technique as previously described (Figure 1).[21] Colistin and meropenem were obtained from AstraZeneca (Turkey). Ceragenins were prepared at a concentration of 2560 µg/mL and stored frozen at -80°C. Colistin and meropenem were prepared at a concentration of 5120 µg/mL. Meropenem was prepared on the day of use. Frozen solutions of antibiotics were used within 6 months.

Media

Mueller-Hinton Broth (MHB, Difco Laboratories, Detroit, MI, USA) supplemented with divalent cations to a final concentration of 25 mg of Mg^{+2} and 50 mg of Ca^{+2} per liter (CSMHB) was used for all the experiments. Pour plates of tryptic soy agar (TSA, Difco Laboratories, Detroit, MI, USA) were used for colony counts.

Determination of MICs and MBCs

Minimum inhibitory concentrations (MICs) were determined by the microbroth dilution technique as described by the CLSI.[22,23] Serial twofold dilutions ranging from 128 to 0.06 µg/mL were prepared in CSMHB. The inoculum was prepared with 4- to 6-h broth culture that gives a final concentration of 5×10^5 cfu/mL in the test tray. Viable cell counts were performed with each test to verify the number of colony-forming units in each inoculum. The trays were covered and placed in plastic bags to prevent evaporation and incubated at 37°C for 18-20 h. The MIC was defined as the lowest concentration of antibiotic giving complete

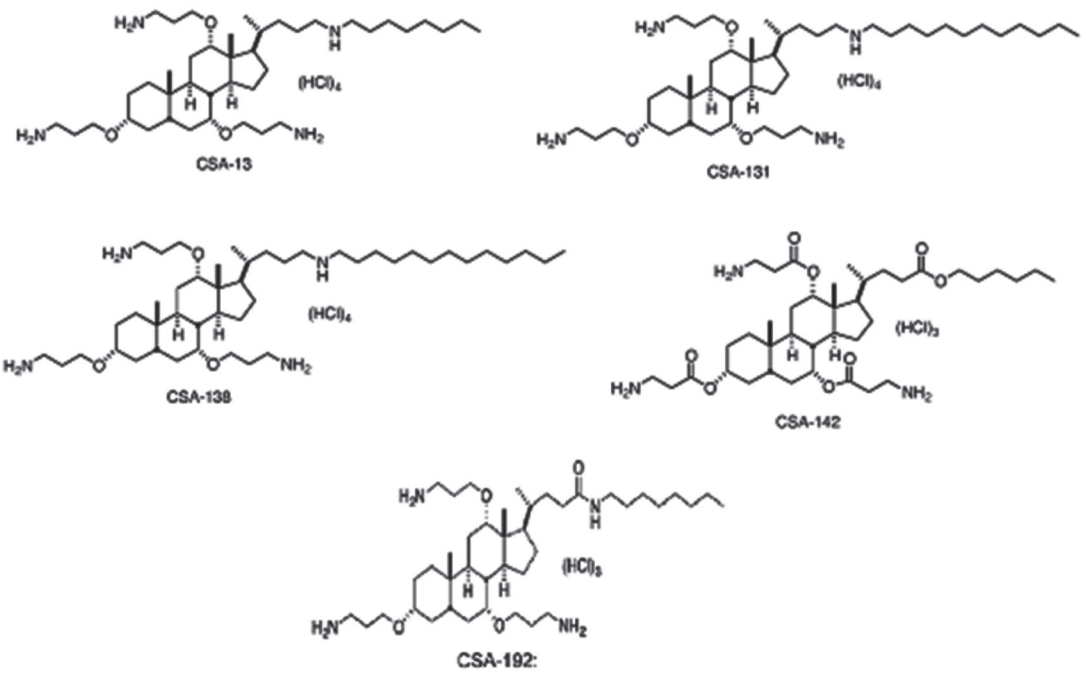

Figure 1. Structures of ceragenins CSA-13, CSA-131, CSA-138, CSA-142, and CSA-192

CSA: Cationic steroid antibiotics

inhibition of visible growth. The experiments were performed in duplicate. Minimum bactericidal concentrations (MBCs) were determined at the conclusion of the incubation period by removing two 0.01-mL samples from each well demonstrating no visible growth and plated onto TSA. Resultant colonies were counted after overnight incubation at 37°C. The MBC was defined as the lowest concentration of antibiotic giving at least 99.9% killing of the initial inocula.[24]

RESULTS

MIC ranges for CSA-13, CSA-131, CSA-138, CSA-142, CSA-192, colistin, and meropenem against 20 clinical CRPA strains were 4-16, 2-8, 4-32, 8-32, 8-32, 0.5-2, and 8-128 (μg/mL), respectively (Table 1, Table 2). The MBCs were generally equal to or twofold greater than those of the MICs (Table 1, Table 3). MIC and MBC studies were conducted with three replicates. CSA-131 and CSA-138 followed by CSA-13 may be good candidates for infections caused by these bacteria. CSA-142 and CSA-192 are less effective. *P. aeruginosa* ATCC 27853 strain was used as a standard strain and the MIC results against quality control strains were as expected (Table 4).

DISCUSSION

Today, the treatment of *P. aeruginosa* infections is becoming increasingly difficult due to growing antibiotic resistance. CRPA is the second microorganism, after carbapenem-resistant *A.baumannii*, in the list of bacteria for which new antibiotics are urgently needed published by the WHO in 2017.[4] This has led researchers to search for new therapeutic agents. One of them is CSA molecules. In the present study, we investigated the *in vitro* effects of CSA-13, CSA-131, CSA-138, CSA-142, and CSA-192 against 20 clinical unrelated CRPA strains.

Table 1. MIC and MBC values

Antimicrobials	MIC range	MIC_{50}	MIC_{90}	MBC range	MBC_{50}	MBC_{90}
CSA-13	4-16	8	16	4-32	16	32
CSA-131	2-8	4	4	2-8	4	8
CSA-138	4-32	8	8	4-32	8	16
CSA-142	8-32	16	32	8-64	32	64
CSA-192	8-32	32	32	8-64	32	32
Colistin	0.5-2	1	2	0.5-4	2	4
Meropenem	8-128	16	32	8-256	32	64

MIC_{50}, MIC_{90}: Defined as the antimicrobial concentration that inhibited growth of 50% and 90% of the strains, MBC_{50}, MBC_{90}: Defined as the bactericidal concentration of 50% and 90% of the strains, MIC: Minimum inhibitory concentration, MBC: Minimum bactericidal concentration, CSA: Cationic steroid antibiotics

There are several studies in the literature investigating the effect of CSA molecules on *P. aeruginosa.* Vila-Farrés et al.[6] investigated the *in vitro* activities of CSA-13, CSA-44, CSA-131, and CSA-138 against colistin-susceptible and resistant strains of *A. baumannii* and *P. aeruginosa* in 2015. They showed that CSA-131 is a good candidate for the treatment of *P. aeruginosa* and *A. baumannii* infections.

In the present study, the MIC_{50} values (μg/mL) of CSA-13, CSA-131, CSA-138, CSA-142, CSA-192, and colistin against 20 CRPA strains isolated from various samples were 8, 4, 8, 16, 32, and 1, respectively. It is thought that CSA-131 has the best activity because it has a long hydrophobic chain at C12 (Figure 1). It is promising that the MIC value of CSA-131 is 4 μg/mL, while the MIC value of colistin is 1 μg/mL. The fact that CSA-13 and

Table 2. MIC, MIC_{50}, and MIC_{90} values of the tested antimicrobial agents (µg/mL)

Antimicrobial agents	MIC	Number of isolates	MIC_{50}	MIC_{90}
CSA-13	4 8 16	2 10 8	8	16
CSA-131	2 4 8	5 14 1	4	4
CSA-138	4 8 16	1 18 1	8	8
CSA-142	8 16 32	7 9 4	16	32
CSA-192	8 16 32	1 8 11	32	32
COL	0.5 1 2	2 8 10	1	2
MER	2 8 16 32 64 128	2 4 7 5 1 1	16	32

COL: Colistin, MER: Meropenem, MIC: Minimum inhibitory concentration, CSA: Cationic steroid antibiotic

CSA-138 have the best activity after CSA-131 is considered to be because of the long hydrophobic chain at C8. As a result, the long hydrophobic chain structure that CSA possesses causes these molecules to move strongly through the bacterial membrane, leading to their strong activity. CSA-142 and CSA-192 were found to be less effective than the others. In our study, the MIC ranges of colistin against 20 CRPA strains were 0.5-2 µg/mL, and the MIC_{50} value was 1 µg/mL and the MIC_{90} value was 2 µg/mL. No colistin resistance was detected against any of the strains.

Sensitivity tests are of great importance for the selection of antibiotics to be used in treatment. One of them is the MIC test. MICs are predictive values of clinical outcome and estimate the bacteriostatic or inhibitory activity of antimicrobial agents. However, it is important to know bactericidal activity in the treatment of serious infections that may result in death due to inadequate treatment. Therefore, it is also important to determine the MBC values of *P. aeruginosa*, which is difficult to treat due to the increasing antibiotic resistance. The MBC values of the antibiotics tested in our study were equal to or twice the MIC values. This suggests that these antibiotics may produce the desired bactericidal effect in the treatment of CRPA infections.

Table 3. MBC, MBC_{50}, and MBC_{90} values of the tested antimicrobial agents (µg/mL)

Antimicrobial agents	MBC	Number of isolates	MBC_{50}	MBC_{90}
CSA-13	4 8 16 32	2 4 8 6	16	32
CSA-131	2 4 8	1 14 5	4	8
CSA-138	4 8 16 32	1 13 5 1	8	16
CSA-142	8 16 32 64	1 8 7 4	32	64
CSA-192	8 16 32 64	1 3 15 1	32	32
COL	0.5 1 2 4	2 4 11 3	2	4
MER	2 4 8 16 32 64 256	1 1 2 3 7 5 1	32	64

COL: Colistin, MER: Meropenem, MBC: Minimum bactericidal concentration, CSA: Cationic steroid antibiotic

Table 4. MIC values (µg/mL) of antimicrobial agents against *Pseudomonas aeruginosa* ATCC 27853 strain

Antibiotics	MIC values
CSA-13	16
CSA-131	8
CSA-138	32
CSA-142	16
CSA-192	32
Colistin	2
Meropenem	1

CSA: Cationic steroid antibiotic MIC: Minimum inhibitory concentration

CONCLUSION

In conclusion, according to our results, ceragenins, especially CSA-131 and CSA-138, appear to be good candidates in the treatment of CRPA infections. However, future *in vivo* and

in vitro studies should be performed to correlate the safety, efficacy, and pharmacokinetic parameters of these molecules.

ACKNOWLEDGEMENTS

This work was supported by the Research Fund of İstanbul University under project no: 23843.

Conflicts of interest: No conflict of interest was declared by the authors.

References

1. Bassetti M, Poulakou G, Ruppe E, Bouza E, Van Hal SJ, Brink A. Antimicrobial resistance in the next 30 years, humankind, bugs and drugs: a visionary approach. Intensive Care Med. 2017;43:1464-1475.
2. Davies TA, Marie Queenan A, Morrow BJ, Shang W, Amsler K, He W, Lynch AS, Pillar C, Flamm RK. Longitudinal survey of carbapenem resistance and resistance mechanisms in Enterobacteriaceae and non-fermenters from the USA in 2007-09. J Antimicrob Chemother. 2011:66:2298-2307.
3. El-Mahdy TS. Expression of ampC, oprD, and mexA, outer membrane protein analysis and carbapenemases in multidrug resistant clinical isolates of Pseudomonas aeruginosa from Egypt. J Chemother. 2014:26:379-381.
4. World Health Organization. WHO publishes list of bacteria for which new antibiotics are urgently needed (2017). Accessed: 14 March. 2017. http://www.who.int/mediacentre/news/releases/2017/bacteria-antibiotics-needed/en/
5. Falagas ME, Bliziotis IA. Pandrug-resistant Gram-negative bacteria: the dawn of the postantibiotic era? Int J Antimicrob Agents. 2007;29:630-636.
6. Vila-Farrés X, Callarisa AE, Gu X, Savage PB, Giralt E, Vila J. CSA-131, a ceragenin active against colistin-resistant Acinetobacter baumannii and Pseudomonas aeruginosa clinical isolates. Int J Antimicrob Agents. 2015:46:568-571.
7. Smeianov V, Scott K, Reid G. Activity of cecropin P1 and FA-LL-37 against urogenital microflora. Microbes Infect. 2000;2:773-777.
8. Epand RM, Epand RF, Savage PB. Ceragenins (Cationic Steroid Compounds), a novel class of antimicrobial agents. Drug News Perspect. 2008:21:307-311.
9. Chin JN, Jones RN, Sader HS, Savage PB, Rybak MJ. Potential synergy activity of the novel ceragenin, CSA-13, against clinical isolates of Pseudomonas aeruginosa, including multidrug-resistant P. aeruginosa. J Antimicrob Chemother. 2008:61:365-370.
10. Chin JN, Rybak MJ, Cheung CM, Savage PB. Antimicrobial activities of ceragenins against clinical isolates of resistant Staphylococcus aureus. Antimicrob Agents Chemother. 2007:51:1268-1273.
11. Durnaś B, Wnorowska U, Pogoda K, Deptuła P, Wątek M, Piktel E, Głuszek S, Gu X, Savage PB, Niemirowicz K, Bucki R. Candidacidal Activity of Selected Ceragenins and Human Cathelicidin LL-37 in Experimental Settings Mimicking Infection Sites. PLoS One. 2016;11:e0157242.
12. Epand RF, Pollard JE, Wright JO, Savage PB, Epand RM. Depolarization, bacterial membrane composition, and the antimicrobial action of ceragenins. Antimicrob Agents Chemother. 2010:54:3708-3713.
13. Epand RF, Savage PB, Epand RM. Bacterial lipid composition and the antimicrobial efficacy of cationic steroid compounds (Ceragenins). Biochim Biophys Acta. 2007;1768:2500-2509.
14. Howell MD, Streib JE, Kim BE, Lesley LJ, Dunlap AP, Geng D, Feng Y, Savage PB, Leung DY. Ceragenins: a class of antiviral compounds to treat orthopox infections. J Invest Dermatol. 2009:129:2668-2675.
15. Lara D, Feng Y, Bader J, Savage PB, Maldonado, RA. Anti-trypanosomatid activity of ceragenins. J Parasitol. 2010;96:638-642.
16. Leszczynska K, Namiot D, Byfield FJ, Cruz K, Zendzian-Piotrowska M, Fein DE, Savage PB, Diamond S, McCulloch CA, Janmey PA, Bucki R. Antibacterial activity of the human host defence peptide LL-37 and selected synthetic cationic lipids against bacteria associated with oral and upper respiratory tract infections. J Antimicrob Chemother. 2013;68:610-618.
17. Polat ZA, Savage PB, Genberg C. *In vitro* amoebicidal activity of a ceragenin, cationic steroid antibiotic-13, against Acanthamoeba castellanii and its cytotoxic potential. J Ocur Pharmacol Ther. 2011;27:1-5.
18. Savage PB, Li C, Taotafa U, Ding B, Guan Q. Antibacterial properties of cationic steroid antibiotics. FEMS Microbiol Lett. 2002;217:1-7.
19. Bozkurt-Guzel C, Savage PB, Gerceker AA. In vitro activities of novel ceragenin, CSA-13, alone or combination with colistin, tobramycin and ciprofloxacin against Pseudomonas aeruginosa strains isolated from cystic fibrosis patients. Chemotherapy. 2011;57:505-510.
20. Saha S, Savage PB, Bal M. Enhancement of the efficacy of erythromycin in multiple antibiotic resistant gram-negative bacterial pathogens. J Appl Microbiol. 2008;105:822-828.
21. Guan Q, Li C, Schmidt EJ, Boswell JS, Walsh JP, Allman GW, Savage PB. Preparation and characterization of cholic acid-derived antimicrobial agents with controlled stabilities. Org Lett. 2000;2:2837-2840.
22. Clinical and Laboratory Standards Institute.Methods for dilution antimicrobial susceptibility tests for bacteria that grow aerobically. Approved Standard-(10 th ed). CLSI document. USA; 2015:7-10.
23. Clinical and Laboratory Standards Institute. Performance standards for antimicrobial susceptibility testing. CLSI document (27th ed). USA; 2016:100-127.
24. National Committee for Clinical Laboratory Standarts. Methods for Determining Bactericidal Activity of Antimicrobial Agents-Approved Guideline, USA; 2005:26.

Turk J Pharm Sci 2020;17(1):68-73
DOI: 10.4274/tjps.galenos.2018.83788

ORIGINAL ARTICLE

The Relationship Between Dipeptidyl Peptidase-4 Inhibitor Usage and Asymptomatic Amylase Lipase Increment in Type 2 Diabetes Mellitus Patients

Tip 2 Diabetes Mellitus Tanılı Hastalarda Dipeptidil Peptidaz-4 İnhibitör Kullanımı ile Asemptomatik Amilaz Lipaz Artışı Arasındaki İlişki

Zeynel Abidin SAYİNER[1]*, Gamze İNAN DEMİROĞLU[2], Ersin AKARSU[1], Mustafa ARAZ[1]

[1]Gaziantep University, School of Medicine, Department of Endocrinology and Metabolism, Gaziantep, Turkey
[2]Gaziantep University, School of Medicine, Department of Internal Medicine, Gaziantep, Turkey

ABSTRACT

Objectives: In different studies, it has been shown that the use of dipeptidyl peptidase-4 (DPP-4) inhibitors (DPP-4 inh) does not increase the risk of pancreatitis or pancreatic cancer. Although the number of studies involving clinical pancreatitis clinics is sufficient, the number of studies involving clinical non-pancreatitis hyperamylasemia is rare. The aim of the study was to investigate the relationship between DPP-4 inh usage and amylase and lipase increment without clinical pancreatitis symptoms.

Materials and Methods: Eighty-seven patients who met the inclusion criteria were enrolled. The patients were divided into 3 groups according to their use of saxagliptin, sitagliptin, or vildagliptin. All patients included in the study were receiving metformin at a dose of 2 g/day. Fasting blood glucose, postprandial blood glucose, HbA1C, serum creatinine, ALT, amylase, and lipase results were recorded at the beginning of treatment and at the end of 3 months.

Results: There was an increase in all groups in terms of amylase and lipase values but there was no significant difference between the groups in terms of increase ($p>0.05$) There was no statistically significant increase in the saxagliptin and vildagliptin groups ($p>0.05$) when the baseline and 3-month values of lipase and amylase increase were examined. However, there was a statistically significant increase in amylase and lipase in the sitagliptin group ($p<0.05$).

Conclusion: The use of DPP-4 inh can increase amylase and lipase levels without clinical findings of acute pancreatitis in the patient. DPP-4 inh should be used with caution in patients at risk for pancreatitis and pancreatic cancer. Patients using DPP-4 inh, especially sitagliptin, should be evaluated carefully for pancreatitis risk factors.

Key words: Oral antidiabetics, dipeptidyl peptidase-4 inhibitors, amylase, lipase

ÖZ

Amaç: Farklı çalışmalarda, dipeptidil peptidaz-4 (DPP-4) inhibitörünün (DPP-4 inh) kullanımının pankreatit ve pankreas kanseri riskini artırdığı gösterilmiştir. Her ne kadar pankreatit klinikleri ile yapılan çalışmaların sayısı yeterli olsa da, klinik olarak pankreatit olmayan hiperaldemi ile yapılan çalışmaların sayısı azdır. Çalışmanın amacı, DPP-4 inh kullanımı ile pankreatit semptomları olmadan amilaz ve lipaz artışı arasındaki ilişkiyi araştırmaktır.

Gereç ve Yöntemler: Çalışmaya dahil edilme kriterlerlerine uyan 87 hasta alındı. Hastalar saksagliptin, sitagliptin ve vildagliptin kullanımlarına göre 3 gruba ayrıldı. Çalışmaya dahil edilen tüm hastalar 2 gram/gün dozda metformin aldı. Açlık kan şekeri, post prandial kan şekeri, HbA1c, serum kreatinin, ALT, amilaz, lipaz sonuçları tedavi başlangıcında ve 3. ayın sonunda kaydedildi.

Bulgular: Amilaz ve lipaz değerleri açısından tüm gruplarda artış vardı ve gruplar arasında artma açısından anlamlı fark yoktu ($p>0,05$). Saksagliptin ve vildagliptin grubunda istatistiksel olarak anlamlı bir artış yoktu ($p>0,05$) Lipaz ve amilaz artışının başlangıç ve 3. ay değerleri incelendiğinde sadece sitagliptin grubunda istatistiksel olarak anlamlı bir amilaz ve lipaz artışı vardı ($p<0.05$).

Sonuç: DPP-4 inh kullanımı, akut pankreatitin klinik bulguları olmaksızın amilaz ve lipaz seviyelerini arttırabilir. DPP-4 inh pankreatit ve pankreatik kanser riski olan hastalarda dikkatli kullanılmalıdır. DPP-4 inh, özellikle sitagliptin kullanan hastalar pankreatit risk faktörleri açısından dikkatle değerlendirilmelidir.

Anahtar kelimeler: Oral antidiyabetikler, dipeptidil peptidaz-4 inhibitörleri, amilaz, lipaz

***Correspondence: E-mail:** zeynelasayiner@hotmail.com, **Phone:** +90 342 360 60 60 **ORCID-ID:** orcid.org/0000-0001-5105-0292
Received: 21.08.2018, **Accepted:** 25.10.2018

INTRODUCTION

Dipeptidyl peptidase 4 (DPP-4), an aminopeptidase that was isolated from the rat liver in 1960, is excreted in the pancreas, brain, lungs, kidneys, intestines, adrenal glands, and lymph nodes.[1,2] Moreover, this enzyme causes glucagon-like peptide-1 (GLP-1) to break down in less than 2 min and gastric inhibitory polypeptide in less than 5 to 7 min.[3,4] Dipeptidyl peptidase-4 inhibitors (DPP-4 inh) are oral antidiabetic agents that increase circulating GLP-1 levels. Thus, they help to inhibit the rapid inactivation of GLP-1 and regulate blood sugar. In other words, they control blood glucose by stimulating insulin secretion in glucose-dependent pathways.[5] Although DPP-4 contains a wide range of substrates including chemokines, hormones, and neuropeptides, DPP-4 inh usually do not negatively affect type 2 diabetes (T2DM) patients. Several studies have evaluated the safety of DPP-4 inh in elderly patients as well as patients with renal insufficiency, liver disease, and/or heart failure. While most observational studies have demonstrated the safety of these inhibitors, they have nevertheless been associated with a slightly increased incidence of acute pancreatitis during placebo-controlled trials. In addition, the possible side effects of long-term DPP-4 inh use remain unclear.[6] Those side effects observed during the preclinical and clinical trials of sitagliptin and vildagliptin treatments are inconsistent with the increased risk of pancreatitis in T2DM patients, but the association between DPP-4 inh and pancreatic cancer, pancreatitis, and pancreatic enzyme elevation has been proven.[7] The Food and Drug Administration (FDA) has also reported that patients using sitagliptin and exenatide should be cautious in terms of developing pancreatic cancer.[7] On the other hand, various studies have demonstrated that the use of DPP-4 inh does not increase the risk of pancreatitis or pancreatic cancer.[8] Finally, although the number of studies involving pancreatic cancer patients is sufficient, those concerning patients with clinical non-pancreatic hyperamylasemia are rare. The present study assessed changes in the amylase and lipase values of various patients who had been using DPP-4 inh but did not exhibit acute pancreatitis symptoms.

MATERIALS AND METHODS

The participants were diabetic patients who had been referred to the endocrinology and metabolism clinic of Gaziantep Şahinbey research and application hospital. Prior to the study, approval (approval no. 17/10/2016/268) was obtained from the Gaziantep University Committee. The study was prospective in nature, with patients being evaluated twice over a 3-month period (i.e. at 0 and 3 months). In addition, it was descriptive in nature and assessed the relationship among variables. All patients involved in this study met the following inclusion criteria developed by the American Diabetes Association :

1. Patients with T2DM
2. Patients who were not using antidiabetic drugs other than metformin and previously had not used sitagliptin, saxagliptin, or vildagliptin
3. Patients with HbA1C level lower than 10
4. Patients without cholelithiasis,
5. Patients without chronic alcohol consumption,
6. Patients with triglyceride levels lower than 150 mg/dL,
7. Patients in whom blood sugar regulation could not be achieved with metformin or any form of sitagliptin, saxagliptin, or vildagliptin treatment,
8. Patients without pancreatitis or pancreatitis history,
9. Patients with no history of renal or hepatic disease,
10. Patients without acute malignancy or malignancy history
11. Patients who were not pregnant,

The 87 patients who met the above criteria were divided into 3 groups according to their use of saxagliptin, sitagliptin, or vildagliptin. All had been taking metformin at a dosage of 2 g/day at the start of the study. Patients using saxagliptin had been taking 1 mg of 5 mg daily, patients using sitagliptin had been taking 100 mg daily, and patients using vildagliptin had been taking 50 mg daily (morning and evening). Prior to and following the 3-month treatment, patients' fasting blood glucose, postprandial blood glucose, hemoglobin A1c (HbA1C), serum creatinine, alanine transaminase (ALT), amylase, and lipase levels were recorded.

Statistical analysis

A minimum of 80 patients were required for the present study based on the results of power analysis conducted for sample selection. The normal distribution fitness of numerical data was tested using the Shapiro-Wilk test, while the Kruskal-Wallis test was used to compare normal nondispersive variables. The relationship among normally undistracted dependent variables was tested via the Wilcoxon test, and the relationship among categorical variables was tested using the chi-square test. SPSS 22.0 was employed for results analysis and a p-value <0.05 was considered significant.

RESULTS

There was no statistically significant difference among the groups in terms of age or sex ($p>0.05$). The demographic characteristics of each group of participants are shown in Table 1.

At the beginning of the study, no significant difference in baseline fasting glucose level or postprandial blood glucose, HbA1C, serum creatinine, ALT, amylase, or lipase was observed ($p>0.05$) (Table 2). A statistically significant decrease in all groups ($p>0.05$) was found in fasting blood glucose, postprandial blood glucose, and HbA1C values after the 3-month treatment. Moreover, amylase and lipase values increased in all groups,

Table 1. Demographic characteristics of the groups

	Saxagliptin n=27	Sitagliptin n=30	Vildagliptin n=30	p
Sex (female/male)	21/6	7/23	12/18	0.241
Age (year)	54.26±7.906	56.33±6.572	54.00±10.316	0.577

but there was no significant difference in these values when comparing the groups (p>0.05) (Table 3). By the end of the study, there was a statistically significant decrease in fasting blood glucose and HbA1C in all groups (p<0.05). However, in comparing the groups, the decline rates did not significantly differ. There was no statistically significant increase in lipase or amylase levels within the saxagliptin and vildagliptin groups (p>0.05) after the 3-month treatment. However, there was a statistically significant increase in amylase and lipase levels within the sitagliptin group (p<0.05). There was no statistically significant increase in ALT levels within the sitagliptin or vildagliptin groups (p>0.05), yet there was a statistically significant increase in ALT level within the saxagliptin group (p<0.05) (Table 4).

Table 2. Comparison of laboratory parameters of the groups at the beginning of treatment

		N	Mean	Std. deviation	p
Fasting glucose (mg/dL)	Saxagliptin	27	204.41	69.841	0.704
	Sitagliptin	30	190.67	66.093	
	Vildagliptin	30	215.73	91.480	
	Total	87	203.57	76.679	
Postprandial glucose (mg/dL)	Saxagliptin	27	344.30	112.314	0.621
	Sitagliptin	30	275.97	114.564	
	Vildagliptin	30	327.90	126.681	
	Total	87	315.08	120.458	
HbA1C (%)	Saxagliptin	27	9.41	2.005	0.700
	Sitagliptin	30	8.97	1.650	
	Vildagliptin	30	9.27	1.874	
	Total	87	9.21	1.831	
Creatinine (mg/dL)	Saxagliptin	27	0.93	0.267	0.885
	Sitagliptin	30	0.90	0.305	
	Vildagliptin	30	0.93	0.254	
	Total	87	0.92	0.274	
ALT (U/L)	Saxagliptin	27	23.07	10.954	0.905
	Sitagliptin	30	24.57	10.448	
	Vildagliptin	30	22.63	9.368	
	Total	87	23.44	10.168	
Amylase (U/L)	Saxagliptin	27	60.74	21.506	0.792
	Sitagliptin	30	56.77	22.660	
	Vildagliptin	30	56.03	21.714	
	Total	87	57.75	21.821	
Lipase (U/L)	Saxagliptin	27	19.65	12.776	0.394
	Sitagliptin	30	25.32	17.035	
	Vildagliptin	30	21.82	14.274	
	Total	87	22.35	15.297	

HbA1C: Hemoglobin A1c, ALT: Alanine transaminase, Std: Standard

DISCUSSION

Sitagliptin, which has been used since 2006, is the longest of the DPP-4 inh in use; thus, more information is available regarding its use compared to other DPP-4 inh. According to the FDA's reported side effect database, patients using sitagliptin or exenatide are more prone to develop pancreatic cancer than

Table 3. Laboratory parameters of the groups by the end of treatment

		N	Mean	Std. deviation	p
Fasting glucose (mg/dL)	Saxagliptin	27	155.48	49.431	0.171
	Sitagliptin	30	162.67	52.948	
	Vildagliptin	30	182.37	61.222	
	Total	87	167.23	55.484	
Postprandial glucose (mg/dL)	Saxagliptin	27	277.67	99.458	0.402
	Sitagliptin	30	251.73	108.690	
	Vildagliptin	30	271.97	109.553	
	Total	87	266.76	105.579	
HbA1C (%)	Saxagliptin	27	8.11	1.450	0.154
	Sitagliptin	30	7.80	1.375	
	Vildagliptin	30	8.57	1.569	
	Total	87	8.16	1.485	
Creatinine (mg/dL)	Saxagliptin	27	0.96	0.192	0.800
	Sitagliptin	30	0.93	0.254	
	Vildagliptin	30	0.97	0.183	
	Total	87	0.95	0.211	
ALT (U/L)	Saxagliptin	27	26.00	10.269	0.937
	Sitagliptin	30	25.13	11.697	
	Vildagliptin	30	25.47	13.364	
	Total	87	25.52	11.763	
Amylase (U/L)	Saxagliptin	27	63.33	22.675	0.646
	Sitagliptin	30	67.13	20.416	
	Vildagliptin	30	62.00	27.188	
	Total	87	64.18	23.456	
Lipase (U/L)	Saxagliptin	27	35.41	18.158	0.249
	Sitagliptin	30	42.23	20.992	
	Vildagliptin	30	34.10	18.713	
	Total	87	37.31	19.482	

HbA1C: Hemoglobin A1c, ALT: Alanine transaminase, Std: Standard

Table 4. Comparison of laboratory parameters at the beginning and end of treatment

Mean ± Std		Beginning	3 Months	
		Mean ± Std	p	
Fasting glucose	Saxagliptin	204.4±69.9	155.5±49.4	0.001
	Sitagliptin	190.7±66.1	162.7±52.9	0.018
	Vildagliptin	215.7±91.5	182.4±61.2	0.005
Postprandial glucose	Saxagliptin	344.3±112.3	277.7±99.5	0.001
	Sitagliptin	275.9±114.6	251.7±108.7	0.098
	Vildagliptin	327.9±126.7	271.9±109.6	0.001
HbA1C	Saxagliptin	9.4±2.0	8.1±1.5	0.001
	Sitagliptin	8.9±1.6	7.8±1.4	0.001
	Vildagliptin	9.3±1.9	8.6±1.6	0.007
Amylase	Saxagliptin	60.7±21.5	63.3±22.7	0.400
	Sitagliptin	56.8±22.7	67.1±20.4	0.001
	Vildagliptin	56.0±21.7	62.0±27.2	0.174
Lipase	Saxagliptin	19.7±12.8	35.4±18.2	0.360
	Sitagliptin	25.3±17.0	42.2±20.9	0.001
	Vildagliptin	21.8±14.3	34.1±18.7	0.090
Creatinine	Saxagliptin	0.9±0.3	0.9±0.2	0.564
	Sitagliptin	0.9±0.3	0.9±0.3	0.564
	Vildagliptin	0.9±0.3	0.9±0.2	0.564
ALT	Saxagliptin	23.1±10.9	26.0±10.3	0.037
	Sitagliptin	24.6±10.5	25.1±11.7	0.789
	Vildagliptin	22.6±9.4	25.5±13.4	0.096

HbA1C: Hemoglobin A1c, ALT: Alanine transaminase, Std: Standard

those using other drugs.[9] Moreover, it has been claimed that chronic subclinical pancreatitis due to GLP-1 therapy may cause an increase in the incidence of pancreatic cancer.[10]

The above assertions have been supported by studies demonstrating that long-term exendin-4-mediated GLP-1R activation proliferates the development of pancreatic duct glands and the formation of dysplastic lesions (low grade intraepithelial neoplasia-mPANIN) in rats as well as chronic pancreatitis in the KrasG12D mouse model.[11] These studies have observed GLP-1-induced changes in pancreatic duct glands as well as genetic predisposition to cellular dysplasia. Therefore, it has been assumed that the absence of both a clear pancreatitis pattern and tumors in lean and nondiabetic animals receiving extendin-4 therapy owes itself to two facts. First, these animals are not genetically predisposed to dysplasia, and, second, the methodological analysis used to detect changes in the pancreas is not suitable for these animals.[12,13] For this reason, it has been suggested that in the case of chronic pancreatitis the pancreatic duct glands can easily transform into PanIN-like lesions.[14,15] Although exendin-4 administration leads to the development of mPanIN, it has not been scientifically proven that drug treatment in subjects does not lead to pancreatic cancer in genetically modified mice since this treatment has not been long enough in terms of duration.[16] At the same time, Butler et al.[17] have reported that patients receiving incretin therapy experience exocrine pancreatic dysplasia and endocrine pancreatic cell proliferation. On the other hand, the limited number of patients and treatment involved in Butler et al.[17] study as well as the lack of statistical data might have caused this link between therapy and cancer.[18,19]

In previous studies, cases of pancreatitis associated with the use of DPP-4 inh have been presented as case reports.[20] However, retrospective studies and meta-analyses have reported that these drugs are not statistically significant in terms of causing pancreatitis compared to other antidiabetic drugs.[21] In the current study, although there was an increase in amylase and lipase in patients, no significant difference was seen in any patient possessing the characteristics of acute pancreatitis. In their study of acute pancreatitis among T2DM patients in Taiwan, Hsin-Chuo et al.[22] determined the use of DPP-4 inh to be a risk factor for the presence of cholelithiasis and uncontrolled diabetes mellitus. On the other hand, in another retrospective cohort study conducted by Daisuke Yabe et al.[23] in Japan among 93,280 antidiabetic patients who had been screened for acute pancreatitis and used 27,962 DPP-4 inh, no significant difference was observed in terms of acute pancreatitis development.

Studies have also emerged regarding the use of DPP-4 inh for elevating amylase and lipase from pancreatic exocrine enzymes. In a 3-month prospective study observing the amylase and lipase levels of 36 patients, 24 of whom were using DPP-4 inh and 12 of whom were taking other antidiabetic drugs, Tokuyama et al.[24] observed an elevation in amylase and lipase levels among 11 out of 24 patients receiving DPP-4 inh that was regarded as statistically significant. In the present study, a baseline increase in amylase and lipase was observed in all groups. However, there was no statistically significant increase in the saxagliptin or vildagliptin groups ($p>0.05$), whereas a statistically significant increase was observed in the sitagliptin group.

The greater number of studies concerning sitagliptin in DPP-4-associated pancreatitis cases presented as case reports may be related to the longer treatment duration of sitagliptin in comparison to other DPP-4 inh. Still, some theoretical information (especially that derived from animal experiments) is available that indicates the cause of the increase in pancreatic enzymes with the use of DPP-4. Studies examining the relationship between sitagliptin and oxidative stress as well as inflammation have indicated that sitagliptin increases the levels of tumor necrosis factor-alpha in serum inflammatory stores. Moreover, it has been found to decrease oxidative stress in serum by decreasing serum IL-1β levels and reducing serum total malondialdehyde levels but not total antioxidant levels. Another study examining the effects of sitagliptin on oxidative

stress has reported that the total oxidant levels in diabetic rat pancreatic tissues did not change but oxidative stress increased due to decreased total antioxidant levels. This increased oxidative stress, which is likely to occur in the pancreas tissue, causes some inflammation in the exocrine pancreas. However, it is unclear whether this level can cause pancreatitis. Despite the inflammation and dysplastic changes in animal experiments examining the exocrine pancreas, the use of DPP-4 inh has been shown to increase function and mass in pancreatic beta cells.[25,26]

Based on the above findings, one could assume that the use of DPP-4 inh may increased amylase and lipase levels in patients who do not exhibit symptoms of acute pancreatitis. Thus, DPP-4 inh should be used with caution in patients at risk for pancreatitis and pancreatic cancer. Moreover, patients using DPP-4 inh, especially sitagliptin, should be evaluated carefully for pancreatitis risk factors.

Conflicts of interest: No conflict of interest was declared by the authors.

REFERENCES

1. Hopsu-Havu VK, Glenner GG. A new dipeptide napthylamidase hydrolyzing glycl-prolyl-beta-naphthylamide. Histochemie. 1966;7:197-201.
2. Gautier JF, Choukem SP, Girard J. Physiology of incretins (GIP and GLP-1) and abnormalities in type 2 diabetes. Diabetes Metab. 2008;34(Suppl 2):65-72.
3. International Diabetes Federation. Diabetes Atlas; (6th ed). 2013:32-34. Available from: https://www.idf.org/e-library/epidemiology-research/diabetes-atlas/19-atlas-6th-edition.html
4. Inzucchi SE, McGuire DK. New drugs for the treatment of diabetes: part II: incretin-based therapy and beyond. Circulation. 2008;117:574-584.
5. Mentlein R, Gallwitz B, Schmidt WE. Dipeptidyl-peptidase IV hydrolyses gastric inhibitory polypeptide, glucagon-like peptide-1 (7-36) amide, peptide histidine mehtionine and is responsible for their degradation in human serum. Eur J Biochem. 1993;214:829-835.
6. Spranger J, Gundert-Remy U, Stammschulte T. GLP-1-based therapies: the dilemma of uncertainty. Gastroenterology. 2011;141:20-23.
7. Elashoff M, Matveyenko AV, Gier B, Elashoff R, Butler PC. Pancreatitis, pancreatic, and thyroid cancer with glucagon-like peptide-1-based therapies. Gastroenterology. 2011;141:150-156.
8. White WB, Cannon CP, Heller SR, Nissen SE, Bergenstal RM, Bakris GL, Perez AT, Fleck PR, Mehta CR, Kupfer S, Wilson C, Cushman WC, Zannad F; EXAMINE Investigators. Alogliptin after Acute Coronary Syndrome in Patients with Type 2 Diabetes. N Engl J Med. 2013;369:1327-1335.
9. Egan AG, Blind E, Dunder K, de Graeff PA, Hummer BT, Bourcier T, Rosebraugh C. Pancreatic safety of incretin-based drugs-FDA and EMA assessment. N Engl J Med. 2014;370:794-797.
10. Butler PC, Dry S, Elashoff R. GLP-1-based therapy for diabetes: what you do not know can hurt you. Diabetes Care. 2010;33:453-455.
11. Gier B, Matveyenko AV, Kirakossian D, Dawson D, Dry SM, Butler PC. Chronic GLP-1 receptor activation by exendin-4 induces expansion of pancreatic duct glands in rats and accelerates formation of dysplastic lesions and chronic pancreatitis in the Kras(G12D) mouse model. Diabetes. 2012;61:1250-1262.
12. Tatarkiewicz K, Smith PA, Sablan EJ, Polizzi CJ, Aumann DE, Villescaz C, Hargrove DM, Gedulin BR, Lu MG, Adams L, Whisenant T, Roy D, Parkes DG. Exenatide does not evoke pancreatitis and attenuates chemically induced pancreatitis in normal and diabetic rodents. Am J Physiol Endocrinol Metab. 2010;299:1076-1086.
13. Koehler JA, Baggio LL, Lamont BJ, Ali S, Drucker DJ. Glucagon-like peptide-1 receptor activation modulates pancreatitis-associated gene expression but does not modify the susceptibility to experimental pancreatitis in mice. Diabetes. 2009;58:2148-2161.
14. Gale EA. GLP-1-based therapies and the exocrine pancreas: more light, or just more heat? Diabetes. 2012;61:986-988.
15. Strobel O, Rosow DE, Rakhlin EY, Lauwers GY, Trainor AG, Alsina J, Fernández-Del Castillo C, Warshaw AL, Thayer SP. Pancreatic duct glands are distinct ductal compartments that react to chronic injury and mediate Shh-induced metaplasia. Gastroenterology. 2010;138:1166-1177.
16. Goggins M. GLP-1 receptor agonist effects on normal and neoplastic pancreata. Diabetes 2012;61:989-990.
17. Butler AE, Campbell-Thompson M, Gurlo T, Dawson DW, Atkinson M, Butler PC. Response to comments on: Butler et al. Marked expansion of exocrine and endocrine pancreas with incretin therapy in humans with increased exocrine pancreas dysplasia and the potential for glucagon-producing neuroendocrine tumors. Diabetes 2013;62:2595-2604. Diabetes. 2013;62:19-22.
18. Heine RJ, Fu H, Kendall DM, Moller DE. Comment on: Butler et al. Marked Expansion of Exocrine and Endocrine Pancreas With Incretin Therapy in Humans With Increased Exocrine Pancreas Dysplasia and the Potential for Glucagon-Producing Neuroendocrine Tumors. Diabetes. 2013;62:16-17.
19. Engel SS, Golm GT, Lauring B. Comment on: Butler et al. Marked expansion of exocrine and endocrine pancreas with incretin therapy in humans with increased exocrine pancreas dysplasia and the potential for glucagon-producing neuroendocrine tumors. Diabetes 2013;62:2595-2604. Diabetes. 2013;62:18.
20. Köroğlu Kale B, Songür Y, Ersoy İH, Köroğlu M, Akın M, Tamer MN. Sitagliptin and Acute Pancreatitis: Cases and Literature Review. Turkiye Klinikleri J Med Sci. 2012;32:859-864.
21. Li L, Shen J, Bala MM, Busse JW, Ebrahim S, Vandvik PO, Rios LP, Malaga G, Wong E, Sohani Z, Guyatt GH, Sun X. Incretin treatment and risk of pancreatitis in patients with type 2 diabetes mellitus: systematic review and meta-analysis of randomised and non-randomised studies. BMJ. 2014;348:2366.
22. Chou HC, Chen WW, Hsiao FY. Acute Pancreatitis in Patients with Type 2 Diabetes Mellitus Treated with Dipeptidyl Peptidase-4 Inhibitors: A Population-Based Nested Case-Control Study. Drug Saf. 2014;37:521-528.
23. Yabe D, Seino Y. Use of the Japanese health insurance claims database to assess the risk of acute pancreatitis in patients with diabetes: comparison of DPP-4 inhibitors with other oral antidiabetic drugs. Diabetes Obes Metab. 2015;17:430-434.
24. Tokuyama H, Kawamura H, Fujimoto M, Kobayashi K, Nieda M, Okazawa T, Takemoto M, Shimada F. A low-grade increase of serum pancreatic exocrine enzyme levels by dipeptidyl peptidase-4 inhibitor in patients with type 2 diabetes. Diabetes Res Clin Pract. 2013;100:66-69.

25. Ferreira L, Teixeira-de-Lemos E, Pinto F, Parada B, Mega C, Vala H, Pinto R, Garrido P, Sereno J, Fernandes F, Santos P, Velada I, Melo A, Nunes S, Teixeira F, Reis F. Effects of Sitagliptin Treatment on Dysmetabolism, Inflammation, and Oxidative Stress in an Animal Model of Type 2 Diabetes (ZDF Rat). Mediators Inflamm. 2010;2010:592760.

26. Nauck MA, Meininger G, Sheng D, Terranella L, Stein PP; Sitagliptin Study 024 Group. Efficacy and safety of the dipeptidyl peptidase-4 inhibitor, sitagliptin, compared with the sulfonylurea, glipizide, in patients with type 2 diabetes inadequately controlled on metformin alone: a randomized, double-blind, non-inferiority trial. Diabetes Obes Metab. 2007;9:194-205.

Turk J Pharm Sci 2020;17(1):74-80
DOI: 10.4274/tjps.galenos.2018.90582

ORIGINAL ARTICLE

Development and Validation of *In Vitro* Discriminatory Dissolution Testing Method for Fast Dispersible Tablets of BCS Class II Drug

BCS Sınıf II İlacının Hızlı Dağılabilir Tabletleri için *İn Vitro* Ayırt Edici Çözünme Test Yönteminin Geliştirilmesi ve Validasyonu

Shailendra BHATT[1]*, Dabashis ROY[1], Manish KUMAR[1], Renu SAHARAN[1], Anuj MALIK[1], Vipin SAINI[2]

[1]Maharishi Markandeshwar (Deemed to be University), Maharishi Markandeshwar College of Pharmacy, Department of Pharmaceutics, Haryana, India
[2]Maharishi Markandeshwar University, Solan, India

ABSTRACT

Objectives: Fast dispersible tablets (FDTs) get dispersed very fast due to which the discrimination of *in vitro* drug release and their evaluation is difficult. Hence in the present study a new *in vitro* discriminatory dissolution method was developed and validated for FDTs of domperidone of BCS class II.

Materials and Methods: FDTs of domperidone were prepared by direct compression method. The dissolution studies were performed in an eight-station Electrolab TDT-082 dissolution testing apparatus, analyzed by ultraviolet spectrophotometer and evaluated in different dissolution mediums i.e. sodium lauryl sulphate (0.5%, 1.0% and 1.5%) with fresh distilled water, simulated intestinal fluid pH 6.8, simulated gastric fluid pH 1.2 without enzymes, phosphate buffer solution (pH 6.8) and 0.1 N hydrochloric acid at different agitation speeds.

Results: The developed method was validated in terms of specificity, accuracy, precision, linearity and robustness. Amongst the different mediums, 0.5% sodium lauryl sulfate (SLS) with distilled water was found to be optimum with higher rate of discriminatory power. The percentage recovery was found to be 96 to 100.12 % and the % relative standard deviation value for precision (intraday and interday) was found to be less than 1%. Also a dissolution profile of prepared FDTs were compared in distilled water containing 0.5% SLS using similarity (f2) and dissimilarity (f1) factor calculation which showed dissimilarity in release profile and confirms the discriminatory nature of developed method.

Conclusion: The discriminatory dissolution method for FDTs was developed and validated. All the obtained results were satisfactory, accurate and in range. The current method could be beneficial for formulation development and for assessment of quality of FDTs.

Key words: Validation, discriminative dissolution method, fast dispersible tablets (FDTs), domperidone

ÖZ

Amaç: Hızlı dağılabilir tabletler (FDT'ler), çok hızlı dağıldıkları için *in vitro* etken madde salımının ayrımı ve değerlendirilmesi zordur. Bu nedenle, bu çalışmada, BCS sınıf II domperidonun FDT'leri için yeni bir *in vitro* ayırt edici çözünme yöntemi geliştirilmiş ve valide edilmiştir.

Gereç ve Yöntemler: Domperidonun FDT'leri direkt basım yöntemi ile hazırlanmıştır. Çözünme çalışmaları sekiz istasyonlu Electrolab TDT-082 çözünme test cihazında gerçekleştirilmiştir, ultraviyole spektrofotometre ile analiz edilmiş ve taze distile su ile sodyum lauril sülfat (%0,5, % 1,0 ve %1,5), simüle bağırsak sıvısı pH 6,8 ile simüle enzimsiz mide sıvısı pH 1,2, fosfat tampon çözeltisi (pH 6,8) ve 0,1N hidroklorik asit gibi farklı çözünme ortamlarında farklı çalkalama hızlarında değerlendirilmiştir.

Bulgular: Geliştirilen yöntem özgüllük, doğruluk, kesinlik, doğrusallık ve sağlamlık açısından doğrulanmıştır. Farklı ortamlar arasında, distile su ile %0,5 sodyum lauril sülfat (SLS)'nin daha yüksek ayrım gücü ile optimum olduğu bulunmuştur. Geri kazanım yüzdesi %96 ila %100,12 ve kesinlik için bağıl standart sapma değerinin (gün içi ve günler arası) %1'den az olduğu bulunmuştur. Ayrıca hazırlanan FDT'lerin %0,5 SLS içeren distile sudaki çözünme profili, salım profilinde farklılığı gösteren ve geliştirilen yöntemin ayırt edici doğasını doğrulayan benzerlik (f2) ve fark (f1) faktörü hesaplaması kullanılarak karşılaştırılmıştır.

Sonuç: FDT'ler için ayırt edici çözünme yöntemi geliştirilmiş ve valide edilmiştir. Elde edilen tüm sonuçlar tatmin edici, doğru ve aralık içindedir. Mevcut yöntem, formülasyon geliştirilmesi ve FDT'lerin kalitesinin değerlendirilmesi için faydalı olabilir.

Anahtar kelimeler: Validasyon, ayırt edici çözünme yöntemi, hızlı dağılabilir tabletler (FDT'ler), domperidon

*Correspondence: **E-mail:** shailu.bhatt@gmail.com, **Phone:** 8107663903 **ORCID-ID:** orcid.org/0000-0001-9405-3311
Received: 15.09.2018, **Accepted:** 25.10.2018

INTRODUCTION

Fast dispersible tablets (FDTs) are one of the formulations that can be used as a substitute for suspensions and they can overcome the problems associated with the swallowing of solid dosage forms. They disperse in liquid to give a homogeneous dispersion before administration and also disperse immediately in the mouth when they come in contact with saliva or rapidly disintegrate in water usually within 3 min to form a stabilized suspension. Such formulations provide an opportunity for those who have difficulty with conventional oral dosage forms, i.e. capsules, tablets, suspensions, and solutions, or who may not have access to water and have problems swallowing etc.[1,2] As the intrinsic solubility of the active pharmaceutical ingredient (API) controls the dissolution rate and as disintegration of FDTs is very rapid, it is difficult to evaluate the effect of the formulation on *in vitro* drug release.

From the discussion above, it can be seen that it is necessary to develop a dissolution strategy specific to FDTs and, in particular, to develop a method that has the capability to discriminate between *in vitro* release profiles with different natures, and to detect possible changes if any in the quality of products before performing *in vivo* to detect changes through an *in vitro* dissolution test for a drug with limited solubility is very challenging. The capability of a dissolution method to detect changes in a drug product is known as its discriminating power and it can be demonstrated by analyzing the dissolution profiles by considering the changes made in the method.[3]

Dissolution is a quantitative and qualitative technique that provides the necessary information regarding bioavailability of a drug to ensure lot-to-lot consistency.

The dissolution test remains incomplete without performing its validation, which ensures accuracy, consistency, and precision with repeatable results. The validation of dissolution can be performed by considering equipment validation that examines the geometrical specifications of the dissolution apparatus and its alignment, and by considering the performance parameters the reliability of the dissolution test is evaluated, especially precision.[4,5]

In the present study a discriminating dissolution test method was developed and validated for FDTs of domperidone, a Biopharmaceutics Classification System Class II drug having poor water solubility and high permeability. It is a D_2 antagonist and is usually prescribed as an antiemetic agent with a molecular weight of 425.91 g/mol, pk_a value of 7.9, and melting point in the range of 244-246°C.

The official dissolution medium prescribed for domperidone 0.1 N hydrocloric acid (HCl) is unable to discriminate the dissolution test of FDTs. Hence the goal of our study was to develop and validate a discriminatory dissolution method for FDTs of domperidone to support product development efforts.[6]

MATERIALS AND METHODS

Materials

Domperidone reference standard was supplied by Metrochem API, Pvt. Ltd., Hyderabad, India, as a gift sample. Vomistop 10 DT tablets (M.L.L./07/436/MNB), Mfd. by Cipla Ltd, 20, Indi Area-1, Baddi (H.P. 173205) containing 10 mg of domperidone IP were obtained commercially. Sodium lauryl sulfate (SLS), disodium hydrogen phosphate, and hydrochloric acid were obtained from Nice Chemicals Pvt. Ltd., Kerala, India. Potassium dihydrogen phosphate, methanol, and sodium bicarbonate were bought from Central Drug House (P) Ltd., New Delhi, India. Sodium chloride was purchased from Chemigens Research and Fine Chemicals, New Delhi, India. Sodium hydroxide pellets, citric acid, magnesium stearate, sodium croscarmellose, and microcrystalline cellulose were purchased from Qualikems Fine Chem; Pvt, Ltd., India. All chemicals were used without any further purification and were of analytical grade. SLS (0.5%, 1.0%, and 1.5%) with fresh distilled water was used throughout the study. Simulated intestinal fluid (SIF) (pH 6.8), simulated gastric fluid (SGF) (pH 1.2) without enzyme, PBS (pH 6.8), and 0.1 N HCl were prepared according to United States Pharmacopeial Convention (USP) 27.

Instruments and apparatus

To detect absorbance a Shimadzu ultraviolet (UV) - visible spectrophotometer model UV-1800 was used and a digital pH meter (model P101, Hanna Instruments, Italy) was used to determine pH. A water bath incubator (model PLT-113, Remi Equipments, Mumbai, India) was used for shaking. An analytical balance (model-SSI/DB 195, Singla Scientific) was applied for weighing. A rotatory tablet machine (12 station) (model-SSI/RTM/5283, Madhur, India) was used for tablet punching. An eight-station Electrolab TDT-08L dissolution tester and model TDT-06L dissolution tester apparatus were used as per USP 27 general guidelines.

Determination of solubility

The equilibrium solubility of domperidone in various solvents was determined by flask-shake method. A surplus amount of drug was added to 50 mL of test solvent, sonicated for 10 min, and subjected to continuous shaking for 24 h on a mechanical shaker at normal temperature. To achieve equilibrium the solution was left undisturbed for 1 h; after that it was filtered (Whatman filter paper no. 42; 2.5-µm pore size) and by UV spectrophotometric method the drug content was calculated. The saturated solubility was determined in 0.1 N HCl dissolution medium, distilled water, distilled water with SLS (0.5% w/v), distilled water with SLS (1% w/v), distilled water with SLS (1.5% w/v), phosphate buffer (pH 6.8), SGF without enzymes pH 1.2, and SIF pH 6.8. The drug content of each solution was determined in triplicate and the results were presented as mean ± standard deviation.[5]

Sink condition

The capability of the medium to dissolve the desired amount of the drug is known as a sink condition. Using sink conditions or too high amount of the sample usually increase the dissolution rate and weaken the discrimination between dissolution profiles. In the European Pharmacopeia, sink conditions are defined as a volume of dissolution medium that is at least three to ten times the saturation volume. In other words, if the maximum

concentration of the sample in the dissolution medium is less than 1/3 times the saturation solubility, i.e. $\phi < 1/3$, it is in sink conditions. Otherwise, it is in non-sink conditions.

The three vessels each containing 10 mL of medium and an excess of drug (100 mg) (n=3) containing 10 mL of medium were gently rotated for 24 h on a mechanical shaker at normal temperature. To achieve equilibrium the solution was kept undisturbed for 4 h and then filtered through Whatman filter paper no. 41 and after appropriate dilution the drug content was calculated by UV spectrophotometry at 284 nm.

Formulation of domperidone FDTs

Tablets were prepared as per the previously published method with slight modification. The raw materials were passed through a screen (60 mesh) prior to mixing and then another screen (40 mesh). Domperidone containing an amount equivalent to 10 mg was blended with the other desired excipients. Sodium bicarbonate and anhydrous citric acid were preheated at 80°C to remove absorbed/residual moisture and were thoroughly mixed in a mortar to get a uniform powder and then mixed with the other ingredients. The blend thus obtained was directly compressed using a 12-station mini press tablet machine equipped with a 9-mm concave punch.[7] The composition of the domperidone FDTs is given in Table 1.

Optimization of dissolution test

On the basis of the results obtained from the solubility study, the optimization of dissolution test for FDTs of domperidone was carried out on two different marketed FDTs of different manufacturer (FDT1 and FDT2). FDTs containing 10 mg of domperidone were used and dissolution studies were carried out using an USP apparatus II. The rate of dissolution was determined in different dissolution media (900 mL), i.e. SLS (0.5 %, 1.0%, 1.5%) with fresh distilled water, SIF (pH 6.8), SGF (pH 1.2) without enzyme, PBS (pH 6.8), and 0.1 N HCl at different agitation speeds of 50 and 75 rpm (Figures 1-4). Further, the dissolution profiles were compared using one-way ANOVA. A p value <0.05 was considered significant.[8]

In vitro drug release study of prepared FDTs (DOM-1 and DOM-2) in selected media

To check the discriminatory power of the dissolution media, *in vitro* drug release studies were performed using the prepared FDTs (DOM-1 and DOM-2) in 0.1 N HCl and 0.5% SLS with distilled water using the USP apparatus II at 50 rpm (Figure 5).

Table 1. Composition of fast dispersible tablets of domperidone

Ingredient	DOM-1	DOM-2
Drug (domperidone)	5%	5%
Sodium bicarbonate	14%	14%
Citric acid	7%	7%
Croscarmellose sodium	6%	-
Microcrystalline cellulose (MCC)	66.5%	72.5%
Magnesium stearate	1.5%	1.5%

Comparison of dissolution profiles by model-independent method

The dissolution profiles of the prepared FDTs (DOM-1 and DOM-2) and marketed FDTs (FDT-1 and FDT-2) were compared by applying a model-independent approach, which was based on the calculation of similarity factor (f_2) and dissimilarity factor

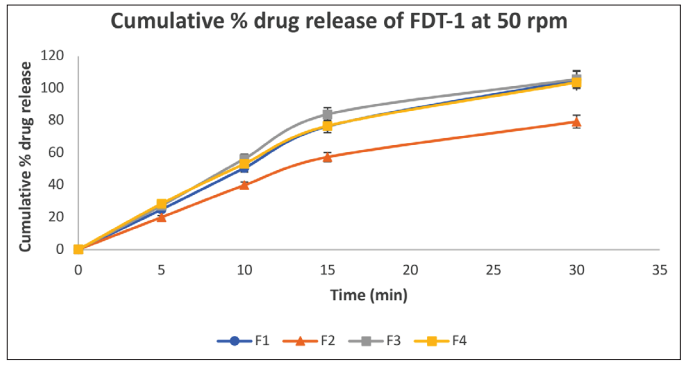

Figure 1. *In vitro* drug release study of marketed fast dispersible tablets (FDTs-1) of domperidonein (F1) 0.1 N HCl, (F2) SGF pH 1.2, (F3) Distilled water with 0.5% SLS, (F4) Distilled water with 1% SLS

FDTs: Fast dispersible tablets, SGF: Simulated gastric fluid, SLS: Sodium lauryl sulfate

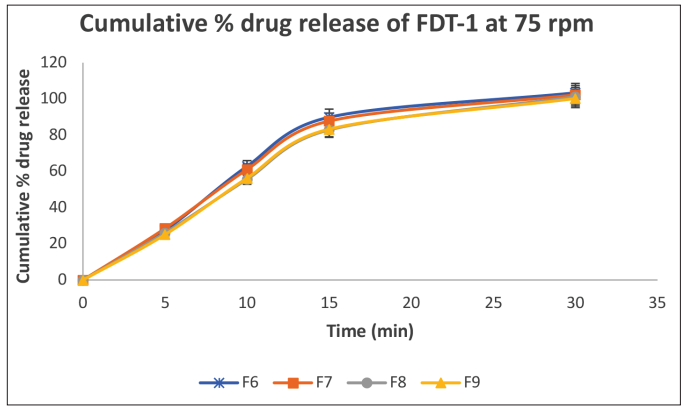

Figure 2. *In vitro* drug release study of marketed fast dispersible tablets (FDTs-1) of domperidone in (F1) 0.1 N HCl, (F2) SGF pH 1.2, (F3) Distilled water with 0.5% SLS, (F4) Distilled water with 1% SLS

FDTs: Fast dispersible tablets, SGF: Simulated gastric fluid, SLS: Sodium lauryl sulfate

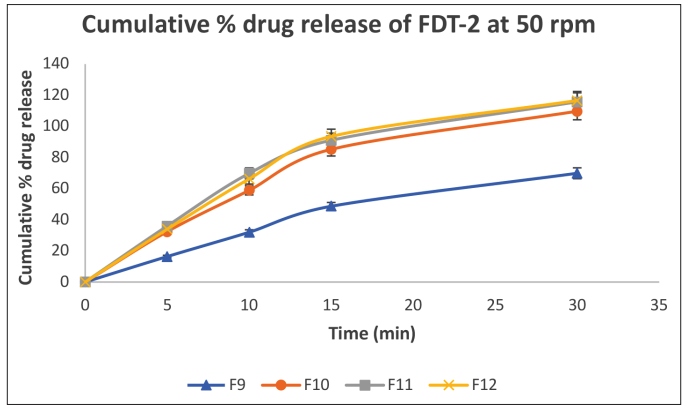

Figure 3. *In vitro* drug release study of marketed fast dispersible tablets (FDTs-1) of domperidone in (F9) SGF pH 1.2, (F10) 0.1 N HCl, (F11) Distilled water with 0.5% SLS, (F12) Distilled water with 1% SLS

FDTs: Fast dispersible tablets, SGF: Simulated gastric fluid, SLS: Sodium lauryl sulfate

(f_1). An f_2 value equal to 50 or greater ensures sameness or equivalence of the two curves and also the performance of the two products. Dissolution profiles of the FDTs were compared in 0.1 N HCl and 0.5% SLS with distilled water (as highest drug release was observed in both media) using similarity and dissimilarity factor calculation.[9-11]

The similarity factor (f_2) and dissimilarity factor (f_1) were calculated using equations 1 and 2.

$f_1=\{[\Sigma\ t=1\ n\ |R-T|]\ /\ [\Sigma\ t=1\ n\ R]\} \times 100$.....1

$f_2=50\times\log\{[1+(1/n)\Sigma t=1n(R-T)2]-0.5x100$.....2

Here n is the number of time points, R is the dissolution value of the reference (prechange) batch at time t, and T is the dissolution value of the test (postchange) batch at time t.

Validation of dissolution test method

The validation of the dissolution method was tested using different parameters such as specificity, linearity, robustness, accuracy, and precision.[12,13]

Specificity

A sample of reference commercial formulation (placebo) of tablets was prepared and transferred to a vessel containing 900 mL of dissolution media and stirred at 50 rpm using a paddle apparatus. The aliquots of sample solution were filtered through Whatman filter paper and analyzed by UV spectroscopy.[14]

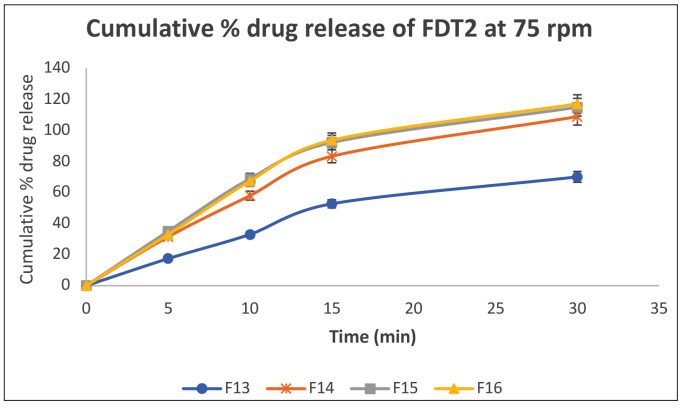

Figure 4. *In vitro* drug release study of marketed fast dispersible tablets (FDTs-1) of domperidone in (F13) SGF pH 1.2, (F14) 0.1 N HCl, (F15) Distilled water with 0.5% SLS, (F16) Distilled water with 1% SLS

FDTs: Fast dispersible tablets, SGF: Simulated gastric fluid, SLS: Sodium lauryl sulfate

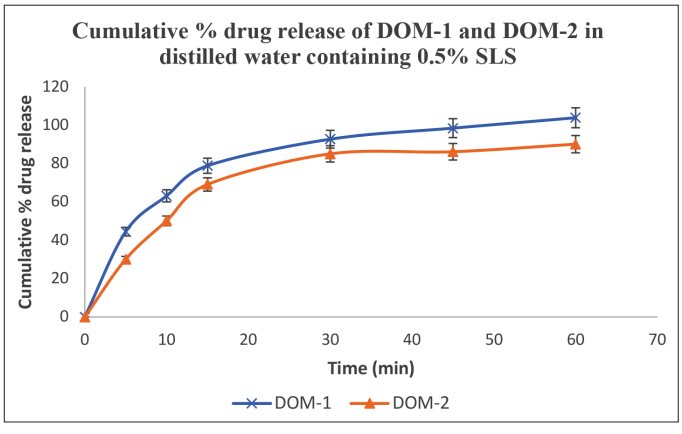

Figure 5. *In vitro* drug release study of prepared fast dispersible tablets (DOM-1 and DOM-2) in distilled water containing 0.5% SLS

SLS: Sodium lauryl sulfate

Accuracy

The domperidone was added to a dissolution vessel in known amount at 80%, 100%, and 120% level along with each 10 mg of domperidone FDT. The dissolution test was performed for 30 min using 900 mL of dissolution media (distilled water with 0.5% SLS) at a paddle speed of 50 rpm. Aliquots of 10 mL were filtered through Whatman filter paper and analyzed by UV spectroscopy at a spiked concentration.[5]

Linearity

To determine the linearity, a standard plot for domperidone was constructed by plotting average absorbance versus concentration. The linearity was evaluated by linear regression analysis.

Precision

The precision of the developed method was determined by repeatability and intermediate precision. For the determination of repeatability the test was performed using six dissolution vessels under the same conditions and the results were compared. Intermediate precision was determined by intraday and interday studies. The intraday study was performed by repeating the test three times in a day.[15] In the interday study, the dissolution test was conducted on a daily basis for 3 days and the results were compared. An relative standard deviation (RSD) value less than 2% indicates the precision of the developed method.

RESULTS AND DISCUSSION

Determination of solubility and sink condition

The solubility profile of domperidone shows that solubility is pH dependent. The maximum solubility shown by domperidone was observed in 0.1 N HCl and it increased as the pH decreases.[16,17] The solubility of domperidone in water is very low and is enhanced by the addition of surfactant (SLS). SLS caused an increase in the solubility with concentration 0.5% and a further increase in concentration had no significant effect on solubility as shown in Table 2. The dose of domperidone in the FDTs was 10 mg/tablet. The solubility to dose ratio (Cs/Cd) represents the closeness to sink condition and it occurs when the amount of drug that can be dissolved is three times higher than the amount of drug to be dissolved. A low ratio of Cs/Cd shows the existence of nonsink condition.[18,19]

Characterization of domperidone FDTs

The friability, hardness, disintegration time, wetting time, drug content, and weight of the formulated tablets were determined. The hardness of all the formulation was in the range of 3.37-3.55 kg/cm^2. The friability of all the formulations was below 1%, which indicates that the tablets had good mechanical resistance. Drug content was in the range of 100.9%-103.95%. The disintegration time of DOM-1 and DOM-2 was 31 and 50 s, respectively, which clearly indicated that the use of a

disintegrating agent in combination with effervescent material had a great impact on disintegration time. The weight variation results revealed that average % deviation of 20 tablets of each formulation was less than ±7.5%, providing good uniformity in all formulations.

Optimization of dissolution test conditions

On the basis of the screening study conducted on FDTs of domperidone and two different marketed FDTs of different manufacturer (FDT1 and FDT2), it was found that FDT-1 and FDT-2 exhibited similar dissolution profiles at 50 and 75 rpm. The highest drug release was observed in 0.1 N HCl and SGF without enzymes (pH 1.2) due to the high solubility to dose ratio (as shown in Table 2), but no significant difference in drug release was observed in either medium. The use of 0.5% SLS in distilled water increased the solubility and more than 100% drug release was observed within 30 min at a paddle speed of 50 rpm. Moreover, irrespective of paddle speed, the dissolution rate was relatively slow and consistent. A further increase in SLS did not increase the dissolution significantly. The use of a dissolution medium containing surfactant in small amounts less than its critical micelles concentration is often sufficient to solubilize certain poorly soluble drugs. The use of the slowest paddle speed (50 rpm) and dissolution media 0.1 N HCl and distilled water containing 0.5% SLS resulted in a better release profile. The drug release of FDT-1 and FDT-2 was similar (f_2>50) in both media, which may be due to the similar formulation parameters in both tablets.[8,20]

Confirmation of discriminating dissolution test conditions

Different dissolution profiles were obtained for FDTs of varying nature (Figures 5 and 6). In the present study dissimilarity in drug release was observed with DOM-1 compared to DOM-2 in 0.5% SLS (f_2=26) and similarity in drug release was observed with 0.1 N HCl (f_2=58). Based upon these results, the developed dissolution test method is considered discriminatory because it discriminates between products having differences in pharmaceutical attributes. From the above results it is possible to establish a dissolution method that can be used as an alternative to the official dissolution test for domperidone FDTs. In the present study distilled water containing 0.5% SLS at a stirring speed of 50 rpm was optimum.[9-11]

Table 2. Solubility and sink condition of domperidone in different media

Dissolution medium	Solubility (µg/mL)	Sink condition (Cs/Cd)
Distilled water	3.56	0.356
Simulated intestinal fluid (pH 6.8)	8.38	0.838
SGF (pH 1.2) without enzymes	214.3	21.43
Phosphate buffer solution (pH 6.8)	16.09	1.609
0.1 N HCl solution	268.7	26.87
0.5% SLS with distilled water	28.9	2.89
1% SLS with distilled water	23.8	2.38
1.5% SLS with distilled water	19.2	1.92

SGF: Simulated gastric fluid, SLS: Sodium lauryl sulfate

Validation of the dissolution method[21-23]

Specificity

When tablets were subjected to dissolution testing and absorbance was recorded, the corresponding absorbance was equivalent to 1.38% domperidone concentration. As per the ICH guidelines, the dissolution method is specific if the interference is not more than 2%. Hence, the developed method was specific.

Accuracy

The accuracy of the developed method was evaluated on the basis of percent recovery. For the accuracy test, recommended percent recovery should be between 95.0% and 105.0%. The mean recovery of domperidone is shown in Table 3, indicating that the dissolution method is accurate.

Linearity

The standard curve (Figure 7) depicts good linearity in the range of 5-35 µg/mL. The equation of the line was y=0.0287x+0.0093 with slope 0.0287 and r^2=0.9992. The RSD was less than 2%. The data clearly indicate that the method is linear and with a specified limit.

Precision

The results for repeatability and intermediate precision are summarized in Tables 4-6. The RSD value was less than 1%,

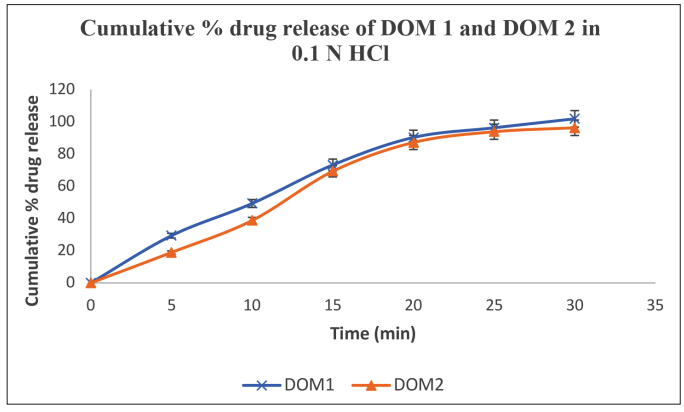

Figure 6. *In vitro* drug release study of prepared fast dispersible tablets (DOM-1 and DOM-2) in 0.1 N HCl

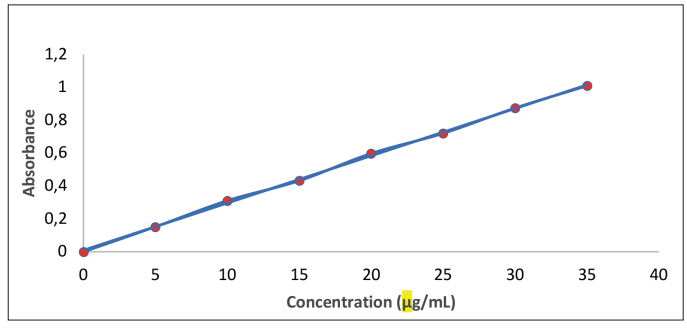

Figure 7. Calibration curve of domperidone in distilled water containing 0.5% SLS

SLS: Sodium lauryl sulfate

which shows that the developed dissolution method has good precision.

CONCLUSION

A dissolution test for domperidone FDTs was developed and validated as per ICH guidelines. The dissolution profiles of FDTs of domperidone were evaluated in different media (900 mL) at different stirring speeds (50 and 75 rpm). The use of distilled water containing 0.5% SLS as dissolution medium at 37±0.5°C and stirring speed of 50 rpm produced satisfactory results. The dissolution testing of domperidone FDTs formulated with different excipients showed different release profiles, which confirms the discriminatory nature of the developed method. The model independent method was used to evaluate the similarity of dissolution profiles. The developed method was found to be adequate for use in quality control testing of domperidone FDTs.

Conflicts of interest: No conflict of interest was declared by the authors.

Table 3. Accuracy test result for domperidone

Sr. no.	Parameter	Levels		
1	Tablet amount (mg)	10	10	10
2	Level of addition (%)	80	100	120
3	Amount added (mg)	8	10	12
4	Average amount recovered (mg)	17.40	20.08	21.59
5	Average % recovery*	96.66±1.132	100.40±1.82	98.13±1.49

* Each reading is mean ± standard deviation (n=3)

Table 4. Dissolution test precision (repeatability) result for domperidone

Dissolution vessels	Average % drug release ± SD (n=3)	RSD%
Vessel 1	98.82±0.81	0.81
Vessel 2	99.71±0.59	0.59
Vessel 3	100.28±0.38	0.37
Vessel 4	99.31±0.75	0.76
Vessel 5	100.89±0.35	0.34
Vessel 6	100.06±0.91	0.90

SD: Standard deviation, RSD: Relative standard deviation

Table 5. Dissolution test precision (intraday) result for domperidone

Time	Average % drug release ± SD (n=3)	RSD%
8.30 a.m.	99.71±0.89	0.89
1.30 p.m.	100.01±0.57	0.56
6.30 p.m.	100.09±0.71	0.70

SD: Standard deviation, RSD: Relative standard deviation

Table 6. Dissolution test precision (interday) result for domperidone

Day	Average % drug release ± SD (n=3)	RSD%
Day 1	100.07±0.79	0.79
Day 2	99.23±0.68	0.68
Day 3	99.01±0.51	0.52

SD: Standard deviation, RSD: Relative standard deviation

REFERENCES

1. Schiermeier S, Schmidt PC. Fast dispersible ibuprofen tablets. European Journal of Pharmaceutical Sciences. 2002;15:295-305.
2. Yasvanth A, Daroi A, Gupta R, Khanolkar A, Kulkarni A, Laud S, Pokale M, Shedge S, Date P. Discriminatory dissolution method development and validation of etoricoxib tablets. Dissolution Technologies. 2016;23:30-34.
3. Shaikh F, Patel V, Patel M, Surt N. Dissolution method development and validation for lercanidipine hydrochloride tablets. Dissolution Technologies. 2018;25:1-38
4. Furlanetto S, Maestrelli F, Orlandini S, Pinzauti S, Mura PJ. Optimization of dissolution test precision for a ketoprofen oral extended-release product. Pharm Biomed Anal. 2003;32:159-165.
5. Khan A. Development and validation of a discriminatory dissolution testing method for orally disintegrating tablets (ODTs) of domperidone. Dissolution Technologies. 2017;24:28-36.
6. Kulkarni AP, Shahnawaz M, Zaheer Z, Dehghan MHG. Development and validation of a dissolution method for pioglitazone tablets. Dissolution Technologies. 2012;19:36-45.
7. Bhatt S, Trivedi P. Development of domperidone: polyethylene glycol 6000 fast dissolving tablets from solid dispersions using effervescent method. J Chem Pharm Res.2011;3:889-898.
8. Kamalakkannan V, Puratchikody A, Ramanathan L, Jayapraba S. Development and validation of a dissolution test with reversed-phase high performance liquid chromatographic analysis for Candesartan cilexetil in tablet dosage forms. Arabian Journal of Chemistry. 2016;9:867-873.
9. Shah V, Tsonga Yi, Sathe P, Williams R. Dissolution profile comparison using similarity factor f2. Office of Pharmaceutical Science. Centre for Drug Evaluation and Research, Food and Drug Administration. Avaible form: https://link.springer.com/article/10.1023%2FA%3A1011976615750
10. Moore JW, Flanner HH. Mathematical comparison of curves with an emphasis on in-vitro dissolution profiles. PharmTech. 1996;20:64-74.
11. Shah VP, Tsong L, Sathe P, Williams RL. Dissolution profile comparison using similarity factor, f2. Dissolution Technologies. 1999;6:21.
12. International Conference of Harmonization. Validation of Analytical Procedures: Text and Methodology, Q2(R1); ICH Harmonized Tripartite Guideline: Geneva, Switzerland. 2005;1-13.
13. The United States Pharmacopeia and National Formulary.
14. USP 32–NF 27. The United States Pharmacopeial Convention, Inc.: Rockville, MD, 2009.

15. Guidance for the Validation of Analytical Methodology and Calibration of Equipment Used for Testing of Illicit Drugs in Seized Materials and Biological Specimens. Laboratory and Scientific Section United Nations Office on Drugs and Crime Vienna. New York; United Nations; 2009.

16. Shah R, Patel S, Patel H, Pandey S, Shah S, Shah D. Development and validation of dissolution method for carvedilol compression-coated tablets. Brazilian Journal of Pharmaceutical Sciences. 2011;47:899-906.

17. Chandran S, Singh RSP. Comparison of various international guidelines for analytical method validation. Pharmazie. 2007;62:4-14.

18. Sahoo R, Panda RK, Himasankar K, Barik BB. In-vitro evaluation of domperidone mouth dissolving tablets. Indian J Pharm Sci. 2010;72:822-825.

19. Khadka P, Ro J, Kim H, Kim I, Kim JK, Kim H, Cho JM, Yun G, Lee J. Pharmaceutical particle technologies: an approach to improve drug solubility, dissolution and bioavailability. Asian Journal of Pharmaceutical Sciences. 2014;9:304-316.

20. Jassim ZE, Hussein AA. Dissolution method development and enhancement of solubility of clopidogrel bisulfate. Int Res J Pharm. 2017;8:25-29.

21. Ministry of Health & Family Welfare, Govt. of India. General Monographs. In: Ministry of Health & Family Welfare, Govt. of India. Indian Pharmacopoeia (2018). 8th ed. The Indian Pharmacopoeia Commission, Ghaziabad, India; 2018: 1879-1881.

22. Santos Júnior ADF, Barbosa IS, Santos VLD, Silva RL, Junior EC. Test of dissolution and comparison of *in-vitro* dissolution profiles of coated ranitidine tablets marketed in Bahia. Brazilian Journal of Pharmaceutical Sciences. 2014;50:83-89.

23. Belouafa S, Habti F, Benhar S, Belafkih B, Tayane B, Hamdouch S, Bennamara A, Abourriche A. Statistical tools and approaches to validate analytical methods: methodology and practical examples. International Journal of Metrology and Quality Engineering. 2017;8:1-10.

Turk J Pharm Sci 2020;17(1):81-93
DOI: 10.4274/tjps.galenos.2018.59389

ORIGINAL ARTICLE

Synthesis and Anticancer and Antimicrobial Evaluation of Novel Ether-linked Derivatives of Ornidazole

Eter Bağlı Yeni Ornidazol Türevlerinin Sentezi, Antikanser ve Antimikrobiyal Etkisinin Değerlendirilmesi

Sevil ŞENKARDEŞ[1]*, Necla KULABAŞ[1], Özlem BİNGÖL ÖZAKPINAR[2], Sadık KALAYCI[3], Fikrettin ŞAHİN[3], İlkay KÜÇÜKGÜZEL[1], Ş. Güniz KÜÇÜKGÜZEL[1]

[1]Marmara University, Faculty of Pharmacy, Department of Pharmaceutical Chemistry, Haydarpaşa, İstanbul, Turkey
[2]Marmara University, Faculty of Pharmacy, Department of Biochemistry, Haydarpaşa, İstanbul, Turkey
[3]Yeditepe University, Faculty of Engineering, Department of Genetics and Bioengineering, Kayışdağı, İstanbul, Turkey

ABSTRACT

Objectives: Some novel 1-(2-methyl-5-nitro-1H-imidazol-1-yl)-3-(substituted phenoxy)propan-2-ol derivatives (**3a-g**) were designed and synthesized.

Materials and Methods: Compounds **3a-g** were obtained by refluxing ornidazole (1) with the corresponding phenolic compounds (**2a-g**) in the presence of anhydrous K_2CO_3 in acetonitrile.

Results: Following the structure elucidation, the *in vitro* antimicrobial activity and cytotoxic effects of compounds **3a-g** on K562 leukemia and NIH/3T3 mouse embryonic fibroblast cells were measured. As a part of this study, the compliance of the compounds with the drug-likeness properties was evaluated. The physico-chemical parameters (log P, TPSA, nrotb, number of hydrogen bond donors and acceptors, logS) were calculated using the software OSIRIS.

Conclusion: All the synthesized compounds except **3a** showed significant activity (MIC=4-16 μg mL^{-1}) against the bacterial strain *Bacillus subtilis* as compared to the standard drug, whereas antileukemic activities were rather limited. Furthermore, all the compounds were nontoxic and the selectivity index outcome indicated that the antileukemic and antimicrobial effects of the compounds were selective with good estimated oral bioavailability and drug-likeness scores.

Key words: Imidazole, ether linked, ornidazole, antimicrobial activity, cytotoxicity

ÖZ

Amaç: Bu çalışmada bazı yeni 1-(2-metil-5-nitro-1H-imidazol-1-il)-3-(sübstitüe fenoksi) propan-2-ol (**3a-g**) türevleri tasarlanmış ve sentezlenmiştir

Gereç ve Yöntemler: 3a-g numaralı bileşikler Ornidazol'ün **(1)** uygun fenolik bileşikler (**2a-g**) ile asetonitril içinde susuz K_2CO_3 eşliğinde ısıtılmasıyla elde edilmiştir.

Bulgular: Yapı aydınlatılmasını takiben, *in vitro* antimikrobiyal aktivite ve K562 lösemi hücresi ve NIH/3T3 fare embriyonik fibroblast hücresi üzerinde sitotoksik etki çalışması yapılmıştır. Bu çalışmanın bir parçası olarak, bileşiklerin ilaç benzerlik özelliklerine uyumu değerlendirilmiştir. OSIRIS yazılımı kullanılarak fizikokimyasal parametreler (log P, TPSA, dönebilen bağ sayısı, hidrojen bağ vericileri ve alıcıları, logS) hesaplanmıştır.

Sonuç: Bileşik **3a** dışında sentezlenen tüm bileşikler, *Bacillus subtilis* suşuna karşı standart ilaca kıyasla anlamlı bir aktivite (MIC=4-16 μg mL^{-1}) göstermiş olmakla birlikte antilösemik aktiviteleri oldukça sınırlıdır. Ayrıca, bütün bileşiklerin hesaplanan iyi oral biyoyararlanım ve ilaç benzerlik özelliklerinin yanında non-toksik özellikte olabilecekleri öngörülmüş olup, seçicilik indeksi sonucuna göre bileşiklerin antimikrobiyal ve antilösemik etkilerinin selektif olduğu tespit edilmiştir.

Anahtar kelimeler: İmidazol, eter bağlı, ornidazol, antimikrobiyal aktivite, sitotoksisite

Presented in: The research was presented at the 12th International Symposium on Pharmaceutical Sciences on 26-29 June 2018 in Ankara, Turkey

***Correspondence: E-mail:** sevil.aydin@marmara.edu.tr, **Phone:** +90 543 474 39 17 **ORCID-ID:** orcid.org/0000-0002-0523-459X
Received: 17.07.2018, **Accepted:** 29.11.2018

INTRODUCTION

Cancer, which is defined as a group of related diseases, not a single disease, is a major health problem worldwide. According to a report by the World Health Organization, cancer is the second leading cause of death globally and resulted in 8.8 million deaths in 2015. Leukemia is a group of cancers that generally start in the bone marrow and end up with high numbers of abnormal white blood cells and forms 3.7% of all new cancer cases.[1] Bloodstream infections resulting in deaths in leukemia patients constitute a major challenge for public health and is a situation that needs attention for cancer patients.[2] Intrinsic immune defense mechanisms protect us against invading pathogens and progression of malignancies; thus there is a relationship between antibacterial and antileukemic effects. Many studies for reducing the threat posed by leukemia showed that progress in antimicrobial protection and chemotherapy has reduced disease severity and improved the survival rate.[3]

Over the years, there has been increased interest in the synthesis and biological research of nitrogen-based heterocycles. Among these, the imidazole ring is a major pharmacophoric substructure in a number of antimicrobial and anticancer agents[4-7] like temozolomide, zoledronic acid, mercaptopurine, azomycin, and ornidazole. Therefore, the search for new therapeutic agents bearing the imidazole ring continues to be an attractive area of investigation in medicinal chemistry. Moreover, it has been hypothesized that a reactive intermediate formed in the microbial reduction of the nitro moiety of nitroimidazoles binds to the DNA of the microorganism with a covalent bond and activates the lethal effect.[8] As shown in Figure 1, analogues of metronidazole and ornidazole have been reported as antimicrobial and anticancer agents.[9-11] Additionally, five-membered heterocyclic compounds containing an ether-linked structure showed significant anticancer activity.[12,13]

In view of the aforementioned premises, we aimed to report herein the synthesis and *in vitro* anticancer and antimicrobial activity of the title compounds. Ornidazole is an antibiotic that is effective only against anaerobic bacterial strains. In the present study paper, we planned the design and synthesis of a series of ornidazole derivatives and investigation of their antimicrobial properties and anticancer activity on the K562 leukemia cell line as well as their cytotoxic effect on the NIH/3T3 cell line.

EXPERIMENTAL

Chemistry

All reagents and solvents were obtained from commercial suppliers and were used without further purification. Merck silica gel 60 F254 plates were used for analytical thin-layer chromatography (TLC). Melting points were determined using a Schmelzpunktbestimmer SMP II apparatus and were uncorrected. ^{1}H-NMR and ^{13}C-NMR spectra were recorded on a Bruker 300 MHz Ultrashield TM spectrometer. Elemental analyses were determined by CHNS-932 (LECO). FT-IR spectra were recorded on a Shimadzu FT-IR-8400S spectrometer. ESI-MS mass spectra were acquired using a PerkinElmer AxION 2 TOF spectrometer. The liquid chromatographic system consisted of an Agilent Technologies 1100 series instrument equipped with a quaternary solvent delivery system and a model Agilent series G1315 A photodiode array detector. Chromatographic data were collected and processed using the software Agilent Chemstation Plus. Chromatographic separation was performed at ambient temperature using a reverse phase ACE C18 (4.0×100 mm) column. All experiments were performed using ACN-H_2O (v/v, 40/60) mobile phase with ultraviolet detection at 254 nm.

*General procedure for the synthesis of compounds **3a-g***

A mixture of phenol derivatives **(2a-g)** (paracetamol, *p*-nitrophenol, thymol, methyl paraben, ethyl paraben, 4-chloro-3-methylphenol, and *m*-cresol) (0.005 mol) and anhydrous

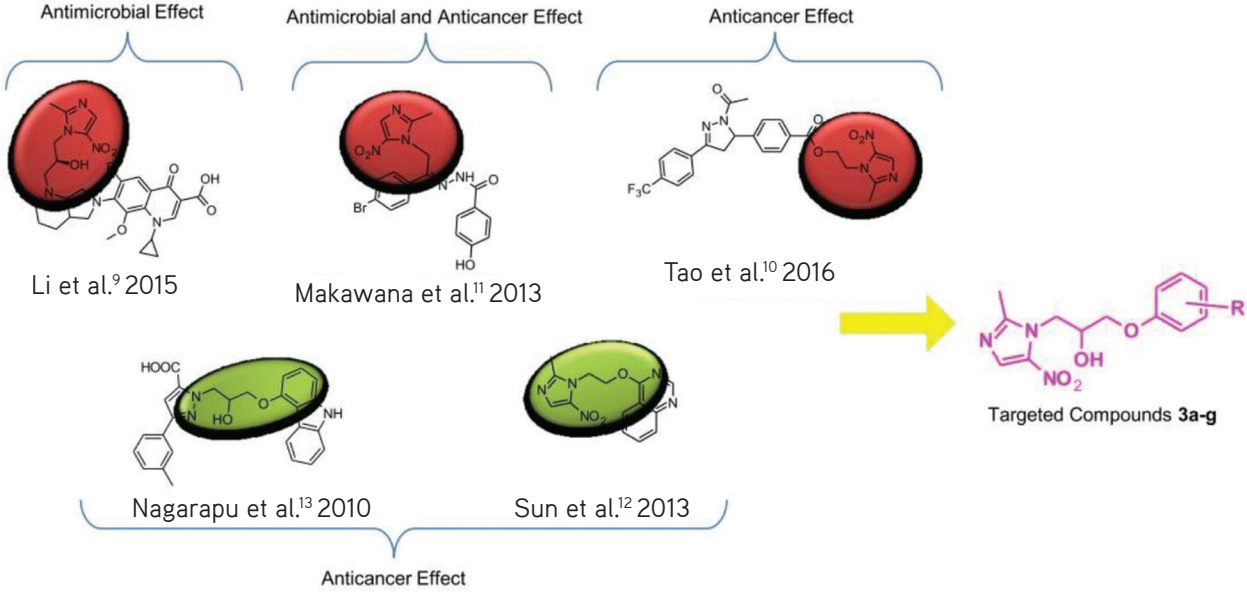

Figure 1. The design of new ornidazole derivatives on the basis of the literature

K_2CO_3 (0.015 mol) in acetonitrile (30 mL) was heated for 1 h. Ornidazole (ODZ) (1) (0.005 mol) was added and the mixture was refluxed for 3 h. The reaction mixture was then poured onto ice and neutralized with 1 N hydrochloric acid. The resulting precipitate consisting of 1-(2-methyl-5-nitro-1*H*-imidazol-1-yl)-3-(substitutedphenoxy) propan-2-ol **(3a-g)** derivatives was collected by filtration and finally purified by recrystallization from methanol (Scheme 1).

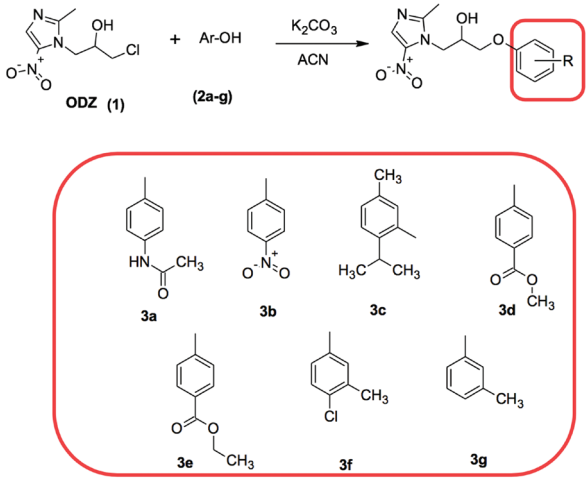

Scheme 1. Synthetic route to ornidazole derivatives

N*-{4-[2-hydroxy-3-(2-methyl-5-nitro-1H-imidazol-1-yl) propoxy]phenyl} acetamide *(3a)

Light yellow solid; Yield 81%; m.p. 189-190°C; Rt (min): 1.15; FT-IR υ_{max} (cm^{-1}): 3377 (O-H); 3219 (N-H); 1659 (C=O amide); 1602, 1553, 1510, 1445, 1370 (N-H bending, C=C, C=N, NO_2); 1240 (C-O). ^{1}H-NMR (300 MHz), (DMSO-d_6/TMS) δ ppm: 2.00 (s, 3H, Ar-**CH_3**); 2.46 (s, 3H, CO**CH_3**); 3.95-3.97 (d, 2H, J=5.1 Hz, N-**CH_2**-**CH**-OH); 4.05-4.13 (m, 1H, CH-**OH**); 4.24-4.62 (m, 2H, **CH_2**-O); 5.55 (bs, 1H, **OH**); 6.87-6.90 (d, 2H, J=9.0 Hz, Ar-**H**); 7.47-7.50 (d, 2H, J=9.0 Hz, Ar-H); 8.04 (s, 1H, **Im-H**); 9.80 (s, 1H, **NH**). ^{13}C-NMR (75 MHz, DMSO-d_6) δ ppm: 14.81 (**CH_3**), 24.27(**CH_3**), 49.37 (**CH_2**), 68.32 (CH-OH), 70.47 (**CH_2**), 114.96 (2CH), 120.92 (2CH), 133.31(C), 133.38 (CH), 139.03 (C-NO_2), 152.58 (C), 154.46 (C), 168.22 (C=O). Anal. Calcd for $C_{15}H_{18}N_4O_5$. 1/2 H_2O: C, 52.47; H, 5.58; N, 16.32 Found: C, 52.96; H, 4.91; N, 16.31. ESI-MS (m/z): 357 $[M+Na]^+$.

*1-(2-Methyl-5-nitro-1H-imidazol-1-yl)-3-(4-nitrophenoxy) propan-2-ol **(3b)***

Light brown solid; Yield 78%; m.p. 181°C; Rt (min): 2.71; FT-IR υ_{max} (cm^{-1}): 3375 (O-H); 3136 (=C-H); 1593, 1531,1498, 1347 (C=C, C=N, NO_2); 1342 (C-O). ^{1}H-NMR (300 MHz), (DMSO-d_6/TMS) δ ppm: 2.47 (s, 3H, **CH_3**); 4.13-4.35 (m, 4H, 2**CH_2**); 4.57-4.63 (m, 1H, **CH**-OH); 5.62-5.64 (d, 1H, *J*=4.5 Hz, **OH**); 7.15-7.21 (d, 2H, *J*=9.3 Hz, Ar-**H**); 8.05 (s, 1H, **Im-H**); 8.21-8.26 (d, 2H, *J*=9.6 Hz, Ar-**H**). ^{13}C-NMR (75 MHz, DMSO-d_6) δ ppm: 14.82 (**CH_3**), 49.12 (**CH_2**), 68.08 (CH-OH), 71.05 (**CH_2**), 115.57 (2CH), 126.36 (2CH), 133.44 (CH), 139.03 (C-NO_2), 141.47 (C-NO_2), 152.61 (C), 164.09 (C). Anal. Calcd for $C_{13}H_{14}N_4O_6$: C, 48.45; H, 4.38; N, 17.38 Found: C, 49.16; H, 4.31; N, 17.36. ESI-MS (m/z): 345 $[M+Na]^+$.

*1-(2-Methyl-5-nitro-1H-imidazol-1-yl)-3-[5-methyl-2-(propan-2-yl)phenoxy]propan-2-ol **(3c)***

Off-white solid; Yield 92%; m.p. 163°C; Rt (min): 7.25; FT-IR υ_{max} (cm^{-1}): 3234 (O-H); 1659 (C=O amide); 1610, 1533, 1469, 1365 (N-H bending, C=C, C=N, NO_2); 1243 (C-O). ^{1}H-NMR (300 MHz), (DMSO-d_6/TMS) δ ppm: 1.15-1.18 [d, 6H, *J*=6.9 Hz, CH-(**CH_3**)$_2$]; 2.27 (s, 3H, Ar-**CH_3**); 2.48(s, 3H, **CH_3**); 3.28-3.35 [m, 1H, CH-(**CH_3**)$_2$]; 3.95-4.05 (m, 2H, N-**CH_2**-CH-OH); 4.13-4.14 (m, 1H, CH-OH); 4.27-4.70 (m, 2H, **CH_2**-O); 5.52 (bs, 1H, **OH**); 6.72-7.08 (m, 3H, Ar-**H**); 8.05 (s, 1H, **Im-H**). ^{13}C-NMR (75 MHz, DMSO-d_6) δ ppm: 14.81(**CH_3**), 21.40 (**CH_3**), 23.13 (**CH_3**), 23.16 (**CH_3**), 26.50 (CH), 49.64 (**CH_2**), 68.44 (CH-OH), 70.16 (**CH_2**), 112.71 (CH), 121.63 (CH), 126.01 (CH), 133.40 (**CH_2**), 133.61 (C), 136.36 (C), 138.98 (C-NO_2), 152.65 (C), 155.72 (C). Anal. Calcd for $C_{17}H_{23}N_3O_4$. 1/2 H_2O: C, 59.63; H, 7.06; N, 12.27 Found: C, 59.00; H, 6.33; N, 12.50. ESI-MS (m/z): 356 $[M+Na]^+$.

*Methyl 4-[2-hydroxy-3-(2-methyl-5-nitro-1H-imidazol-1-yl) propoxy]benzoate **(3d)***

Dark brown solid; Yield 80%; m.p. 181-183°C; Rt (min): 2.48; FT-IR υ_{max} (cm^{-1}): 1699 (C=O ester); 1602, 1533, 1475, 1363 (N-H bending, C=C, C=N, NO_2) 1317 (C-O). ^{1}H-NMR (300 MHz), (DMSO-d_6/TMS) δ ppm: 2.47 (s, 3H, **CH_3**); 3.82 (s, 3H, COO**CH_3**); 4.08-4.34 (m, 4H, 2**CH_2**); 4.57-4.63 (m, 1H, **CH**); 5.58-5.59 (d, 1H, *J*=4.8 Hz, **OH**); 7.05-7.09 (d, 2H, *J*=9.0 Hz, Ar-**H**); 7.90-7.95 (d, 2H, *J*=9.0 Hz, Ar-**H**); 8.05 (s, 1H, **Im-H**). ^{13}C-NMR (75 MHz, DMSO-d_6) δ ppm: 14.81 (**CH_3**), 49.23 (**CH_2**), 52.29 (**CH_3**), 68.15 (CH-OH), 70.46 (**CH_2**), 115.00 (2CH), 122.57 (C), 131.71 (2CH), 133.41 (CH), 139.02 (C-NO_2), 152.59 (C), 162.62 (C), 166.32 (C=O). Anal. Calcd for $C_{15}H_{17}N_3O_6$: C, 53.73; H, 5.11; N, 12.53 Found: C, 53.19; H, 4.77; N, 12.33. ESI-MS (m/z): 358 $[M+Na]^+$.

*Ethyl 4-[2-hydroxy-3-(2-methyl-5-nitro-1H-imidazol-1-yl) propoxy]benzoate **(3e)***

Yellow solid; m.p. 81-82°C, Rt (min): 3.73; FT-IR υ_{max} (cm^{-1}): 3208 (O-H); 1690 (C=O ester); 1607, 1537, 1472, 1427, 1364 (N-H bending, C=C, C=N, NO_2); 1314 (C-O). ^{1}H-NMR (300 MHz), (DMSO-d_6/TMS) δ ppm: 1.29-1.34 (t, 3H, *J*=7.2 Hz, CH_2-**CH_3**); 2.47 (s, 3H, **CH_3**); 4.11-4.62 (m, 7H, **CH_2**-CH_3 and **CH**-OH); 5.58-5.60 (d, 1H, *J*=4.8 Hz, **OH**); 7.05-7.08 (d, 2H, *J*=8.7 Hz, Ar-**H**); 7.91-7.94 (d, 2H, *J*=9.0 Hz, Ar-**H**); 8.05 (s, 1H, **Im-H**). ^{13}C-NMR (75 MHz, DMSO-d_6) δ ppm: 14.68 (CH_3), 14.81 (CH_3), 49.24 (CH_2), 60.81 (CH_2), 68.15 (CH-OH), 70.46 (CH_2), 114.94 (2CH), 122.84 (C), 131.66 (2CH), 133.41 (CH), 139.02 (C-NO_2), 152.59 (C), 162.57 (C), 165.81 (C=O). Anal. Calcd for $C_{16}H_{19}N_3O_6$: C, 55.01; H, 5.48; N, 12.03 Found: C, 54.74; H, 5.05; N, 12.13. ESI-MS (m/z): 372 $[M+Na]^+$.

*1-(4-Chloro-3-methylphenoxy)-3-(2-methyl-5-nitro-1H-imidazol-1-yl)propan-2-ol **(3f)***

Dark brown solid; Yield 87%; m.p. 139-140°C; Rt (min): 7.40; FT-IR υ_{max} (cm^{-1}): 3144 (O-H); 1593, 1530, 1483, 1362 (N-H bending, C=C, C=N, NO_2); 1292 (C-O). ^{1}H-NMR (300 MHz), (DMSO-d_6/TMS) δ ppm: 2.30 (s, 3H, Ar-**CH_3**); 2.49 (s, 3H, Im-**CH_3**); 3.99-4.00 (m, 2H, N-**CH_2**-CH-OH); 4.10 (m, 1H, **CH**-OH); 4.24-4.61 (m, 2H, **CH_2**-O); 5.54-5.55 (d, 1H, *J*=3.9 Hz, **OH**); 6.80-7.32 (m, 3H, Ar-**H**); 8.04 (s, 1H, **Im-H**). ^{13}C-NMR (75 MHz, DMSO-d_6) δ

ppm: 14.81 (CH_3), 20.25 (CH_3), 49.30 (CH_2), 68.22 (CH-OH), 70.52 (CH_2), 114.15 (CH), 117.70 (CH), 125.28 (C), 129.97 (CH), 133.40 (CH), 136.98 (C), 139.02 (C-NO_2), 152.58 (C), 157.53 (C). Anal. Calcd for $C_{14}H_{16}ClN_3O_4$: C, 51.62; H, 4.95; N, 12.90 Found: C, 51.68; H, 4.55; N, 12.75. ESI-MS (m/z): 348 $[M+Na]^+$.

1-(2-Methyl-5-nitro-1H-imidazol-1-yl)-3-(3-methylphenoxy) propan-2-ol ***(3g)***

Light brown solid; Yield 76% ; m.p. 103°C (lit. 105-106°C).[14] Rt (min): 3.44; FT-IR υ_{max} (cm^{-1}): 3140 (O-H); 1586, 1530, 1497, 1470, 1370 (N-H bending, C=C, C=N, NO_2); ^{1}H-NMR (300 MHz), (DMSO-d_6/TMS) δ ppm: 2.29 (s, 3H, Ar-**CH_3**); 2.47 (s, 3H**,** Im-**CH_3**); 3.97-3.99 (m, 2H, N-**CH_2**-CH-OH); 4.10 (m, 1H, **CH**-OH); 4.57-4.63 (m, 2H, **CH_2**-O); 5.51-5.53 (d, 1H, *J*=5.4 Hz, **OH**); 6.73-7.20 (m, 4H, Ar-**H**); 8.04 (s, 1H, **Im-H**). ^{13}C-NMR (75 MHz, DMSO-d_6) δ ppm: 14.80 (CH_3), 21.56 (CH_3), 49.38 (CH_2), 68.32 (CH-OH), 70.11 (CH_2), 111.93 (CH), 115.62 (CH), 122.02 (CH), 129.71 (CH), 133.38 (CH), 139.03 (C-NO_2), 139.47 (C), 152.58 (C), 158.76 (C). Anal. Calcd for $C_{14}H_{17}N_3O_4$: C, 57.72; H, 5.88; N, 14.42 Found: C, 58.25; H, 5.45; N, 14.24. ESI-MS (m/z): 314 $[M+Na]^+$.

Biological part

Antimicrobial activity

All synthesized compounds were evaluated for antimicrobial activity. The activity experiments were carried out in Yeditepe University, Faculty of Engineering, Department of Genetics and Bioengineering. The gram-positive and gram-negative bacteria *Escherichia coli* ATCC 10536, *Staphylococcus aureus* ATCC 6538, *Pseudomonas aeruginosa* ATCC 15442, and *Bacillus subtilis (B. subtilis)* ATCC 6633 and *Candida albicans* ATCC 10231 were used in the activity studies. Antimicrobial activities of the compounds tested against these species were based on disc-diffusion and micro-well dilution assays.

Disc-diffusion assay

The antimicrobial properties of the compounds were investigated by disc-diffusion assay as described in the literature.[15] For this aim, 100 µL of freshly prepared microbial suspensions containing 10^8 CFU/mL of bacteria and 10^4 spore/mL of fungi were spread on nutrient agar, Sabouraud dextrose agar, and potato dextrose agar, respectively. Black discs (6 mm) impregnated with imidazole derivatives (20 µL) of the specified concentrations were placed on the inoculated plates. Distilled water (20 µL) was used as a negative control. The inoculated plates were incubated at 36±1°C for 24 h for the bacterial strains and 27±1°C for 72 h for the fungal isolate. Antimicrobial activity was determined by measuring the zone of inhibition around the discs.

Micro-well dilution assay

The sensitivity of the bacterial strains towards the compounds was quantitatively evaluated from the minimum inhibitory concentration (MIC) values obtained by the micro-well dilution method.[16]

The inocula of the bacterial strains were prepared from 12-h broth cultures and the suspensions were adjusted to 0.5 McFarland standard turbidity. Compounds dissolved in DMSO were first prepared at the highest concentration to be tested (1024 µg/mL), and then serial two-fold dilutions were made in order to obtain a concentration range from 2 to 1024 µg/mL in 15-mL sterile test tubes containing nutrient broth. The 96-well plates were prepared by dispensing into each well 95 µL of nutrient broth and 5 µL of the inoculum. Two hundred microliters of nutrient broth without inoculum was transferred into the first wells as a positive control. Aliquots (100 µL) taken from the 200 µg/mL stock solution were added to the second well. One hundred microliters from the respective serial dilutions was transferred into 5 consecutive wells. The last well containing 195 µL of nutrient broth without compound and 5 µL of the inoculum on each strip was used as a negative control. The contents of each well were mixed on a plate shaker at 300 rpm for 20 s and then incubated at appropriate temperatures for 24 h. Microbial growth in each medium was determined by reading the absorbance (Abs) at 630 nm using an ELx800 universal microplate reader (BioTek Instruments Inc., Highland Park, VT, USA) and confirmed by plating 5-µL samples from clear wells on nutrient agar medium. The MIC was defined as the lowest concentration of the compounds to inhibit the growth of microorganisms. Ampicillin and fluconazole were used as positive controls for the bacteria and fungi, respectively.

Anticancer activity

Cell culture

The human leukemic cell line K562 (ATCC, CCL-243) and mouse embryonic fibroblast cell line NIH/3T3 (ATCC, CRL-1658) were maintained in Dulbecco's Modified Eagle Medium supplemented with 10% fetal bovine serum, 1% L-glutamine, and penicillin/streptomycin (Gibco) at 37°C in a humidified incubator with 5% CO_2.

Cell viability assay

The cell viability effects of compounds **3a-g** were evaluated *in vitro* using the MTT colorimetric method against the K-562 and NIH/3T3 cell lines at different doses[17,18] at the Marmara University, Faculty of Pharmacy, Department of Biochemistry. Briefly, the cells (1×10^4 cells/well) were seeded onto 96-well plates and incubated overnight. Then the cells were treated with different concentrations of compounds for 48 h. After the incubation period, MTT was added to each well to a final concentration of 0.5 mg/mL followed by incubation for 4 h. The culture medium was removed and 100 µL of the SDS buffer was added to solubilize the purple formazan product. Abs at wavelengths of 570 and 630 nm was measured by a microplate reader (BioTek, Winooski, VT, USA). Cell viability was expressed as a percentage of the untreated control cells.

Statistical analysis

The data were reported as means±standard deviations and analyzed by one-way analysis of variance followed by Tukey's multipl comparison test using GraphPad Prism 5. Differences between means at $p<0.05$ level were considered significant.

RESULTS AND DISCUSSION

Chemistry

Scheme 1 outlines the synthetic pathway used to obtain the ether-linked derivatives **3a-g**. The reaction of ornidazole (**1**) with phenol compounds **2a-g** yielded the 1-(2-methyl-5-nitro-1*H*-imidazol-1-yl)-3-(substituted phenoxy)propan-2-ol (**3a-g**) derivatives. The TLC and high performance liquid chromatography data confirmed the new products. The purity of the compounds was established from sharp melting points and elemental analysis data. Compound **3g** was reported to be synthesized previously but no theoretical or biological information about this compound has been presented in the available literature.[14]

The FT-IR, ^{1}H NMR, ^{13}C-NMR, and ESI-MS data were in agreement with the proposed structures of compounds **3a-g** (Figures S1-S28, in the *Supplementary File)*. In particular, the FT-IR spectrum of **3a** showed absorption bands at 1659 cm^{-1} and 3129 cm^{-1} due to C=O and NH functions, respectively. In the NMR spectra the NH proton resonated at the expected regions. The FT-IR spectra of compounds **3d** and **3e** revealed the presence of bands for C=O ester groups, while the ^{1}H-NMR spectra of compounds **3d** and **3e** revealed the presence of methyl and ethyl protons attributed to the ester group. The aryl methyl groups in the **3f** and **3g** molecules were clearly demonstrated by their typical signals at δ 2.29-2.30 ppm along with a singlet in the aliphatic region. The LC-MS/MS analysis data displayed $[M+Na]^{+}$ corresponding to new compounds.

Pharmacological screening

Cytotoxicity of compounds towards K562 and NIH/3T3 cells

In the MTT test, the K562 cell line and NIH/3T3 cell line were incubated with compounds **3a-g** at various concentrations. After the completion of the incubation period, the cytotoxic effects of the compounds were examined and the IC_{50} values with the selectivity index were calculated. The results are presented in Table 1.

The MTT assay was performed to determine the antiproliferative effects of compounds **3a-g** on the K562 leukemia cell line. In order to check for toxicity on healthy cells, the effects of compounds **3a-g** on NIH/3T3 mouse embryonic fibroblast cells were investigated using the MTT test. The selectivity index values of all of the compounds were also determined to compare their selectivity (Table 1). Compounds **3a-g** showed weaker cytotoxicity on the K562 cell line, while all the synthesized compounds were found to be nontoxic on healthy cells and safe for human consumption. Among them, compound **3a** was the most effective, with an IC_{50} value of 116.55 μM. Moreover, these compounds exhibited selectivity due to their low cytotoxicity on healthy cells with selectivity indices between 1.94 and 4.02.

Table 1. IC_{50} values of the compounds against K562 and NIH/3T3 cells for 24 h

Compound	IC_{50} (μM)		SI*
	K562 cell line	NIH/3T3 cell line	
3a	116.55	341.75	2.93
3b	131.68	479.25	3.64
3c	126.33	317.00	2.51
3d	166.75	324.10	1.94
3e	276.59	773.75	2.80
3f	127.88	178.10	1.39
3g	166.46	669.40	4.02
Imatinib	11.22	1104.00	98.39

SI: IC_{50} on normal cells/IC_{50} on cancer cells

The IC_{50} values of these compounds for the NIH/3T3 cell line were higher than those for the K562 cell line. These results suggested that this series of compounds possessed selectivity for the K562 cancer cell line. As a result, compounds **3b** and **3g** showed more selective antileukemic activity than the other compounds.

Antimicrobial activity

The synthesized derivatives were screened for their antimicrobial activity against two gram-positive (*B. subtilis* and *Staphylococcus aureus*) and two gram-negative (*Escherichia coli* and *Pseudomonas aeruginosa*) bacterial strains and *Candida albicans* fungus strain. The zone of inhibition and minimum inhibitory concentration results are presented in Table 2.

The results of the antimicrobial screening of the tested compounds revealed that **3f**, bearing chlorine, showed moderate antibacterial activity against *Staphylococcus aureus* only (MIC: 64 μg/mL). On the other hand, all the tested compounds exhibited significant activity against *B. subtilis* (MIC: 4-16 μg/mL, with a range of inhibition zones 12-20 mm) comparable with that of the reference compound ampicillin except **3a**. Compounds **3b** and **3f**, bearing nitro and chloro groups at the *para* position, were the most effective synthetic compounds, having lower MIC values compared to the other compounds. *B. subtilis* was used as a model organism as it belongs to the same group as pathogenic *Bacillus anthracis* etc. and is a gram-positive, aerobic, and spore-forming microorganism belonging to the genus *Bacillus*.[19] *B. subtilis* ATCC 6633 is used in EN 13704 as an obligatory test organism in the form of endospores.[20]

SI is commonly used to estimate the therapeutic window of a drug and to identify drug candidates for further studies. According to the literature,[21,22] candidates for new drugs must have a SI>10, with MIC values lower than 6.25 μg/mL and low cytotoxicity, as is indeed the case for compounds **3b-3f**. The synthesized compounds were evaluated for cytotoxicity in NIH/3T3 cells at concentrations ten times the MIC (Table 2).

The rest of the compounds showed no significant activity against the other microorganisms tested when compared to that of standard drugs at the same concentration as that of the test compounds.

*Prediction of the drug-likeness properties of **3a-g***

The *in silico* drug-likeness properties obtained by OSIRIS Property Explorer (http://www.openmolecules.org/

Table 2. ***In vitro*** **antimicrobial activity of the synthesized compounds 3a-g, MIC in μg mL^{-1} (zones of inhibition, mm)**

Compound	Gram-positive bacteria		Gram-negative bacteria		Fungus	SI* IC_{50}/MIC
	S. aureus	*B. subtilis*	*E. coli*	*P. aeruginosa*	*C. albicans*	
3a	256 (8)	256 (10)	512 (0)	256 (0)	512 (0)	1.28
3b	256 (9)	4 (20)	512 (0)	256 (0)	512 (0)	119.81
3c	128 (8)	8 (12)	512 (0)	512 (0)	256 (0)	39.63
3d	128 (9)	8 (18)	512 (0)	512 (0)	512 (0)	40.51
3e	128 (9)	8 (19)	512 (0)	512 (0)	512 (0)	96.72
3f	64 (0)	4 (17)	256 (0)	512 (0)	512 (0)	44.53
3g	256 (7)	16 (18)	256 (0)	512 (0)	512 (0)	41.84
Ampicillin	10	10	25	50	-	
Fluconazole	-	-	-	-	6.25	

*Evaluation for cytotoxicity in NIH/3T3 cells at concentrations up to ten times the MIC for *B. subtilis*. The activity/cytotoxicity criterion is SI>10, MIC: Minimum inhibitory concentration

Table 3. Drug-likeness calculations and Lipinski parameters of the compounds

Comp.	Mol. weight	cLogP[a]	cLogS[b]	TPSA[c]	%ABS[d]	HBA[e]	HBD[f]	nrotb[g]	nviol[h]	Drug-likeness[i]
3a	334.331	0.0263	-1.875	122.20	66.84	9	2	7	0	2.9626
3b	322.275	-0.5985	-1.993	138.92	61.07	10	1	7	0	2.3314
3c	333.337	1.854	-2.748	93.10	76.88	7	1	7	0	2.1639
3d	335.315	0.2361	-1.674	119.40	67.81	9	1	8	0	0.08249
3e	349.342	0.6424	-1.974	119.4	67.81	9	1	9	0	-1.3929
3f	325.751	1.273	-2.613	93.1	76.88	7	1	6	0	2.3696
3g	291.306	0.667	-1.877	93.1	76.88	7	1	6	0	2.3314
ODZ	219.627	-0.4663	-0.984	83.87	80.07	6	1	4	0	1.8208

[a] Octanol/water partition coefficient (in log), calculated lipophilicity; [b]water solubility in log (moles/L); [c]topological polar surface area; [d]absorbtion; [e]number of hydrogen bond acceptors; [f]number of hydrogen bond donors; [g]rotatable bond; [h]number of violations; [i]drug-likeness score, ODZ: Ornidazole

datawarrior/) are given in Table 3. Drug-likeness prediction evaluates the acceptability of derivatives as drug molecules based on Lipinski[23] rule of five. ABS% was calculated by %ABS=109-[0.345 × topological polar surface area (TPSA)] according to the method described by Zhao et al.[24] TPSA,[25] cLogP, number of rotatable bonds, and violations of Lipinski's rule of five were calculated using the online property calculation toolkit OSIRIS.

The rule of five is a set of defined parameters to predict if a chemical compound has promising or viable pharmacological or biological activity as a drug in oral administration. These parameters are: 1) The molecule should not contain more than 5 hydrogen bond donors, 2) And no more than 10 hydrogen bond acceptors, 3) The molecular weight should be lower than 500, 4) The value for cLogP should not be higher than 5) The parameters in the rule of five were fully covered for the set of our synthesized compounds. The values of log P ranged from -0.59 to 1.273 for all designed molecules, while the values of log S were between -1.674 and -2.748. More than 80% of the drugs on the market have an estimated S value greater than 4.[26,27] TPSA values are closely related to the hydrogen bonding potential of a compound; those around of 160 or more indicate poor intestinal absorption. Hence, these parameters suggest that the compounds are expected to exhibit good oral bioavailability and intestinal absorption.

Drug-likeness estimations have been used to minimize attrition in the process of drug discovery and refer to the similarity of compound properties to those of existing oral drugs. Generally, the drug-likeness scores of compounds were greater than that of ornidazole using a starting compound, except **3d** and **3e**.

CONCLUSION

A series of ether-linked imidazole compounds that are derivatives of ornidazole were synthesized, structurally identified, and tested for antimicrobial and antileukemic activity. All the synthesized molecules were achieved in good yields by following a simple method. The projected structures of synthesized compounds **3a-g** were well supported by the spectral characterization data using IR, ^{1}H-NMR, and ESI-MS.

As a result, all compounds showed a minor anticancer effect on the K562 leukemia cell line. In addition, they were found to be the most promising antimicrobial agents in the series due to their selective antimicrobial activity against *B. subtilis* with

MIC values of 4-8 µg/mL when compared with the reference agent, except **3a** and **3g**. The compounds with nitro and chloro substituents were the most active in the series against *B. subtilis*. We can surmise that the inhibition of spores of *B. subtilis* is related to their sporicidal activity.

In particular, all the compounds were nontoxic. This outcome indicated that the antileukemic and antimicrobial effects of the compounds were selective and they had good oral bioavailability and drug-likeness properties. Thus, we can conclude that these ether-linked imidazole derivatives could be an excellent starting point to design new anticancer and antibacterial agents.

Conflict of Interest: No conflict of interest was declared by the authors.

REFERENCES

1. Yan J, Liang X, Bai C, Zhou L, Li J, Wang K, Tang Y, Zhao L. NK-18, a promising antimicrobial peptide: anti-multidrug resistant leukemia cells and LPS neutralizing properties. Biochimie. 2018;147:143-152.
2. Papanicolas LE, Gordon DL, Wesselingh SL, Rogers GB. Not Just antibiotics: ıs cancer chemotherapy driving antimicrobial resistance? Trends Microbiol. 2018;26:393-400.
3. Bosso M, Ständker L, Kirchhoff F, Münch J. Exploiting the human peptidome for novel antimicrobial and anticancer agents. Bioorg Med Chem. 2018;26:2719-2726.
4. Rani N, Sharma A, Singh R. Imidazoles as Promising Scaffolds for Antibacterial Activity: A Review. Mini Rev Med Chem. 2013;13:1812-1835.
5. Ali I, Lone MN, Aboul-Enein HY. Imidazoles as potential anticancer agents. Medchemcomm. 2017;8:1742-1773.
6. Narasimhan B, Sharma D, Kumar P. Biological importance of imidazole nucleus in the new millennium. Med Chem Res. 2011;20:1119-1140.
7. Zhang L, Peng XM, Damu GL, Geng RX, Zhou CH. Comprehensive review in current developments of imidazole-based medicinal chemistry. Med Res Rev. 2014;34:340-437.
8. Moreno SN, Docampo R. Mechanism of toxicity of nitro compounds used in the chemotherapy of trichomoniasis. Environ Health Perspect. 1985;64:199-208.
9. Li Q, Xing J, Cheng H, Wang H, Wang J, Wang S, Zhou J, Zhang H. Design, synthesis, antibacterial evaluation and docking study of novel 2-hydroxy-3- (nitroimidazolyl) - propyl-derived quinolone. Chem Biol Drug Des. 2015;85:79-90.
10. Tao XX, Duan YT, Chen LW, Tang DJ, Yang MR, Wang PF, Xu C, Zhu HL. Design, synthesis and biological evaluation of pyrazolyl- nitroimidazole derivatives as potential EGFR / HER-2 kinase inhibitors. Bioorg Med Chem Lett. 2016;26:677-683.
11. Makawana JA, Sun J, Zhu HL. Schiff 's base derivatives bearing nitroimidazole moiety: New class of antibacterial, anticancer agents and potential EGFR tyrosine kinase inhibitors. Bioorg Med Chem Lett. 2013;23:6264-6268.
12. Sun J, Li DD, Li JR, Fang F, Du QR, Qian Y, Zhu HL. Design, synthesis, biological evaluation, and molecular modeling study of 4-alkoxyquinazoline derivatives as potential VEGFR2 kinase inhibitors. Org Biomol Chem. 2013;11:7676-7686.
13. Nagarapu L, Gaikwad HK, Sarikonda K, Mateti J, Bantu R, Raghu PS, Manda KM, Kalvendi SV. Synthesis and cytotoxicity evaluation of 1-[3-(9H-carbazol-4-yloxy)-2-hydroxypropyl]-3-aryl-1H-pyrazole-5-carboxylic acid derivatives. Eur J Med Chem. 2010;45:4720-4725.
14. Sunjic V, Kolbah D, Kajfez F, Blazevic N. 1-Imidazolyl derivatives of 2-hydroxy-3-phenoxypropane. J Med Chem. 1968;11:1264-1265.
15. Kalaycı S, Demirci S, Sahin F. Determination of antimicrobial properties of Picaridin and DEET against a broad range of microorganisms. World J Microbiol Biotechnol. 2014;30:407-411.
16. Kalaycı S, Demirci S, Fikrettin Ş. Antimicrobial properties of various psychotropic drugs against broad range microorganisms. Current Psychopharmacology. 2014;3:195-202.
17. Grever MR, Schepartz SA, Chabner BA. The National Cancer Institute: Cancer drug discovery and development program. Semin Oncol. 1992;19:622-638.
18. Boyd MR, Paul KD. Some practical considerations and applications of the national cancer institute in vitro anticancer drug discovery screen. Drug Dev Res. 2018;34:91-109.
19. Mckenney PT, Driks A, Eichenberger P. The Bacillus subtilis endospore: assembly and functions of the multilayered coat. Nat Rev Microbiol. 2013;11:33-44.
20. BS EN 13704:2002. Chemical disinfectants. Quantitative suspension test for the evaluation of sporicidal activity of chemical disinfectants used in food, industrial, domestic and institutional areas. Test method and requirements. (phase 2, step 1).
21. Orme I; Tuberculosis Drug Screening Program. Search for new drugs for treatment of tuberculosis. Antimicrob Agents Chemother. 2001;45:1943-1946.
22. Pavan FR, da S Maia PI, Leite SR, Deflon VM, Batista AA, Sato DN, Franzblau SG, Leite CQ. Thiosemicarbazones, semicarbazones, dithiocarbazates and hydrazide/hydrazones: anti-mycobacterium tuberculosis activity and cytotoxicity. Eur J Med Chem. 2010;45:1898-1905
23. Lipinski CA, Lombardo F, Dominy BW, Feeney PJ. Experimental and computational approaches to estimate solubility and permeability in drug discovery and development settings. Adv Drug Deliv Rev. 2001;46:3-26.
24. Zhao YH, Abraham MH, Le J, Hersey A, Luscombe CN, Beck G, Sherborne B, Cooper I. Rate-Limited steps of human oral absorption and QSAR studies. Pharm Res. 2002;19:1446-1457.
25. Ertl P, Rohde B, Selzer P. Fast calculation of molecular polar surface area as a sum of fragment-based contributions and its application to the prediction of drug transport properties. J Med Chem. 2000;43:3714-3717.
26. Parvez A, Meshram J, Tiwari V, Sheik J, Dongre R, Youssoufi MH, Ben Hadda T. Pharmacophores modeling in terms of prediction of theoretical physico-chemical properties and verification by experimental correlations of novel coumarin derivatives produced via Betti 's protocol. Eur J Med Chem. 2010;45:4370-4378.
27. Uddin N, Sirajuddin M, Uddin N, Tariq M, Ullah H, Ali S, Tirmizi SA, Khan AR. Synthesis, spectroscopic characterization, biological screenings, DNA binding study and POM analyses of transition metal carboxylates. Spectrochim Acta A Mol Biomol Spectrosc. 2015;140:563-574.

N-{4-[2-Hydroxy-3-(2-methyl-5-nitro-1*H*-imidazol-1-yl)propoxy]phenyl}acetamide (3a)

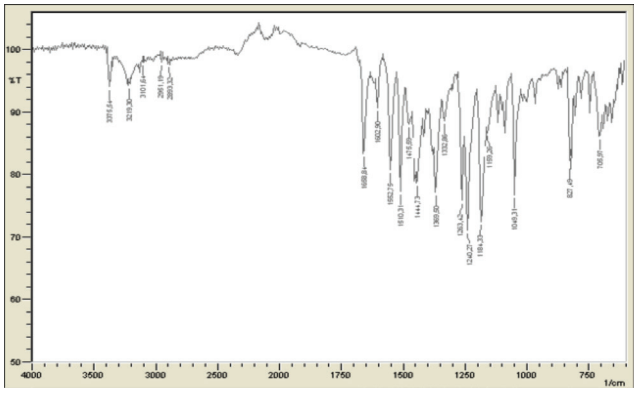

Figure S1. IR spectrum for compound 3a

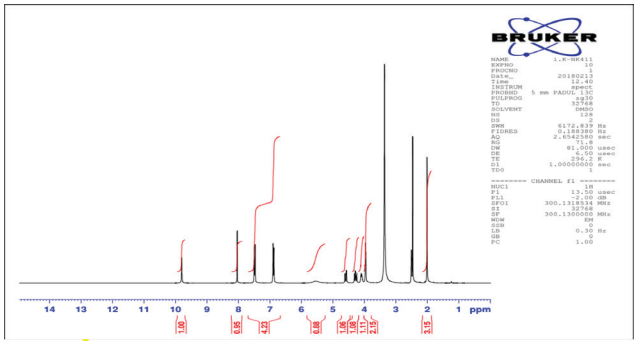

Figure S2. ^{1}H-NMR spectrum for compound 3a

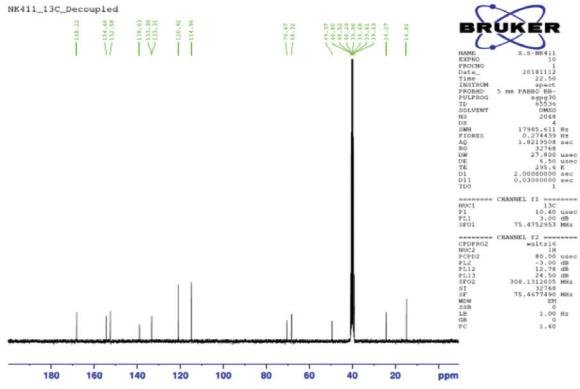

Figure S3. ^{13}C-NMR spectrum for compound 3a

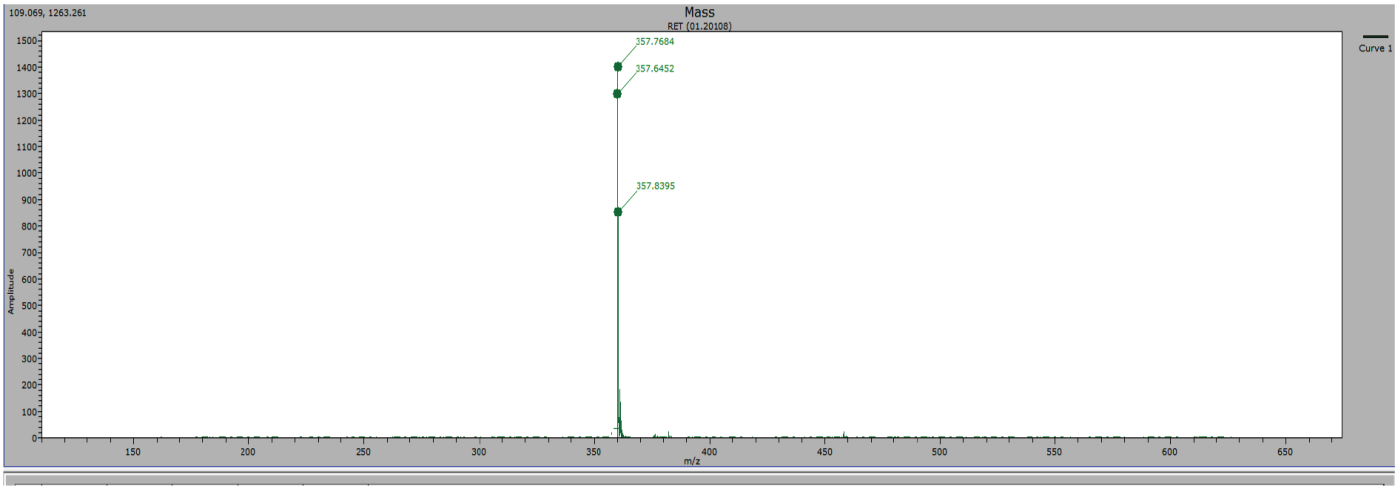

Figure S4. MS spectrum for compound 3a

1-(2-Methyl-5-nitro-1*H*-imidazol-1-yl)-3-(4-nitrophenoxy)propan-2-ol (3b)

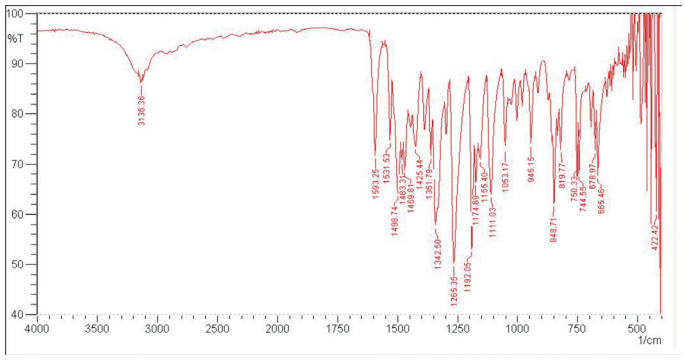

Figure S5. IR spectrum for compound 3b

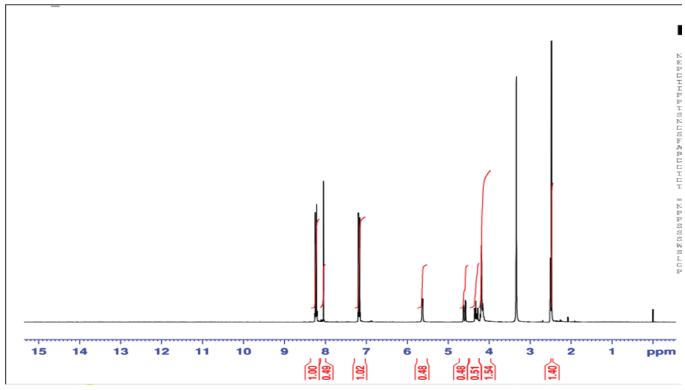

Figure S6. [1]H-NMR spectrum for compound 3b

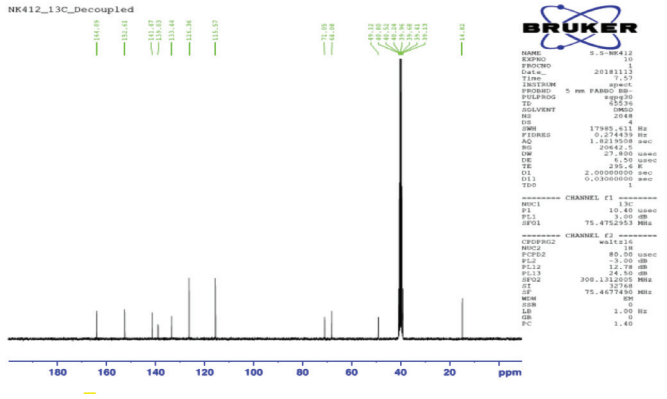

Figure S7. [13]C-NMR spectrum for compound 3b

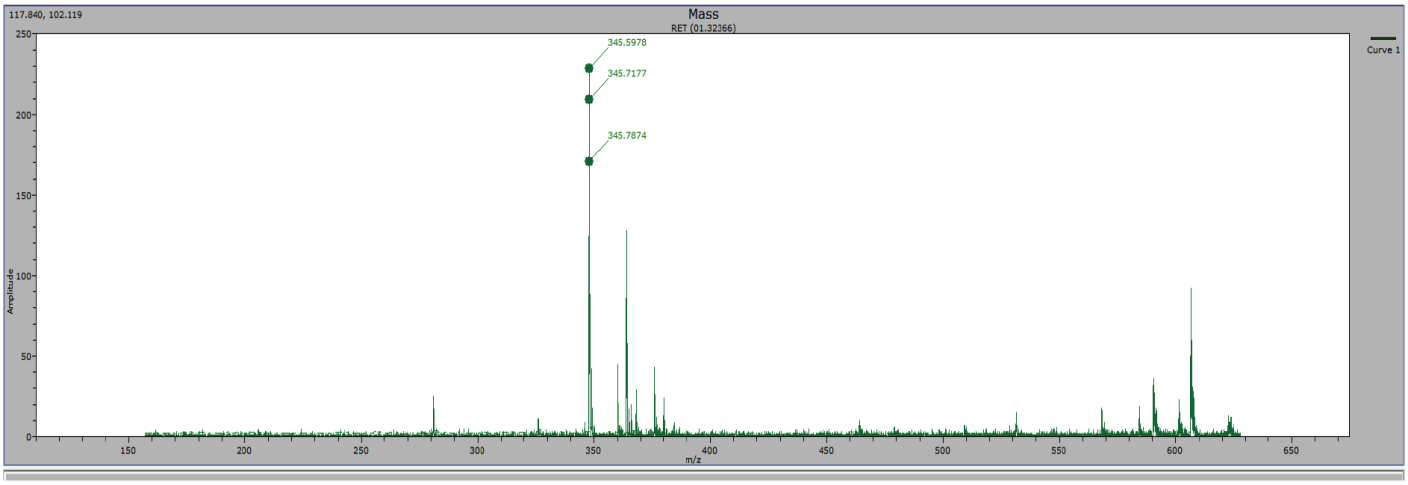

Figure S8. MS spectrum for compound 3b

1-(2-Methyl-5-nitro-1*H*-imidazol-1-yl)-3-[5-methyl-2-(propan-2-yl)phenoxy]propan-2-ol (3c)

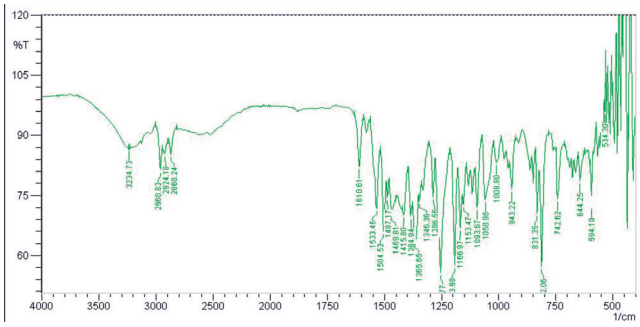

Figure S9. IR spectrum for compound 3c

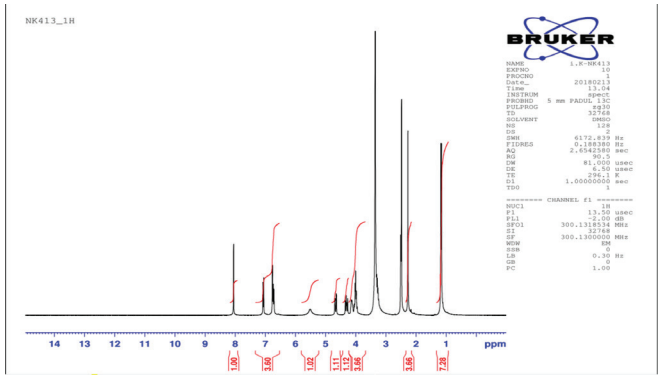

Figure S10. [1]H-NMR spectrum for compound 3c

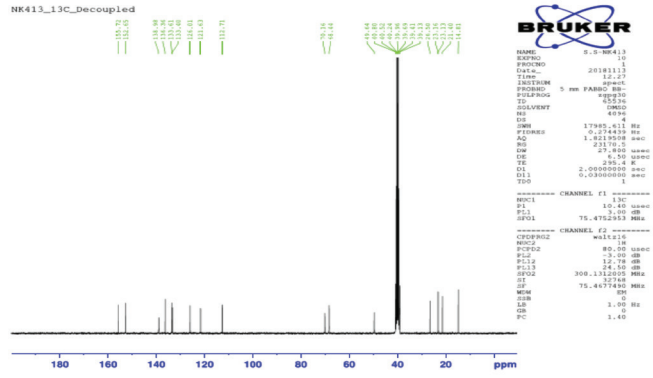

Figure S11. [13]C-NMR spectrum for compound 3c

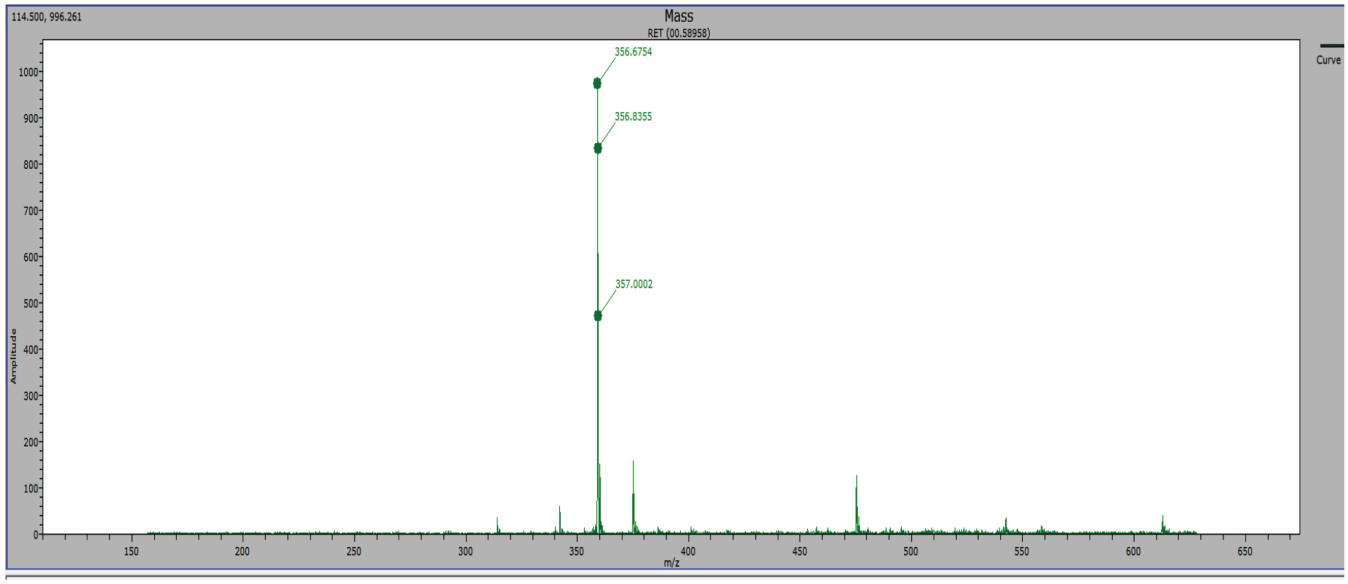

Figure S12. MS spectrum for compound 3c

Methyl 4-[2-hydroxy-3-(2-methyl-5-nitro-1*H*-imidazol-1-yl)propoxy]benzoate (3d)

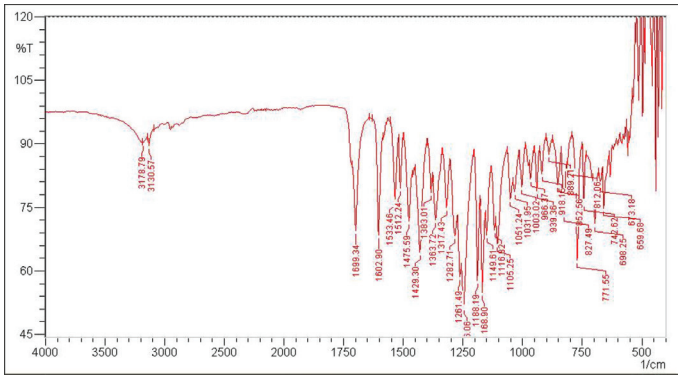

Figure S13. IR spectrum for compound 3d

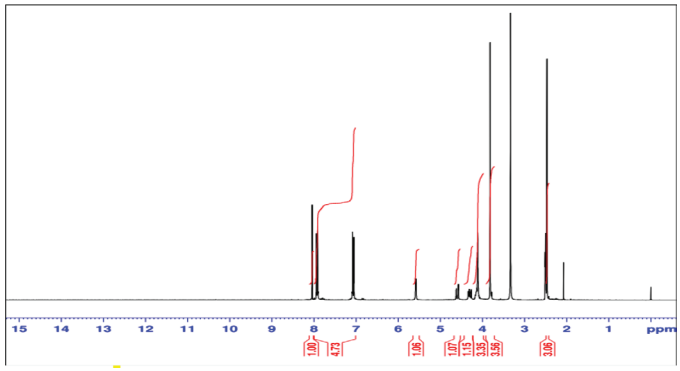

Figure S14. ^{1}H-NMR spectrum for compound 3d

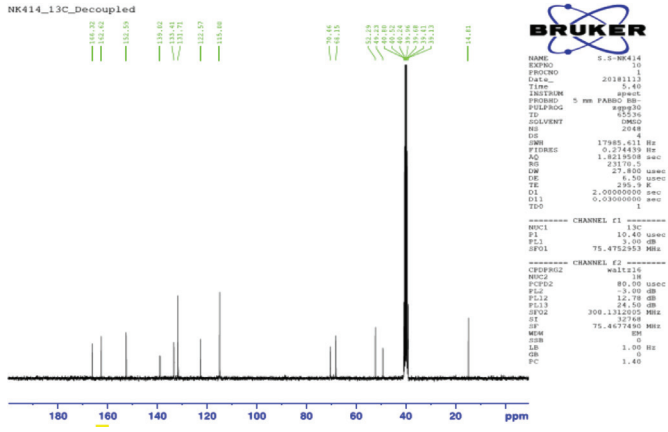

Figure S15. ^{13}C-NMR spectrum for compound 3d

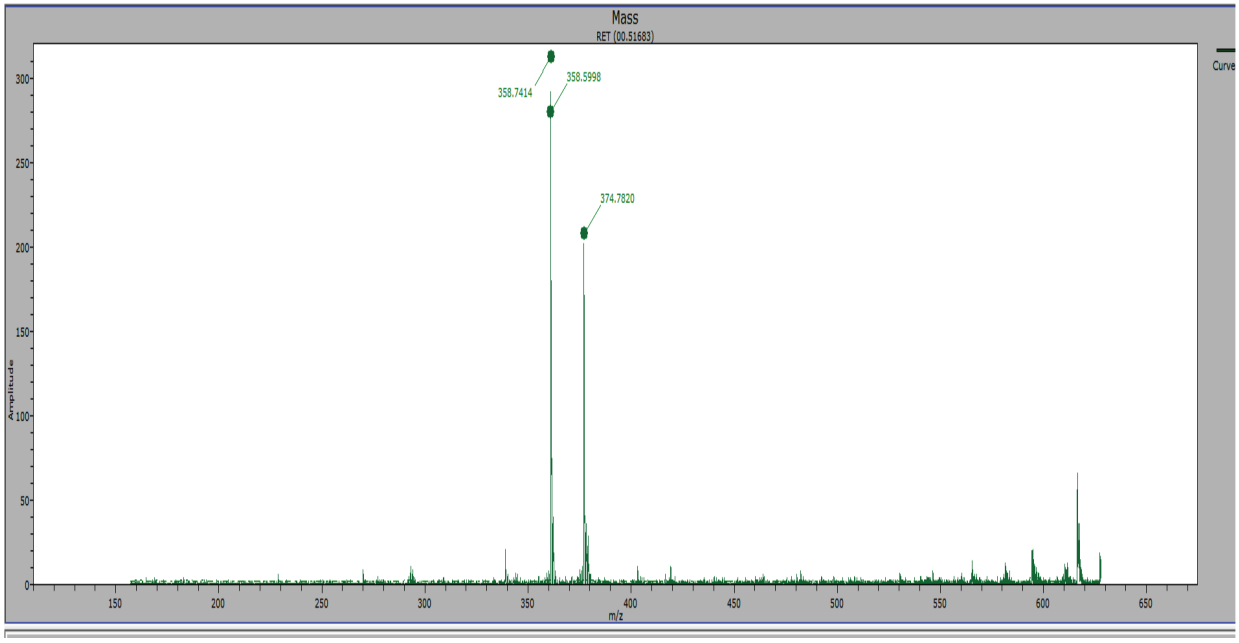

Figure S16. MS spectrum for compound 3d

Ethyl 4-[2-hydroxy-3-(2-methyl-5-nitro-1*H*-imidazol-1-yl)propoxy]benzoate (3e)

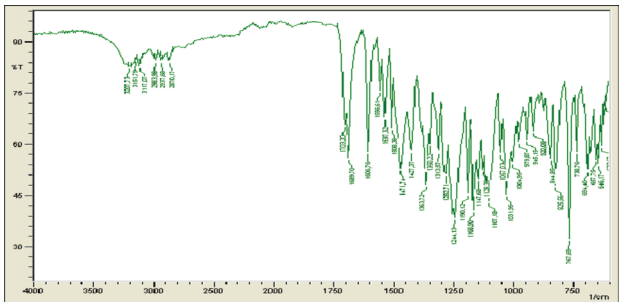

Figure S17. IR spectrum for compound 3e

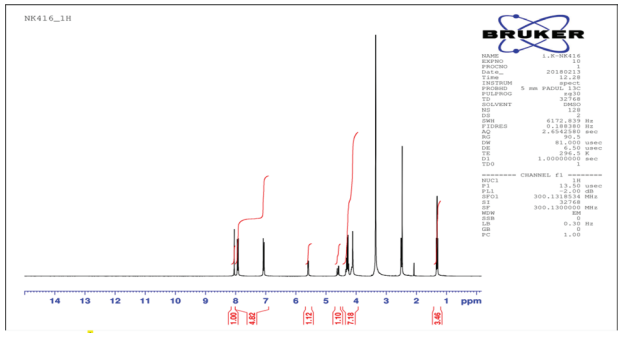

Figure S18. ^{1}H-NMR spectrum for compound 3e

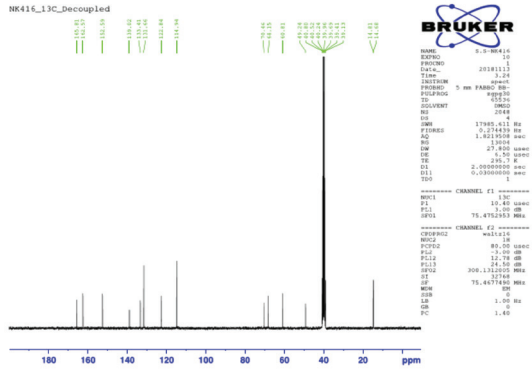

Figure S19. ^{13}C-NMR spectrum for compound 3e

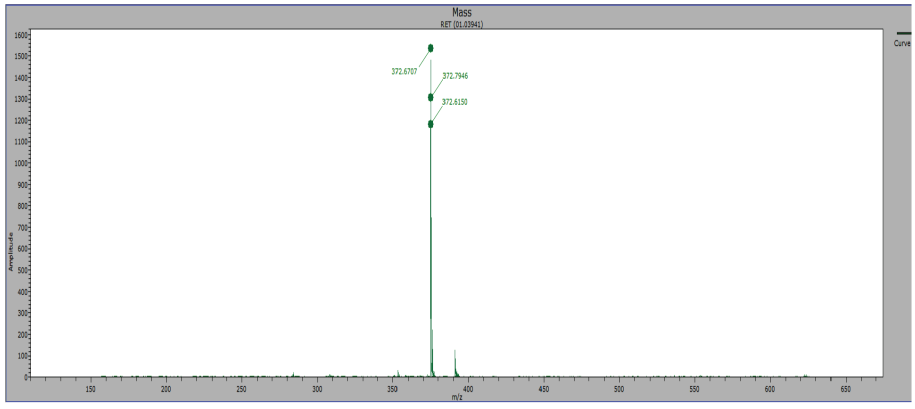

Figure S20. MS spectrum for compound 3e

1-(4-Chloro-3-methylphenoxy)-3-(2-methyl-5-nitro-1*H*-imidazol-1-yl)propan-2-ol (3f)

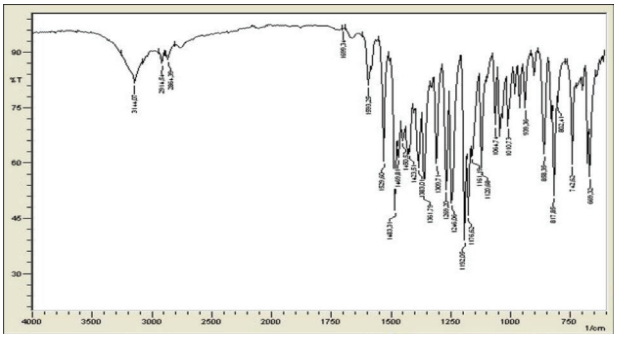

Figure S21. IR spectrum for compound 3f

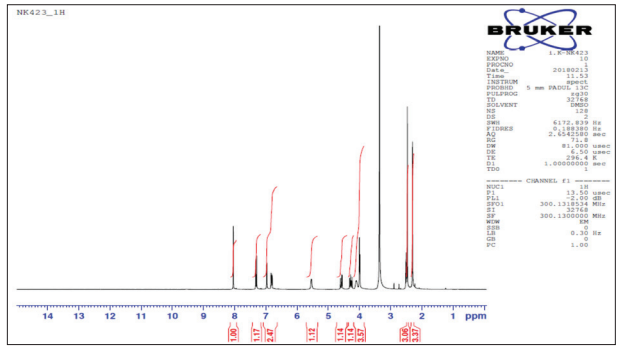

Figure S22. ^{1}H-NMR spectrum for compound 3f

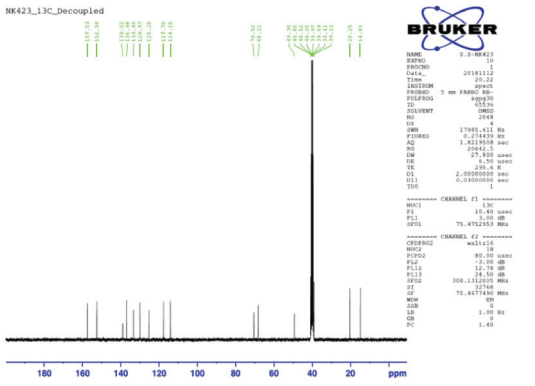

Figure S23. ^{13}C-NMR spectrum for compound 3f

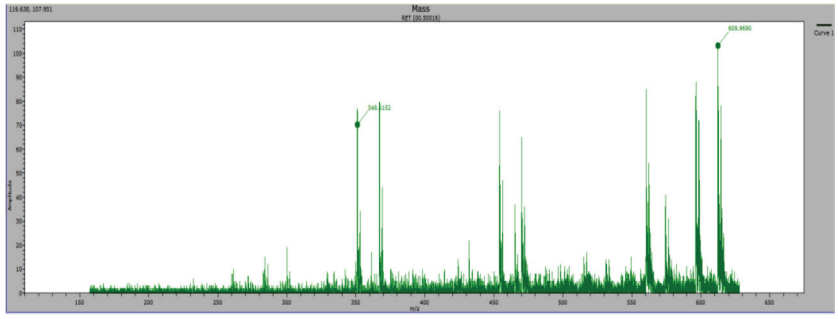

Figure S24. MS spectrum for compound 3f

1-(2-Methyl-5-nitro-1*H*-imidazol-1-yl)-3-(3-methylphenoxy)propan-2-ol (3g)

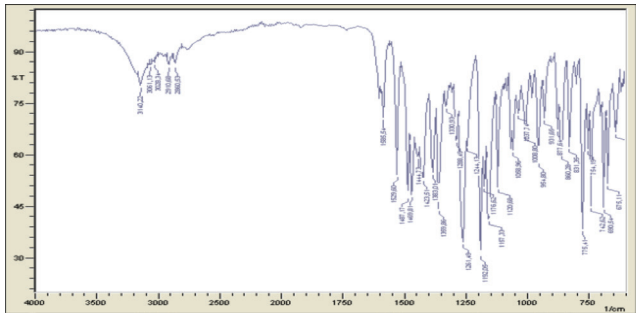

Figure S25. IR spectrum for compound 3g

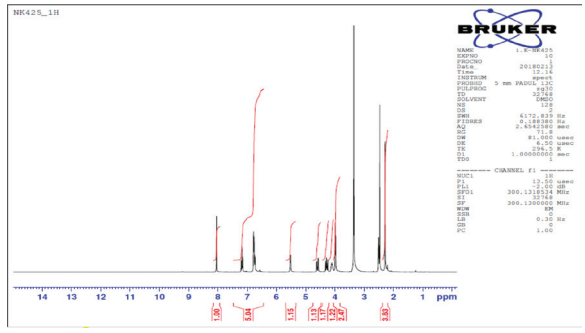

Figure S26. 1H-NMR spectrum for compound 3g

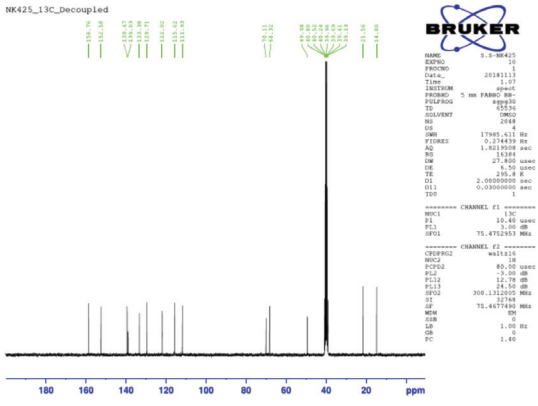

Figure S27. 13C-NMR spectrum for compound 3g

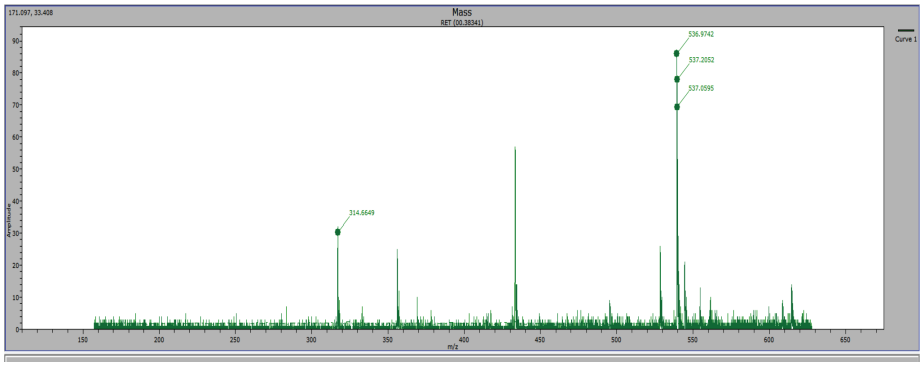

Figure S28. MS spectrum for compound 3g

Turk J Pharm Sci 2020;17(1):94-8
DOI: 10.4274/tjps.galenos.2018.53386

ORIGINAL ARTICLE

Local Use of Apisan Gel, A New Oral Care Product in the Treatment of Experimental Periodontitis Against the Background of Hyperacid Gastritis and Intoxication with Tobacco Smoke

Hiperasit Gastrit ve Tütün ile Zehirlenmeye Karşı Deneysel Periodontitis Tedavisinde Yeni Bir Ağız Bakım Ürünü, Apisan Jelinin Lokal Kullanımı

Lyudmila KRAVCHENKO[1]*, Irina BORISYUK[2], Natali FIZOR[2], Liana UNHURIAN[2], Elena ZOLOTUKHINA[1], Olga GONCHARENKO[1]

[1]Odessa National Medical University, Faculty of Dentistry, Department of Therapeutic Dentistry, Odessa, Ukraine
[2]Odessa National Medical University, Faculty of Pharmacy, Department of Organization and Economics of Pharmacy, Odessa, Ukraine

ABSTRACT

Objectives: The aim of the work was to substantiate the use of a newly created oral care product in the treatment of periodontal disease reconstructed against the background of hyperacidic gastritis under the conditions of tobacco smoke intoxication.

Materials and Methods: The study was conducted in 2 stages. In the first stage, all experimental animals were divided into 4 groups: 1) intact, 2) with simulated periodontitis, 3) with reproduced periodontitis against the background of reproduced hyperacidic gastritis, 4) with reproduced periodontitis against the background of hyperacid gastritis under the conditions of tobacco smoking. Biochemical studies of gum homogenate with periodontitis in rats were conducted to determine the impact of stomach pathology and tobacco smoke as endogenous and exogenous risk factors. In stage 2, the effectiveness of local therapy with the use of the newly created oral care product and a comparator was studied in rats with reproduced periodontitis against the background of hyperacidic gastritis under the conditions of smoking.

Results: In the experimental periodontitis against the background of hyperacidic gastritis under the conditions of tobacco smoking, there were significant changes in the periodontal tissues characteristic of the inflammatory process: the activity of peroxide oxidation of lipid (POL) increased, activity of the antioxidant system decreased, and inflammatory markers increased when nonspecific protection was reduced. Local therapy in the rats using the new "Apisan" gel resulted in the correction of certain metabolic disorders, faster elimination of the harmful effects of the damaging factors, and restoration of the condition of periodontal tissues compared with the use of the comparator, the Asepta gel.

Conclusion: The therapeutic effectiveness of the new Apisan gel is due to the normalizing effect on the processes of POL, and inflammation and activation of the oral cavity protective systems during inflammatory periodontal disease occurring against the background of a concomitant stomach pathology, hyperacidic gastritis.

Key words: Apigel, periodontitis, hyperacidic gastritis, tobacco smoking, inflammation

ÖZ

Amaç: Çalışmanın amacı, tütün dumanı intoksikasyonu koşullarında hiperasidik gastritin zemininde oluşan periodontal hastalığın tedavisinde yeni oluşturulan ağız bakım ürününün kullanımını gerçekleştirmektir.

Gereç ve Yöntemler: Çalışma 2 aşamada gerçekleştirilmiştir. İlk aşamada, tüm deney hayvanları 4 gruba ayrılmıştır: 1) bozulmamış, 2) simüle edilmiş periodontitis ile, 3) çoğaltılmış hiperasidik gastritin zemininde oluşturulan periodontitis ile, 4) tütün içme koşulları. Endojen ve eksojen risk faktörleri olarak mide patolojisi ve tütün dumanının etkisini belirlemek için periodontitisli sıçanlarda sakız homojenatının biyokimyasal çalışmaları yapılmıştır. ikinci aşamada, sigara içme koşulları altında hiperasidik gastrit zemininde oluşturulan periodontitisli sıçanlarda yeni oluşturulan ağız bakım ürünü ve karşılaştırıcı kullanımı ile lokal tedavinin etkinliği incelenmiştir.

Bulgular: Tütün içme koşulları altında hiperasidik gastrit zeminine karşı oluşan deneysel periodontitiste, enflamatuvar sürecin karakteristiği olan periodontal dokularda önemli değişiklikler vardı: lipit peroksit oksidasyonu (POL) aktivitesi artmış ve antioksidan sistemin aktivitesi azalmış spesifik

*Correspondence: E-mail: lianau@ukr.net, Phone: +38 (048) 723-35-67 ORCID-ID: orcid.org/0000-0001-5391-9676
Received: 10.10.2018, Accepted: 15.11.2018

olmayan koruma azaltıldığında enflamatuvar belirteçler artmıştır. Sıçanlarda yeni "Apisan" jeli kullanılarak lokal terapi, belirli metabolik bozuklukların düzeltilmesi, zarar verici faktörlerin zararlı etkilerinin daha hızlı ortadan kaldırılması ve karşılaştırıcının Asepta jelinin kullanımından daha çok periodontal dokuların durumunun yenilenmesi ile sonuçlanmıştır.

Sonuç: Yeni Apisan jelinin terapötik etkinliği, POL süreçleri, mide patolojilerinin zemininde hiperasidik gastrite eşlik eden enflamatuvar periodontal hastalık sürecinde oral kavite koruyucu sistemlerin iltihaplanması ve aktivasyonu üzerindeki normalleştirici etkiden kaynaklanmaktadır.

Anahtar kelimeler: Apigel, periodontitis, hiperasidik gastrit, tütün içme, enflamasyon

INTRODUCTION

Changes in the tissues of the oral cavity with manifestations of inflammation are often associated with diseases of the gastrointestinal tract (GIT), due to the morphofunctional unity of the digestive apparatus. There are ulcerative lesions, erosion, and aphthae of the oral cavity mucosa (OCM) in the pathology of the GIT due to trophic disorders. The presence of harmful habits, especially smoking, in patients with concomitant diseases of the GIT further enhances the severity of the inflammatory symptoms in the oral cavity. Dental deposit of smokers is a major provocative factor in the development of gum diseases and caries.[1,2]

In inflammatory diseases of the oral cavity, gastritis, among the concomitant GIT pathologies, makes up more than 70% of cases, the form and duration of which affect the functional state of the OCM. Changes in the oral cavity during chronic gastritis depend on the secretion and acid forming function of the stomach. Increased acidity in the stomach is accompanied by hypersalivation, pallor, edema and gingival inflammation, bleeding, decreased capillary stability, and reactivity of the OCM.[3] By weakening the immune defense of the body, the concomitant GIT diseases create conditions for the affecting influence on the OCM and periodontium by the microflora present in the oral cavity and the endogenous periodontal pathogenic factors. In addition, current data suggest a negative impact of *Helicobacter pylori* infection[4] and tobacco smoking[5] on the incidence of OCM and periodontium diseases.

The mechanisms underlying the influence of changes in the GIT on the pathobiochemical reactions of the inflammatory process in the periodontal tissues and OCM and the possibility of treating such a combined pathology, taking into account the harmful habit of tobacco smoking, require a specific study. Therefore, we consider it relevant and promising for dentistry to search for and study the effectiveness of new means of local therapy of the OCM and periodontal diseases as a concomitant pathology of hyperacidic gastritis under the conditions of tobacco smoking.

The aim of the present work was to substantiate the local application of a newly created oral care product in the treatment of periodontal disease reconstructed against the background of hyperacidic gastritis under the condition of intoxication with tobacco smoke.

MATERIALS AND METHODS

The study was conducted on 72 male wistar rats, 1-1.5 months of age, weighing 180-220 g, which were in the vivarium of Odessa National Medical University on a standard feed for laboratory rats. According to the tasks of the experiment, the study was conducted in 2 stages. In the first stage the rats were divided into 4 groups (10 animals in each). The first group consisted of intact rats (control). In the second group of rats periodontitis was modeled. The third group consisted of rats in which, after reproduction of hyperacidic gastritis, periodontitis was modeled. The fourth group included rats in which, against the background of reproduced hyperacidic gastritis, periodontitis was modeled under the condition of tobacco smoke dosing. After conducting the first series of the experiment to determine the effect of concomitant stomach and tobacco smoke on metabolic disorders in the tissues of the oral cavity of rats upon reproduction of periodontitis, the effectiveness of local treatment with the use of the newly created drug was studied on the basis of apiproducts and other biologically active substances with anti-inflammatory, antimicrobial, and antioxidant effects[6] and a comparator preparation, aseptic gel. The experimental animals were also divided into 4 groups: 1) intact (control); 2) rats with a reproduced model of periodontitis against the background of hyperacidic gastritis under the conditions of exposure to tobacco smoke; 3) the main one, which included newly treated rats with periodontal disease reproduced against the background of hyperacidic gastritis under the conditions of intoxication with tobacco smoke; 4) a comparison group, which included rats with a periodontitis model in groups 2 and 3 receiving local treatment with Asepta gel.

The gastroduodenal zone in the rats was affected by the addition of ammonium acetate 2 g/L to drinking water for 10 days and then 0.4 mg of *Helicobacter pylori* suspension 5×10^8 KU/mL given per os twice daily for 7 days in 3 days.[7,8] Hyperacidic gastritis was reproduced by the introduction of a single 5% solution of acetic acid at 4 mL/kg of mass through a probe 5 days before the trial. For control intragastric pH-metry was conducted under intraperitoneal anesthesia using sodium thiopental at a dose of 20 mg/kg of the rat's mass by insertion of a glass electrode (EL-40) into the cavity of the stomach during supramedial laparotomy using a pH meter (pH-340). The level of basal acidity in the simulation of hyperacidic gastritis was 1.80-2.00.

In the rats in groups 3 and 4 after the reproduction of hyperacidic gastritis and in group 2 on the first day of the experiment in the first series of experiments under thiopental anesthesia (20 mg/kg) periodontitis was modeled by applying a ligature to the central incisor. The essence of the model consists of the formation of a retention point for the dental plaque, which initiates the development of inflammation and destruction of the periodontal tissues.[9] In the rats in group 4 in the first series of the experiment and in groups 2, 3, and 4 of the second series

the conditions for tobacco smoking were created by exposure to the effect of tobacco smoke.

To reproduce the conditions of tobacco smoking, a plastic hermetic chamber of 28 L with three different sections was used, to which tobacco smoke from 15 cigarettes (primma red with a content of 1.0 mg of nicotine and 10 mg of resin in 1 cigarette) was introduced inside by pressure of the engine, through the holes for 30 min, daily, for 15 days. At the same time, there were 7 animals in the chamber. During cigarette smoking, the behavioral reactions of the rats were observed: initially, the supply of tobacco smoke to the chamber made the rats anxious, looking for a place to breathe normally, and in 10 min they calmed down and fell asleep. After finishing the inhalation of tobacco smoke and supply of fresh air, the rats became active, began to breathe frequently, and 15 min later they returned to normal.

The animals were removed from the experiment in several stages. Euthanasia of rats in groups 1, 2, 3, and 4 of the first series was performed immediately after the last procedure of inhalation of tobacco smoke (on day 15) under thiopental anesthesia (20 mg/kg) by total bloodletting from the heart. All animals treated after reproduced periodontitis against the background of hyperacidic gastritis under tobacco-smoking conditions were slaughtered 8 or 14 days after the beginning of treatment.

A tissue sample of the gum for biochemical studies was taken. In the supernatant fluid of the gum homogenates the final level of the peroxide oxidation of lipid (POL) malondialdehyde (MDA) by the thiobarbituric method was determined[10] and the antioxidant protection (AOP) status was assessed by activity of catalase[11] as well as inflammation level by elastase activity[12] and nonspecific activity protection index lysozyme.[13] The antioxidant-prooxidant index of API was calculated by the ratio of catalase activity to MDA concentration.

During the study, the procedures used adhered to the general principles of animal experiments approved at the National Congress on Bioethics (Kyiv, Ukraine, 2001) and were in accordance with the provisions of the European Convention for the Protection of Vertebrate Animals used for experimental and other scientific purposes (Strasbourg, France, 1985). The statistical processing of the data was carried out using the program "Statistica 6.0" using Students t-criterion. The changes were considered to be significant at $p<0.05$.

RESULTS AND DISCUSSION

The experimental animals had an intact mucous membrane of the gum before the reproduction of pathological conditions, with no apparent pathological changes; gum bleeding was not found on probing. There were manifestations of the clinical symptoms of periodontal tissue inflammation, namely hyperemia, edema, and bleeding of the gum in the area of the incisors in all rats after ligature-induced periodontitis on day 3. On day 5, inflammation was seen in the area of the molars, that is, there was a generalization of the inflammatory process in the periodontal tissues. The animals in which hyperacidic gastritis was reproduced became weak, ate little, and showed inflammatory symptoms of OCM in their oral cavity: hyperemia and edema. After modeling periodontal disease in these animals there was an explicit picture of inflammation in the gums in the form of edema and hyperemia of the marginal region and gingivitis on day 2. There were metabolic changes in the periodontal tissues of the rats, as evidenced by the biochemical parameters of the gum biopsy in the rats in groups 2 and 3 compared to intact animals. The analysis of changes in the biochemical markers of inflammation in the gum tissues of animals determined the most significant deviations in the rats with periodontitis against the background of hyperacidic gastritis under the conditions of intoxication with tobacco smoke (group 4).

Taking into account that one of the main factors that trigger the inflammatory processes is the activation of free radical lipid oxidation, the prooxidant system has been studied for the level of MDA and the activity of AOP in the activity of catalase. Modeling of periodontitis led to an increase in the content of MDA in the gum tissues, which pointed to intensification of POL with decreased activity of AOP (catalase activity decreased) in the periodontal tissues. Even more significant similar changes occurred in the gum biopsy of the animals, in which periodontitis was reproduced against the background of hyperacidic gastritis. The most expressed metabolic disorders in the tissues of the oral cavity were found in group 4 of rats, in which periodontitis was simulated against the background of hyperacidic gastritis under the conditions of smoking, when the combination of the influences of two affecting factors, especially in the system of POL/AOP, was observed. The process of POL activation as the main factor of cell membrane damage due to the action of an excessive stimulus was realized in all tissues, including the mucous membranes of the digestive system. In the tissues of rats, there is a system for counteracting damage and activation of POL; such a counteracting factor is AOP, in particular, the enzyme catalase. The activity of catalase was reduced as a result of its consumption during active participation in the processes of decontamination of the POL products. In group 4, the animals showed the lowest activity of catalase in the gum (4.96±0.39 mcat/kg) and the highest level of MDA (19.70±1.30 μmol/kg), which exceeded this index 2.3 times in the intact animals ($p<0.05$) and 1.3 times in rats in group 2 with periodontitis (Table 1).

Elastic activity, which characterizes the development of inflammation in the gum during reproduction of periodontitis, was most increased under the conditions of combined stomach pathology and the action of tobacco smoke, which indicated high activity of neutrophils that in large numbers infiltrated the periodontal tissues during the development of inflammation.

In the tissues of rats with periodontitis against the background of hyperacidic gastritis, which was influenced by tobacco smoke, elastase activity was 1.35 times higher than that in intact animals ($p<0.05$) without intoxication with tobacco smoke; the studied index increased by 25% less ($p<0.05$). Concomitant hyperacid gastritis significantly influenced the degree of metabolic disorders of the oral cavity tissues in animals with induced inflammation of the periodontal tissues, enhancing the

manifestations of oxidative stress, suppressing the functional state of the system of antioxidant protection, and causing damage to biological membranes, and structural and functional changes in the gum mucosa with elements of inflammation. Elastase activity in the gum tissues was increased 1.26 times in rats with periodontitis against the background of hyperacid gastritis compared to intact ones, exceeding values in the rats without combined pathology. At the same time, there was a decrease in the local resistance of the tissues of the oral cavity in groups 3 and 4, which was evidenced by 36.3% and 44.3% less lysozyme activity in the gum homogenates compared with intact animals. It is known that lysozyme has a local anti-inflammatory and immunomodulating effect: it inhibits the chemotaxis of neutrophils and the production of toxic oxygen radicals.[14] Reduction in the activity of lysozyme may be the cause of maintaining a local inflammatory process.

The application of a new mucosal apigel Apisan in the local therapy of periodontal disease reconstructed against the background of hyperacidic gastritis under the conditions of intoxication with tobacco smoke contributed to the reduction in the influence of the affecting factors on the animal oral cavity and the restoration of the tissue condition. During the examination of the oral cavity, much less damage to the mucosa was detected, namely swelling and redness of the gums decreased. After local use of the Apisan gel, the condition of the periodontal tissues improved within 5 days of the beginning of treatment, and with application of the comparator (the Asepta gel) in only 10 days. The results of the biochemical studies showed that the newly created drug significantly reduced the markers of inflammation in the gum tissue. Their parameters in the substrate that was studied in the animals in which the new gel was applied to the areas with induced periodontitis had lower values compared with the data of the comparison group. On day 8 after treatment with the new gel, most animals (86%) were found to have normalization of the antioxidant-prooxidant system, markers of inflammation in the gum tissues.

During the application of the Asepta gel a positive effect was determined in only 38% of rats on day 8 after the beginning of application, and metabolic disturbances, which were eliminated mainly at the end of the observation, were recorded in the remaining animals (62%). In the course of a comprehensive study it was found that the Apisan gel gave a more pronounced therapeutic effect than the Asepta gel, characterized by an improvement in the biochemical indices of the rat periodontal tissues (Table 2).

Thus, summing up the results of experimental studies, it is possible to state that rats during the reproduction of periodontitis against the background of hyperacidic gastritis under the conditions of intoxication with tobacco smoke had increased activity of the prooxidant system and decreased activity of the antioxidant system, and elastase activity increased in decreasing nonspecific protection in the periodontal tissues, indicating the development of the inflammatory process. The application of the newly created Apisan apigel for application in periodontal disease in rats against the background of hyperacidic gastritis after intoxication with tobacco smoke significantly reduced the processes of inflammation in the periodontal tissues, affecting the normalization of the POL processes, inflammation, and activation of the protective systems of the oral cavity.

CONCLUSION

1. In experimental periodontitis against the background of hyperacidic gastritis under the conditions of intoxication with tobacco smoke, changes in the periodontal tissue are characteristic of the inflammatory process: the activity of lipid peroxidation increases and the activity of the antioxidant system decreases, and the markers of inflammation increase in decreasing nonspecific protection.

2. Local therapy of periodontal disease reconstructed against the background of hyperacidic gastritis with the effect of tobacco smoke in rats using the newly created apigel Apisan

Table 1. Changes in biochemical parameters in the gum tissues in the rats in which periodontitis was reproduced against the background of hyperacid gastritis

Group of animals	Contents of MDA µmol/kg	Elastase µcat/kg	Catalase mcat/kg	Lysozyme µ/kg	API
Intact (control), n=10	8.42±0.34	34.0±2.00	7.18±0.33	276±24	8.52±0.32
Periodontitis, n=10	14.70±0.62	40.0±3.00	6.74±0.41	188±14	4.58±0.52
p	<0.05	>0.05	>0.05	<0.05	<0.05
Hyperacidic gastritis+periodontitis, n=10	17.80±1.20	43.0±3.00	5.86±0.48	176±22	3.29±0.84
p					
p_1	<0.05	<0.05	<0.05	<0.05	<0.05
	<0.05	>0.05	>0.05	>0.05	>0.05
Hyperacidic gastritis+periodontitis+tobacco smoke, n=10	19.70±1.30	46.0±4.00	4.96±0.39	154±22	2.52±0.60
p	<0.05	<0.05	<0.05	<0.05	<0.05
p_1	<0.05	>0.05	<0.05	>0.05	<0.05
p_2	>0.05	>0.05	>0.05	>0.05	>0.05

p: Probability relative to the control group, p_1: Probability of the periodontitis group, p_2: Probability of differences between groups 3 and 4, MDA: Malondialdehyde

Table 2. Correction of metabolic disorders in the periodontal tissues of rats in the local treatment of reconstructed periodontitis against the background of hyperacidic gastritis (M ± t)

Group of animals	Contents of MDA μmol/kg	Elastase μcat/kg	Catalase mcat/kg	Activity Lysozyme μ/kg	API
Intact (control) n=10	8.42±0.34	34.0±2.0	7.18±0.33	276±24	8.52±0.32
Hyperacidic gastritis+periodontitis+tobacco smoke, n=10	19.7±1.30	46.0±4.0	4.96±0.39	154±34	2.52±0.80
p	<0.05	<0.05	<0.05	<0.05	<0.05
The main group, n=10	9.87±0.48	37.0±2.0	6.88±0.58	218±28	7.07±0.53
p	<0.05	>0.05	>0.05	>0.05	>0.05
Comparison group, n=10	13.31±0.74	40.0±3.0	6.23±0.42	197±22	4.68±0.58
p	<0.05	>0.05	<0.05	<0.05	<0.05
p_1	<0.05	>0.05	<0.05	>0.05	<0.05
p_2	<0.05	>0.05	>0.05	>0.05	<0.05

p: Probability relative to the control group, p_1: Probability relative to the data before treatment, p_2: probability of differences between the main group and the comparison group
MDA: Malondial dehyde

led to the correction of certain metabolic disorders in the gum homogenate, and faster elimination of the harmful effects of the damaging factors and restoration of the state of the periodontal tissues than in comparative application of Asepta gel.

3. The therapeutic efficacy of the Apisan gel is due to a normalizing effect on the processes of POL, inflammation, and activation of the oral protective systems.

4. The results of the studies give grounds for recommending the local application of the new Apisan apigel to prevent inflammatory processes in the tissues of the oral cavity against the background of concomitant hyperacidic gastritis and to create optimal conditions for the elimination of structural and functional disorders caused by endogenous and exogenous risk factors such as tobacco smoke.[15]

PROSPECTS FOR FURTHER RESEARCH

The results obtained in the experiment indicate the expediency of studying the effect of the developed treatment on indices of nonspecific resistance and immune reactivity in the oral cavity during periodontitis against the background of concomitant GIT pathology and the creation of recommendations for its application in the complex therapy of dental diseases.

Conflicts of interest: No conflict of interest was declared by the authors.

REFERENCES

1. Yarova S. Features of the distribution and course of inflammatory and dystrophic processes in the periodontium against the background of diseases of the gastrointestinal tract. Ukr Dent Almanac. 2014;2:105-107.
2. Orekhova LYu. Clinical features and tendencies in the periodontal status of smokers. Parodontology. 2011;1:47-50.
3. Gazhva S. An integrated approach to the treatment of the oral mucous membranes in patients with chronic gastritis. Dentistry. 2013;6:16-19.
4. Beloklitskaya G. Dental manifestations in the oral cavity in patients with diseases of the gastrointestinal tract. Ukr Dent Almanac. 2010;2:66-68.
5. Oshakbayev K, Abilayuly Zh, Amanov T, Kozhazbekova B. Factors associated with tobacco smoking. Prevention of Diseases and Strengthening of Health. 2007;2:22-26.
6. Kravchenko L. A patent for the useful model of Ukraine №119715 IPC (2015.01) A61K31 / 235 Apisan gel for local treatment and prevention of traumatic lesions of the oral mucosa. Applicant and patent holder of Odessa National Medical University, №201702028 of 10, 03.2017, 2017; 21. Available from: http://uapatents.com/6-119715-gel-apisan-dlya-miscevo-profilaktiki-ta-likuvannya-travmatichnikh-urazhen-slizovo-obolonki-porozhnini-rota.html
7. Khomenko L, Savichuk O, Kostiuk O. A patent of Ukraine for invention 38149 A7A61B13 / 00 A61B10 / 00 Method of modeling of chronic relapsing aphthous stomatitis. Applicant and Patent holder of National Medical University named after O.O. Bogomolets, №2000063173 of 02.06.2000; published on May 15, 2001; 4. Available from: http://uapatents.com/3-38149-sposib-modelyuvannya-khronichnogo-recidivuyuchogo-aftoznogo-stomatita.html
8. Li H, Mellgard B, Helander H. Inoculation of VacA- and CagA-*Helicobacter pylori* delays gastric ulcers healing in the rat. Scand J Gastroenterol. 1997;32:439-444.
9. Struillou X, Boutigny H, Soueidan A, Layrolle P. Experimental animal models in periodontology: a review. Open Dent J. 2010;4:37-47.
10. Stalnaya I, Garishvili T. A method for the determination of malonic diaaldehyde with tiobarbituric acid. Modern Methods in Biochemistry. 1977:66-68.
11. Koroliuk MA, Ivanova LI, Maĭorova IG, Tokarev VE. A method of determining catalase activity. Lab Delo. 1988;1:16-19.
12. Levitsky A, Denga O, Makarenko O. Biochemical markers of inflammation of the tissues of the oral cavity: study guide. Odessa. 2010:16.
13. Kulakov E, Zorina O, Boriskinf A. The role of protective factors of the organism in the pathogenesis of inflammatory periodontal diseases. Dentistry. 2010;6:72-76.
14. Apatzidou D, Riggio MP, Kinane DF. Impact of smoking on the clinical, microbiological and immunological parameters of adult patients with periodontitis. J Clin Periodontol. 2005;32:973-983.
15. Batsaeva YuG, Begimbetova K, Fedorov D, Yakushenko V, Zharmaev S. Clinical and laboratory study of preparations based on propolis in the treatment of periodontal and oral mucosa. Saratov Scientific Medical Journal. 2018;2:133-136.

Turk J Pharm Sci 2020;17(1):99-107
DOI: 10.4274/tjps.galenos.2018.24381

ORIGINAL ARTICLE

Anti-inflammatory Effects of Deuterium-Depleted Water Plus *Rosa Damascena* Mill. Essential Oil Via Cyclooxygenase-2 Pathway in Rats

Döteryumu Azaltılmış Su ve *Rosa Damascena* Mill. Uçucu Yağının Sıçanlarda Siklooksijenaz-2 Yolağı Üzerinden Anti-enflamatuvar Etkileri

Faezeh FATEMI[1]*, Abbas GOLBODAGH[2], Reza HOJIHOSSEINI[2], Abolfazl DADKHAH[3], Kambiz AKBARZADEH[4], Salome DINI[5], Mohammad Reza Mohammadi MALAYERI[6]

[1]Nuclear Science and Technology Research Institute, Materials and Nuclear Fuel Research School, Tehran, Iran
[2]Payame Noor University, Faculty of Sciences, Department of Biochemistry, Tehran, Iran
[3]Islamic Azad University, Qom Branch, Faculty of Medicine, Department of Medicine, Qom, Iran
[4]Mashhad University of Medical Science, Faculty of Medicine, Mashhad, Iran
[5]Islamic Azad University, Karaj Branch, Young Researchers and Elite Club, Karaj, Iran
[6]Islamic Azad University, Garmsar Branch, Faculty of Veterinary Medicine, Department of Pathobiology, Garmsar, Iran

ABSTRACT

Objectives: Natural medicine has been proposed for treating sepsis worldwide. Therefore, in this study, the effect of deuterium-depleted water (DDW) alone and adjuvant with *Rosa damascena* Mill. (RD) essential oils was considered through the evaluation of oxidative stress-antioxidant parameters and the expression of cyclooxygenase-2 (COX-2) inflammatory gene in liver damage caused by sepsis.

Materials and Methods: The rats were randomly divided into 5 groups: 1) laparotomy group; 2) cecal ligation and puncture (CLP) group; 3) DDW (15 ppm and 30 ppm doses) group; 4) DDW (15 ppm and 30 ppm doses) plus RD essential oil (100 mg/kg.bw); 5) indomethacin (2 mg/kg.bw) as a positive control. The treatments were daily administrated for 2 weeks and the CLP model was created on the day 15. Then, the animals were killed and their liver tissue was separated for histopathologic and biochemical assessment.

Results: Our results demonstrated that the treatment of animals with DDW and DDW plus RD essential oil was effective due to the regulation of the oxidative stress-antioxidant parameters including lipid peroxidation, glutathione (GSH), GSH s-transferases, myeloperoxidase, ferric reducing ability of plasma and inflammatory parameters such as prostaglandin E2 and COX-2. Pathological studies also showed that sepsis led to the liver tissue injuries, which can be reduced by treatments.

Conclusion: Sepsis caused oxidative stress in the liver tissue, but the administration of DDW and DDW plus RD essential oil can be useful to prevent and heal these injuries.

Key words: Deuterium-depleted water, *Rosa damascena* Mill essential oil, cecal ligation and puncture, oxidative stress-antioxidant parameters, sepsis

ÖZ

Amaç: Dünyada sepsis tedavisi için doğal kaynaklı ilaçlar önerilmektedir. Bu nedenle, bu çalışmada, döteryumu azaltılmış suyun (DDW) tek başına ve *Rosa damascena* (RD) Mill. uçucu yağı ile birlikte etkisi oksidatif stres-antioksidan parametrelerin ve sepsisten kaynaklanan karaciğer hasarında siklooksijenaz-2 (COX-2) enflamatuvar genin ekspresyonunun değerlendirilmesi yoluyla belirlenmiştir.

Gereç ve Yöntemler: Sıçanlar rastgele 5 gruba ayrılmıştır: 1) laparotomi grubu; 2) çekal ligasyon ve punksiyon (CLP) grubu; 3) DDW'ler (15 ppm ve 30 ppm dozlar) grupları; 4) DDW'ler (15 ppm ve 30 ppm dozlar) ile RD (100 mg/kg); 5) pozitif bir kontrol olarak indometasin (2 mg/kg). Tedaviler günlük olarak iki hafta boyunca yapılmış ve 15. günde CLP modeli oluşturulmuştur. Daha sonra hayvanlar öldürülmüş ve karaciğer dokuları histopatolojik ve biyokimyasal değerlendirmeler için ayrılmıştır.

*Correspondence: E-mail: fatemi81@yahoo.com, Phone: +989124186349 ORCID-ID: orcid.org/0000-0002-1092-9038
Received: 15.09.2018, Accepted: 15.11.2018

Bulgular: Sonuçlarımız, DDW ve DDW ile RD uygulamalarının, hayvanların lipid peroksidasyon, glutatyon (GSH), GSH s-transferaz, miyeloperoksidaz, plazma demir indirgeme kabiliyeti dahil olmak üzere oksidatif stres-antioksidan parametrelerinin; prostaglandin E2 ve COX-2 gibi enflamatuvar parametrelerinin düzenlenmesinden dolayı etkili olduğunu göstermiştir. Patolojik çalışmalar da sepsisin karaciğer doku yaralanmalarına yol açtığını ve söz konusu uygulamalarla azaltılabileceğini göstermiştir.

Sonuç: Sepsis karaciğer dokusunda oksidatif strese neden olmuştur, ancak DDW ve DDW ile RD'nin birlikte uygulanması bu hasarı önlemek ve iyileştirmek için yararlı olabilir.

Anahtar kelimeler: Döteryumu azaltılmış su, *Rosa damascena* Mill, uçucu yağ, çekal ligasyon ve punksiyon, oksidatif stres-antioksidan parametreler, sepsis

INTRODUCTION

Natural products are increasingly becoming one of the most important resources for replacing chemical compounds. They will undergo continual use toward meeting the urgent need to develop effective drugs, and they will play a leading role in the discovery of drugs for treating human diseases, especially chronic disorders.[1]

Deuterium-depleted water (DDW), known as light water, has a lower concentration of naturally occurring deuterium (20-25 ppm vs. 150 ppm).[2] The use of DDW for a long period may reduce the concentration of deuterium in the liquids and tissues of organisms due to isotopic exchange reactions. These reactions may impact the cellular cycle and cell proliferation.[3,4] Previous studies stated that a decreased amount of deuterium in drinking water caused different biological activities such as anticancer, antioxidant, and chemopreventive properties.[5-8]

On the other hand, our recent study reported that *Rosa damascena* Mill. (RD) essential oils with the main chemical compositions of citranellol (66.11%), transgeraniol (11.56%), and phenylethyl alcohol (5.33%) had antioxidant and anti-inflammatory effects in a sepsis model.[9] RD essential oil, belonging to the family Roseaceae,[10] is one of the most valuable sources of flavors and fragrances worldwide and has some applications in the medicine and food industries.[11]

A study showed that RD essential oil has beneficial effects in the treatment of various disorders, e.g., inflammatory reactions, premenstrual breast tenderness, and spasms.[12] It is traditionally used for the treatment of abdominal and chest pain and depression.[13] Several biological activities of RD essential oil have also been reported, including analgesic, antitussive, antidepressant, antispasmodic, antioxidant, and anti-HIV activities.[14-17] A study showed that the oil extracted from RD essential oil exhibited antimicrobial activity against a large number of microorganisms, especially against *Proteus vulgaris* and *Klebsiella pneumoniae*.[18]

Regarding the beneficial therapeutic properties of these natural products, their probable anti-inflammatory and antioxidant effects in treating severe diseases such as sepsis should be considered.

Sepsis is a systemic body reaction to invasive microorganisms like bacteria and fungi. It is one of the top ten main causes of death among all patients admitted to hospital. It causes inflammation, microvascular damage, and coagulopathy, hemodynamic instability, multiple organ dysfunction, and immunosuppression. It is an important medical problem all over the world and is the most common cause of death among critically ill patients.[19,20] The cecal ligation and puncture (CLP) model as a stable, repetitive, and applicable model leads to the pollution of the abdominal cavity by bacteria-carrying intestinal contents and induces a wide range of systemic inflammatory responses leading to sepsis.[21,22] In the CLP model, bacteria spreading from infection sites and entering the bloodstream are rapidly trapped in many organs, such as the liver, kidney, lung, and spleen, and bound to the surface of specific target cells and macrophages in the target organ and subsequently killed by infiltrating neutrophils.[23,24] The organs are damaged in mice with lethal sepsis induced by CLP and also in humans with sepsis. This injury is mainly associated with ineffective bacterial clearance, leading to bacterial dissemination and high mortality rates.[24] Several reports have demonstrated that inflammatory cytokines can serve as both makers and mediators of the severity of sepsis and elevated levels of these cytokines predict mortality following CLP.[25-27]

Regarding the increase in resistance to and side effects of antibiotics and synthetic drugs in sepsis treatment, natural products with high antibacterial and antioxidant capacities could be a suitable alternative. In the current study, inflammation was induced by a CLP inflammatory model in rats in order to consider the preventive anti-inflammatory effects of DDW alone and concomitant with RD through the estimation of cyclooxygenase-2 (COX-2) gene expression and prostaglandin E2 (PGE2) as well as the assessment of oxidative stress-antioxidant parameters such as glutathione (GSH), lipid peroxidation (LP), GSH *s-transferases* (GST), myeloperoxidase (MPO), and ferric reducing ability of plasma (FRAP).

MATERIALS AND METHODS

Plant materials and DDW preparations

DDW (15 and 30 ppm) obtained from the Atomic Energy Organization of Iran was used in our study. In addition, the essential oils of RD were obtained from Barij Essence Pharmaceutical Co, Kashan Iran (Batch No: 714043, Sample Serial No: AE932009).

Animals

The study was carried out on 70 male Wistar rats (200-250 g). The rats were kept under standard conditions (12 h light/12 h dark) at 20-25°C for 2 weeks. The animal studies had been approved by the Medical Ethics Committee of Tarbiat Modares

University based on the World Medical Association Declaration of Helsinki. The CLP model was used to cause sepsis in rats.[9]

The rats (10 rats in each group) were randomly divided into 7 groups: 1) laparotomy (LAP) group (LAP) as a negative control group; 2) CLP group as a control group; 3) DDW: the rats received DDW orally (at a dose of 15 ppm and 30 ppm) for 2 weeks; 4) DDW+RD: the rats received RD essential oil at 100 mg/kg.bw dose plus DDW 15 ppm and 30 ppm for 2 weeks; *5)* indomethacin: the rats received 2 mg/kg.bw indomethacin orally, serving as a positive control group. After 15 days, CLP surgery was performed in all groups.

Next, 24 h after CLP surgery, the rats were anesthetized and heparinated blood samples were collected by heart puncture from all the animals and centrifuged at 3000×g for 10 min to obtain the plasma. Then the rats were killed and their livers were removed and processed for histological and biochemical assays.

Assessment of PGE2

Plasma PGE2 level was measured by enzyme-linked immunosorbent assay kit (ELISA Kit; BioAssay System) according to the producer's instructions.

Assessment of COX-2 gene expression

Total RNA from liver tissues was prepared with an RNA total kit (BioBasic Inc, Canada). cDNA was synthesized with a PrimeScript™ RT reagent kit (Takara Bio Inc, Japan) and oligo dt primers (Takara Bio Inc, Japan), according to the manufacturer's protocol.

Then the primers for PCR were designed with the Gene Runner software version 3.05 and primer 3 servers (COX2 forward: 5'ACCTCTGCGATGCTCTTC3'; COX-2 reverse: 5' AGGAATCTCGGCGTAGTAC3'; Glyceraldehyde 3-phosphate dehydrogenase (GAPDH) forward: 5' TGCCAGCCTCGTCTCATAG 3'; GAPDH reverse: 5''ACTGTGCCGTTGAACTTGC 3'). Blast N searches were used to check primer specificity. The cDNA samples were amplified by PCR amplification and then checked by 2.5% agarose gel electrophoresis to ensure whether the PCRs contained a product with the expected size.

The relative expression of the selected gene was measured with a real-time PCR system (Rotor-Gene Q, QIAGEN). The reaction mixture contained 5 µL of SYBR Green real-time PCR Master Mix (QIAGEN), which includes Taq DNA polymerase, dNTP, $MgCl_2$, and SYBR Green I dye, 0.2 µL of a 10 mM solution of sense-anti-sense primer, 0.5 µL of template cDNA added with H_2O to a total of 10 µL. The negative controls were also designed as above but without cDNA. The thermal cycling conditions consisted of an initial denaturation stage at 95°C for 2 min, followed by 40 cycles at 95°C for 15 s, 60°C for 20 s, and 72°C for 20 s. At the completion of each run, melting curves for the amplicons were measured by raising the temperature by 0.3°C from 57 to 95°C while monitoring fluorescence. All expression data were normalized using GAPDH expression as the internal standard.

Assessment of antioxidant and liver parameters

GSH test

It was estimated in liver homogenates according to the procedure reported by Seldak and Lindsay.[28] A weighed portion of the liver was homogenized in ethylenediaminetetraacetic acid (EDTA) (0.02 M). Then 5 mL of homogenate was immediately precipitated with 1 mL of 50% trichloroacetic acid and 4 mL of distilled water; the precipitate was removed after centrifugation at 3000×g for 15 min. To determine the GSH level, 2 mL of supernatant was mixed with 4 mL of tris buffer (0.4 M), containing EDTA (0.2 M) and 0.1 mL of 5,5'-dithiobis (2-nitrobenzoic acid) (0.01 M). Absorbance was measured at 412 nm using a spectrophotometer.

LP test

The concentration of thiobarbituric acid reactive substances as an indicator for LP production was measured spectrophotometrically using thiobarbituric acid reagent based on the procedure described by Buege and Aust.[29]

GST test

GST was measured spectrophotometrically using 1-chloro-2, 4-dinitrobenzene (a general substrate) according to the procedures described by Habig et al.[30]

FRAP test

FRAP was performed using 2,4,6-Tris (2-pyridyl)-s-triazine reagent as described by Benzie and Strain.[31] FRAP level was calculated by plotting a standard curve of absorbance against µmol/L concentration of Fe (2) standard solution.

MPO test

MPO activity was measured, with minor modification, according to the procedure reported by Hillegass et al.[32]

Assessment of liver enzymes

To confirm the liver function and injury, serum alanine transaminase (ALT), aspartate transaminase (AST) (Pars Azmoon, Co, Iran), alkaline phosphatase (ALP) (Ziest Chem Diagnostics Co, Iran), and total bilirubin (BILI) (Darman Faraz Kave Co, Iran) were determined spectrophotometrically according to the procedure described in the kit purchased.

Histological analysis

Liver biopsies were collected from all the control and treated animals 24 h after sepsis induction. The tissue samples were fixed in 10% phosphate-buffered saline of formaldehyde solution. Dehydration was performed in graded ethanol, followed by embedding in paraffin, and a 5-µm section was stained with hematoxylin and eosin. For histopathological analysis, the sections were examined by light microscopy (Olympus CX31RBSF). The histological changes were quantitatively and semiquantitatively analyzed by a veterinary pathologist. The histologic index was scored from 0 (minimal) to 4 (maximal); score 0= from 0 to 9 neutrophils, score 1= from 10 to 19 neutrophils, score 2= from 20 to 29 neutrophils, score 3= from 30 to 39 neutrophils, score 4= more than 40 neutrophils. The scoring system included: zero (0) for normal condition, 1+ for

mild changes, 2+ for average changes, 3+ for severe changes, and 4+ score for more severe changes.

Statistical analysis

The data was analyzed with Statistical Package for the Social Sciences v.19. The data was expressed as mean±standard error. One-way analysis of variance was applied to compare the mean values. The normal distribution of the data was examined by Kolmogorov-Smirnov normality *test*. A p-value of less than 0.05 was considered statistically significant.

RESULTS

Effect of DDW and DDW plus RD essential oil on PGE2 and COX-2 in sepsis

The results indicated that the level of PGE2 value increased as evidenced by the significant rise ($p<0.05$) in the level of COX-2 in the CLP group. However, the administration of DDW reduced considerably ($p<0.05$) the level of COX-2 compared to the CLP group. Indeed, the PGE2 level returned significantly ($p<0.05$) to normal levels after using DDW plus RD essential oil ($p<0.05$) but there was no significant change ($p>0.05$) in COX-2 gene expression. Likewise, indomethacin as a positive control decreased significantly ($p<0.05$) the levels of PGE2 and COX-2 gene expression when compared to the CLP group (Table 1).

Effect of DDW and DDW plus RD essential oil on oxidative stress-antioxidant parameters in sepsis

As shown in Table 2, the levels of LP and MPO significantly ($p<0.05$) increased in the CLP group, while the level of FRAP went down remarkably ($p<0.05$). Moreover, sepsis led to a significant decrease in the liver GSH as compared to the LAP group ($p<0.05$). The DDW and DDW plus RD essential oil restored the levels of LP, MPO, and GSH in comparison to the CLP group. However, the administration of DDW plus RD essential oil returned the level of FRAP to the normal one ($p>0.05$). Meanwhile, administration of indomethacin to rats showed the same results in the treatment groups ($p<0.05$), whereas GST level did not show any significant changes ($p>0.05$) in the groups even after using indomethacin as a positive control (Table 2).

Table 1. The effect of DDW and DDW + RD on PGE2 and COX-2 gene expression in septic rats

Groups	PGE2 (ng/mL)	COX-2 gene expression
LAP	508±26.7	0±0.03
CLP	796±20.7[a]	0.43±0.05[a]
DDW15	584±18.4[b]	0.32±0.03[b]
DDW30	709±18[b]	0.23±0.02[b]
RD100+DDW15	486±24.6[b]	0.48±0.05
RD100+DDW30	530±17.4[b]	0.45±0.05
Indomethacin	536±32.8[b]	0.15±0.11[b]

[a]$p<0.05$ is considered significant between LAP and CLP group, [b]$p<0.05$ is considered significant between CLP and treatment groups, DDW: Deuterium-depleted water, RD: *Rosa damascena* Mill, PGE2: Prostaglandin E2, *COX-2*: cyclooxygenase-2, LAP: Laparotomy, CLP: Cecal ligation and puncture

Effect of DDW and DDW plus RD on liver enzymes in sepsis

The levels of AST and ALT significantly increased ($p<0.05$) as compared to the LAP group (Table 3). In contrast, the rats pretreated with DDW and DDW plus RD essential oil surprisingly ($p<0.05$) had restored AST and ALT levels as compared to the CLP group. Similarly, indomethacin (2 mg/kg.bw) as a positive control returned the levels of AST and ALT to normal levels ($p<0.05$) (Table 2), whereas the levels of ALP and BILI had no remarkable changes in all groups even after using DDW and DDW plus RD essential oil (Table 3).

Histological findings

There were some mild changes in the hepatocytes in the LAP group (Figure 1A), whereas severe congestion, interstitial edema, and margination of neutrophils in the venules and sinusoids were observed in the CLP group. Neutrophils and mononuclear cells were also infiltrated in the portal tracts and sinusoids in the septic group. Kupffer cell hyperplasia and granular degeneration were seen in the CLP group. There were no signs of necrosis in the hepatocytes. All the changes in the CLP group revealed a kind of hepatitis called nonspecific reactive hepatitis (Figures 1B1 and B2). The treated groups showed improved histopathological lesions except for the DDW30 plus RD essential oil treated group. The portal tract and the parenchyma were nearly in normal condition in the DDW15 and DDW30 treated groups (Figures 1C and D). Moreover, the presence of a few neutrophils in the sinusoids of the DDW15 plus RD essential oil treated group was observed (Figure 1E). However, there were neutrophil infiltrations in the sinusoids in the DDW30 plus RD essential oil treated group. Kupffer cells that show hypertrophy and hyperplasia were also obvious in this group (Figure 1F). Furthermore, in the indomethacin group, reduced amounts of neutrophils were seen (Figure 1G).

As shown in Table 4, the CLP group obviously showed neutrophil margination and infiltration, mononuclear cell infiltration, and Kupffer cell hyperplasia as compared with the LAP group ($p\leq0.05$). Concerning portal inflammation, it was also meaningful in the CLP group in comparison with the LAP group ($p\leq0.05$). However, there were no obvious differences regarding granular degeneration or inflammatory foci between the study groups ($p>0.05$). All the treatment groups, except the RD+DDW30 treated group, had prominently reduced neutrophil margination and infiltration, mononuclear cells infiltration, Kupffer cell hyperplasia, and portal inflammation in comparison with the CLP group ($p\leq0.05$).

DISCUSSION

Our previous results demonstrated that medicinal plants with bioactive constituents such as RD essential oil as well as *Berberis integerrima* and *Ferula assafoetida* extracts significantly affect oxidative stress-antioxidant parameters and detoxifying enzymes as well as COX-2 gene expression.[9, 33,34] There is also evidence indicating hepatoprotective activity of DDW against acetaminophen.[7] Following this, the present study was designed

to consider, for the first time, the therapeutic efficacy of DDW and DDW plus RD essential oil against liver injury induced by CLP in septic rats.

Our results revealed that the sepsis induced by CLP significantly increased ($p<0.05$) the levels of LP and MPO along with PGE2 level and COX-2 expression. Likewise, the levels of AST and ALT activities went up sharply due to CLP surgery compared with the LAP group (Table 3), while there was a considerable decrease in the amount of GSH and FRAP (as an important factor in the oxidative stress-antioxidant balance) in comparison with the LAP group (Tables 1 and 2; Figure 1).

Sepsis reflects a systemic inflammatory syndrome in response to an infection and represents the leading cause of death in the

Table 2. The effect of DDW and DDW+RD on oxidative stress-antioxidant parameters in septic rats

Groups	LP (pmol/mg protein)	GSH (nmol/mg protein)	MPO (U/mg protein)	GST (nmol/min/mg protein)	FRAP (µmol/L)
LAP	10.34±1.18	11.42±1.1	9.46±0.7	1126±61.61	407±21.76
CLP	18.51±1.53[a]	7.28±0.67[a]	26.13±0.7[a]	1173±32.11	257±10.98[a]
DDW15	11.95±1[b]	9.86±0.75[b]	18.9±0.98[b]	1355±46.02	265±15.54
DDW30	12.39±1.04[b]	9.65±0.75[b]	18.34±1.89[b]	1246±52.97	246±9.7
RD+DDW15	10.23±0.908[b]	13.9±1.03[b]	10.34±0.75[b]	1976±66.67	374±7.33[b]
RD+DDW30	11.15±0.86[b]	14.25±1[b]	11.24±0.8[b]	1878±45.09	383±6.2[b]
Indomethacin	11.8±0.87[b]	11.26±0.95[b]	6.58±0.2[b]	1076±48.22	280±18.2[b]

[a]$p<0.05$ is considered significantly between LAP and CLP groups, [b]$p<0.05$ is considered significantly between CLP and treatment groups, DDW: Deuterium-depleted water, RD: *Rosa damascena* Mill, LAP: Laparotomy, CLP: Cecal ligation and puncture, LP: Lipid peroxidation, GSH: Glutathione, MPO: Myeloperoxidase, FRAP: Ferric reducing ability of plasma, GST: Glutathione s-transferases

Table 3. The effect of DDW and DDW+RD the on liver enzymes in septic rats

Groups	AST (U/L)	ALT (U/L)	ALP (U/L)	BILI (mg/dL)
LAP	132±9.58	61±5.35	364±33.8	0.54±0.05
CLP	317±13.58[a]	136±8.76[a]	400±25.8	0.6±0.05
DDW15	168±11.76[b]	74±7.63[b]	394±33	0.59±0.04
DDW30	171±9.91[b]	78±8.01[b]	377±30.8	0.58±0.04
RD+DDW15	135±7.92[b]	64±5.93[b]	357±27.4	0.55±0.04
RD+DDW30	143±10.06[b]	67±6.65[b]	368±20.5	0.55±0.04
Indomethacin	150±11.72[b]	73±4.48[b]	371±30	0.54±0.04

[a]$p<0.05$ is considered significantly between LAP and CLP groups, [b]$p<0.05$ is considered significantly between CLP and treatment groups, DDW: Deuterium-depleted water, RD: *Rosa damascena* Mill, LAP: Laparotomy, CLP: Cecal ligation and puncture, AST: Aspartate transaminase, ALT: Alanine transaminase, BILI: Bilirubin, ALP: Alkaline phosphatase

Table 4. Mean values and standard error of histopathologic variables of the liver specimens in the study groups

Groups	Neutrophil margination and infiltration	Granular degeneration	Inflammatory foci	Mononuclear cells infiltration and Kupffer cell hyperplasia	Portal inflammation
LAP	0±0	0.4±0.24	0±0	0±0	0±0
CLP	2.75±0.25[a]	0.75±0.75	1.5±0.86	3±0.4[a]	2.25±0.25[a]
DDW15	0.4±0.24[b]	0.4±0.24	0±0	1.4±0.4[b]	0.4±0.24[b]
DDW30	1±0[b]	0±0	0.8±0.8	0.8±0.2[b]	0.2±0.2[b]
RD+DDW15	1.4±0.24[b]	0±0	0.2±0.2	1.4±0.24[b]	1±0[b]
RD+DDW30	3±0	0.8 ±0.37	0.4 ±0.4	3±0	3±0
Indomethacin	1.6±0.16[b]	0.29±0.19	0.45±0.21	1.3±0.21[b]	0.5±0.21[b]

[a]$p<0.05$ is considered significantly between LAP and CLP groups, [b]$p<0.05$ is considered significantly between CLP and treatment groups, LAP: Laparotomy, CLP: Cecal ligation and puncture, DDW: Deuterium-depleted water, RD: *Rosa damascena* Mill

intensive care unit. During the process of sepsis, the liver plays an important role in defensive responses to scavenge bacteria and produce an inflammatory mediator.[35] Recent studies have also observed that liver dysfunction is an early event in sepsis.[36] The hepatocellular liver enzymes AST and ALT have been regarded as markers of liver injury.[37]

Our results (Table 3) clearly showed that sepsis increased liver enzymes such as AST and ALT caused by liver damage. The biochemical results along with the histological findings (Figure 1) confirmed the pathophysiological changes in liver function damaged by sepsis. Other studies also proved that there is a direct link between the oxidative stress conditions and organ

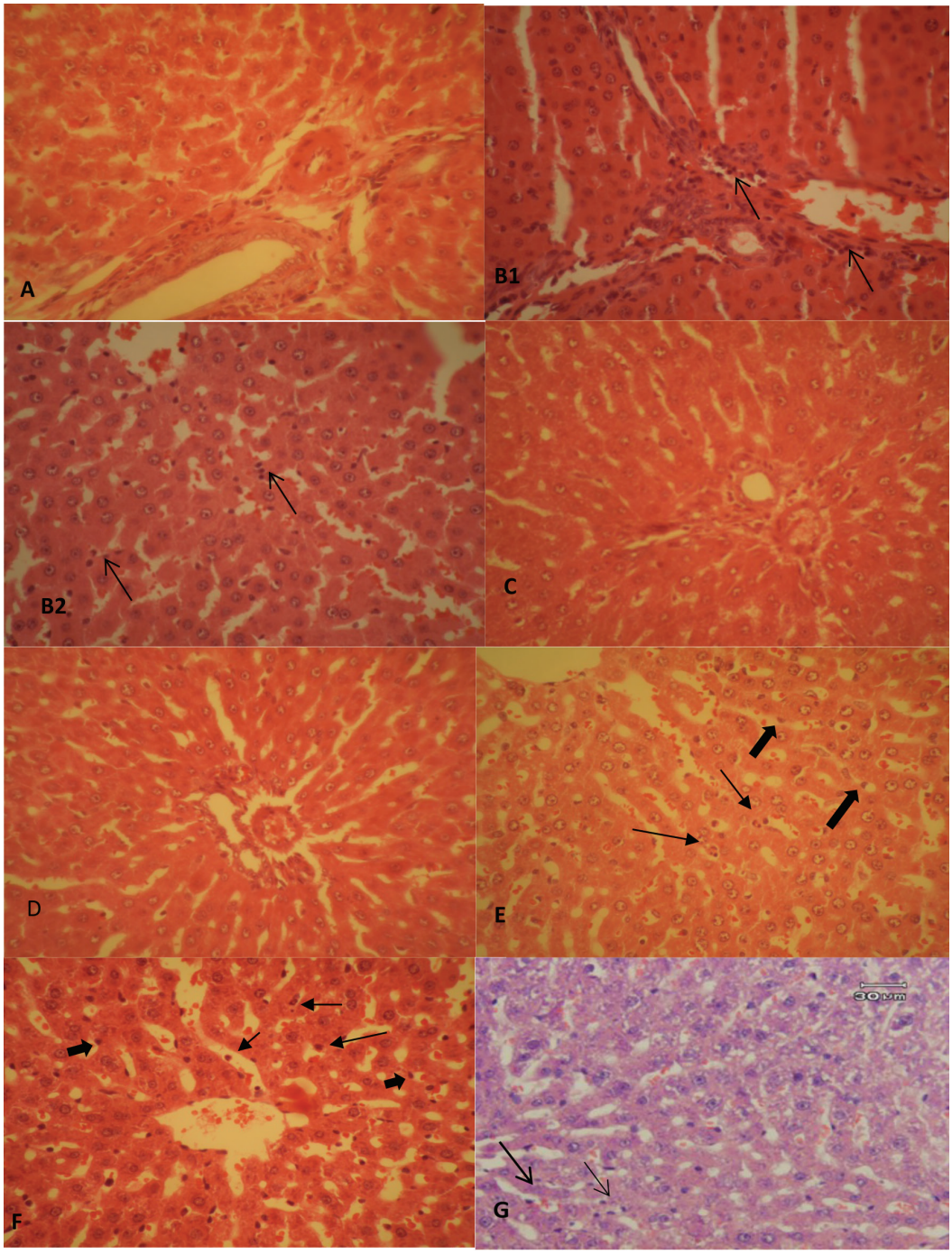

Figure 1. Histopathological studies. A) LAP group, the portal tract and the hepatocytes in normal condition. B1) CLP group, neutrophil infiltration in the portal tract (arrows). B2) CLP group, neutrophil infiltration in the sinusoids that can be seen easily with their dark nuclei (arrows). C) DDW15 group, the portal tract and the parenchyma in normal condition. H and E, 400×. D) DDW30 group, the portal tract and the parenchyma in normal condition. H and E, 400×. E) DDW15+RD, presence of a few neutrophils in the sinusoids (thin arrows). Kupffer cells can also be seen in the picture (thick arrows). H and E, 400×. F) DDW30+RD group, neutrophil infiltration in the sinusoids (thin arrows). Kupffer cells showing hypertrophy and hyperplasia are also obvious (thick arrows). H and E, 400×. G) Indomethacin group, a few infiltrated neutrophils (arrows) can be seen. H and E, 400×

LAP: Laparotomy, CLP: Cecal ligation and puncture, DDW: Deuterium-depleted water, RD: *Rosa damascena* Mill, H: Hematoxylin, E: Eosin

injuries in the CLP model.[38,39] In addition, initiation of oxidative stress was identified by the increase in malondialdehyde level.[40] GSH also plays a principal role in protecting cells from oxidative damage.[41] Therefore, the fall in GSH level in the liver in the septic groups and the rise in LP demonstrated that sepsis promoted destruction in balancing antioxidants and oxidative stress. While MPO is a protein in neutrophils that participates in the early inflammatory process in patients with sepsis,[42,43] its elevation in septic animals concomitant with LP production led to hepatic dysfunction.

Furthermore, COX-2 as an early expressed gene is not only detected in most normal tissues, but it is also induced by stimuli such as pro-inflammatory cytokines,[44] leading to PGE2 production, which acts on neurons and contributes to the systemic responses to inflammation.[45] In our study, an increase in the level of COX-2 expression was detected in septic rats as well as PGE2 concentration in plasma level compared to the control group (Table 1).

Regarding the importance of treatment of sepsis, studies confirmed the main role of antioxidants in reducing the tissue damage due to scavenging free radicals.[9,46-48] To confirm, our results demonstrated that the administration of DDW and DDW plus RD essential oil was effective in sepsis treatment, where the levels of LP, MPO, and GSH returned to the normal levels. Moreover, these treatments significantly ($p<0.05$) protected the liver (based on histological analysis) and decreased the AST and ALT levels as compared to the CLP group. The PGE2 level also fell considerably ($p<0.05$) after using DDW alone and the combination of DDW with RD. The COX-2 gene expression diminished when the rats were treated with only DDW, while there were no considerable changes in the DDW plus RD essential oil groups, which may be due to the transient state of expression of some genes in sepsis. In fact, the natural agents (DDW and DDW+RD) protect the liver from injuries in a sepsis model as potently as indomethacin, a nonsteroidal anti-inflammatory drug, used clinically for its anti-inflammatory, antipyretic, and analgesic properties (Tables 2 and 3; Figure 1).

The reduction in deuterium content in the body's liquids due to isotope metabolism reactions is the main effect of DDW as light water. The decrease in this element's concentration in erythrocytes, in blood plasma, and in homogenates of laboratory animals' hearts can be achieved with the use of water with low deuterium content. Such changes induce in turn the recovery of prooxidant-antioxidant system balance and a decrease in prooxidant load in organisms, which is further accompanied by higher immunity of laboratory animals.[49,50] One study reported that DDW with its antioxidant property was effective in protecting the liver against acetaminophen toxicity.[51] We demonstrated that DDW alone and in combination with *Satureja rechingeri* essential oil had synergistic effects in prevention of acetaminophen-induced hepatotoxicity in rats due to the reduction in oxidative stresses.[7] Other research reported that the DDW pretreatment protected the liver from chromium toxicity by restoring the levels of AST and ALT activities.[51] Furthermore, DDW has an anticancer action due to the influence on gene expression regulation and consequently on protein biosynthesis.[52]

Moreover, the protective effects of the oils may be due to the antioxidant activity and free radical scavenging effects of phenolic compounds and flavonoids present in them. Our current study indicated the *in vivo* anti-inflammatory activities of RD essential oils may be associated with their antioxidant compounds, namely citronellol, trans-geraniol and phenylethyl alcohol as the main constituents of the essential oils, which exhibited antioxidant activities by 2,2-difenil-1-pikrilhidrazil and β-carotene-linoleic acid bleaching assays.[9] A previous study also revealed that the essential oil of rosemary containing antioxidant compounds has strong antioxidant and hepatoprotective activities by modulating the malondialdehyde and GSH levels and also catalase, peroxidase, GSH peroxidase, and GSH reductase activities. That study showed that hepatoprotective activity can be attributed to 1,8-cineole as its major compound as well.[53] Nithianantham et al. [54] also reported that the hepatoprotective activity of *Clitoria ternatea* leaf may be due to its free radical-scavenging and antioxidant activity. One study reported that the treatment of rats with ethyl acetate extracted from *Asparagus cochinchinensis* root suppressed inflammatory responses through inhibition of NO, COX-2, and reactive oxygen species production.[55]

CONCLUSION

The current findings indicated that the pretreatment of rats with DDW and DDW plus RD essential oil exerted beneficial effects on the prevention of liver damage, induced by a CLP inflammatory model, through not only reducing the levels of liver enzymes and oxidative stress-antioxidant parameters, but also through the balance of COX-2 and PGE2 levels. The histopathological studies proved that the hepatic injuries were improved via the administration of DDW and DDW plus RD essential oil as well.

Conflicts of interest: No conflict of interest was declared by the authors.

REFERENCES

1. Galm U, Shen B. Natural product drug discovery: The times have never been better. Chem Biol. 2007;14:1098-1104.
2. Rehakova R, Klimentova J, Cebova M, Barta A, Matuskova Z, Labas P, Pechanova O. Effect of deuterium-depleted water on selected cardiometabolic parameters in fructose-treated rats. Physiol Res. 2016;65(Supll 3):401.
3. Bykov MI, Dzhimak SS, Basov AA, Arcybasheva OM, Shashkov D, Baryshev MG. Comparative characteristics of the isotopic D/H composition and antioxidant activity of freshly squeezed juices from fruits and vegetables grown in different geographical regions. Vopr Pitan. 2015;84:89-96.
4. Sergeevich DS, Alexandrovich BA, Anatolyevna EA, Viacheslavovna FL, Alexandrovna KE, Romanovna VE, Mikhailovna LO, Gennadievich BM. Influence of Deuterium-Depleted Water on Hepatorenal Toxicity. Jundishapur J Nat Pharm Prod. 2018.

5. Olariu L, Petcu M, Tulcan C, Buiga-Chis I, Pup M, Florin M, Brudiu I. Deuterium depleted water-antioxidant or prooxidant. Scientific Papers Veterinary Medicine. 2007;15:265-269.
6. Somlyai G, Molnár M, Laskay G, Szabó M, Berkényi T, Guller I, Kovács A. Biological significance of naturally occurring deuterium: the antitumor effect of deuterium depletion. Orv Hetil. 2010;151:1455-1460.
7. Rasooli A, Fatemi F, Akbarzadeh K, Dini S, Bahremand S. Synergistic Protective Activity of Deuterium Depleted Water (DDW) and Satureja rechingeri Essential Oil on Hepatic Oxidative Injuries Induced by Acetaminophen in Rats. Journal of Essential Oil Bearing Plants. 2016;19:1086-1101.
8. Fatemi F, Dadkhah A, Akbarzadeh K, Dini S, Hatami S, Rasooli A. Hepatoprotective Effects of Deuterium Depleted Water (DDW) Adjuvant with *Satureja rechingeri* Essential Oils. Electronic Journal of Biology. 2015;11:23-32.
9. Dadkhah A, Fatemi F, Mohammadi Malayeri MR, Karvin Ashtiyani MH, Noureini SK, Rasooli A. Considering the effect of *Rosa Damascena* essential oil on oxidative stress and COX-2 gene expression in liver of septic rats. Turk J Pharm Sci. 2019;16(4):16-24.
10. Pellati F, Orlandini G, van Leeuwen KA, Anesin G, Bertelli D, Paolini M, Benvenuti S, Camin F. Gas chromatography combined with mass spectrometry, flame ionization detection and elemental analyzer/ isotope ratio mass spectrometry for characterizing and detecting the authenticity of commercial essential oils of *Rosa damascena* Mill. Rapid Commun Mass Spectrom. 2013;27:591-602.
11. Shafei MN, Saberi Z, Amini S. Pharmacological effects of *Rosa damascena*. Iran J Basic Med Sci. 2011;14:295-307.
12. Kaul VK, Singh V, Singh B. Damask rose and marigold: prospective industrial crops. Int J Med Arom Plants. 2000:313-318.
13. Shakeri F, Boskabady MH. A review of the relaxant effect of various medicinal plants on tracheal smooth muscle, their possible mechanism(s) and potency. J Ethnopharmacol. 2015;175:528-548.
14. Mahmood N, Piacente S, Pizza C, Burke A, Khan AI, Hay AJ. The anti-HIV activity and mechanisms of action of pure compounds isolated from *Rosa damascena*. Biochem Biophys Res Commun. 1996;229:73-79.
15. Achuthan CR, Babu BH, Padikkala J. Antioxidant and hepatoprotective effects of *Rosa damascena*. J Padikkala Pharm Biol. 2003;41:357-361.
16. Özkan G, Sagdic O, Baydar NG. Antioxidant and antibacterial activities of *Rosa damascena* flower extracts. Food Sc Technol Int. 2004;10:277-281.
17. Nunes HS, Miguel MG. *Rosa damascena* essential oils: a brief review about chemical composition and biological properties. Trends Phytochem Res. 2017;1:111-128.
18. Mahboubi M, Kazempour N, Khamechian T, Fallah MH, Kermani MM. Chemical Composition and Antimicrobial Activity of *Rosa damascena* Mill. Essential Oil. Journal of Biologically Products from Nature. 2011;1:19-26.
19. Seymour CW, Liu VX, Iwashyna TJ, Brunkhorst FM, Rea TD, Scherag A, Rubenfeld G, Kahn JM, Shankar-Hari M, Singer M, Deutschman CS, Escobar GJ, Angus DC. Assessment of clinical criteria for sepsis: for the Third International Consensus Definitions for Sepsis and Septic Shock (Sepsis-3). JAMA. 2016;315:762-774.
20. Singer M, Deutschman CS, Seymour CW, Shankar-Hari M, Annane D, Bauer M, Bellomo R, Bernard GR, Chiche JD, Coopersmith CM, Hotchkiss RS, Levy MM, Marshall JC, Martin GS, Opal SM, Rubenfeld GD, van der Poll T, Vincent JL, Angus DC. The third international consensus definitions for sepsis and septic shock (Sepsis-3). JAMA 2016;315:801-810.
21. Liu MW, Su MX, Wang YH, Wei W, Qin LF, Liu X, Tian ML, Qian CY. Effect of melilotus extract on lung injury by upregulating the expression of cannabinoid CB2 receptors in septic rats. BMC Complement Altern Med. 2014;14:94.
22. Ritter C, Andrades M, FrotaJúnior ML, Bonatto F, Pinho RA, Polydoro M, Klamt F, Pinheiro CT, Menna-Barreto SS, Moreira JC, Dal-Pizzol F. Oxidative parameters and mortality in sepsis induced by cecal ligation and perforation. Intensive Care Med. 2003;29:1782-1789.
23. Gregory SH, Barczynski LK, Wing EJ. Effector function of hepatocytes and Kupffer cells in the resolution of systemic bacterial infections. J Leukoc Biol. 1992;51:421-424.
24. Owen KA, Pixley FJ, Thomas KS, Vicente-Manzanares M, Ray BJ, Horwitz AF, Parsons JT, Beggs HE, Stanley ER, Bouton AH. Regulation of lamellipodial persistence, adhesion turnover, and motility in macrophages by focal adhesion kinase. J Cell Biol. 2007;179:1275-1287.
25. Moreno SE, Alves-Filho JC, Rios-Santos F, Silva JS, Ferreira SH, Cunha FQ, Teixeira MM. Signaling via platelet-activating factor receptors accounts for the impairment of neutrophil migration in polymicrobial sepsis. J Immunol. 2006;177:1264-1271.
26. Remick DG, Bolgos G, Copeland S, Siddiqui J. Role of interleukin-6 in mortality from and physiologic response to sepsis. Infect Immun. 2005;73:2751-2757.
27. Sherwood ER, Enoh VT, Murphey ED, Lin CY. Mice depleted of CD8+ T and NK cells are resistant to injury caused by cecal ligation and puncture. Lab Invest. 2004;84:1655-1665.
28. Sedlak J, Lindsay RH. Estimation of total, protein-bound, and nonprotein sulfhydryl groups in tissue with Ellman's reagent. Anal Biochem. 1968;25:192-205.
29. Buege JA, Aust SD. Microsomal lipid peroxidation. Methods Enzymol. 1978;52:302-310.
30. Habig WH, Pabst MJ, Jakoby WB. Glutathione S-transferases. The first enzymatic step in mercapturic acid formation. J Biol Chem. 1974;249:7130-7139.
31. Benzie IF, Strain JJ. The ferric reducing ability of plasma (frap) as a measure of "antioxidant power: the frap assay. Anal Biochem. 1996;239:70-76.
32. Hillegass LM, Griswold DE, Brickson B, Albrightson-Winslow C. Assessment of myeloperoxidase activity in whole rat kidney. J Pharmacol Methods. 1990;24:285-295.
33. Malayeri MR, Dadkhah A, Fatemi F, Dini S, Torabi F, Tavajjoh MM, Rabiei J. Chemotherapeutic effect of *Berberis integerrima* hydroalcoholic extract on colon cancer development in the 1,2-dimethyl hydrazine rat model. Z Naturforsch C J Biosci. 2016;71:225-232.
34. Torabi F, Dadkhah A, Fatemi F, Dini S, Taghizadeh M, Mohammadi Malayeri MR. Prevention and therapy of 1,2-dimethyl hydrazine induced colon carcinogenesis by *Ferula assafoetida* hydroalcoholic extract. Turkish Journal of Biochemistry. 2015;40:390-400.
35. Angus DC, van der Poll T. Severe sepsis and septic shock. N Engl J Med. 2013;369:840-851.
36. Marshall JC. New translational research provides insights into liver dysfunction in sepsis. PLoS Med. 2012;9:1001341.
37. Alonso A, Misialek JR, Amiin MA, Hoogeveen RC, Chen LY, Agarwal SK, Loehr LR, Soliman EZ, Selvin E. Circulating levels of liver enzymes and

incidence of atrial fibrillation: the Atherosclerosis Risk in Communities cohort. Heart. 2014;100:1511-1516.

38. Hubbard WJ, Choudhry M, Schwacha MG, Kerby JD, Rue LW 3rd, Bland KI, Chaudry IH. Cecal ligation and puncture. Shock. 2005;24(Suppl 1):52-57.

39. Toscano MG, Ganea D, Gamero AM. Cecal ligation puncture procedure. J Vis Exp. 2011.

40. Dadkhah A, Fatemi F, Alipour M, Ghaderi Z, Zolfaghari F, Razdan F. Protective effects of Iranian Achillea wilhelmsii essential oil on acetaminophen-induced oxidative stress in rat liver. Pharm Biol. 2015;53:220-227.

41. Villa P, Saccani A, Sica A, Ghezzi P. Glutathione protects mice from lethal sepsis by limiting inflammation and potentiating host defense. J Infect Dis. 2002;185;1115-1120.

42. Metzler KD, Fuchs TA, Nauseef WM, Reumaux D, Roesler J, Schulze I, Wahn V, Papayannopoulos V, Zychlinsky A. Myeloperoxidase is required for neutrophil extracellular trap formation: Implications for innate immunity. Blood. 2011;117:953-959.

43. Kothari N, Keshari RS, Bogra J, Kohli M, Abbas H, Malik A, Dikshit M, Barthwal MK. Increased myeloperoxidase enzyme activity in plasma is an indicator of inflammation and onset of sepsis. J Crit Care. 2011;26:435.

44. Konturek PC, Kania J, Burnat G, Hahn EG, Konturek SJ. Prostaglandins as mediators of COX-2 derived carcinogenesis in gastrointestinal tract. J Physiol Pharmacol. 2005;56(Suppl 5)57-73.

45. Samad TA, Sapirstein A, Woolf CJ. Prostanoids and pain: unraveling mechanisms and revealing therapeutic targets. Trends Mol Med. 2002;8:390-396.

46. Khan R, Sultana S. Farnesol attenuates 1,2-dimethylhydrazine induced oxidative stress, inflammation and apoptotic responses in the colon of Wistar rats. Chem-Biol Interact. 2011;192:193-200.

47. Rasooli A, Fatemi F, Hajihosseini R, Vaziria A, Akbarzadeh K, Mohammadi Malayerid MR, Dini S, Foroutanrad M. Synergistic effects of deuterium depleted water and Mentha longifolia L. essential oils on sepsis-induced liver injuries through regulation of cyclooxygenase-2. Pharm Biol. 2019;57:125-132.

48. Kharpate S, Vadnerkar G, Jain D, Jain S. Evaluation of Hepatoprotective Activity of Ethanol Extract of Ptrospermum acerifolium Ster Leaves. Indian J Pharm Sci. 2007;69:850-852.

49. Barishev MG, Dzhimak SS, Frolov VU, Bolotin SN, Dolgov MA. Technologies For Obtaining Deuterium Depleted Water. Membranes. 2013;3:523-526.

50. Basov AA, Elkina AA, Samkov AA, Volchenko NN, Moiseev AV, Fedulova LV, Baryshev MG, Dzhimak SS. Influence of Deuterium-Depleted Water on the Isotope D/H Composition of Liver Tissue and Morphological Development of Rats at Different Periods of Ontogenesis. Iran Biomed J. 2019; 23:129-41.

51. Doina PM, Olariu V, Scurtu M, Tulcan C, Brudiu I, Muntean D, Petcu F, Pădeanu I, Ostan M. The effect of deuterum depleted water on some hepatic enzymes' activity in rats intoxicated with chromium (VI). Fascicula: Ecotoxicologie, Zootehnie si Tehnologii de Industrie Alimentară. 2012:521-526.

52. Krempels K, Somlyai I, Somlyai G. A retrospective evaluation of the effects of deuterium depleted water consumption on 4 patients with brain metastases from lung cancer. Integr Cancer Ther. 2008;7:172-181.

53. Rašković A, Milanović I, Pavlović N, Cebović T, Vukmirović S, Mikov M. Antioxidant activity of rosemary (Rosmarinus officinalis L.) essential oil and its hepatoprotective potential. BMC Complement Altern Med. 2014;14:225.

54. Nithianantham K, Shyamala M, Chen Y, Latha LY, Jothy SL, Sasidharan S. Hepatoprotective potential of Clitoria ternatea leaf extract against paracetamol induced damage in mice. Molecules. 2011;16:10134-10145.

55. Lee HA, Koh EK, Sung JE, Kim JE, Song SH, Kim DS, Son HJ, Lee CY, Lee HS, Bae CJ, Hwang DY. Ethyl acetate extract from Asparagus cochinchinensis exerts anti-inflammatory effects in LPS-stimulated RAW264. 7 macrophage cells by regulating COX-2/iNOS, inflammatory cytokine expression, MAP kinase pathways, the cell cycle and anti-oxidant activity. Mol Med Rep. 2017;15:1613-1623.

Turk J Pharm Sci 2020;17(1):108-14
DOI: 10.4274/tjps.galenos.2019.44270

ORIGINAL ARTICLE

Synthesis and Structure Elucidation of New Benzimidazole Amidoxime Derivatives

Yeni Benzimidazol Amidoksim Türevlerinin Sentezleri ve Yapı Aydınlatmaları

Cigdem KARAASLAN*

Ankara University Faculty of Pharmacy, Department of Pharmaceutical Chemistry, Ankara, Turkey

ABSTRACT

Objectives: In our previous studies we synthesized some potent antiparasitic, anticancer and antimicrobial amidine derivatives. Despite all their potent activities, it is well known that due to their cationic charge, amidine derivatives pose a serious problem in terms of bioavailability. The main purpose of this study is to prepare amidoxime derivatives of previously synthesized potent amidine derivatives as prodrugs in order to increase their bioavailabilities.

Materials and Methods: The targeted benzimidazole amidoximes were synthesized from their nitrile derivatives. The nitrile groups of these benzimidazole carbonitriles were converted to N-hydroxy benzamidine derivatives (amidoxime derivatives, 20-29) in the presence of $NH_2OH.HCl$ and KO-t-Bu in dimethyl sulfoxide. Structures of newly synthesized amidoxime derivatives were elucidated with 1H-NMR, 13C-NMR and some 2D NMR techniques like COSY, NOESY, HSQC and HMBC.

Results: A new series of benzimidazole amidoximes were synthesized and their structural elucidations were done in this study.

Conclusion: In order to solve the potential bioavailability problem of potent amidine derivatives, we prepared the prodrugs of those potent amidine derivatives as their amidoxime derivatives. *In vivo* studies of both previous amidine derivatives and amidoxime prodrugs of those amidines which were synthesized in this study are planned to perform in our ongoing studies.

Key words: Amidoxim, amidinobenzimidazole, prodrug, 1H-NMR, 2DNMR

ÖZ

Amaç: Daha önce yaptığımız çalışmalarda, antiparaziter, antikanser ve antimikrobiyal etkili potent aktiviteye sahip bazı amidin türevleri sentezledik. Ancak potent aktivitelerine rağmen, amidin türevlerinin, katyonik yükleri nedeniyle biyoyararlanım açısından ciddi bir sorun oluşturduğu bilinmektedir. Bu çalışmanın temel amacı, daha önce sentezlenen etkili amidin türevlerinin biyoyararlanımlarını artırmak için, ön ilaçları olarak bilinen amidoksim türevlerini hazırlamaktır.

Gereç ve Yöntemler: Hedeflenen benzimidazol amidoksimler, nitril türevlerinden hareketle sentezlenmiştir. Bu benzimidazol karbonitrillerin nitril grupları, dimetil sülfoksit içerisinde $NH_20H.HCl$ ve KO-t-Bu varlığında N-hidroksi benzamidin türevlerine (amidoksim türevleri, 20-29) dönüştürülmüştür. Yeni sentezlenmiş olan amidoksim türevlerinin yapıları ise 1H-NMR, 13C-NMR ve COSY, NOESY, HSQC ve HMBC gibi bazı 2D NMR teknikleri ile açıklanmıştır.

Bulgular: Bu çalışmada yeni bir seri benzimidazol amidoxim türevi bileşik sentezlenmiş ve yapıları aydınlatılmıştır.

Sonuç: Daha önceki çalışmalarımızda sentezlediğimiz amidin türevleri ile literatürlerde biyolojik açıdan etkili bulduğumuz amidin türevlerinin potansiyel biyoyararlanım problemlerini çözebilmek için, bu çalışmada söz konusu potent amidinlerin ön ilaç formları olan amidoksim türevlerini hazırladık. Etkili amidin türevleri ile bu çalışmada sentezlenen amidoksim türevlerinin *in vivo* çalışmalarının devam eden araştırmalarımız kapsamında yapılması planlanmaktadır.

Anahtar kelimeler: Amidoksim, amidinobenzimidazol, önilaç, 1H-NMR, 2DNMR

***Correspondence: E-mail:** karaslan@pharmacy.ankara.edu.tr, **Phone:** +90 312 203 30 63 **ORCID-ID:** orcid.org/0000-0002-2006-5421
Received: 04.12.2019, **Accepted:** 16.12.2019

INTRODUCTION

A biologically active compound with intended pharmacological activity may have unwanted properties that limit its bioavailability or structure which negatively effect its activities in the organism. Amidoximes are generally developed to overcome low oral bioavailability of amidines which are pharmacologically effective in many areas including antiparasitic,[1] antimicrobial[2] and anticancer activities.[3]

Amidine derivatives which are known as DNA interactive compounds, have been used in clinic for many years especially against protozoal diseases. The most important example of this group is pentamidine (Figure 1) which has been used effectively in the treatment of several protozoal diseases for many years.[1,4] Amidino group bearing compounds with similar structures such as berenil, furamidine (Figure 1) and some amidino benzimidazoles are also used as effective antiprotozoal compounds based on their selective binding to AT-rich sequences of DNA.[5] Furthermore, it is also known that these compounds have shown very good activities in anticancer therapy.[6-8] Pentamidine has been emphasized as a potential anticancer agent also.[9-11] Although amidine group is essential for the pharmacological effect of several active compounds, their oral bioavailability is too low and they have several toxic effects. Due to hydrophilic and very strong basic properties of amidines, after protonation they form highly mesomerically stabilized cations and so they are usually incapable of passing through membranes and cannot be absorbed from the gastrointestinal system after oral administration.[12] In order to avoid this problem, several prodrug attempts have been performed on the amidine moiety of drugs and hydroxylation of amidine group to amidoxime has been found the most promising alternative. Amidoximes instead of amidines principle was first performed to pentamidine and then it has been transferred to several other amidine derivatives (Furamidin-Pafuramidin) (Figure 1) for increasing oral absorption and improving bioavailability.[12-14]

Amidoxime derivatives indicate a prodrug class used to enhance the oral bioavailability of amidine containing drugs. Because of their lower basicity and higher lipophilicity than amidine derivatives, they can be quickly absorbed by the gastrointestinal tract after oral administration.[12,15]

Over the past decade, we have focused our effort on the design of amidino benzimidazole derivatives possessing antiprotozoal and anticancer activity.[1,3]

Mono-di amidino 2-anilino benzimidazoles were designed, synthesized and their antiprotozoal activities were determined against *Trypanosoma brucei rhodesiense* and *Plasmodium falciparum.* In this study some of dicationic compounds (Figure 2a) showed almost equal activity with melarsoprol against *Trypanosoma brucei rhodesiense* and they showed close activity with chloroquine against *Plasmodium falciparum*.[1]

Furthermore, the anticancer activities of these compounds with additional new analogues were studied against MCF-7 human breast adenocarcinoma cells. Some of them (Figure 2b) strongly inhibited MCF-7 cell viability compared to clinically used reference compounds, docetaxel and imatinib mesylate.[3]

Recently we reported synthesis and antimicrobial-anticancer activities of 2-(3,4-dimethoxyphenyl) benzazoles and imidazopyridine derivatives with very important results[16] some of which bearing amidine groups (Figure 2c).

As a part of our continuing research program, focused on developing new antimicrobial and anticancer benzimidazole

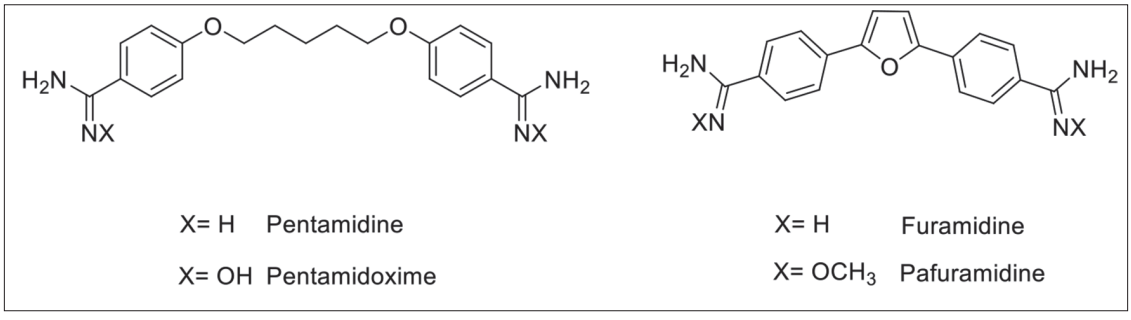

Figure 1. Chemical structures of some amidine derivatives and their amidoxime prodrugs

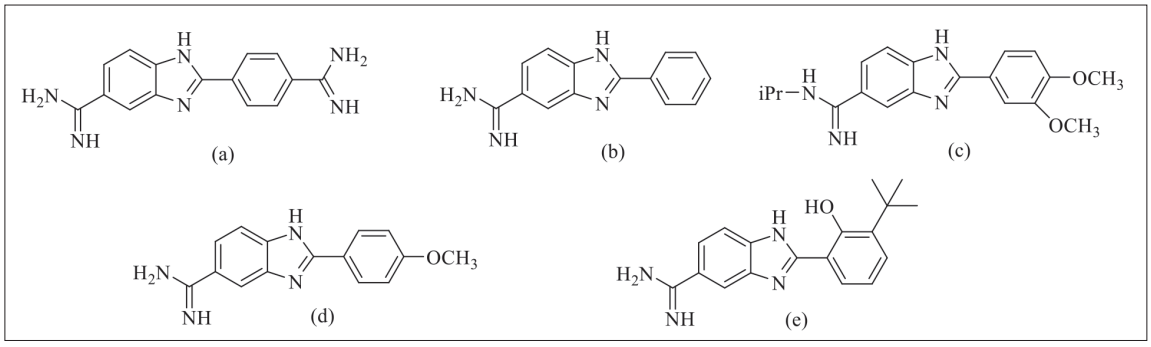

Figure 2. Previously synthesized potent benzimidazole carboxamidines

carboxamidines, we have planned to prepare prodrug structures of some of our effective amidine derivatives which have been previously reported.[1,3,16] Furthermore we designed new amidoxime derivatives according to literature including amidine derivatives which have potent activities (Figure 2d, e).[17,18] *In vivo* studies of these newly synthesized benzimidazole amidoximes are planned to test efficacy in an animal model and to determine their pharmacokinetic profiles in further analysis.

MATERIALS AND METHODS

Experimental

Uncorrected melting points were detected by a capillary melting point device (Büchi B-540). The ^{1}H, ^{13}C, COSY (Evaluated as only primary neighbourhood), NOESY, HSQC and HMBC - nuclear magnetic resonance (NMR) spectra were performed by VARIAN (Agilent) MERCURY 400 MHz (Varian, Palo Alto, CA, USA) at a proton resonance frequency of 400 MHz and a carbon resonance frequency of 100 MHz. The optimisation of NMR spectrum was directed by Agilent Vnmr J version 3.2 revision Asoftware. The samples to be analysed (5-20 mg) were prepared in 0.7 ml of CD_3OD, $CDCl_3$ or dimethyl sulfoxide (DMSO) -d_6 and tetramethylsilane was used as an internal standard. The liquid chromatography-mass spectrometry (LC-MS) spectra were obtained by using the electrospray-ionization (ESI) (+) method on a Waters Micro mass ZQ connected with Waters Alliance high-performance liquid chromatography (Waters Corporation, Milford, USA), with a C-18 column (X Terra, 4.6 X 250mm, 5µm). Because of the tautomeric forms of these compounds, ^{1}H and ^{13}C-NMR spectra of some unsubstituted analogues could not be clearly seen and appearance of some proton and carbon signals as broad peaks and unobservable some hinge carbon signals are normal. In order to remove the tautomeric effect, some of the benzimidazoles were dissolved in $CDCl_3$, CD_3OD or DMSO-d_6, followed by dry NaH, and D_2O were added to the NMR tube and stirred well. Besides substitution of this "nitrogen atom's proton" with an alkyl/aryl group has appeared to prevent the tautomerism.

Chemistry

The synthetic pathways for preparation of targeted compounds are outlined in Scheme1. All commercially available compounds were supplied from Sigma Aldrich. 4-Amino-3-nitrobenzonitrile is a commercially available compound. Compound **1-4**[2,19] and compound **5-7,9**[20-22] were prepared according to the given literature methods. Compound **8** was prepared from compound 3 by hydrogenation reaction. Compound **10-19** were obtained by condensation of 3-amino-4-(*N*-substituteamino)-benzonitriles with $Na_2S_2O_5$ adduct of related arylaldehydes in dimethylformamide (DMF).[23] Compound **19** was prepared from compound 11 according to the literature.[24] The nitrile groups of these benzimidazole carbonitriles were converted to *N*-hydroxy benzamidine derivatives (amidoxime derivatives, **20-29**) with the presence of $NH_2OH.HCl$ and KOtBu in DMSO.[25]

3-Amino-4- (phenylamino) benzonitrile 8

Compound **3** (2 mmol) was dissolved in ethanol (50mL) and was hydrogenated by H_2 (40 psi) and Pd-C (10%, 25 mg) until uptake of H_2 ceased. Then the Pd-C was filtered off from celite and washed with ethanol several times. The filtrate was concentrated in vacuo and the crude product was used for further steps without crystallization. Yield, 0.67g (92%). Mp: 152-154°C . ^{1}H-NMR δ (DMSO-d_6): 5.21 (s, 2H, -NH_2), 6.86-6.90 (m, 2H), 6.97-7.01(m, 3H), 7.06 (d, 1H, *J*= 8 Hz), 7.24 (t, 2H, *J*= 7.6 Hz), 7.47 (s, 1H), ^{13}C-NMR δ (DMSO-d_6): 102.1, 116.3, 116.8, 118.3, 120.1, 120.8, 121.1, 129.2, 134.2, 139.3, 142.5. MS (ESI+) m/z: 209.2 (M+H, 100%).

Sodium metabisulphite adduct of arylaldehyde derivatives

The corresponding arylaldehydes (5 mmol) were dissolved in ethanol (25 mL) and the solution of sodium metabisulfite (0.5 g) in water (5 mL) was added piece by piece. Then reaction was stirred and kept in refrigerator until all precipitation finished and the resulting precipitate was filtered off and dried, and used without purification for further steps.

General synthesis of compounds 10-19

The mixture of related 3-amino-4- (*N*-substituted-amino) benzonitriles 5-9 (1 mmol) and related sodium metabisulphite adduct of arylaldehydes (1 mmol) in DMF (1 mL) were heated at 120°C, for 3-4 h. At the end of the time the reaction was cooled and dilute K_2CO_3 solution were added. The final precipitate was collected by filtration and dried. If the product was not pure, it was purified with crystallization. Compound **10**,[19] **11**,[24] **12**,[26] **14**,[27] and **16**[24] were prepared according to the given literature methods. Compound **19** was prepared from compound **11** (0.43mmol) with the reaction of 4-chlorobenzyl chloride (0.6mmol) and sodium hydride (95%) (0.8mmol) in DMF (1 mL) and isolated as described in the literature.[24]

1-Butyl-2-(3-(tert-butyl)-2-hydroxyphenyl)-1H-benzo[d] imidazole-5-carbonitrile 13

Prepared from compound **7** (0.189 g) and sodium metabisulphite adduct of 2-hydroxy-3-*tert*-butylbenzaldehyde (0.282 g) as given in general method and the crude product was crystallized from ethanol. Yield, 0.159 g (46%). Mp: 184-187°C. ^{1}H-NMR δ (DMSO-d_6) : 0.77 (t,3H, *J*= 7.2 Hz, -CH_3), 1.82-1.24(m, 2H, -CH_2), 1.41(s, 9H, -CH_3), 1.66-1.74(m, 2H, -CH_2), 4.37 (t, 2H, *J*= 7.6 Hz, -CH_2), 6.98 (t, 1H, *J*= 8 Hz, H-5'), 7.41 (dd, 1H, *J*= 8 & 1.2 Hz, H-4'), 7.52 (dd, 1H, *J*= 8 & 1.2 Hz, H-6'), 7.71 (dd, 1H, *J*= 8.4 & 1.2 Hz, H-6), 7.91 (d, 1H, J= 8.8Hz, H-7), 8.27 (d, 1H, J= 0.8 Hz, H-4), 11.59 (s, 1H, OH). NOESY δ (DMSO-d_6): (N-CH_2/H-7), (N-CH_2/H-6'). COSY δ (DMSO-d_6): (H-6/H-7), (H-5'/H-6'), (H-5'/H-4'). ^{13}C-NMR & HSQC δ (DMSO-d_6): 13.1, 19.1, 29.3, 30.9, 34.7, 44.7, 104.5, 112.4 (CH-7), 114.5, 118.9 (CH-5'), 119.6, 123.3 (CH-4), 126.1(CH-6), 126.7 (CH-6'), 129.0 (CH-4'), 137.6, 138.1, 140.2, 153.9, 155.7. MS (ESI+) m/z: 348.94 (M+H, 100%).

1-Butyl-2-(naphthalen-2-yl)-1H-benzo[d]imidazole-5-carbonitrile 15

Prepared from compound **7** (0.189 g) and sodium metabisulphite adduct of 2-napthaldehyde (0.260 g) as given in general method and the crude product was crystallized from ethanol. Yield, 0.133 g, (41%). Mp: 126-129°C. ^{1}H-NMR δ (DMSO-d_6): 0.72 (t,3H, *J*= 7.6 Hz, -CH_3), 1.11-1.16(m, 2H, -CH_2), 1.63-1.71 (m, 2H, -CH_2),

4.47 (t, 2H, *J*= 7.2 Hz, -CH_2), 7.63-7.69 (m, 2H), 7.73 (dd, 1H, *J*= 8.4 & 1.2 Hz), 7.92-7.96 (m, 2H), 8.05-8.15(m, 3H), 8.29 (d, 1H, *J*= 0.8 Hz), 8.42 (s, 1H). ^{13}C-NMR δ (DMSO-d_6): 13.1, 19.1, 31.0, 44.2, 104.2, 112.5, 119.8, 124.1, 125.7, 125.9, 126.89, 126.96, 127.5, 127.7, 128.5, 129.0, 132.4, 133.2, 138.7, 142.0, 155.5. MS (ESI+) m/z: 326.68 (M+H, 100%).

2-(3,4-Dimethoxyphenyl)-1-phenyl-1H-benzo[d]imidazole-5-carbonitrile 17

Prepared from compound **8** (0.209 g) and sodium metabisulphite adduct of 3,4-dimethoxy benzaldehyde (0.270 g) as given in general method and the crude product was crystallized from ethanol. Yield, 0.220 g (62%). Mp: 175-176°C. ^{1}H-NMR δ ($CDCl_3$): 3.69 (s, 3H, OCH_3), 3.87 (s, 3H, OCH_3), 6.77 (d, 1H, *J*= 8.4 Hz, H-5'), 7.10 (dd, 1H, *J*= 8 & 2 Hz, H-6'), 7.13 (d, 1H, J= 2Hz, H-4), 7.24 (d, 1H, J= 8.8 Hz, H-7), 7.33 (dd, 2H, *J* = 8 & 2 Hz, H-2'',6''), 7.49 (dd, 1H, *J*= 8.8 & 1.6 Hz, H-6), 7.53-7.58 (m, 3H, H-3'',4'',5''), 8.16 (d, 1H, J= 1.6Hz, H-2'). COSY δ ($CDCl_3$): (H- 6/H-7), (H-5'/H-6'), (H-2'',6''/H-3'',5''). ^{13}C-NMR δ ($CDCl_3$): 55.7, 55.9, 106.2, 110.7, 111.3, 112.2, 119.8, 121.1, 122.8, 124.4, 126.5, 127.4, 129.3, 130.2, 136.4, 139.9, 142.4, 148.7, 150.7, 154.7. MS (ESI+) m/z: 356 (M+H, 100%).

1-Benzyl-2-(3,4-dimethoxyphenyl)-1H-benzo[d]imidazole-5-carbonitrile 18

Prepared from compound **9** (0.223 g) and sodium metabisulphite adduct of 3,4-dimethoxy benzaldehyde (0.270 g) as given in general method the crude product was crystallized from

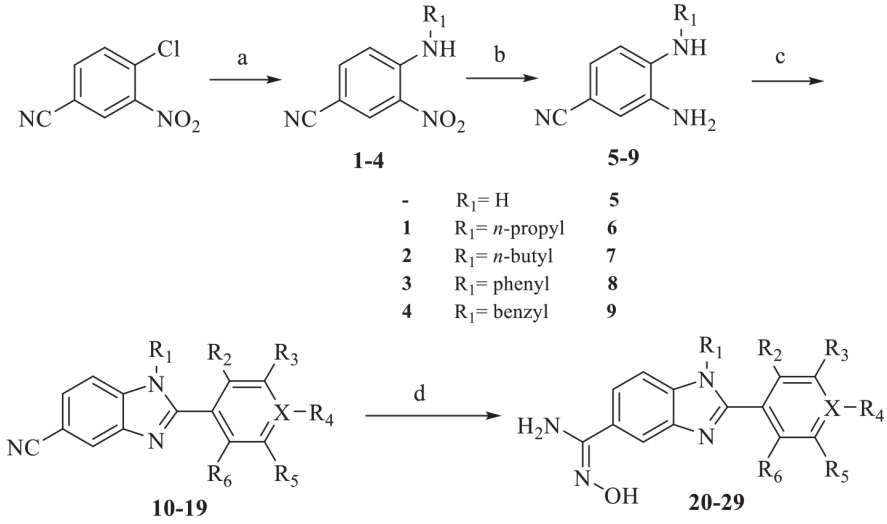

No	R_1	R_2	R_3	R_4	R_5	R_6	X	No
10	H	H	H	OCH_3	H	H	CH	20
11	H	H	OCH_3	OCH_3	H	H	CH	21
12	H	OH	*t*-butyl	H	H	H	CH	22
13	*n*-butyl	OH	*t*-butyl	H	H	H	CH	23
14	*n*-butyl	H	H	H	H	H	N	24
16	*n*-propyl	H	OCH_3	OCH_3	H	H	CH	26
17	phenyl	H	OCH_3	OCH_3	H	H	CH	27
18	benzyl	H	OCH_3	OCH_3	H	H	CH	28
19	4-Cl-benzyl	H	OCH_3	OCH_3	H	H	CH	29

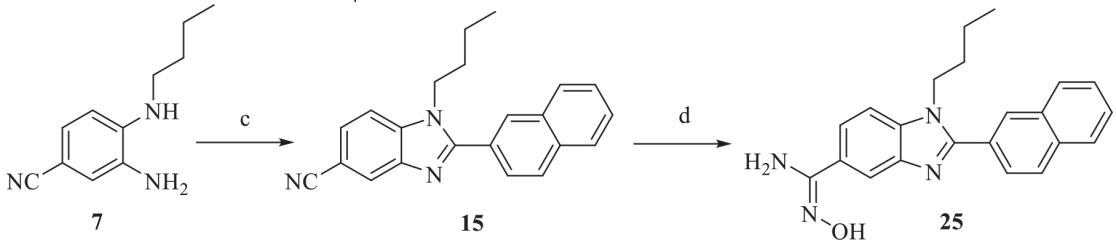

Reagents. a: corresponding amines; b:H_2/Pd-C; c:corresponding $Na_2S_2O_5$ adduct of arylaldehydes in DMF; d: $NH_2OH.HCl$ / KO.*t*-Bu, DMSO.

Scheme1. Synthesis of targeted benzimidazole amidoximes, DMF: Dimethylformamide, DMSO: Dimethyl sulfoxide

ethanol. Yield, 0.191 g (52%). Mp: 203-204°C. ^{1}H-NMR δ ($CDCl_3$): 3.73 (s, 3H, OCH_3), 3.93 (s, 3H, OCH_3), 5.51 (s, 2H, -CH_2 benzyl), 6.93 (d, 1H, *J*= 8.4 Hz, H-5'), 7.10 (dd, 2H, *J*= 8 & 1.2 Hz, H-2'',6''), 7.22 (dd, 1H, *J*= 8.8 & 2 Hz, H-,6'), 7.25 (d, 1H, *J*= 2 Hz, H-4), 7.29 (d, 1H, *J*= 8 Hz, H-7), 7.33-7.40 (m, 3H, H-3'',4'',5''), 7.49 (dd, 1H, *J*= 8.8 & 1.6 Hz, H-6), 8.17 (d, 1H, *J*= 0.8 Hz, H-2'). COSY δ ($CDCl_3$): (H- 6/H-7), (H-5'/H-6'), (H-2'',6''/H-3'',5''). ^{13}C-NMR δ ($CDCl_3$): 48.7, 55.7, 56.0, 105.9, 111.1, 111.3, 112.1, 119.8, 121.2, 122.0, 124.6, 125.6, 126.3, 128.2, 129.3, 135.6, 138.9, 144.6, 149.2, 151.1, 156.6. MS (ESI+) m/z: 369 (M+H, 100%).

General synthesis of compounds 20-29

Benzimidazole carbonitriles **10-19** (1 mmol) were stirred with a mixture of hydroxylamine hydrochloride (10 mmol) and potassium *tert*-butoxide (10 mmol) in DMSO (1 mL) at room temperature for 24h, to furnish the benzimidazole carboxamidoximes **20-29**. Then the reaction mixture was cooled and poured into water. The resulting precipitate was collected by filtration and washed with water plenty of time and then dried.

2-(4-Methoxyphenyl)-N-hydroxy-1H-benzo[d]imidazole-5-carboximidamide 20

Prepared from compound **10** (0.249 g) as given in general method. Yield, 0.231g (82%). Mp: 268-272°C. ^{1}H-NMR δ (DMSO-d_6): 3.82 (s, 3H, OCH_3), 5.76 (s, 2H, amidoxime NH_2), 7.09 (d, 2H, *J*= 8.4 Hz, H-3',5'), 7.46-7.92 (m, 3H), 8.10 (d, 2H, *J*= 8.8 Hz, H-2',6'), 9.49 (s, 1H, amidoxime OH), 12.75 (s, 1H, imidazole NH). COSY δ (DMSO-d_6): (H- 2',6'/H-3',5'). NOESY δ (DMSO-d_6): (-OCH_3/ H-3',5') (H-2',6'/ H-3',5'). ^{13}C-NMR δ (DMSO-d_6): 55.3, 71.3, 108.2, 114.3, 117.7, 119.7, 120.0, 122.5, 127.5, 128.0, 151.6, 152.1, 160.7. MS (ESI+) m/z: 283.6 (M+H, 100%).

2-(3,4-Dimethoxyphenyl)-N-hydroxy-1H-benzo[d]imidazole-5-carboximidamide 21

Prepared from compound **11** (0.279 g) as given in general method. Yield, 0.237g (76%). Mp: 217-219°C. ^{1}H-NMR δ (DMSO-d_6 + NaH+D_2O): 3.76 (s, 3H, OCH_3), 3.83 (s, 3H, OCH_3), 6.91 (d, 1H, *J*= 8.8 Hz, H-5'), 7.15 (dd, 1H, *J*= 8 & 1.6 Hz, H-6), 7.30 (d, 1H, *J*= 8.8 Hz, H-7), 7.68 (d, 1H, *J*= 1.2 Hz, H-4), 7.80 (d, 1H, *J*= 8 & 2 Hz, H-6'), 7.93 (d, 1H, *J*= 1.6 Hz, H-2'). COSY δ (DMSO-d_6+NaH+D_2O): (H- 6/H-7), (H-5'/H-6'). ^{13}C-NMR δ (DMSO-d_6+NaH+D_2O): 48.7, 55.7, 55.8, 110.9 (CH-2'), 111.8 (CH-5'), 112.9 (CH-4), 114.9, 115.5, 119.2 (CH-6'), 123.1, 130.8, 147.1, 148.2, 148.5, 153.3, 161.2. MS (ESI+) m/z: 313 (M+H, 100%).

2-[3-(tert-Butyl)-2-hydroxyphenyl]-N-hydroxy-1H-benzo[d]imidazole-5-carboximidamide 22

Prepared from compound **12** (0.291 g) as given in general method. Yield, 0.233 g 72%. Mp: 199-201°C. ^{1}H-NMR δ (CD_3OD): 1.47 (s, 9H), 6.87 (t, 1H, *J*= 8 Hz), 7.36 (dd, 1H, *J*= 7.6 & 1.2 Hz), 7.57-7.59 (m, 2H), 7.73 (d, 1H, *J*= 6.8 Hz), 7.92-7.94 (m, 1H). ^{13}C-NMR δ (CD_3OD): 30.0, 35.9, 40.5, 110.6, 111.9, 113.7, 117.5, 118.8, 119.5, 122.9, 124.9, 129.3, 130.0, 139.0, 145.2, 155.4, 156.4, 159.2 MS (ESI+) m/z: 325.43 (M+H, 100%).

1-Butyl-2-(3-(tert-butyl)-2-hydroxyphenyl)-N-hydroxy-1H-benzo[d]imidazole-5-carboximidamide 23

Prepared from compound **13** (0.347 g) as given in general method. Yield, 0.296 g 78%. Mp: 205-208°C. ^{1}H-NMR δ (DMSO-d_6): 0.85 (t, 3H, *J*= 7.2 Hz, -CH_3), 1.25-1.30 (m, 2H, -CH_2), 1.47 (s, 9H, -CH_3), 1.76-1.82 (m, 2H, -CH_2), 3.37 (t, 2H, *J*= 7.6 Hz, H-5'), 7.43-7.48 (m,2H, H-4',6'), 7.58 (d, 1H, *J*= 8.8 Hz, H-7), 7.67 (dd, 1H, *J*= 8.4 & 1.6 Hz, H-6), 7.99 (d, 1H, *J*= 1.2 Hz, H-4). COSY δ (DMSO-d_6): (H- 6/H-7), (H-5'/H-4'), (H-5'/H-6'). NOESY δ (DMSO-d_6): (-N-CH_2/ H-7), (-N-CH_2/ H-6'). ^{13}C-NMR δ (DMSO-d_6): 13.8, 20.8, 30.1, 32.7, 36.1, 46.2, 111.7, 116.3, 117.8, 120.0, 122.9, 127.7, 129.2, 130.1, 137.7, 139.6, 142.5, 154.5, 157.4. MS (ESI+) m/z: 381.83 (M+H, 100%).

1-Butyl-N-hydroxy-2-(pyridin-4-yl)-1H-benzo[d]imidazole-5-carboximidamide 24

Prepared from compound **14** (0.276 g) as given in general method. Yield, 0.200 g (65%). Mp: 232-235°C. ^{1}H-NMR δ (DMSO-d_6): 0.76 (t, 3H, *J*= 7.2 Hz, -CH_3), 1.12-1.18 (m, 2H, -CH_2), 1.64-1.68 (m,2H, -CH_2), 4.38 (t, 2H, *J*= 6.8 Hz, N-CH_2), 5.87 (s, 2H, amidoxime NH_2), 7.68 (d, 1H, *J*= 8.8 Hz, H-7), 7.74 (dd, 1H, *J*= 8.8 & 1.6 Hz, H-6), 7.82 (dd, 2H, *J*= 4.8 & 1.6 Hz, H-2',6'), 8.04 (s, 1H, H-4), 8.80 (dd, 2H, *J*= 4.8 & 1.6 Hz, H-3',5'), 9.59 (s, 1H, amidoxime OH). COSY δ (DMSO-d_6): (H- 6/H-7), (H-2',6'/H-3',5'). NOESY δ (DMSO-d_6): (N-CH2/H-2',6'), (N-CH_2/H-7), (amidoxime NH_2/ H-4), (amidoxime OH/ H-6). ROESY δ (DMSO-d_6): (N-CH_2/ H-2',6'), (N-CH_2/H-7), (amidoxime NH2/ H-4). ^{13}C-NMR & HSQC & HMBC δ (DMSO-d_6): 13.2, 19.1, 31.2, 43.9, 110.6 (CH-7), 116.5 (CH-4), 120.9 (CH-6), 123.2 (CH-2',6'), 127.9 (C-5), 136.3 (amidoxime C), 137.7 (C-1'), 142.2 (C-3a), 150.2 (CH-3',5'), 150.8 (C-2), 151.2 (C-7a). MS (ESI+) m/z: 310.48 (M+H, 100%).

1-Butyl-N-hydroxy-2-(naphthalen-2-yl)-1H-benzo[d]imidazole-5-carboximidamide 25

Prepared from compound **15** (0.325 g) as given in general method. Yield, 0.243 g (68%). Mp: 231-233°C. ^{1}H-NMR δ (CD_3OD): 0.72 (t, 3H, *J*= 7.6 Hz, -CH_3), 1.10-1.16(m, 2H, -CH_2), 1.67-1.70 (m, 2H, -CH_2), 4.42 (t, 2H, *J*= 7.2 Hz, -CH_2), 5.89 (s, 2H, amidoxime NH_2), 7.63-7.69 (m, 4H), 7.92 (dd, 1H, *J*= 8.4 & 1.2 Hz), 8.03-8.13 (m, 4H), 8.38(s, 1H), 9.61 (s, 1H, amidoxime OH). ^{13}C-NMR δ (CD_3OD): 13.2, 19.1, 31.2, 43.9, 110.5, 116.3, 120.4, 126.3, 127.3, 127.6, 127.7, 127.8, 128.3, 128.5, 128.7, 132.5, 133.1, 136.3, 142.4, 151.4, 153.6. MS (ESI+) m/z: 359.8 (M+H, 100%).

2-(3,4-Dimethoxyphenyl)-N-hydroxy-1-propyl-1H-benzo[d]imidazole-5-carboximidamide 26

Prepared from compound **16** (0.321g) as given in general method. Yield, 0.290 g 82%. Mp: 245-247°C. ^{1}H-NMR δ (DMSO-d_6): 0.76 (t, 3H, *J*= 7.2 Hz, -CH_3), 1.71 (m, 2H, -$CH_{2(2'')}$), 3.84 (s, 3H, OCH_3), 3.85 (s, 3H, OCH_3), 4.27 (t, 2H, *J*= 7.2 Hz, -$CH_{2(1'')}$), 5.83 (s, 2H, amidine NH), 7.14 (d, 1H, *J*= 8.4 Hz, H-5'), 7.30-7.33 (m, 2H, H-4, 6'), 7.60-7.66 (m, 2H, H-6,7), 7.97 (d, 1H, *J*= 0.8 Hz, H-2'), 9.55 (s, 1H, amidoxime OH). COSY δ (DMSO-d_6): (H- 6/H-7), (H-5'/H-6'). ^{13}C-NMR δ (DMSO-d_6): 10.9(CH_3), 22.6($CH_{2(2'')}$), 45.8 ($CH_{2(1'')}$), 55.5 (OCH_3), 55.6 (OCH_3), 110.3 (CH-7), 111.6 (CH-5'), 112.5 (CH-4), 115.9 (CH-2'), 120.1 (CH-6), 121.7 (CH-6'), 122.7, 127.4, 136.3, 142.2, 148.6, 149.9, 151.4, 153.7. MS (ESI+) m/z: 355 (M+H, 100%).

2-(3,4-Dimethoxyphenyl)-N-hydroxy-1-phenyl-1H-benzo[d]imidazole-5-carboximidamide 27

Prepared from compound **17** (0.355 g) as given in general method. Yield, 0.295 g (76%). Mp: 244-246°C. ^{1}H-NMR δ (CD_3OD): 3.62 (s, 3H, OCH_3), 3.83 (s, 3H, OCH_3), 6.93 (d, 1H, *J*= 8 Hz, H-5'), 7.08 (d, 1H, *J*= 2 Hz, H-2'), 7.16 (dd, 1H, *J*= 8.8 & 2 Hz, H-6'), 7.23 (d, 1H, *J*= 8.4 Hz, H-7), 7.39-7.42 (m, 2H, H-2'',6''), 7.56-7.62 (m, 4H, H-6,3'',4'',5''), 8.04 (d, 1H, J= 1.6 Hz, H-4). COSY δ (CD_3OD): (H- 6/H-7), (H-5'/H-6'), (H-2'',6''/H-3'',5''). ^{13}C-NMR δ (DMSO-d_6+NaH+D_2O): 55.1, 55.5, 109.7, 111.3, 112.3, 116.0, 120.9, 121.7, 122.0, 127.6, 128.2, 128.9, 130.1, 136.6, 137.5, 142.2, 148.0, 149.9, 151.2, 152.3. MS (ESI+) m/z: 389 (M+H, 100%).

1-Benzyl-2-(3,4-dimethoxyphenyl)-N-hydroxy-1-propyl-1H-benzo[d]imidazole-5-carboximidamide 28

Prepared from compound **18** (0.369 g) as given in general method. Yield, 0.289 g (72%). Mp: 224-226°C. ^{1}H-NMR δ (DMSO-d_6+NaH+D_2O): 3.68 (s, 3H, OCH_3), 3.83 (s, 3H, OCH_3), 5.59 (s, 2H, -CH_2 benzyl), 7.03 (d, 2H, *J*= 6.8 Hz, H-2'',6''), 7.10 (d, 1H, *J*= 8.4 Hz, H-5'), 7.25-7.34 (m, 5H, H-2',6',3'',4'',5''), 7.43 (d, 1H, *J*= 8.8 Hz, H-7), 7.59 (dd, 1H, *J*= 8.8 & 1.2 Hz, H-6), 8.02 (s, 1H, H-4). COSY δ ($CDCl_3$): (H- 6/H-7), (H-5'/H-6'), (H-2'',6''/H-3'',5''). ^{13}C-NMR δ ($CDCl_3$): 47.5, 55.3, 55.5, 110.2, 111.7, 112.4, 116.1, 120.3, 121.6, 122.1, 125.8, 127.3, 127.7, 128.7, 136.5, 136.9, 142.3, 148.6, 150.1, 151.3, 153.8. MS (ESI+) m/z: 403 (M+H, 100%).

1-(4-Chlorobenzyl)-2-(3,4-dimethoxyphenyl)-N-hydroxy-1H-benzo[d]imidazole-5-carboximidamide 29

Prepared from compound **19** (0.403 g) as given in general method. Yield, 0.305 g (70%). Mp: 245-247°C. ^{1}H-NMR δ (DMSO-d_6): 3.70 (s, 3H, OCH_3), 3.81 (s, 3H, OCH_3), 5.59 (s, 2H, -CH_2 benzyl), 5.80 (s, 2H, amidoxime NH2), 7.04 (d, 2H, *J*= 8.4 Hz, H-2'',6''), 7.08 (d, 1H, *J*= 8.8 Hz, H-5'), 7.22-7.24 (m, 2H, H-2',6'), 7.37 (d, 2H, *J*= 8 Hz, H-3'',5''), 7.43 (d, 1H, *J*= 8.8 Hz, H-7), 7.60 (d, 1H, *J*= 8.8 Hz, H-6), 8.01 (s, 1H, H-4). COSY δ (DMSO-d_6): (H- 6/H-7), (H-5'/H-6'), (H-2'',6''/H-3'',5''). NOESY δ (DMSO-d_6): (CH_2 benzyl / H-2',6'), (CH_2 benzyl / H-2'',6''), (amidoxime NH_2/ H-4), (amidoxime NH_2/ H-6). ^{13}C-NMR & HSQC & HMBC δ (DMSO-d_6): 46.9 (benzyl CH_2), 55.4 (OCH_3), 55.6 (OCH_3), 110.2 (CH-7), 111.7 (CH-5'), 112.4 (CH-2'), 116.2 (CH-4), 120.5 (CH-6), 121.6 (CH-6'), 121.9 (C-3'), 127.8 (CH-2'',6''), 128.7 (CH-3'',5''), 131.9, (C-4''), 136.0 (C-1''), 136.4 (C-7a), 142.3 (C-3a), 148.6 (C-1'), 150.2 (C-4'), 151.4 (amidoxime C), 153.9 (C-2). MS (ESI+) m/z: 437.77 (M+H, 100%).

RESULTS AND DISCUSSION

As shown in Scheme 1, uncommercial starting materials, 4-(*N*-substituted-amino) -3-nitrobenzonitriles **1-4**, were prepared by nucleophilic displacement of the chloro group of 4-chloro-3-nitrobenzonitril with corresponding amine derivatives in *N,N*-dimethylformamide. Non-susbstituted-4-amino-3-nitrobenzonitril is a commercially available compound. Then Pd/C-catalyzed hydrogenation of these compounds gave *N*-substituted-3,4-diamino benzonitriles 5-9. The benzimidazole carbonitriles **10-18** were obtained by condensation of these *N*-substituted-3,4-diamino benzonitriles with sodium metabisulfite adduct of related arylaldehydes. Compound **19** was prepared from compound **11** by the alkylation of tautomeric hydrogen with 4-chlorobenzyl chloride with the presense of sodium hydride (95%) in DMF. Finally targeted *N*-hydroxy benzamidine derivatives **20-29** (amidoxime derivatives) were achieved by the reaction of benzimidazole carbonitriles with $NH_2OH.HCl$ and KOtBu in DMSO. The structures of novel compounds were determined by ^{1}H-NMR, ^{13}C-NMR, some 2D-NMR techniques (COSY, NOESY, HSQC and HMBC) and LC-MS. Benzimidazoles are condensed systems of imidazole and benzene ring, and their hydrogen bearing nitrogen atom resembles the pyrole *N*-atom and the other nitrogen atom resembles the pyridine *N*-atom. Hydrogen atom of this pyrole *N*-atom can easily tautomerise in the 1,3-position and because of these tautomeric forms, ^{1}H and ^{13}C-NMR spectra of unsubstituted compounds may not be clearly seen. Both appearence of some proton and carbon signals as broad peaks and unobservable some hinge carbon signals are normal in that case. Substitution of this NH proton with an alkyl group would prevent tautomerism and can lead to clearly seen spectra. In this study we can easily see the hydrogen signals of even amidoxime NH_2 and OH in *N*-alkylated benzimidazoles.

In this study, 10 new amidoxime compounds designed as prodrugs of effective amidine derivatives, were synthesized and their structures were elucidated with advanced NMR techniques.

CONCLUSION

As a result in this study, a new series of benzimidazole amidoximes **20-29**, were synthesized starting from 3-amino-4- (substituted-amino) benzonitrile derivatives and sodium bisulfite adduct of corresponding arylaldehydes. The structures of novel compounds were determined by ^{1}H-NMR, ^{13}C-NMR, some 2D-NMR techniques and LC-MS. In our previous studies[1,3,16] we reported several types of amidino benzimidazoles with their potent antiparasitic, anticancer and antimicrobial activities; however most of the compounds' pharmocokinetic properties and *in vivo* studies have not been investigated yet. Because of the amidine groups, it seems very likely to have problems in their pharmacokinetic properties, especially in terms of bioavailability. In order to solve this potential problem, in this study we have prepared amidoxime derivatives of these potent amidino benzimidazoles as their prodrugs. *In vivo* studies of both previous amidine derivatives and amidoxime prodrugs which have been synthesized in this study, are under progress in our ongoing studies.

ACKNOWLEDGEMENTS

Ankara University Faculty of Pharmacy, Central Laboratory provided support for NMR and Mass spectrometer analysis.

Conflict of Interest: No conflict of interest was declared by the authors.

REFERENCE

1. Karaaslan C, Kaiser M, Brun R, Göker H. Synthesis and potent antiprotozoal activity of mono/di amidino 2-anilinobenzimidazoles versus Plasmodium falciparum and Trypanosoma brucei rhodesiense. Bioorg Med Chem. 2016;24:4038-4044.

2. Göker H, Alp M, Yıldız S. Synthesis and Potent Antimicrobial Activity of Some Novel *N*-(Alkyl)-2-Phenyl-1*H*-Benzimidazole-5-Carboxamidines. Molecules. 2005;10:1377-1386.

3. Karaaslan C, Bakar F, Goker H. Antiproliferative activity of synthesized some new benzimidazole carboxamidines against MCF-7 breast carcinoma cells. Z Naturforsch C J Biosci. 2018;73:137-145.

4. Ismail MA, Batista-Parra A, Miao Y, Wilson WD, Wenzler T, Brun R, Boykin DW. Dicationic near-linear biphenyl benzimidazole derivatives as DNA-targeted antiprotozoal agents. Bioorg Med Chem. 2005;13:6718-6726.

5. Baraldi PG, Bovero A, Fruttarolo F, Preti D, Tabrizi MA, Pavani MG, Romagnoli R. DNA minor groove binders as potential antitumor and antimicrobial agents. Med Res Rev. 2004;24:475-528.

6. Hranjec M, Piantanida I, Kralj M, Suman L, Pavelic K, Karminski- Zamola G. Novel amidino-substituted thienyl- and furylvinylbenzimidazole: derivatives and their photochemical conversion into corresponding diazacyclopenta[c]fluorenes. Synthesis,interactions with DNA and RNA, and antitumor evaluation. J Med Chem. 2008;51:4899-4910.

7. Starcevic K, Kralj M, Ester K, Sabol I, Grce M, Pavelic K, Karminski-Zamola G. Synthesis, antiviral and antitumor activity of 2-substituted-5-amidino-benzimidazoles. Bioorg Med Chem. 2007;15:4419-4426.

8. Hranjec M, Starcevic K, Piantanida I, Kralj M, Marjanovic M, Hasani M, Westman G, Karminski-Zamola G. Synthesis, antitumor evaluation and DNAbinding studies of novel amidino-benzimidazolyl substituted derivatives of furyl-phenyl- and thienyl-phenyl-acrylates, naphthofurans and naphthothiophenes. Eur J Med Chem. 2008;43:2877-2890.

9. Qiu G, Jiang J, Liu XS. Pentamidine sensitizes chronic myelogenous leukemia K562 cells to trail-induced apoptosis. Leuk Res. 2012;36:1417-1421.

10. Pathak MK, Dhawan D, Lindner DJ, Borden EC, Farver C, Yi T. Pentamidine is an inhibitor of PRL phosphatases with anticancer activity. Mol Cancer Ther. 2002;1:1255-1264.

11. Jung HJ, Suh SI, Suh MH, Baek WK, Park JW. Pentamidine reduces expression of hypoxia-inducible factor-1α in DU145 and MDAMB- 231 cancer cells. Cancer Lett. 2011;303:39-46.

12. Reeh C, Wundt J, Clement B. *N,N'*-Dihydroxyamidines: A New Prodrug Principle To Improve the Oral Bioavailability of Amidines. J Med Chem. 2007;50:6730-6734.

13. Berger O, Ortial S, Wein S, Denoyelle S, Bressolle F, Durand T, Escale R, Vial H J, Vo-Hoang Y. Evaluation of amidoxime derivatives as prodrug candidates of potent biscationic antimalarials. Bioorg Med Chem Lett. 2019;29:2203-2207.

14. Boykin DW. Antimicrobial activity of the DNA minor groove binders furamidine and analogs. J Braz Chem Soc. 2002;13:763.

15. Clement B. Pharmaceutical preparations that contain an active substance with modified amidine groups. Patents DE 4321444, WO 9501168, EP 0708640, US 5786383, and JP 3838657, 1995.

16. Karaaslan C, Duydu Y, Ustundag A, Yalcin CO, Kaskatepe B, Goker H. Synthesis & Anticancer Evaluation of New Substituted 2-(3,4-Dimethoxyphenyl) benzazoles. Med Chem. 2019;15:287-297.

17. Chavda S, Dittenhafer K, Wu K, Merrick C, Desta D, Cordes E, Babu B, Tzou S, Brockway O, Sjoholm R, Lee M . DNA sequence-selective monoheterocyclic analog of Hoechst 33258: cytotoxicity and antiparasitic properties. Heterocycl Commun. 2010;16:227-230.

18. Weidner-Wells MA, Ohemeng KA, Nguyen VN, Fraga-Spano S, Macielag MJ, Werblood HM, Foleno BD, Webb GC, Barrett JF, Hlasta DJ. Amidino Benzimidazole Inhibitors of Bacterial Two-Component Systems. Bioorg Med Chem Lett. 2001;11:1545-1548.

19. Goker H, Kus C, Boykin DW, Yildiz S, Altanlar N. Synthesis of Some New 2 Substituted-phenyl-1*H*-benzimidazole-5-carbonitriles and Their Potent Activity Against Candida Species. Bioorg Med Chem. 2002;10:2589-2596.

20. Fairley TA, Tidvell RR, Donkor I, Naiman NA, Ohemeng KA, Lombardy RJ, Bentley JA, Cory M. Structure, DNA Minor Groove Binding, and Base Pair Specificity of Alkyl- and Aryl-Linked Bis (amidinobenzimidazoles) and Bis (amidinoindoles). J Med Chem. 1993;36:1746-1753.

21. Goker H, Tuncbilek M, Suzen S, Kus C, Altanlar N. Synthesis and Antimicrobial Activity of Some New 2-Phenyl-*N*-substituted Carboxamido-1*H*-benzimidazole Derivatives, Arch Pharm Pharm Med Chem. 2001;334:148-152.

22. Goker H, Boykin DW. Ring Cleavage of bis-cyanosubstituted benzimidazoles by DIBAL. Heterocyc Comm. 2001;7:6,529-534.

23. Ridley HF, Spickett RGW, Timmis GM. A new synthesis of benzimidazoles and aza-analogs. J Heterocycl Chem. 1965;2:453-456.

24. Doganc F, Alp M, Goker H. Separation and identification of the mixture of 2-(3,4-dimethoxyphenyl)-1-n-propyl or (4-chlorobenzyl)-5 and (6)-1*H*-benzimidazole carbonitriles. Magn Reson Chem. 2016;54:851-857.

25. Farahat AA, Bennett-Vaughn C , Mineva EM, Kumar A, Wenzler T, Brun R, Liu Y, Wilson WD, Boykin DW. Synthesis, DNA binding and antitrypanosomal activity of benzimidazole analogues of DAPI. Bioorg Med Chem Lett. 2016;26:5907-5910.

26. Puskullu MO, Yıldız S, Goker H. Synthesis and Antistaphylococcal Activity of N-Substituted-1*H*-benzimidazole-sulphonamides. Arch Pharm Chem Life Sci. 2010;343:31-39.

27. Goker H, Alp M, Ates-Alagoz Z, Yıldız S. Synthesis and Potent Antifungal Activity Against Candida Species of Some Novel 1H-Benzimidazoles. J Het Chem. 2009;46:936-948.

Turk J Pharm Sci 2020;17(1):115-18
DOI: 10.4274/tjps.galenos.2020.09471

ORIGINAL ARTICLE

Assessment of *In Vitro* Antigenotoxic Effect of *Nigella Sativa* Oil

Nigella Sativa Yağının *İn Vitro* Antigenotoksik Etkisinin Değerlendirilmesi

Murat ZOR[1]*, Elçin Latife ASLAN[2]

[1]Lokman Hekim University, Department of Pharmacognosy, Ankara, Turkey
[2]Lokman Hekim University, Department of Medical Biology, Ankara, Turkey

ABSTRACT

Objectives: Cyclophosphamide (CP) is an alkylating agent widely used as an antineoplastic and immunosuppressive agent. The genotoxicity of CP has been studied in a variety of *in vivo* and *in vitro* systems and is routinely used as a positive control in genotoxicity tests. Traditional medicine *Nigella sativa L*., (*N. sativa*), Ranunculaceae family, especially in the Eastern Mediterranean countries, especially in many countries, and is widely used in many countries as a spice and folk medicine since the time of Dioscorides used as a plant. In this study, it was aimed to show the protective effects of *N. sativa* oil at different concentrations against the genotoxic effects of CP by micronucleus test.

Materials and Methods: For this purpose, healthy cells were treated *in vitro* with N. sativa oil at concentrations of 1, 5, 10 µg/mL and CP as positive control for 68 hours. The micronuclei were then counted.

Results: No significant increase in micronucleus frequency was observed when the application of *N. sativa* oil at concentrations of 1, 5, 10 µg/mL compared with the negative control. There was a decrease in the number of micronucleus in all three concentrations (1, 5, 10 µg/mL) compared to the CP group in the groups treated with *N. sativa* oil and CP.

Conclusion: It has been shown that *N. sativa* oil may have protective effects against genotoxicity agents *in vitro*. But more work is needed to understand the mechanism of the genotoxicity effects of *N. sativa* oil.

Key words: Cyclophosphamide, *Nigella sativa* oil, micronucleus, genotoxicity

ÖZ

Amaç: Siklofosfamid, antineoplastik ve immünosüpresif ajan olarak yaygın olarak kullanılan alkilleyici bir ajandır. Siklofosfamid'in genotoksisitesi çeşitli *in vivo* ve *in vitro* sistemde çalışılmış ve rutin olarak genotoksisite testlerinde pozitif kontrol olarak kullanılmaktadır. Geleneksel tıp da *Nigella sativa L*. (*N. sativa*), Ranunculaceae familyasından olup günümüzde başta Doğu Akdeniz ülkeleri olmak üzere birçok ülkede yaygın olarak yetişen ve hem baharat hem de halk ilacı olarak Dioscorides zamanından beri kullanılan bir bitkidir. Bu çalışmada Siklofosfamid'in genotoksik etkilerine karşı çörek otu yağının değişik konsantrasyonlardaki koruyucu etkilerininin mikronükleus testi ile gösterilmesi amaçlanmıştır.

Gereç ve Yöntemler: Bu amaçla, sağlıklı hücreler 1, 5, 10 µg/mL konsantrasyonlarında *N. sativa* yağı ile ve pozitif kontrol olarak Siklofosfamid ile 68 saat boyunca *in vitro* muamele edildi. Daha sonra ise mikronükleuslar sayıldı.

Bulgular: *N. sativa* yağının 1, 5, 10 µg/mL konsantrasyonlarındaki uygulaması negatif kontrolle karşılaştırıldığında mikronükleus frekansında anlamlı bir artış gözlenmedi. *N. sativa* yağı ve Siklofosfamid'in birlikte uygulandığı gruplarda her üç konsantrasyonda da (1, 5, 10 µg/mL) Siklofosfamid grubuna göre mikronükleus sayısında azalma olduğu görüldü.

Sonuç: *N. sativa* yağının genotoksisite ajanlarına karşı *in vitro* koruyucu etkilerinin olabileceği gösterilmiştir. *N. sativa* yağının genotoksisiteyi giderici etkilerinin mekanizmasının anlaşılması için daha fazla çalışmaya ihtiyaç vardır.

Anahtar kelimeler: Siklofosfamid, *Nigella sativa* yağı, mikronükleus, genotoksisite

*Correspondence: E-mail: murat.zor@lokmanhekim.edu.tr, Phone: +90 536 495 65 96 ORCID-ID: orcid.org/0000-0001-6014-2930
Received: 18.12.2019, Accepted: 02.01.2020

INTRODUCTION

Cyclophosphamide (CP) is a oxazophosphorine derivative of nitogen mustard and is an alkylating agent commonly used as an antineoplastic and immunosuppressive agent.[1-3] CP is one of the universally known anti-neoplastic drugs whose therapeutic efficacy against hematological and solid malignancies and autoimmune diseases such as rheumatoid arthritis, systemic lupus erythematosus and multiple sclerosis.[4] CP is used in high doses for the chemotherapy of various forms of cancer, in low doses in the treatment of autoimmune diseases, and also as an immunosuppressant after organ transplants.[5] CP's chemically reactive metabolic products induce cytotoxicity by alkylating DNA and proteins.[3] CP is known as human carcinogen and has an increased incidence of chromosome aberrations in lymphocytes from patients with malignant and non-malignant diseases.[6] The genotoxicity of CP has been studied in a variety of *in vivo* and *in vitro* systems, mutagenic, teratogenic and carcinogenic, and is routinely used as a positive control in genotoxicity tests.[1,6]

Natural compounds find application in the treatment of refractory diseases, a new trend in modern clinical medicine.[7] *Nigella sativa* (*N. sativa)* is a short-lived annual plant of the Ranunculaceae family, known as black seed, black cumin and fennel flower.[8,9] *N. sativa* is an aromatic plant with tremendous therapeutic properties such as hypotensive, gastroprotective, nephrocurative, nephroprotective, antioxidative, antimicrobial, genoprotective, neuroprotective, immunomodulatory, anti-inflammatory, hypoglycemic, hypolipidemic, anticarcinogenic and hepatoprotective.[9,10] It increases the production of two substances, interferon and interleukin, the first defense shield of the immune system against tumor cells.[11] *N. sativa* seeds are very rich in fixed oil, essential fatty acids, alkaloids, phytosterols, glycolipids and phospholipids, saponins and essential oil components. In seed essential oil; thymoquinone, *p*-cymene and thymol are the active components. Thymoquinone has been shown as a cytotoxic agent in several human tumor cell lines resistant to various multidrug drugs.[1] It has also been shown in another study that gastric cancer cells inhibit their growth.[12] The effect of high dose thymoquinone on stomach was found to be equal to Omeprazole.[13] Molecular mechanisms underlying these anticancer effects; cell cycle arrest, apoptosis, oxidative damage of cellular macromolecules, blockade of tumor angiogenesis and inhibition of tumor migration.[1] Micronucleus analysis methods are widely used in genotoxicity studies at chromosome level. The frequency of micronucleus formation is considered to be an indicator of damage to the genetic material. Micronuclei are those that occur during cell division, originating from centric or ascentric chromosome fragments that are not involved in the core nucleus.[14]

In this study, it was aimed to show the healing effects of *N. sativa* oil at different concentrations against the genotoxic effects of CP by micronucleus test.

MATERIALS AND METHODS

Materials

Micronucleus testing is usually performed in peripheral blood lymphocytes to determine genotoxicity in humans. Because in the studies performed, the increase in the micronucleus frequency in peripheral blood lymphocytes from cancer patients was found to be as much as the micronucleus frequency in the target tissue.[15-17] *N. sativa* oil was obtained from a local vegetable urea shop and stored in dark brown bottles until use. It was dissolved in dimethyl sulfoxide and then applied to the cells at a final concentration of 1, 5 and 10 µg/mL. CP, cytochalasine B, RPMI medium, phytohemaglutinin, antibiotic, fetal calf serum, L-Glutamine and Giemsa solution were obtained from Sigma.

Methods

Micronucleus test was performed according to the method described by Fenech and Morley.[18] For the analysis of micronucleus in binucleated lymphocytes, cell culture was established from 0.2 mL of fresh heparinized blood. Cells were treated with *N. sativa* oil at a final concentration of 1 µg/mL, 5 µg/mL, 10 µg/mL. Cytochalasin B was added to each tube at a final concentration of 6 µg/mL at 44 hours of incubation. After 24 hours of incubation at 37°C, the cells were centrifuged and micronucleus test in peripheral lymphocytes was performed.[18] Cells were harvested with hypotonic (0.4% KCl) and fixative (methanol: acetic acid) solution. Cell suspensions were stained with Giemsa after dropping onto clean glass slides. CP was also used as a positive control. CP was given to the tubes at a final concentration of 0.16 µg/mL. Micronucleus scoring was limited to binuclear lymphocytes with cytoplasm according to the criteria determined by Fenech et al.[19] Two thousand binucleated lymphocytes were scored for each donor (8000 binucleated cells per concentration).[20]

Statistical analysis

Windows for SPSS version 22 statistical software program was used to analyze the data. Experimental and control groups were analyzed with one way Anova. Arithmetic mean (X) ± and standard deviation was determined. $P<0.05$ was considered significant.

RESULTS

Micronucleus data in cells treated with CP and *N. sativa* oil and both are shown in Table 1. Micronucleus frequency for the control group was determined as 3.5. CP treatment increased the micronucleus ratio to 25.2. This value was significantly higher than the control group ($p<0.05$). No significant increase in micronucleus frequency was observed when the application of *N. sativa* oil at concentrations of 1, 5, 10 µg/mL compared with the negative control. There was a decrease in the number of micronucleus in all three concentrations (1, 5, 10 µg/mL) compared to the CP group in the groups treated with *N. sativa* oil and CP (Table 1).

Table 1. Frequency of MN in cultured human lymphocytes treated with *N. sativa* oil

Test substance	Concentrations	MN (X±SD)
Control	-	3.5±0,57
Cyclophosphamide	0.16 µg/mL	25.2±3.8[a]
***N.sativa* oil**	1 µg/mL	3.5±1.29[b]
	5 µg/mL	5.25±0.95[b]
	10 µg/mL	2.75±0.95[b]
Cyclophosphamide + *N.sativa* oil	0.16 µg/mL+1 µg/mL	19.75±2.5[ac]
	0.16 µg/mL+5 µg/mL	17.75±4.64
	0.16 µg/mL+10 µg/mL	20.5±3.55[ac]

SD: Standart deviation, p<0.05, 2000 cells were scored for each tube, [a]: Significant difference from control, [b]: Significant difference from cyclophosphamide,[c]: Significant difference from *Nigella sativa* oil, MN: Micronucleus

DISCUSSION

Phytotherapy is an area that uses plants as health promoting agents to treat diseases. In the conventional use of phytotherapies, the original composition of the plant or a certain percentage of certain components of the plant is generally used.[21] Medicinal plants are considered to be the main source of potentially therapeutically effective new chemicals. According to the data of the World Health Organization, 70-80% of the population in developing countries relies on plants for primary health care.[22] *N. sativa* oil, including the main components of thymoquinone and P-cymene, is considered to have anti-inflammatory, hepatoprotective and reno-protective effects.[23] One of the most commonly used cytogenetic assays for genotoxic evaluation of different agents is Cytokinesis Blocked Micronuclei test in cultured human leukocytes.[22] In this study we investigated the effect of *N. sativa* oil on genotoxicity in human leukocytes. *N. sativa* oil was used in different concentrations (1, 5, 10 µg/mL). Unlike our study, Abdel-Moneim et al.[24] investigated the protective effects of *N. sativa* seeds against genotoxicity and chromotomal aberrations induced by carbon tetrachloride in mouse spermatocytes. In our study, the therapeutic effects of *N. sativa* oil were investigated in spite of the application of CP in lymphocyte cells from healthy individuals instead of mouse spermatocytes. Abdel-Moneim et al.[24] have shown that *N.sativa* is effective in the prevention of CCl_4-induced genetic damage in germ cells and can be used as an adjunct nutritional supplement in the early stages of exposure to mutagens. Similarly, in our study, it was observed that the amount of micronucleus decreased in the group in which CP was used together with *N. sativa* oil compared to the positive control group. In the study of Galhena et al.[25], a mixture of 100-600 µg/mL consisting of *N. sativa* seeds, *Hemidesmus indicus* (*H. indicus*) roots and *Smilax glabra* (*S. glabra*) rhizomes was applied to human lymphocyte culture together with bleomycin and chromosome aberrations such as dicentric chromosome, ascentric fragment, chromatid fractures were examined. According to the results of this study; *N. sativa* seeds, *H. indicus* roots and *S. glabra* rhizomes showed that the mixture has the potential to protect against cytogenetic damage caused by bleomycin in human peripheral lymphocytes. In our study, *N. sativa* oil was used instead of *N. sativa* seeds and only micronucleus frequency was examined. However, when the results were examined, similar to the results of Galhena et al.[25], Hashem et al.[10] concluded that *N. sativa* oil is potentially protective against carbendazim-induced hematoxixity, hepatotoxicity and genotoxicity. In this study, it was determined that *N. sativa* oil moderately improved in terms of micronucleus percentage and DNA fragmentation when applied together with carbendazim and mancozeb. In our study, positive control CP was used to determine the healing effect of *N. sativa* oil and *in vitro* cell culture experiments were performed. Al-Okbi et al.[23] investigated the effect of using *N. sativa* oil alone and in combination with fish oil in CCl_4 treated rats. According to the results of this study, it was observed that combined oral administration of *N. sativa* oil and fish oil-*N. sativa* oil combined with anti-inflammatory and antioxidant activity reduced liver and kidney damage. Nguyen et al.[26] in Morocco investigated the *in vitro* cytotoxicity, genotoxicity and antigenotoxicity of aqueous plant extracts from three different regions (Erfoud, Fkih ben Salah, Settat) by the neutral red uptake test in human C3A cells, the bacterial Vitotox, Ames assays, comet assay and micronucleus test. *N. sativa* seed extracts showed varying degrees of antigenotoxicity depending on where the test specimens came from. Extracts from Fkih ben Salah and Settat were reported to exhibit antigenotoxic effects by significantly reducing the micronucleus number at concentrations of 9 mg/mL. Similarly, in our study, the effects of *N. sativa* oil on micronucleus formation in healthy human lymphocyte cell culture at concentrations of 1, 5 and 10 µg/mL were examined and the genotoxic effects of CP used as positive control were reduced by *N. sativa* oil in all three concentrations. Although *N. sativa* oil concentrations and cell type used in our study were different from those of Nguyen et al.[26], similar results were found. However, the location of the samples, the test and other test conditions may affect the research result.

CONCLUSION

In this study, it was shown that *N. sativa* oil may have curative effects against mutation inducing agents. To understand the mechanism of the genotoxicity effects of *N. sativa* oil, molecular tests, testing of different concentrations and *in vivo* experiments are needed.

Conflict of Interest: No conflict of interest was declared by the authors.

REFERENCES

1. Yuksel S, Tasdemir S, Korkmaz S. Protective effect of thymoquinone against cyclophosphamide-induced genotoxic damage in human lymphocytes. Bratisl Lek Listy. 2017;118:208-211.
2. Tuorkey MJ. Therapeutic Potential of *Nigella sativa* Oil Against Cyclophosphamide-Induced DNA Damage and Hepatotoxicity. Nutr Cancer. 2017;69:498-504.
3. Habibi E, Shokrzadeh M, Ahmadi A, Chabra A, Naghshvar F, Keshavarz-Maleki R. Genoprotective effects of Origanum vulgare ethanolic extract against cyclophosphamide-induced genotoxicity in mouse bone marrow cells. Pharm Biol. 2015;53:92-97.

4. Basu A, Bhattacharjee A, Samanta A, Bhattacharya S. Prevention of cyclophosphamide-induced hepatotoxicity and genotoxicity: Effect of an L-cysteine based oxovanadium(IV) complex on oxidative stress and DNA damage. Environ Toxicol Pharmacol. 2015;40:747-757.
5. Ince S, Kucukkurt I, Demirel HH, Acaroz DA, Akbel E, Cigerci IH. Protective effects of boron on cyclophosphamide induced lipid peroxidation and genotoxicity in rats. Chemosphere. 2014;108:197-204.
6. Doherty AT, Hayes J, Holme P, O'Donovan M. Chromosome aberration frequency in rat peripheral lymphocytes increases with repeated dosing with hexamethylphosphoramide or cyclophosphamide. Mutagenesis. 2012;27:533-539.
7. Ijaz H, Tulain UR, Qureshi J, Danish Z, Musayab S, Akhtar MF, Saleem A, Khan KK, Zaman M, Waheed I, Khan I, Abdel-Daim M. Review: *Nigella sativa* (Prophetic Medicine): A Review. Pak J Pharm Sci. 2017;30:229-234.
8. Edizer DT, Yigit O, Cinar Z, Gul M, Kara E, Yigitcan B, Hayır D, Atas A. Protective role of intratympanic *Nigella sativa* oil against gentamicin induced hearing loss. Int J Pediatr Otorhinolaryngol. 2017;97:83-88.
9. Mosbah R, Djerrou Z, Mantovani A. Protective effect of *Nigella sativa* oil against acetamiprid induced reproductive toxicity in male rats. Drug Chem Toxicol. 2018;41:206-212.
10. Hashem MA, Mohamed WAM, Attia ESM. Assessment of protective potential of *Nigella sativa* oil against carbendazim- and/or mancozeb-induced hematotoxicity, hepatotoxicity, and genotoxicity. Environ Sci Pollut Res Int. 2018;25:1270-1282.
11. Swamy SM, Tan BK. Cytotoxic and immunopotentiating effects of ethanolic extract of N*igella sativa* L. seeds. J Ethnopharmacol. 2000;70:1-7.
12. Badary OA, Al-Shabanah OA, Nagi MN, Al-Rikabi AC, Elmazar MM. Inhibition of benzo(a)pyrene-induced forestomach carcinogenesis in mice by thymoquinone. Eur J Cancer Prev. 1999;8:435-440.
13. Magdy MA, Hanan el A, Nabila el M. Thymoquinone: Novel gastroprotective mechanisms. Eur J Pharmacol. 2012;697:126-131.
14. Norppa H, Falck GC. What do human micronuclei contain? Mutagenesis. 2003;18:221-233.
15. Kirsch-Volders M, Elhajouji A, Cundari E, Van Hummelen P. The in vitro micronucleus test: a multi-endpoint assay to detect simultaneously mitotic delay, apoptosis, chromosome breakage, chromosome loss and non-disjunction. Mutat Res. 1997;392:19-30.
16. Vanparys P, Vermeiren F, Sysmans M, Temmerman R. The micronucleus assay as a test for the detection of aneugenic activity. Mutat Res. 1990;244:95-103.
17. Cheng TJ, Christiani DC, Xu X, Wain JC, Wiencke JK, Kelsey KT. Increased micronucleus frequency in lymphocytes from smokers with lung cancer. Mutat Res. 1996;349:43-50.
18. Fenech M, Morley AA. Cytokinesis-block micronucleus method in human lymphocytes: effect of in vivo aging and low dose X irradiation. Mutat Res.1986; 161:193-198.
19. Fenech M, Chang WP, Kirsch-Volders M, Holland N, Bonassi S, Zeiger E; HUman MicronNucleus project. HUMN project: detailed description of the scoring criteria for the cytokinesis-block micronucleus assay using isolated human lymphocyte cultures. Mutat Res. 2003;534:65-75.
20. Ionescu ME, Ciocirlan M, Becheanu G, Nicolaie T, Ditescu C, Teiusanu AG, Gologan SI, Arbanas T, Diculescu MM. Nuclear Division Index may Predict Neoplastic Colorectal Lesions. Maedica (Buchar). 2011;6:173-178.
21. Falzon CC, Balabanova A. Phytotherapy: An Introduction to Herbal Medicine. Prim Care. 2017;44:217-227.
22. Milosevic-Djordjevic O, Radovic Jakovljevic M, Markovic A, Stankovic M, Ciric A, Marinkovic D, Grujičić D. Polyphenolic contents of Teucrium polium L. and Teucrium scordium L. associated with their protective effects against MMC-induced chromosomal damage in cultured human peripheral blood lymphocytes. Turk J Biol. 2018;42:152-162.
23. Al-Okbi SY, Mohamed DA, Hamed TE, Edris AE, Fouda K. Hepatic Regeneration and Reno-Protection by Fish oil, *Nigella sativa* Oil and Combined Fish Oil/*Nigella sativa V*olatiles in CCl4 Treated Rats. J Oleo Sci. 2018;67:345-353.
24. Abdel-Moneim AM, Essawy AE, Hamed SS, Abou-Gabal AA, Alzergy AA. Protective effect of *Nigella sativa* seeds against spermatocyte chromosomal aberrations and genotoxicity induced by carbon tetrachloride in mice. Environ Sci Pollut Res Int. 2017;24:11677-11682.
25. Galhena BP, Samarakoon SSR, Thabrew MI, Paul SFD, Perumal V, Mani C. Protective Effect of a Polyherbal Aqueous Extract Comprised of *Nigella sativa* (Seeds), Hemidesmus indicus (Roots), and Smilax glabra (Rhizome) on Bleomycin Induced Cytogenetic Damage in Human Lymphocytes. Biomed Res Int. 2017;2017:1856713.
26. Nguyen T, Talbi H, Hilali A, Anthonisse R, Maes A, Verschaeve L. *In vitro* toxicity, genotoxicity and antigenotoxicity of *Nigella sativa* extracts from different geographic locations. South African Journal of Botany. 2019;126:132-141.

Turk J Pharm Sci 2020;17(1):119-26
DOI: 10.4274/tjps.galenos.2018.35403

REVIEW

The Contribution of Serotonergic Receptors and Nitric Oxide Systems in the Analgesic Effect of Acetaminophen: An Overview of the Last Decade

Asetaminofenin Analjezik Etkisinde Serotonerjik Reseptörlerin ve Nitrik Oksit Sisteminin Katkısı: Son On Yıla Genel Bakış

Yeşim HAMURTEKİN, Ammar NOUILATI, Cansu DEMİRBATIR, Emre HAMURTEKİN*

Eastern Mediterranean University, Faculty of Pharmacy, Department of Pharmacology, Famagusta, North Cyprus Via Mersin 10, Turkey

ABSTRACT

Acetaminophen is a widely used analgesic and antipyretic agent. It is also available in over the counter formulations, which has increased its wide use. There have been many studies to date that have aimed to evaluate the mechanism of the analgesic action of acetaminophen. Additional to the inhibition of the cyclooxygenase pathway in the central nervous system, the involvement of opioidergic, cannabinoidergic, dopaminergic, cholinergic, and nitrergic systems as well as the contribution of descending pain inhibitory systems like the bulbospinal serotonergic pathway has been proposed as possible mechanisms of the analgesic action of acetaminophen. In this review, we aimed to collect the data from studies revealing the contribution of the central serotonergic system and the role of central nervous system-located serotonergic receptor subtypes in the analgesic effect of acetaminophen. While doing this, we mainly focused on the research that has been performed in the last ten years and tried to link the previous data with the lately added results. In addition to serotonergic system involvement, we also reviewed the role of nitric oxide in the analgesic action of acetaminophen, especially with the new findings reported over the last decade.

Key words: Acetaminophen, serotonin, pain, nitric oxide

ÖZ

Asetaminofen yaygın kullanılan analjezik ve antipiretik bir ajandır. Reçetesiz verilebilen formülasyonlarının da mevcudiyeti sık kullanımını artırmıştır. Günümüze kadar asetaminofenin analjezik etki mekanizmasını inceleyen bir çok çalışma bulunmaktadır. Santral sinir sisteminde siklooksijenaz yolağını inhibe etmesinin yanında, opioiderjik, kannabinoiderjik, dopaminerjik, kolinerjik ve nitrerjik sistemler kadar, bulbospinal serotonerjik yolaklar gibi analjezik etkili inen inhibitör yolakların da asetaminofenin analjezik etkisinde katkısı olan olası mekanizmalar olduğu önerilmiştir. Bu derlemede santral serotonerjik sistem ve santral sinir sistemindeki serotonerjik reseptör alt tiplerinin parasetamolün analjezik etkisine katkısını ortaya koyan verileri bir araya getirmeyi amaçladık. Bunu yaparken, esas olarak son on yılda yapılmış çalışmalara odaklandık ve önceki verilerle son eklenenler arasında bir bağlantı kurmaya çalıştık. Serotonerjik sistemin katkısına ek olarak, aynı zamanda son on yıldaki yeni bulgularla asetaminofenin ağrı kesici etkisinde nitrik oksidin rolünü de derledik.

Anahtar kelimeler: Asetaminofen, serotonin, ağrı, nitrik oksit

INTRODUCTION

Although acetaminophen is one of the most commonly used medications, its exact analgesic mechanism of action is still a mystery. Not only has decreased prostaglandin production via cyclooxygenase (COX) enzyme inhibition (especially COX-2, and a central splice variant of COX-1, which is COX-3) been proposed as the primary mechanism of analgesic action,[1-3] but also the contribution of cannabinoidergic[4] and opioidergic[5] systems has been shown. In addition to these main contributions, cholinergic[6] and dopaminergic[7] systems have also been shown to be involved in acetaminophen analgesia. Not only the above neuronal systems, but also the role of calcium channels (T-type voltage-gated calcium channels) has been proposed to be involved in the analgesic effect of acetaminophen.[8]

The aim of this review is to discuss the two other proposed mechanisms for the analgesic action of acetaminophen, namely the serotonergic system with its various receptor subtypes and nitric oxide (NO) systems. It is focused on the findings in the last decade regarding the contribution of these two systems in acetaminophen analgesia with the intention of comparing these

*Correspondence: E-mail: emre.hamurtekin@emu.edu.tr, Phone: +90 392 630 2449 ORCID-ID: orcid.org/0000-0001-8305-9283
Received: 17.08.2018, Accepted: 18.10.2018

new findings with the previous results and combining these novel findings.

The role of the central serotonergic system in acetaminophen analgesia

In 1991, the antinociceptive effect of acetaminophen in a formalin test was reduced following the chemical impairment of spinal serotonergic pathways (bulbospinal serotonergic pathway) by intrathecal 5,6-dihydroxytryptamine (5,6-DHT) administration in rats. That study indicated the contribution of the spinal serotonergic system in the analgesic action of acetaminophen.[9] This was followed by the finding that the antinociceptive effect of systemic acetaminophen administration to rats was reduced by the administration of *p*-chlorophenylalanine, which was known to deplete the brain's serotonin levels. Additionally, acetaminophen increased serotonin levels in the brain cortex and pons. As a result, these findings showed the involvement of the supra-spinal serotonergic system in acetaminophen analgesia.[10]

These previous results have been confirmed and also expanded with some additional studies performed in the last decade. In animal studies, central serotonergic system impairment with intrathecal and intracerebroventricular 5,7-DHT administration and assessment of brain serotonin levels were the most commonly used methods. These methods enabled the evaluation of serotonergic system involvement in acetaminophen analgesia. Among these studies, some differences were observed in the effects of chemical destruction of the central serotonergic system on the analgesic effect of acetaminophen between different animal pain models and doses of acetaminophen. Recent results are summarized in Table 1.

Acetaminophen-induced serotonin increases have also been confirmed in recent studies. Intraperitoneal acetaminophen administration (400 mg/kg) induced approximately 40% and 75% increases in serotonin levels in the pons and frontal cortex, respectively. These increases in serotonin levels have been found to be related to central (hydroxytryptamine) 5-HT_2 receptors as well as opioid receptors (μ_1 and κ).[5] These data were confirmed in a study by Vijayakaran et al.[14] in which acetaminophen (400 mg/kg; oral) caused increases in serotonin levels in the rat frontal cortex and brain stem. Serotonin increases were observed not only following acute applications but also following chronic acetaminophen applications. Subcutaneous acetaminophen in 10 and 50 mg/kg doses was administered to 3-month-old rats and serotonin levels in the prefrontal cortex, hippocampus, hypothalamus, and striatum were analyzed. Serotonin levels increased after the 10 mg/kg acetaminophen dose (not with 50 mg/kg) in the prefrontal cortex but not in the other brain regions analyzed in this study. Additionally, 5-HIAA levels decreased in the hypothalamus and striatum.[15] All these recent studies have confirmed the idea that systemic acetaminophen administration increases serotonin levels in the brain cortex and brain stem (pons) and meet at a common point, which is that acute and chronic systemic administration of acetaminophen induces changes in central serotonergic neurotransmission. It can be concluded that, despite the involvement of 5-HT_2-serotonergic and opioid receptors in acetaminophen-induced serotonin increases in some brain regions,[5] apparently the exact mechanism (alterations in serotonin metabolism, release, or uptake) is still not clear and needs to be clarified.

The signs of serotonergic involvement in acetaminophen-induced analgesia in humans were also studied. However, despite some supportive results, serotonergic contribution seems still doubtful in human studies due to the challenges in studying pain in humans. Controversial data have been observed between the results in healthy volunteers and patients with pain.[16] The findings of these studies will be discussed in the following sections.

Some metabolites of acetaminophen and the central serotonergic system

Acetaminophen, following its systemic administration, has been shown to be biotransformed to an amine compound, *p-aminophenol*, which occurs mainly in the liver. Enzymatic conversion of *p-aminophenol* to N-arachidonoyl-phenolamine

Table 1. Effect of the deterioration of the bulbospinal serotonergic pathway with 5,7-dihydroxytryptamine (5,7 DHT) in the antinociceptive effect of acetaminophen in different pain models in some studies performed in the last decade

5,7-DHT	Acetaminophen	Pain model	Effect	Animal	References
100 µg; i.t.	3 mg/kg; i.p.	Paw pressure test	decrease	Rat (Sprague Dawley)	[11]
50 µg; i.t.	200-600 mg/kg	Tail flick test	decrease	Mouse (BALB/c)	[12]
50 µg; i.t.	200-600 mg/kg	Hot plate test	decrease	Mouse (BALB/c)	[12]
50 µg; i.t.	200-600 mg/kg	Plantar incision (thermal hyperalgesia)	decrease	Mouse (BALB/c)	[12]
70 µg; i.c.v. (neonatal age)	100 mg/kg; oral	Hot plate test	decrease	Adult rat (Wistar)	[13]
70 µg; i.c.v. (neonatal age)	100 mg/kg; oral	Writhing test	decrease*	Adult rat (Wistar)	[13]
70 µg; i.c.v. (neonatal age)	100 mg/kg; oral	Tail immersion	no change	Adult rat (Wistar)	[13]
70 µg; i.c.v. (neonatal age)	100 mg/kg; oral	Paw pressure test	no change	Adult rat (Wistar)	[13]
70 µg; i.c.v. (neonatal age)	100 mg/kg; oral	Formalin test	no change	Adult rat (Wistar)	[13]

*Decrease in the hot plate test was more obvious than the decrease in the writhing test, i.t.: Intrathecal, i.c.v.: Intracerebroventricular, DHT: Dihydroxytryp tamine

(AM404), which is catalyzed by fatty acid amide hydrolase (FAAH) enzyme with the conjugation of arachidonic acid, occurs in the brain, spinal cord, and dorsal root ganglia.[17] AM404 metabolite of acetaminophen has been shown to activate TRPV1 (transient receptor potential vanilloid-1, capsaicin receptor) channels and act as a CB1 (cannabinoid receptor type-1) ligand.[17,18] Mallet et al.[11] showed that CB1 receptors are vital for the analgesic action of orally administered acetaminophen, because CB1 receptor antagonism as well as gene deletion totally inhibited the analgesic action of acetaminophen in various pain models, i.e. thermal, mechanical, and chemical (formalin) painful stimuli in rats. CB1 receptor related activation of the descending serotonergic pathway has been suggested as the following step, because the antinociceptive effect of systemic acetaminophen was negated following the chemical impairment of the spinal serotonergic pathway. As a CB1 receptor ligand, AM404 metabolite of acetaminophen has been claimed to be responsible for this action. Spinal $5HT_{1A}$ and $5HT_{3/4}$ receptors have been shown to contribute at the spinal cord level to the analgesic action of acetaminophen eventually. On the other hand, Ruggieri et al.[5] claimed that AM404 can only partially contribute to the analgesic action of systemically administered acetaminophen, depending on the fact that the observed analgesic action of AM404 was approximately half of the analgesic action of acetaminophen. This AM404 contribution seems to be related to the central $5HT_3$ receptors, but not to $5HT_{1A}$ or $5HT_2$ receptor subtypes. Interestingly, a central $5HT_2$ receptor subtype, but not $5HT_3$ or $5HT_{1A}$, has been found to be involved in the analgesic action of acetaminophen depending on the dose-dependent inhibition of acetaminophen's analgesic action with systemic ketanserin. Another important finding of their study was the increase in serotonin levels in the pons and frontal cortex following the administration of acetaminophen, but not with AM404. All these results of this study pointed out that acetaminophen and its metabolite AM404 have both analgesic actions but the mechanisms that play a role in this analgesic action differ between these two compounds. These differences regarding the contribution of AM404 to acetaminophen analgesia and the involvement of different serotonergic receptor subtypes may be related to the use of different types and different administration routes of serotonergic receptor subtype antagonists as well as the dose of acetaminophen, which was different in the two studies.

Finally, Barrière et al.[19] showed the contribution of a descending serotonergic antinociceptive pathway in the analgesic effect of 4-aminophenol, another metabolite of acetaminophen as mentioned above. The analgesic effect of intraperitoneally administered 4-aminophenol was reported to depend on AM404 formation in the brain, which is catalyzed by FAAH enzyme, and TRPV1 and CB1 receptor stimulation-induced descending antinociceptive serotonergic system activation and spinal $5\text{-}HT_3$ and $5\text{-}HT_{1A}$ serotonergic receptor subtypes were claimed to play an important role.

As a result, studies showed that not only acetaminophen itself but also its metabolites like AM404 and 4-aminophenol may play an important role in the analgesic action of acetaminophen. It can be concluded that AM404 metabolite contributes to the analgesic action of systemic acetaminophen to some extent and activates the descending serotonergic antinociceptive pathway via the contribution of central TRPV1 and CB1 receptors. Spinal serotonergic receptor subtypes eventually play a role in the antinociceptive action, which may act differently to acetaminophen and its metabolites.

Role of $5\text{-}HT_1$ receptors

It is known that $5\text{-}HT_{1A}$ and $5\text{-}HT_{1B}$ serotonergic receptor subtypes are largely located at the supra-spinal level: $5\text{-}HT_{1A}$ on the cell bodies and dendrites of serotonergic neurons and $5\text{-}HT_{1B}$ mainly on the axon terminals. Both $5\text{-}HT_{1A}$ and $5\text{-}HT_{1B}$ serotonergic receptor subtypes have important effects on extracellular serotonin levels via modulation of nerve firing mainly for $5\text{-}HT_{1A}$ receptors and by modification of serotonin release for mainly $5\text{-}HT_{1B}$ serotonergic receptor subtypes.[20] Blockade of $5\text{-}HT_{1A}$ receptor subtypes has been shown to enhance the extracellular levels of serotonin.[21] Involvement of $5\text{-}HT_1$ serotonergic receptor subtypes in the analgesic effect of acetaminophen has been studied in various studies with different animal pain models and with different ligands for $5\text{-}HT_{1A}$ and $5\text{-}HT_{1B}$ receptor subtypes. Incompatible results were obtained in earlier studies regarding the contribution of $5\text{-}HT_1$ serotonergic receptors in the analgesic effect of acetaminophen. An earlier study showed that pre-administered WAY-100635 ($5HT_{1A}$ receptor antagonist, 10 µg/rat; intrathecal) did not change the analgesic effect of intravenous acetaminophen (200 mg/kg) in a rat paw pressure test.[22] However; intrathecal administration of WAY-100635 (40 µg/rat) has been shown to block acetaminophen analgesia (3 mg/kg, i.p.) in both phase I and II of a rat formalin test.[11] In addition, intraperitoneal administration of NAN-190 ($5\text{-}HT_1$ serotonergic receptor antagonist, 1-5 mg/kg) did not change the acetaminophen analgesia in hot plate or paw pressure tests and did not show any blockage of acetaminophen-induced serotonin increases in the frontal cortex and pons.[5] However, it should not be underestimated that NAN-190 could also block the α_2-adrenergic receptors and this finding can raise some suspicions regarding NAN-190 when using it as a specific $5\text{-}HT_{1A}$ receptor antagonist.[23] Interestingly, another earlier study showed that systemic administration of $5\text{-}HT_{1A}$ and $5\text{-}HT_{1B}$ receptor antagonists enhanced the acetaminophen analgesic action, whereas stimulation of the same receptor subtypes blocked the acetaminophen analgesia in a hot plate test.[24] This was in close agreement with the findings reported by Sandrini et al.[25] in which systemic administration of CP 93129 ($5\text{-}HT_{1B}$ receptor agonist) prevented acetaminophen analgesia in hot plate and paw pressure tests. These two findings suggested that increased serotonin release and/or enhanced firing of serotonergic nerves, which liberate themselves from the suppressing effects of $5\text{-}HT_{1A}$ and $5\text{-}HT_{1B}$ receptors, augment the antinociceptive action of acetaminophen. The findings of a recent study also were in good accordance with those previous results. Oral buspirone as a $5HT_1$ serotonergic receptor agonist blocked the antinociceptive action of intraperitoneal acetaminophen (200 mg/kg) in a hot plate test and in the early phase of a formalin test in mice.[26]

As a result, when taken together it can be concluded that despite some negative results 5-HT_{1A} and 5-HT_{1B} serotonergic receptor subtypes are likely to contribute to acetaminophen analgesia. However, characteristics of this contribution seem to depend on the ligands and animal pain models tested as well as the location (spinal/supra-spinal or presynaptic/postsynaptic) of 5-HT_1 serotonergic receptors and still needs to be evaluated.

Role of 5-HT_2 receptors

The possible involvement of 5-HT_2 serotonergic receptor subtypes in the analgesic effect of acetaminophen has also been examined in recent studies. Ruggieri et al.[5] showed a statistically significant reduction in the antinociceptive action of acetaminophen when ketanserin (5 mg/kg; subcutaneous) was administered systemically before acetaminophen (400 mg/kg; intraperitoneal), whereas it did not change the antinociceptive effect of AM404 in hot plate and paw pressure tests. In another study, Dogrul et al.[12] showed that intrathecally administered ketanserin (10 µg) did not change the antinociceptive effect of acetaminophen (200-600 mg/kg; oral) in hot plate or tail flick tests or in thermal hyperalgesia after incision of the hind paw. This recent study seems to reveal findings opposite those from the study by Courade et al.[22] due to the fact that intrathecally administered ketanserin (5-HT_{2A} antagonist) as well as mesulergine (5-HT_{2C} antagonist) decreased vocalization thresholds, which had been increased by intravenously administered propacetamol (water soluble prodrug form of acetaminophen). The differences in the study designs, like the animals (mice/rat), the animal pain models (tail flick-hot plate/paw pressure test) that were used, and the timing of ketamine administration (before or after acetaminophen), between these two studies should be considered. Even so, when these studies are considered together, although the involvement of spinally located 5-HT_2 receptors in acetaminophen analgesia needs to be elucidated, it can be speculated that supra-spinal 5-HT_2 serotonergic receptors may contribute to the analgesic effects of acetaminophen. Additionally, 5-HT_2 receptors are likely to be involved in the antinociceptive effect of acetaminophen, not in the antinociceptive effect of its metabolite, AM404. Supporting this assumption, systemic ketanserin has also been shown to block acetaminophen-induced serotonin increases in the frontal cortex and pons.[5] Acetaminophen administration has also been shown to increase the serotonin levels in supra-spinal structures and led to a down-regulation of 5-HT_{2A} receptor subtypes in the frontal cortex and brain stem.[14] In that study, the authors stated that an increase in serotonin release triggered by acetaminophen caused down-regulation of 5-HT_{2A} receptors related to the long duration of stimulus by serotonin. This assertion was supported by the study by Srikiatkhachorn et al.[27] claiming that 5-HT_{2A} receptor down-regulation is important for the analgesic effect of acetaminophen. Thus, it may be speculated that supra-spinal located (most likely post-synaptic) 5-HT_2 receptor stimulation by serotonin, which is enhanced following acetaminophen administration, contributes to the analgesic action of acetaminophen. Recent results are summarized in Table 2.

Role of 5-HT_3 receptors

The contribution of 5-HT_3 receptors in the analgesic effect of acetaminophen has been tested in various animal pain models as well as in human studies. Different 5-HT_3 receptor antagonists, like granisetron, ondansetron, and tropisetron, have been used to study the interaction of these receptor subtypes in acetaminophen analgesia. In 1996, the indirect contribution of spinal 5-HT_3 serotonergic receptor subtypes was pointed out based on the findings of research. In that research, it was shown that spinal tropisetron totally inhibited the antinociceptive action of systemically and spinally administered acetaminophen in a rat paw pressure test.[28] This finding had also been confirmed in inflammatory pain models.[29] In the last decade, a study by Mallet et al.[11] showed that intrathecal application of 0.5 µg of tropisetron pre-treatment blocked the increased vocalization thresholds by systemic administration of acetaminophen, which was in good accordance with the previous findings. However, studies with the other tested 5-HT_3 receptor antagonists revealed mostly opposite results. Ondansetron administration (systemic as well as intrathecal) was shown not to alter the analgesic effect of acetaminophen significantly.[25,30] Recent studies also confirmed this finding. Systemic ondansetron pretreatment (2 mg/kg; subcutaneous) did not alter the effect of acetaminophen in hot plate or paw pressure tests in rats,[5] in good accordance with the finding that spinally administered ondansetron caused no change in the effect of orally administered acetaminophen-induced analgesia in hot plate or tail flick tests or in thermal hyperalgesia in a plantar-incision model.[12] An exception is a study in which acetaminophen-induced analgesia was blocked by ondansetron in a mouse formalin test.[31] Among these studies, differential involvement of 5-HT_3 receptors in acetaminophen and AM404-induced analgesia (similar to ketanserin) has been shown in which ondansetron administration was able to block the analgesic effect of AM404.[5] Another 5-HT_3 receptor antagonist, granisetron, caused no significant changes in the analgesic effect of acetaminophen in a paw pressure test.[22,30] As a result, when the animal studies over the last ten years are considered together with the previous data, we can conclude that administration of ondansetron and granisetron is not likely to alter the effect of acetaminophen-induced analgesia, whereas tropisetron inhibits the analgesic effect of acetaminophen in various animal pain models. These different contributions can be explained by the differences between these antagonists regarding their pharmacokinetical properties (especially primary responsible cytochrome p450 system in the liver for their metabolism), 5-HT_3 receptor binding affinities, selectivity and specificity on 5-HT_3 receptors, and their duration of action.[32,33] However, another issue raised at this point was the examination of 5-HT_3 receptor subtype contribution in the interaction between tropisetron- and acetaminophen-induced analgesia due to the finding that acetaminophen analgesia was not altered by other 5-HT_3 receptor antagonists like ondansetron and granisetron. Additionally, spinal 5-HT_3 receptor antisense oligodeoxynucleotide pre-treatment, which aimed to decrease the synthesis of 5-HT_3 receptors, did not inhibit the antinociceptive action of acetaminophen.[30] As a result, it

Table 2. Some studies on the effect on the role of 5-HT_2 receptors on the analgesic effect of acetaminophen in different pain models

Acetaminophen	5-HT_2 antagonist	Animal	Pain model	Effect on acetaminophen analgesia	Reference
200 mg/kg, i.v.	Ketanserin & mesulergine (10 µg, i.t.)-5 min before acetaminophen	Rat	Paw pressure	Decrease	22
400 mg/kg, i.p.	Ketanserin (5 mg/kg, s.c.)	Rat	Hot plate	Decrease	5
400 mg/kg, i.p.	Ketanserin (5 mg/kg, s.c.)	Rat	Paw pressure	Decrease	5
200-600 mg/kg, oral	Ketanserin (10 µg, i.t.)- 60 min after acetaminophen	Mice	Tail flick test	No effect	12
200-600 mg/kg, oral	Ketanserin (10 µg, i.t.)- 60 min after acetaminophen	Mice	Hot plate	No effect	12
200-600 mg/kg, oral	Ketanserin (10 µg, i.t.)- 60 min after acetaminophen	Mice	Post-incision	No effect	12

i.v.: Intravenous, i.p.: Intraperitoneal, s.c.: Subcutaneous, i.t.: Intrathecal

has been started to be speculated that not the spinal 5-HT3 receptor subtypes but another tropisetron-sensitive receptor may play a role in the analgesic action of acetaminophen.[30] Additionally, it has been indicated that tropisetron can also show affinity to other receptors like α7-nicotinic receptor subtypes.[30,34] When all these are considered together, the role of central 5-HT3 serotonergic receptors in the analgesic effect of acetaminophen seems to be clarified with further studies.

The contribution of 5-HT_3 receptors in the analgesic effect of acetaminophen has also been studied in humans using tropisetron, granisetron, and ondansetron. These studies had two important goals: to reveal the involvement of 5-HT_3 serotonergic receptors in acetaminophen analgesia in humans and evaluate the possible drug interaction between 5-HT_3 blockers and acetaminophen, which are used in cancer patients together for vomiting and pain management, respectively. The first report showed blockage of the analgesic effect of acetaminophen (1 g, oral) when administered after tropisetron (5 mg, i.v.) or granisetron (3 mg, i.v.) in healthy volunteers tested with electrically stimulated pain.[35] The results of another study revealed that descending serotonergic inhibitory pathway stimulation by acetaminophen contributed to acetaminophen analgesia in healthy volunteers where central 5-HT_3 receptors were involved.[36] These data were confirmed by a randomized, double-blind, and placebo-controlled study conducted in 16 healthy volunteers in which the combination of 1 g intravenous acetaminophen with 5 mg of tropisetron exerted no analgesic action in electrically stimulated pain. In that study, tropisetron and acetaminophen alone both led to analgesic actions.[37] The analgesic action of tropisetron administration alone was also confirmed by Tiippana et al.[16] in healthy volunteers. Due to the fact that co-administration of acetaminophen with tropisetron in healthy volunteers did not lead to statistically significant changes in the blood levels of acetaminophen,[35,37] it has been claimed that the interaction between acetaminophen and tropisetron was pharmacodynamic. However, studies performed in post-operative patients revealed confusing results that were not totally parallel with the results of healthy volunteers. Ondansetron (4 mg) did not change the analgesic action of acetaminophen in women who underwent laparoscopic hysterectomy.[38] In a study performed in 36 patients who underwent ear surgery, those receiving a combination of tropisetron and acetaminophen reported higher pain scores but the increase was not statistically significant. However, patients who received tropisetron and acetaminophen needed more rescue analgesic agent.[39] A randomized, double-blinded study showed that ondansetron (8 mg) reduced the analgesic effect of acetaminophen (1 g) in patients who had undergone abdominal hysterectomy; however, this reduction was in a short period of time.[40]

The results of those human studies indicate that there is a questionable interaction between acetaminophen analgesia and 5-HT_3 blockers due to some conflicting results. Those conflicting results, showing a lack of obvious interaction, were mainly related to post-operative pain conditions.[38,39] However, in healthy volunteers, the interaction between acetaminophen and 5-HT_3 blockers (tropisetron and granisetron) seems more obvious and is likely to be a pharmacodynamic interaction.[35-37] Apparently, studies with larger patient populations with different painful conditions are needed to clarify the interaction between 5-HT_3 blockers and acetaminophen in humans.

Role of 5-HT_7 receptors

5-HT_7 receptors are G protein-coupled receptors linked with adenylyl cyclase and detected in the central nervous system regions that are involved in pain transmission, like the cerebral cortex, the thalamus, and the superficial lamina of the dorsal horn.[41] Despite the fact that 5-HT_7 receptors are one of the serotonergic receptor subtypes that have been studied less compared to the other subtypes (5-HT_1, 5-HT_2, and 5-HT_3 subtypes),[41] some studies pointed out the contribution of these receptors to the antinociceptive action of acetaminophen in the last decade. Dogrul et al.[12] used SB-269970 as a selective 5-HT_7 receptor antagonist to evaluate the role of these receptors in acetaminophen analgesia and administered intrathecally (10 µg) after the oral administration of 200-600 mg/kg acetaminophen in mice. Intrathecal administration of SB-269970 blocked the antinociceptive action of acetaminophen in tail flick and hot plate tests. Similarly, intrathecal SB-269970 blocked the antihyperalgesic action of oral acetaminophen in a plantar-incision model. This study was the first to reveal the contribution of spinal 5-HT_7 receptors in the antinociceptive action of acetaminophen. A following study showed that an

intrathecally administered lower dose of SB-269970 (3 µg) was again successful in reversing the analgesic action of systemic acetaminophen in phase II of a formalin test in mice. This finding was important to confirm the contribution of spinal 5-HT_7 receptors in acetaminophen analgesia, but also revealed reduction in the reversing effect of SB-269970 administration on acetaminophen analgesia in mice lacking adenosine type-1 receptors, which additionally indicated a strong interaction between the adenosinergic system and 5-HT_7 receptors in the analgesic action of acetaminophen.[42]

The role of nitric oxide in acetaminophen analgesia

NO is widely accepted as an important messenger molecule and neurotransmitter in the central nervous system that is involved in various physiological functions.[43,44] NO plays important roles in pain transmission, either inducing hyperexcitability leading to hyperalgesia or exerting antinociceptive actions.[45-47]

Björkman et al.[48] in 1994 showed that suppression of N-methyl-D-aspartate and substance P-induced pain related behaviors with acetaminophen administration was reversed by L-arginine administration to rats. Their study pointed out the involvement of neuronal NO systems in the analgesic action of acetaminophen. Additionally and in good accordance with that study, neuronal NO synthase was found to be involved in the analgesic effect of acetaminophen when acetaminophen was used in lower doses (especially with 100 mg/kg, oral) in the Randall-Selitto pain model, whereas both neuronal and inducible NO synthases were found to be involved in the analgesic action of acetaminophen in lower doses (especially 50 and 100 mg/kg, oral) in a writhing test. However, the involvement of NO systems was weak or nonexistent with the maximal doses of acetaminophen.[49] It has also been shown that acetaminophen inhibited induced NO synthesis in spinal cord tissue.[50] As a result, it can be concluded that NO systems are involved in acetaminophen analgesia and it is more likely that suppression of the central NO systems contributes to the central analgesic mechanisms of acetaminophen.

When focusing on the findings related to the interaction between acetaminophen and NO in the last decade, it might be appropriate not to underestimate the recent studies related to NO-acetaminophen (NCX-701). NO-acetaminophen is a novel compound with a combination of NO releasing moiety with acetaminophen.[51] This novel compound has been shown to exert enhanced analgesic activity compared to the parent compound in non-inflamed, acetic-acid induced, and inflammatory pain models[51-53] and was also analgesic in arthritis-related pain.[54] Additionally, NO-acetaminophen had considerable anti-inflammatory activity and less hepatotoxic potential compared to acetaminophen.[51,52] The mechanism of action of NO-acetaminophen has been suggested to be different from that of acetaminophen itself. It has been proposed that although NO-acetaminophen and acetaminophen may share some common mechanisms like COX inhibition, the sustained release of low amounts of NO when combined with specific pharmacological actions of acetaminophen may add different but not clearly understood pharmacological properties. Inhibition of the wind-up phenomenon indicating a mechanism of action in the central nervous system level, more probably in the spinal cord, and reduction in the amounts of some cytokines in the peripheral tissues has been proposed.[53,55]

Additional to the above accumulated data related to the promising effects of NO-acetaminophen, the antinociceptive effect of intravenously as well as intrathecally administered NO-acetaminophen has also been shown in a neuropathic pain model (partial ligation of the sciatic nerve) in rats, where acetaminophen alone was ineffective. In good accordance with the previous speculations, the spinal cord was claimed to be the anatomic region involved in this antihyperalgesic action of NO-acetaminophen. Addition of gabapentin to NO-acetaminophen showed a synergistic effect.[56] Similar to gabapentin, lowered doses of NO-acetaminophen also have been shown to enhance the analgesic effect of an α_2-adrenergic receptor agonist, medetomidine, when combined with the sub-effective doses of NO-acetaminophen in a carrageenan-induced inflammatory model in rats.[57] These two recent studies with NO-acetaminophen pointed out the beneficial effects of this novel acetaminophen compound in neuropathic and inflammatory pain conditions. Additionally, it is important to note that NO-acetaminophen was effective in conditions in which acetaminophen alone did not show analgesic action or NO-acetaminophen enhanced the analgesic potency of α_2-adrenergic receptor agonist when acetaminophen alone did not. As a result, these studies showed that NO-acetaminophen can be an effective analgesic in neuropathic and inflammatory painful conditions and also can lead to synergistic actions when used in combination with gabapentin or α_2-adrenergic receptor agonists in related painful conditions.

CONCLUSION

Findings in the last decade related to the contribution of the serotonergic system and NO in the analgesic effect of acetaminophen confirmed and expanded the involvement of these systems in acetaminophen analgesia. Due to the finding that direct binding of acetaminophen has not been shown with 5-HT_1, 5-HT_2, or 5-HT_3 serotonergic receptor subtypes,[58] interactions between these serotonergic receptors and acetaminophen are likely to be indirect. Recent studies confirmed bulbospinal serotonergic pathway involvement in acetaminophen analgesia and acetaminophen-induced serotonin increases in the central nervous system. The metabolite of acetaminophen, AM404, contributes to the analgesic effect of acetaminophen; however, the serotonergic receptor subtypes that contribute to the antinociceptive actions of acetaminophen and AM404 may be different. The involvement of 5-HT_1 receptors in acetaminophen analgesia is still not clear due to the conflicting results and requires to be evaluated with further studies. Despite the conflicting data, the contribution of 5-HT_2 receptors has been shown in acetaminophen analgesia (but not in AM404), and the localization is most likely to be the supra-spinal centers of the central nervous system. In animal studies, the blockage of acetaminophen analgesia with tropisetron is more obvious compared to ondansetron

and granisetron. It seems that the speculation regarding the involvement of tropisetron-sensitive receptors instead of 5-HT_3 receptors in the analgesic action of acetaminophen is still valid and waiting to be confirmed and clarified with further studies. Recent studies showed the contribution of 5-HT_7 serotonergic receptor subtypes as well. Despite the fact that there are some conflicting results between the studies in volunteers and post-operative patients, an important number of human studies expanded the data regarding the contribution of serotonergic receptors. Although there were not many additional findings related to the contribution of NO systems in the antinociceptive action of acetaminophen, the latest findings expanded the beneficial analgesic effects of the NO releasing derivative of acetaminophen, NO-acetaminophen.

Conflict of Interest: No conflict of interest was declared by the authors.

REFERENCES

1. Botting R, Ayoub SS. COX-3 and the mechanism of action of acetaminophen/acetaminophen. Prostaglandins Leukot Essent Fatty Acids. 2005;72:85-87.
2. Graham GG, Scott KF. Mechanism of action of paracetamol. Am J Ther. 2005;12:46-55.
3. Anderson BJ. Paracetamol (Acetaminophen): mechanisms of action. Paediatr Anaesth. 2008;18:915-921.
4. Păunescu H, Coman OA, Coman L, Ghiţă I, Georgescu SR, Drăghia F, Fulga I. Cannabinoid system and cyclooxygenases inhibitors. J Med Life. 2011;4:11-20.
5. Ruggieri V, Vitale G, Pini LA, Sandrini M. Differential involvement of opioidergic and serotonergic systems in the antinociceptive activity of N-arachidonoyl-phenolamine (AM404) in the rat: comparison with paracetamol. Naunyn Schmiedebergs Arch Pharmacol. 2008;377:219-229.
6. Tariq SA, Khan H, Popalzai AJ, Niazi IU, Safiullah. Attenuation of erythrocytic acetyl cholinesterase by acetaminophen and chloroquine: evidence in an *in vitro* study. Pak J Pharm Sci. 2014;27:261-264.
7. Bhagyashree A, Manikkoth S, Sequeira M, Nayak R, Rao SN. Central dopaminergic system plays a role in the analgesic action of acetaminophen: Preclinical evidence. Indian J Pharmacol. 2017;49:21-25.
8. Kerckhove N, Mallet C, François A, Boudes M, Chemin J, Voets T, Bourinet E, Alloui A, Eschalier A. Ca(v)3.2 calcium channels: the key protagonist in the supraspinal effect of paracetamol. Pain. 2014;155:764-772.
9. Tjølsen A, Lund A, Hole K. Antinociceptive effect of paracetamol in rats is partly dependent on spinal serotonergic systems. Eur J Pharmacol. 1991;193:193-201.
10. Pini LA, Sandrini M, Vitale G. The The antinociceptive action of paracetamol is associated with changes in the serotonergic system in the rat brain. Eur J Pharmacol. 1996;308:31-40.
11. Mallet C, Daulhac L, Bonnefont J, Ledent C, Etienne M, Chapuy E, Libert F, Eschalier A. Endocannabinoid and serotonergic systems are needed for acetaminophen-induced analgesia. Pain. 2008;139:190-200.
12. Dogrul A, Seyrek M, Akgul EO, Cayci T, Kahraman S, Bolay H. Systemic paracetamol-induced analgesic and antihyperalgesic effects through activation of descending serotonergic pathways involving spinal 5-HT_7 receptors. Eur J Pharmacol. 2012;677:93-101.
13. Muchacki R, Szkilnik R, Malinowska-Borowska J, Żelazko A, Lewkowicz Ł, Nowak PG. Impairment in Pain Perception in Adult Rats Lesioned as Neonates with 5.7-Dihydroxytryptamine. Adv Clin Exp Med. 2015;24:419-427.
14. Vijayakaran K, Kesavan M, Kannan K, Sankar P, Tandan SK, Sarkar SN. Arsenic decreases antinociceptive activity of acetaminophen: possible involvement of serotonergic and endocannabinoid receptors. Environ Toxicol Pharmacol. 2014;38:397-405.
15. Blecharz-Klin K, Piechal A, Pyrzanowska J, Joniec-Maciejak I, Kiliszek P, Widy-Tyszkiewicz E. Paracetamol--the outcome on neurotransmission and spatial learning in rats. Behav Brain Res. 2013;253:157-164.
16. Tiippana E, Hamunen K, Kontinen V, Kalso E. The effect of paracetamol and tropisetron on pain: experimental studies and a review of published data. Basic Clin Pharmacol Toxicol. 2013;112:124-131.
17. Högestätt ED, Jönsson BA, Ermund A, Andersson DA, Björk H, Alexander JP, Cravatt BF, Basbaum AI, Zygmunt PM. Conversion of acetaminophen to the bioactive N-acylphenolamine AM404 via fatty acid amide hydrolase-dependent arachidonic acid conjugation in the nervous system. J Biol Chem. 2005;280:31405-31412.
18. De Petrocellis L, Bisogno T, Davis JB, Pertwee RG, Di Marzo V. Overlap between the ligand recognition properties of the anandamide transporter and the VR1 vanilloid receptor: inhibitors of anandamide uptake with negligible capsaicin-like activity. FEBS Lett. 2000;483:52-56.
19. Barrière DA, Mallet C, Blomgren A, Simonsen C, Daulhac L, Libert F, Chapuy E, Etienne M, Högestätt ED, Zygmunt PM, Eschalier A. Fatty acid amide hydrolase-dependent generation of antinociceptive drug metabolites acting on TRPV1 in the brain. PLoS One. 2013;8:e70690.
20. Tiger M, Varnäs K, Okubo Y, Lundberg J. The 5-HT(1B) receptor - a potential target for antidepressant treatment. Psychopharmacology (Berl). 2018;235:1317-1334.
21. Dreshfield LJ, Wong DT, Perry KW, Engleman EA. Enhancement of fluoxetine-dependent increase of extracellular serotonin (5-HT) levels by (-)-pindolol, an antagonist at 5-HT1A receptors. Neurochem Res. 1996;21:557-562.
22. Courade JP, Chassaing C, Bardin L, Alloui A, Eschalier A. 5-HT receptor subtypes involved in the spinal antinociceptive effect of acetaminophen in rats. Eur J Pharmacol. 2001;432:1-7.
23. Foong JP, Bornstein JC. 5-HT antagonists NAN-190 and SB 269970 block alpha2-adrenoceptors in the guinea pig. Neuroreport. 2009;20:325-330.
24. Roca-Vinardell A, Ortega-Alvaro A, Gibert-Rahola J, Micó JA. The role of 5-HT1A/B autoreceptors in the antinociceptive effect of systemic administration of acetaminophen. Anesthesiology. 2003;98:741-747.
25. Sandrini M, Pini LA, Vitale G. Differential involvement of central 5-HT1B and 5-HT3 receptor subtypes in the antinociceptive effect of acetaminophen. Inflamm Res. 2003;52:347-352.
26. Karandikar YS, Belsare P, Panditrao A. Effect of drugs modulating serotonergic system on the analgesic action of acetaminophen in mice. Indian J Pharmacol. 2016;48:281-285.
27. Srikiatkhachorn A, Tarasub N, Govitrapong P. Acetaminophen-induced antinociception via central 5-HT(2A) receptors. Neurochem Int. 1999;34:491-498.
28. Pelissier T, Alloui A, Caussade F, Dubray C, Cloarec A, Lavarenne J, Eschalier A. Paracetamol exerts a spinal antinociceptive effect involving

an indirect interaction with 5-hydroxytryptamine3 receptors: *in vivo* and *in vitro* evidence. J Pharmacol Exp Ther. 1996;278:8-14.

29. Alloui A, Chassaing C, Schmidt J, Ardid D, Dubray C, Cloarec A, Eschalier A. Paracetamol exerts a spinal, tropisetron-reversible, antinociceptive effect in an inflammatory pain model in rats. Eur J Pharmacol. 2002;443:71-77.
30. Libert F, Bonnefont J, Bourinet E, Doucet E, Alloui A, Hamon M, Nargeot J, Eschalier A. Acetaminophen: a central analgesic drug that involves a spinal tropisetron-sensitive, non-5-HT(3) receptor-mediated effect. Mol Pharmacol. 2004;66:728-734.
31. Girard P, Pansart Y, Coppé MC, Niedergang B, Gillardin JM. Modulation of paracetamol and nefopam antinociception by serotonin 5-HT(3) receptor antagonists in mice. Pharmacology. 2009;83:243-246.
32. Gan TJ. Selective serotonin 5-HT3 receptor antagonists for postoperative nausea and vomiting: are they all the same? CNS Drugs. 2005;19:225-238.
33. Ho KY, Gan TJ. Pharmacology, pharmacogenetics, and clinical efficacy of 5-hydroxytryptamine type 3 receptor antagonists for postoperative nausea and vomiting. Curr Opin Anaesthesiol. 2006;19:606-611.
34. Macor JE, Gurley D, Lanthorn T, Loch J, Mack RA, Mullen G, Tran O, Wright N, Gordon JC. The 5-HT3 antagonist tropisetron (ICS 205-930) is a potent and selective alpha7 nicotinic receptor partial agonist. Bioorg Med Chem Lett. 2001;11:319-321.
35. Pickering G, Loriot MA, Libert F, Eschalier A, Beaune P, Dubray C. Analgesic effect of acetaminophen in humans: first evidence of a central serotonergic mechanism. Clin Pharmacol Ther. 2006;79:371-378.
36. Pickering G, Estève V, Loriot MA, Eschalier A, Dubray C. Acetaminophen reinforces descending inhibitory pain pathways. Clin Pharmacol Ther. 2008;84:47-51.
37. Bandschapp O, Filitz J, Urwyler A, Koppert W, Ruppen W. Tropisetron blocks analgesic action of acetaminophen: a human pain model study. Pain. 2011;152:1304-1310.
38. Jokela R, Ahonen J, Seitsonen E, Marjakangas P, Korttila K. The influence of ondansetron on the analgesic effect of acetaminophen after laparoscopic hysterectomy. Clin Pharmacol Ther. 2010;87:672-678.
39. Pickering G, Faure M, Commun F, de Boissy EC, Roche G, Mom T, Simen E, Dubray C, Eschalier A, Gilain L. Tropisetron and paracetamol association in post-operative patients. Fundam Clin Pharmacol. 2012;26:432-437.
40. Koyuncu O, Leung S, You J, Oksar M, Turhanoglu S, Akkurt C, Dolapcioglu K, Sahin H, Sessler DI, Turan A. The effect of ondansetron on analgesic efficacy of acetaminophen after hysterectomy: A randomized double blinded placebo controlled trial. J Clin Anesth. 2017;40:78-83.
41. Leopoldo M, Lacivita E, Berardi F, Perrone R, Hedlund PB. Serotonin 5-HT7 receptor agents: Structure-activity relationships and potential therapeutic applications in central nervous system disorders. Pharmacol Ther. 2011;129:120-148.
42. Liu J, Reid AR, Sawynok J. Antinociception by systemically-administered acetaminophen (acetaminophen) involves spinal serotonin 5-HT7 and adenosine A1 receptors, as well as peripheral adenosine A1 receptors. Neurosci Lett. 2013;536:64-68.
43. Dawson TM, Dawson VL, Snyder SH. A novel neuronal messenger molecule in brain: the free radical, nitric oxide. Ann Neurol. 1992;32:297-311.
44. Džoljić E, Grbatinić I, Kostić V. Why is nitric oxide important for our brain? Funct Neurol. 2015;30:159-163.
45. Meller ST, Gebhart GF. Nitric oxide (NO) and nociceptive processing in the spinal cord. Pain. 1993;52:127-136.
46. Lothe A, Li P, Tong C, Yoon Y, Bouaziz H, Detweiler DJ, Eisenach JC. Spinal cholinergic alpha-2 adrenergic interactions in analgesia and hemodynamic control: role of muscarinic receptor subtypes and nitric oxide. J Pharmacol Exp Ther. 1994;270:1301-1306.
47. Millan MJ. The induction of pain: an integrative review. Prog Neurobiol. 1999;57:1-164.
48. Björkman R, Hallman KM, Hedner J, Hedner T, Henning M. Acetaminophen blocks spinal hyperalgesia induced by NMDA and substance P. Pain. 1994;57:259-264.
49. Bujalska M, Gumułka WS. Effect of cyclooxygenase and NO synthase inhibitors on antinociceptive action of acetaminophen. Pol J Pharmacol. 2001;53:341-350.
50. Godfrey L, Bailey I, Toms NJ, Clarke GD, Kitchen I, Hourani SM. Paracetamol inhibits nitric oxide synthesis in murine spinal cord slices. Eur J Pharmacol. 2007;562:68-71.
51. Moore PK, Marshall M. Nitric oxide releasing acetaminophen (nitroacetaminophen). Dig Liver Dis. 2003;35(Suppl 2):49-60.
52. al-Swayeh OA, Futter LE, Clifford RH, Moore PK. Nitroparacetamol exhibits anti-inflammatory and anti-nociceptive activity. Br J Pharmacol. 2000;130:1453-1456.
53. Romero-Sandoval EA, Mazario J, Howat D, Herrero JF. NCX-701 (nitroparacetamol) is an effective antinociceptive agent in rat withdrawal reflexes and wind-up. Br J Pharmacol. 2002;135:1556-1562.
54. Alfonso Romero-Sandoval E, Del Soldato P, Herrero JF. The effects of sham and full spinalization on the antinociceptive effects of NCX-701 (nitroparacetamol) in monoarthritic rats. Neuropharmacology. 2003;45:412-419.
55. Romero-Sandoval EA, Curros-Criado MM, Gaitan G, Molina C, Herrero JF. Nitroacetaminophen (NCX-701) and pain: first in a series of novel analgesics. CNS Drug Rev. 2007;13:279-295.
56. Curros-Criado MM, Herrero JF. Antinociceptive effects of NCX-701 (nitro-paracetamol) in neuropathic rats: enhancement of antinociception by co-administration with gabapentin. Br J Pharmacol. 2009;158:601-609.
57. Molina C, Herrero JF. Subeffective doses of nitroparacetamol (NCX-701) enhance the antinociceptive activity of the α_2-adrenoceptor agonist medetomidine. Pharmacol Biochem Behav. 2011;99:385-390.
58. Raffa RB, Codd EE. Lack of binding of acetaminophen to 5-HT receptor or uptake sites (or eleven other binding/uptake assays). Life Sci. 1996;59:37-40.